Journal of Physical and Chemical Reference Data

Experimental Stark Widths and Shifts for Spectral Lines of Neutral and Ionized Atoms (A Critical Review of Selected Data for the Period 1989 Through 2000)

Cite as: Journal of Physical and Chemical Reference Data **31**, 819 (2002); https://doi.org/10.1063/1.1486456
Submitted: 12 October 2001 . Accepted: 18 January 2002 . Published Online: 12 September 2002

N. Konjević, A. Lesage, J. R. Fuhr, and W. L. Wiese

View Online Export Citation

ARTICLES YOU MAY BE INTERESTED IN

Experimental Stark widths and shifts for spectral lines of neutral and ionized atoms
Journal of Physical and Chemical Reference Data **19**, 1307 (1990); https://doi.org/10.1063/1.555847

Experimental Stark Widths and Shifts for Spectral Lines of Neutral Atoms (A Critical Review of Selected Data for the Period 1976 to 1982)
Journal of Physical and Chemical Reference Data **13**, 619 (1984); https://doi.org/10.1063/1.555715

Stark broadening for diagnostics of the electron density in non-equilibrium plasma utilizing isotope hydrogen alpha lines
Journal of Applied Physics **115**, 163106 (2014); https://doi.org/10.1063/1.4873960

© 2002 by the U.S. Secretary of Commerce on behalf of the United States. All rights reserved.

Experimental Stark Widths and Shifts for Spectral Lines of Neutral and Ionized Atoms
(A Critical Review of Selected Data for the Period 1989 Through 2000)

N. Konjević
Institute of Physics, P.O. Box 68, 11081 Belgrade, Yugoslavia

A. Lesage
Observatoire de Paris–Meudon, 92195 Meudon Cedex, France

J. R. Fuhr[a] and W. L. Wiese
National Institute of Standards and Technology (NIST), Gaithersburg, Maryland 20899

(Received 12 October 2001; accepted 18 January 2002; published 12 September 2002)

A critical review of the available experimental data on Stark widths and shifts for spectral lines of nonhydrogenic neutral atoms and positive ions has been carried out. The review covers the period from 1989 through the end of 2000 and represents a continuation of earlier critical reviews up to 1988. Data tables containing the selected experimental Stark broadening parameters are presented with estimated accuracies. Guidelines for the accuracy estimates, developed during the previous reviews, are summarized again. The data are arranged according to elements and spectra, and these are presented in alphabetical and numerical order, respectively. A total of 77 spectra are covered, and the material on multiply charged ions has significantly increased. Comparisons with comprehensive calculations based on semiclassical theory are made whenever possible, since the comparison with theory has often been a principal motivation for the experiments. © *2002 by the U.S. Secretary of Commerce on behalf of the United States. All rights reserved.*

Key words: critically evaluated data; full width at half maximum intensity; neutral atoms; positive ions; Stark broadening parameters; Stark shifts; Stark widths.

Contents

1. Introduction. 820
2. General Discussion of Our Evaluation Procedure. 821
3. Comparisons with Theory. 822
4. Arrangement of the Tables. 823
5. Summary and Conclusions. 823
6. Acknowledgments. 824
7. References. 824
Appendix A: Principal Properties and Specifications of the Plasma Sources Applied. . . . 825
Appendix B: Advanced Procedures for the Deconvolution of Line Profiles. 826
8. Tables of Stark Widths and Shifts. 827
Aluminum. 827
Al II. 827
Al III. 827
Argon. 828
Ar I. 828
Ar II. 834
Ar III. 843
Ar IV. 844
Boron. 845
B I. 845
B II. 845
B III. 846
Bromine. 847
Br I. 847
Br II. 848
Br III. 848
Br IV. 849
Cadmium. 850
Cd II. 850
Calcium. 850
Ca II. 850
Carbon. 851
C I. 851
C II. 852
C III. 855
C IV. 856

[a]Electronic mail: jeffrey.fuhr@nist.gov
© 2002 by the U.S. Secretary of Commerce on behalf of the United States. All rights reserved.

Chlorine. 857
Cl I. 857
Cl II. 858
Cl III. 859
Copper. 859
Cu I. 859
Cu II. 860
Fluorine. 861
F I. 861
F II. 861
F III. 862
F IV. 863
F V. 864
F VII. 865
Helium. 865
He I. 865
Iodine. 868
I I. 868
I II. 869
I III. 870
Iron. 870
Fe I. 870
Fe II. 873
Krypton. 874
Kr I. 874
Kr II. 875
Kr III. 877
Lead. 879
Pb I. 879
Pb II. 880
Mercury. 881
Hg II. 881
Hg III. 882
Neon. 882
Ne I. 882
Ne II. 884
Ne III. 887
Ne IV. 888
Ne V. 889
Ne VI. 889
Ne VII. 890
Ne VIII. 891
Nickel. 891
Ni I. 891
Ni II. 892
Nitrogen. 892
N I. 892
N II. 894
N III. 898
N IV. 900
N V. 902
Oxygen. 902
O I. 902
O II. 903
O III. 906
O IV. 906
O V. 908
O VI. 908
Silicon. 909
Si I. 909
Si II. 910
Si III. 912
Si IV. 913
Sodium. 914
Na I. 914
Sulfur. 915
S II. 915
S III. 916
Tin. 917
Sn I. 917
Sn II. 918
Xenon. 919
Xe I. 919
Xe II. 920
Xe III. 923
Zinc. 927
Zn II. 927

List of Figures

1 Stark widths for the $3s\,^2\mathrm{S}-3p\,^2\mathrm{P}^\circ$ transition of lithium-like spectral lines (in units of angular frequency) as a function of $\log_{10} Z$ according to Blagojević *et al.*[10]. 821
2 Ratio of experimental Stark widths to semiclassical calculations as a function of the temperature for the lithium-like $3s\,^2\mathrm{S}-3p\,^2\mathrm{P}^\circ$ transition of N V. 822
3 Ratio of experimental Stark widths to semiclassical calculations as a function of the temperature for the boron-like $3s\,^2\mathrm{S}-3p\,^2\mathrm{P}^\circ$ transition of O IV. 822
4 Ratio of experimental Stark widths to semiclassical calculations as a function of the temperature for the boron-like $3s\,^2\mathrm{S}-3p\,^2\mathrm{P}^\circ$ transition of N III. 822
5 Measured temperature dependence for the halfwidth of the Fe I 5383 Å line. 822

1. Introduction

This tabulation is a continuation of a series of critical reviews and tables on experimental Stark broadening data for spectral lines of nonhydrogenic atoms and ions which we started in 1976[1,2] and continued in 1984[3,4] and 1990.[5] In this new installment, we cover the period from 1989 to the end of 2000, and, as in the last review, we have presented the data on atoms and ions in a single set of tables. Generally, we have adhered to the format of our previous reviews, and we have subjected the data again to the same evaluation criteria as those established earlier.

Our main source of literature references has been the master file of the Data Center on Atomic Line Shapes and Shifts at the National Institute of Standards and Technology (formerly the National Bureau of Standards).[6,7] Also, two of the authors have maintained independent searches in the litera-

ture during the entire period. A principal reason for many Stark-broadening experiments is to provide comparisons for theoretical Stark width and shift data. We have therefore also presented comparisons with the generally successful and widely applied semiclassical calculations, similar to our previous reviews. Another reason for such experiments is (especially for heavier and higher ionized elements) the importance of Stark broadening parameters in stellar atmosphere opacity calculations,[8] and in the analysis of dense laboratory plasmas.

2. General Discussion of Our Evaluation Procedure

We have evaluated and tabulated the two principal Stark broadening parameters obtained from the experiments: the full width of a spectral line at half maximum intensity (FWHM) and the shift of a line, usually determined at peak intensity. But in several cases the shifts are reported for the position of the halfwidth, and this is noted in the tables for these spectra. The shifts are listed as positive when they occur toward longer wavelengths (redshift), and as negative when they occur toward shorter wavelengths (blueshift).

We provide detailed discussions of our evaluation procedure and of the criteria adopted in our earlier reviews[1–5,9] and give extensive references from the literature there. Therefore, we only summarize below our principal criteria for the selection of the experimental results and for the estimates of the uncertainties.

(a) The plasma source must be well characterized, i.e., it must be homogeneous in the observation region, be quasisteady state during the observation time and must be highly reproducible. The last requirement is especially important for shot-to-shot line scanning techniques with pulsed plasmas. A detailed listing of the applied plasma sources, their range of applications, power requirements, etc., is given in Appendix A of this introduction. Three properties of the plasma sources principally affect the accuracy of the Stark broadening data: the geometry of the source (especially its homogeneity or inhomogeneity and the presence or absence of boundary layers); its stability during the observation time; and its reproducibility (this is especially important for pulsed sources, when shot-to-shot scanning techniques are used). These features are often discussed in some detail in the references of Appendix A.

(b) The electron density in the observed plasma region must have been determined accurately by an independent method (i.e., a method other than one that utilizes the Stark broadening of the investigated lines).

(c) A temperature determination with an accuracy similar to that for the electron density must have been carried out.

(d) Competing line broadening and shift mechanisms must have been considered, such as Doppler, van der Waals, and instrumental broadening, and their contributions must have been estimated and subtracted. A discussion of recent line shape deconvolution techniques, especially those for the slightly asymmetric profiles of neutral atoms, is given in Appendix B.

(e) Optically thin conditions must prevail at the line centers, or appropriate corrections must be made. Also, inhomogeneous plasma boundary layers must be either eliminated by appropriate experimental arrangements or must be taken into account in the uncertainty estimates.

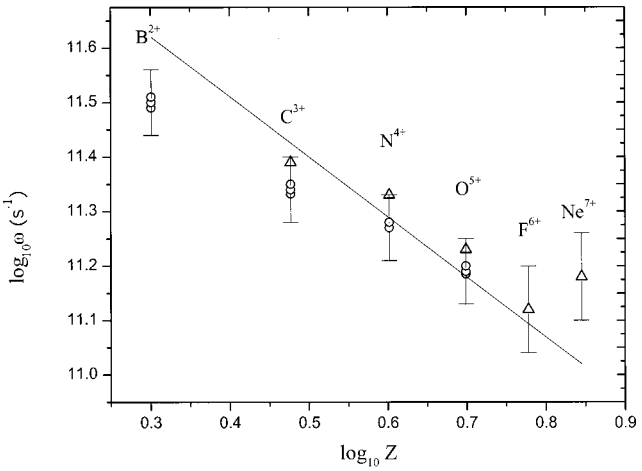

FIG. 1. Stark widths for the $3s\ ^2S-3p\ ^2P°$ transition of lithium-like spectral lines (in units of angular frequency) as a function of $\log_{10} Z$ according to Blagojević *et al.*[10] The experimental data are scaled linearly to a value of the electron density of 10^{17} e/cm^3 and to an electron temperature value of 87 000 K (7.5 eV) using w_e (T_e) dependence from the theoretical data in Ref. 10. Experimental results: Δ, Glenzer *et al.*;[11] and ○, Blagojević *et al.*[10] Error flags are calculated uncertainties including the error in the determination of the full width at half maximum and electron density measurements. The results of semiclassical calculations by Blagojević *et al.*,[10] shown for comparison, are given by the solid line.

We have generally found that in the large majority of the experiments, the above listed critical factors, (a)–(e), have been addressed. Occasionally, one of the factors—like the measurements of the plasma temperature or the effects of plasma end-layers—has not been discussed, and we have either noted this in the tables which list ''Key Data on Experiments,'' or have commented on this in the introduction to the pertinent spectrum.

As in our earlier reviews, we have again selected a few specific cases with fairly large amounts of experimental as well as some semiclassical theoretical comparison data for graphical illustrations of the quality of the data.

In Fig. 1 we show the measured Stark widths (in units of angular frequency) of the lithium-like $3s\ ^2S-3p\ ^2P°$ transition for six successive ions, B III–Ne VIII. Clearly the nuclear charge (Z) dependence is also reasonably well predicted by the semiclassical theory. In Figs. 2, 3, and 4 we illustrate ratios of measured Stark widths to semiclassically calculated ones as a function of temperature for the $3s\ ^2S-3p\ ^2P°$ transition of Li-like N V (Fig. 2) and of boron-like N III and O IV. For Li-like N V the experimen-

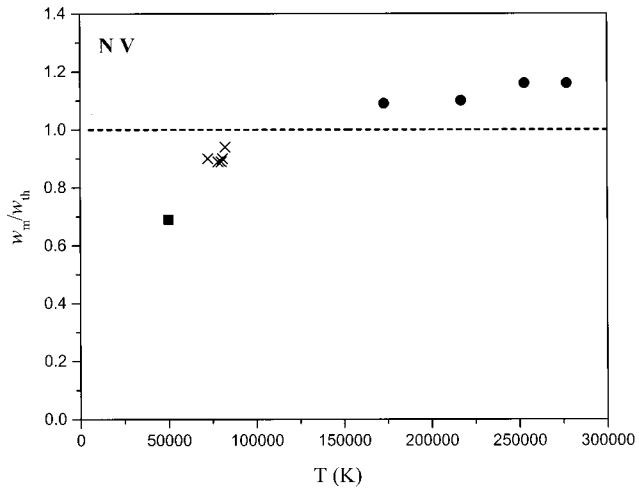

FIG. 2. Ratio of experimental Stark widths to semiclassical calculations as a function of the temperature for the lithium-like $3s\ ^2S-3p\ ^2P°$ transition of N V. The experimental sources are ■, Puric *et al.*;[12] ●, Glenzer *et al.*;[11] and ×, Blagojević *et al.*[10] The semiclassical calculations were carried out by Blagojević *et al.*[10]

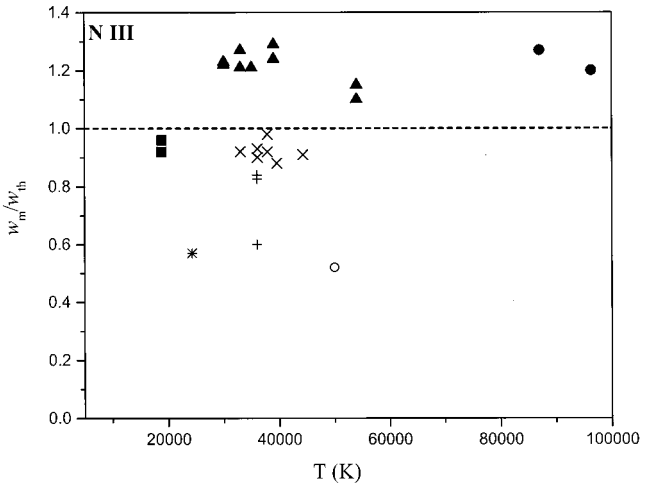

FIG. 4. Ratio of experimental Stark widths to semiclassical calculations as a function of the temperature for the boron-like $3s\ ^2S-3p\ ^2P°$ transition of N III. The sources of experimental data are *, Popović *et al.*;[16] +, Purcell and Barnard;[17] ○, Purić *et al.*;[18] ▲, Glenzer *et al.*;[15] ■, Blagojević *et al.*;[18] ●, Blagojević *et al.*;[19] and ×, Djenize and Milosavljević.[20] Compared to the data for the same transition of the isoelectronic ion O^{+3} (see Fig. 3), the scatter among the experimental data is much larger. This is not unexpected since the number of experiments has more than doubled compared to O^{+3}, and include several early experiments that contribute appreciably to the scatter. The theoretical comparison data were taken from the semiclassical calculations by Blagojević *et al.*[18]

tally established temperature dependence is noticeably different from the semiclassically calculated one, where as for O IV the agreement is very close. For N III, for which seven experimental sources[15–20] are available, the various results scatter appreciably, with early experiments[16–18] contributing a great deal. In Fig. 5 we show the temperature dependence of the Stark width for the 5383 Å line of Fe I obtained from numerous shock-tube measurements.[21–23] In spite of considerable scatter, a trend is clearly visible.

3. Comparisons with Theory

Whenever theoretical data are available, we have provided comparisons with the semiclassical theory developed by Griem[24] in 1962. For neutral atoms and singly charged ions, the semiclassical results by Griem[25] are normally used. For a few exceptions the source of the theoretical data is clearly noted. For multiply charged ions the results of another semiclassical perturbation mechanism are used.[26] This approach was then modified and extended, especially by Sahal-Bréchot, and Dimitrijević, and a large number of additional

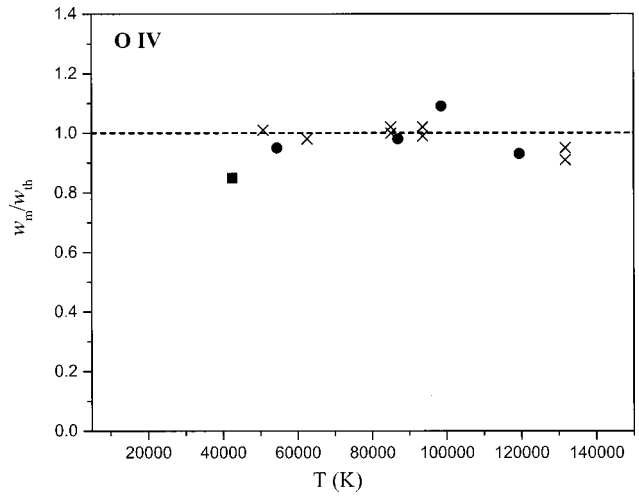

FIG. 3. Ratio of experimental Stark widths to semiclassical calculations as a function of the temperature for the boron-like $3s\ ^2S-3p\ ^2P°$ transition of O IV. The sources of experimental data are ■, Puric *et al.*;[13] ×, Blagojević *et al.*;[14] and ●, Glenzer *et al.*[15] The measurements are compared with the semiclassical calculations of Blagojević *et al.*[14]

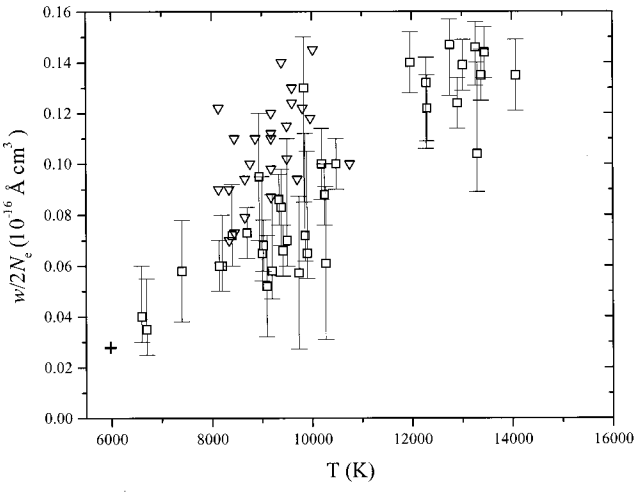

FIG. 5. Measured temperature dependence for the halfwidth of the Fe I 5383 Å line. (All measurements are normalized to an electron density of 10^{16} cm^{-3}.) The sources of experimental data are □, Lesage *et al.*;[21] ▽, Freudenstein and Cooper;[22] and +, de Frutos *et al.*[23] (corrected using a Stark width given by Lesage *et al.*[21] for the electron density determination).

numerical results were provided by these authors (see the NBS/NIST bibliographies on spectral line broadening[6,7] for numerous references).

The ratios of measured-to-calculated widths and shifts tabulated by us for the various spectra provide guidance on the degree of agreement between the experiments and theory, and thus provide a valuable indication of the quality of the calculated as well as measured data. It is seen that, for most transitions, the semiclassical calculations compare well with the experimental data, which was also observed in our earlier reviews.

We should note that the theoretical width data for ionic radiators are for the electron width only, and the usually very small additional width caused by ion broadening is neglected. Also, small shifts contributed by ions are neglected in the theoretical shift data for ionic radiators.

4. Arrangement of the Tables

The data are presented in separate tables for each spectrum (or stage of ionization) and the spectra are arranged according to the chemical elements, which are given in alphabetical order.

Each data table is preceded by short comments that provide important information on the literature selected and by a short tabular overview that provides some key points on each experiment selected, such as the type of plasma source employed. For spectra containing more than 20 transitions, we provide a finding list in which the lines selected are given in order of increasing wavelength.

The data tables are subdivided into four principal parts. In the first part, which comprises three columns, each spectral line is identified by transition array, multiplet designation (wherever available), and wavelength (given in units of angströms). The wavelengths are usually taken from the Atomic Spectra Database (ASD) of NIST,[27] or, in a few cases, from more recent NIST compilations[28] or the earlier data tables of Striganov and Sventitskii.[29]

In the second part of the table, the principal plasma data are listed. Normally, these are the ranges of temperatures and electron densities at which the width and shift data have been measured. However, in a number of papers the authors have not listed the actual electron densities at which the measurements were made, but have presented their data scaled to nominal electron densities of 10^{16} cm^{-3} (mainly for neutrals) or 10^{17} cm^{-3} in order to facilitate comparisons with theory. We have always listed the electron densities in units of 10^{17} cm^{-3}.

In the third part of the table, we present the measured Stark broadening data, specifically the FWHM, i.e., the Stark width, w_m, and the Stark shift, d_m. We also present the ratios of measured to theoretical, i.e., semiclassically calculated, widths and shifts, $w_m/w_{\rm th}$ and $d_m/d_{\rm th}$, when available.

In the fourth part of the table, we provide estimates of the uncertainties of the data and we also identify references from the literature. When Stark widths as well as shifts are measured, we provide two estimates of the uncertainties, where the first one refers to the width, while the second pertains to the shift. For the estimates we again use code letters which indicate the following:

A=uncertainties within 15%,
B^+=uncertainties within 23%,
B=uncertainties within 30%,
C^+=uncertainties within 40%,
C=uncertainties within 50%, and
D=uncertainties larger than 50%.

D is used very sparingly, i.e., for important transitions only when no other data are available, and for uncertainties estimated not to exceed factors of 3.

In this critical review we have expressed the relative uncertainties as ''combined standard uncertainties'' according to recommendations by Taylor and Kuyatt.[30] This means that the overall uncertainties of the measurements are given as the root of the sum of the squares (rss) of the individual contributions. All reported, or otherwise estimated, individual standard uncertainties that contribute have been combined to the rss relative error. This new procedure differs from the preceding reviews[1–5] where the straight sum of individual uncertainties was taken as the overall uncertainty. For example, in Refs. 1–5 the total error in the Stark width from uncertainties of $\pm 10\%$ in the electron density and $\pm 15\%$ in the halfwidth measured was $\pm 25\%$, while the rss estimate used here yields $\pm 18\%$. In many experiments, the two dominant contributions are the uncertainties in the electron density and linewidth, or shift, measurement. Smaller contributions arise usually from the deconvolution process, from plasma inhomogeneities such as cooler, lower electron-density end layers, from optical depth problems and corrections, and from plasma temperature measurements.

In arriving at our uncertainty estimates, we have also taken into account occasional disagreements between authors outside their mutual error estimates. Furthermore, whenever possible, we have tested the adherence of the data to regularities and similarities predicted on the basis of atomic structure considerations.[31,32] For example, Stark halfwidths should normally be nearly the same for all lines within multiplets, and we have commented on cases where significant departures from this rule have occurred. Studies of isoelectronic ions of the Li sequence have shown clear systematic trends of the Stark widths with nuclear charge.

5. Summary and Conclusions

We have critically evaluated and compiled experimental Stark broadening data for isolated spectral lines of neutral and ionized atoms published since our last compilation, that is, for the 12-year period 1989 through the end of 2000. The growth of experimental data has been especially pronounced for multiply charged ions due to the development and application of new plasma sources (see also Ref. 9).

We have found that the new experimental data are generally very consistent with the earlier material, as well as with the results of semiclassical theory. But most of the new data

are not significantly better than those in our last review, indicating that improvements in the experimental techniques have not advanced significantly in recent years.

For lines of neutral atoms we observe that for Stark widths the agreement between different experiments, as well as between experiment and theory, is usually within $\pm 20\%$, and often within 10%. Stark width data of especially good quality and mutual consistency are found for several lines of Ar I, C I and He I, so that these Stark widths can compete with other techniques as a high-accuracy plasma diagnostic approach for the determination of electron densities.

For lines of singly ionized atoms, the accuracy of the experimental data is, however, not as well established yet, and more measurements are highly desirable. A few exceptions are several multiplets of Ar II and the first multiplet of Si II. For multiply charged ions, good progress has been achieved in the last decade. For several spectra these are the first measurements. Stark widths have been measured over a large electron density and temperature range, and the agreement between experiments and theory is usually good.

6. Acknowledgments

The authors gratefully acknowledge the valuable assistance of Amandine Pikon in the process of data collection and of Suzanne Sullivan in preparing this article for publication.

7. References

[1] N. Konjević and J. R. Roberts, J. Phys. Chem. Ref. Data **5**, 209 (1976).
[2] N. Konjević and W. L. Wiese, J. Phys. Chem. Ref. Data **5**, 259 (1976).
[3] N. Konjević, M. S. Dimitrijević, and W. L. Wiese, J. Phys. Chem. Ref. Data **13**, 619 (1984).
[4] N. Konjević, M. S. Dimitrijević, and W. L. Wiese, J. Phys. Chem. Ref. Data **13**, 649 (1984).
[5] N. Konjević and W. L. Wiese, J. Phys. Chem. Ref. Data **19**, 1307 (1990).
[6] J. R. Fuhr, W. L. Wiese, and L. J. Roszman, *Bibliography on Atomic Line Shapes and Shifts*, Spec. Publ. No. 366 (1972); Suppl. 1 (1974); Suppl. 2 (1975) (with G. A. Martin and B. J. Specht); Suppl. 3 (1978) (with B. J. Miller and G. A. Martin); Suppl. 4 (1993) (with A. Lesage).
[7] J. R. Fuhr and H. R. Felrice, *Atomic Spectral Line Broadening Bibliographic Database*, http://physics.nist.gov/linebrbib.
[8] A. Lesage, in *Astrophysical Applications of Powerful New Databases*, edited by S. J. Adelman and W. L. Wiese, Astron. Soc. Pacific Conf. Ser., Vol. 78 (1994).
[9] N. Konjević, Phys. Rep. **316**, 339 (1999).
[10] B. Blagojević, M. V. Popović, N. Konjević, and M. S. Dimitrijević, J. Quant. Spectrosc. Radiat. Transf. **61**, 361 (1999).
[11] S. Glenzer, N. I. Uzelac, and H.-J. Kunze, Phys. Rev. A **45**, 8795 (1992).
[12] J. Purić, A. Srećković, S. Djenize, and M. Platisa, Phys. Rev. A **36**, 3957 (1987).
[13] J. Purić, S. Djenize, A. Srećković, M. Platisa, and J. Labat, Phys. Rev. A **37**, 498 (1988).
[14] B. Blagojević, M. V. Popović, N. Konjević, and M. S. Dimitrijević, Phys. Rev. E **50**, 2986 (1994).
[15] S. Glenzer, J. D. Hey, and H.-J. Kunze, J. Phys. B **27**, 413 (1994).
[16] M. Popović, M. Platisa, and N. Konjević, Astron. Astrophys. **41**, 463 (1975).
[17] S. T. Purcell and A. J. Barnard, J. Quant. Spectrosc. Radiat. Transf. **32**, 205 (1984).
[18] B. Blagojević, M. V. Popović, N. Konjević, and M. S. Dimitrijević, Phys. Rev. E **54**, 743 (1996).
[19] B. Blagojević, M. V. Popović, and N. Konjević, *Spectral Line Shapes*, AIP Conf. Proc. Vol. 10, edited by R. M. Herman (AIP, Woodbury, NY, 1999), pp. 187–190; 467.
[20] S. Djenize and V. Milosavljević, Astron. Astrophys., Suppl. Ser. **131**, 355 (1998).
[21] A. Lesage, J. L. Lebrun, and J. Richou, Astrophys. J. **360**, 737 (1990).
[22] S. Freudenstein and J. Cooper, Astron. Astrophys. **71**, 283 (1979).
[23] A. M. de Frutos, A. Poueyo, L. Sabatier, R. Fabbro, and J. M. Orza, *Spectral Line Shapes*, edited by R. Stamm and B. Talin (Nova Science, Commack, NY, 1993), Vol. 7, pp. 143–144.
[24] H. R. Griem, Phys. Rev. **128**, 515 (1962).
[25] H. R. Griem, *Spectral Line Broadening by Plasmas* (Academic, New York, 1974).
[26] S. Sahal-Bréchot, Astron. Astrophys. **1**, 91 (1969); **2**, 322 (1969).
[27] NIST Atomic Spectra Database, http://physics.nist.gov/asd.
[28] A. Musgrove, J. Reader, and C. J. Sansonetti (private communications).
[29] A. R. Striganov and N. S. Sventitskii, *Tables of Spectral Lines: Neutral and Ionized Atoms* (Atomizdat, Moscow, 1966).
[30] B. N. Taylor and C. E. Kuyatt, NIST Tech. Note 1297, U.S. Government Printing Office, Washington, DC, (1994).
[31] W. L. Wiese and N. Konjević, J. Quant. Spectrosc. Radiat. Transf. **28**, 185 (1982).
[32] W. L. Wiese and N. Konjević, J. Quant. Spectrosc. Radiat. Transf. **47**, 185 (1992).

Appendix A: Principal Properties and Specifications of the Plasma Sources Applied

Plasma source	Element and spectrum	Effective plasma size, (mm) $d-l$[a]	Mode of observation	Arc current (A) or energy (J)	Duration (μs)	Temperature (10^3 K)	Electron density (10^{16} cm^{-3})
I. Stationary Plasma Sources							
Wall-stabilized arcs and jets							
NIST,[1] U.S.	Ar I, C I, N I	4–88	End on	40–60 A	Stationary	11.6–12.6	6.20–7.90
University of Idaho,[2] U.S.	Ar I	10	Side on	300 A	Stationary	~11.9	3.8–6.0
Institute of Physics,[3] Belgrade, Yugoslavia	F I, Cl I, Br I, Br II	5–50	End on	25–35 A	Stationary	9.3–10.0	2.0–3.2
Institute of Physics,[4] University of Novi Sad, Yugoslavia	Ar I	5	Side on	30 A	Stationary	8.9–11.1	0.5–3.5
Institute de Science,[5] Font Romeu, France	Ar I	6	Side on	30–80 A	Stationary	5–20	0.9–6.5
Assiut University,[6] Egypt	Ar I, Ar II	4–48	End on	80 A	Stationary	14.2	~14.4
University of Orleans,[7] France	Ar II	5	Side on	200 A	Stationary	24	20
Opole University,[8] Poland	Ar I, Br I	4–55	End on	25–60 A	Stationary	11.5	10
University of Hannover,[9] Germany	C I, N I, O I, Ar I, Ar II, Kr I, Kr II	4–90	End on	40–80 A	Stationary	14	10
II. Pulsed discharges[b]							
1. Gas-liner pinch, Ruhr University,[10] Bochum, Germany	B III, C IV, N III, N IV, N V, O IV, O V, O VI, F IV, F V, F VII, Ne II, Ne III, Ne IV, Ne V, Ne VI, Ne VII, Ne VIII, Ar IV, Kr III	~20	Side on	2220–11200 J	0.1–0.5	81.2	240
2. Low-pressure pulsed arc, University of Valladolid,[11] Spain	He I, C I, C II, N II, O II, Ne II, Si II, Si III, Xe II	20–155	End on	560–1200 J	40–350	11–43	2–18
University of Caracas,[12] Venezuela	He I	50–250	End on	180 J	45	23.3–25.5	0.77–0.99
University of Belgrade,[13] Yugoslavia	B I, B II, B III, C II, C III, C IV, N II, O II, F II, F III, Na I, Si I, Si III, Si IV, S II, S III, S IV, Ar II, Ca II, Fe II, Ni I, Ni II, Cu I, Zn II, Br II, Br III, Br IV, Kr II, Kr III, Cd II, Sn I, Sn II, I II, I III, Hg I, Hg II, Hg III, Pb II	5–55 or 80	End on	12–83 J	10–105	1.0–6.4	1.4–26
3. Low-pressure pulsed arc (variable plasma length), Institute of Physics,[14] Belgrade, Yugoslavia	He I, B II, B III, C III, C IV, N III, N IV, N V, O III, O IV, O V, O VI, F III, F V, Ne III, S II, Cl II, Cl III, Ar III, Ar IV	13.5–280 31–280 11–180 10–161 24–161	End on	200–1000 J	8–600	12–131	2–110
4. Flash tube of variable plasma observation length, Institute of Physics,[15] Belgrade, Yugoslavia	Xe I, Xe II, Kr I, Kr II	7–70	End on	~300 J	~600	11.5–12.8	4.5–10.2
5. Low-pressure pulsed discharge National University,[16] Tandil, Argentina	Kr II, Kr III, Xe II, Xe III	3–800	End on	0.2–4 J	2.5	14.5	2.65
6. *Z* pinch, University of Orleans,[17] France	F I, S II	50	Side on	1920 J	20	20	20
7. Capillary discharge, Kazan State University,[18] Kazan, Russia	Cu II, Pb I, Pb II	2.5	Side on	2030 J	200	24	100
III. Shock tubes[c]							
University of Maryland,[19] U.S.	Kr I, Kr II, Xe II	92.5×67.1	Side on		35–150	<12.5	<17
Observatory of Meudon,[20] France	Fe I	40×40	Side on		~100	<14	<11
University of Düsseldorf,[21] Germany	Si II	52×52	Side on		~100	~15	<30
IV. Laser-produced plasmas[d]							
1. CO_2 TEA laser, Axicon, Institute of Physics,[22] Belgrade, Yugoslavia	He I	8	Side on		20	30	17
2. Nd–YAG laser, University of Madrid,[23] Spain	Al II, Al III, Sn I, Sn II	0.7 or 2.75	Side on	10^{10}–10^{11}	1	10.5–93	4–1600
3. CO_2 laser, University of Valladolid,[24] Spain	Fe I		Side on	5×10^6	Stationary	6	9
4. Perpendicularly crossed laser beams at 1.054 μm, Naval Research Laboratory,[25] U.S.	Al III	1×1	Side on	Two beams 10^{10}–10^{11}	0.005–0.008	50	230–2000

[a] d=diameter, l=length of plasma.

[b] Pulse duration in s.

[c] Cross section of shock tube (in mm^2) is given as effective plasma size.

[d] Power on target (in W cm^{-2}) is given instead of energy.

References for Appendix A

[1] D. W. Jones and W. L. Wiese, Phys. Rev. A **29**, 2597 (1984).
[2] V. Bakshi and R. J. Kearney, J. Quant. Spectrosc. Radiat. Transf. **42**, 405 (1989).
[3] S. Djurović and N. Konjević, Z. Phys. D **10**, 425 (1988).
[4] S. Djurović, Z. Mijatović, R. Kobilarov, and N. Konjević, J. Quant. Spectrosc. Radiat. Transf. **57**, 695 (1997).
[5] J. M. Badie and G. Vallbona, J. Phys. E **21**, 724 (1988).
[6] A. Abbas, T. S. Basha, and Z. A. A. El-Aal, Nuovo Cimento **10**, 597 (1988).
[7] S. Pellerin, K. Musiol, and J. Chapelle, J. Quant. Spectrosc. Radiat. Transf. **57**, 349 (1997).
[8] T. Wujec, A. Baclawski, A. Goly, and I. Ksiazek, J. Quant. Spectrosc. Radiat. Transf. **61**, 533 (1999); J. Musielok, Acta Phys. Pol. A **86**, 315 (1994).
[9] J. P. Knauer and M. Kock, J. Quant. Spectrosc. Radiat. Transf. **56**, 563 (1996).
[10] K. H. Finken and U. Ackerman, J. Phys. D **16**, 773 (1983).
[11] J. A. Del Val, S. Mar, M. A. Gigosos, I. de la Rosa, C. Perez, and V. Gonzalez, Jpn. J. Appl. Phys., Part 1 **37**, 4177 (1998).
[12] Y. Guimerans, E. J. Iglesias, D. Mandelbaum, and A. Sanchez, J. Quant. Spectrosc. Radiat. Transf. **42**, 39 (1989).
[13] J. Purić, S. Djenize, A. Srećković, J. Labat, and Lj. M. Ćirković, Phys. Rev. A **35**, 2111 (1987); **37**, 4380 (1988).
[14] R. Kobilarov, M. V. Popović, and N. Konjević, Phys. Rev. A **37**, 1021 (1988).
[15] N. Konjević and N. I. Uzelac, J. Quant. Spectrosc. Radiat. Transf. **44**, 61 (1990); N. I. Uzelac and N. Konjević, J. Phys. B **22**, 2517 (1989).
[16] D. Bertuccelli, G. Bertuccelli, and H. O. Di Rocco, Rev. Sci. Instrum. **62**, 966 (1991).
[17] D. Hong and C. Fleurier, *Spectral Line Shapes*, edited by R. Stamm and B. Talin (Nova Science, Commack, NY, 1993), Vol. 7, pp. 123–124.
[18] I. S. Fishman, E. V. Sarandaev, and M. Kh. Salakhov, J. Quant. Spectrosc. Radiat. Transf. **52**, 887 (1994).
[19] A. Lesage, S. Sahal-Bréchot, and M. H. Miller, Phys. Rev. A **16**, 1617 (1977).
[20] A. Lesage, J. L. Lebrun, and J. Richou, Astrophys. J. **360**, 737 (1990).
[21] F. Wollschläger, J. Mitsching, D. Meiners, M. Depiesse, J. Richou, and A. Lesage, J. Quant. Spectrosc. Radiat. Transf. **58**, 135 (1997).
[22] Lj. M. Ćirković, B. T. Vujićić, and S. M. Glisić, J. Phys. D **15**, 229 (1982).
[23] C. Colon, G. Hatem, E. Verdugo, P. Ruiz, and J. Campos, J. Appl. Phys. **73**, 4752 (1993).
[24] A. M. de Frutos, L. Sabatier, A. Poueyo, R. Fabbro, D. Bermejo, and J. M. Orza, Proc. SPIE **1397**, 717 (1991).
[25] L. Y. Chan, A. N. Mostovych, and K. J. Kearney, J. Quant. Spectrosc. Radiat. Transf. **55**, 815 (1996); A. N. Mostovych, L. Y. Chan, K. J. Kearney, D. Garren, C. A. Iglesias, M. Klapisch, and F. J. Rogers, Phys. Rev. Lett. **75**, 150 (1995).

Appendix B: Advanced Procedures for the Deconvolution of Line Profiles

In most Stark broadening experiments that deal with symmetric line profiles, a standard line shape deconvolution technique is used which is, for example, well described by Davies and Vaughan.[1] These authors supply convenient correction tables for the width of the Lorentzian components and their work is therefore widely cited.

However, most lines of neutral atoms are slightly asymmetric since their Stark profiles usually contain a small asymmetric ion broadening component (which becomes negligible for ion lines). Thus, the above cited standard method to deconvolute Voigt profiles developed by Davies and Vaughan[1] is not strictly applicable, and two methods, generalized to include the deconvolution of asymmetric profiles, were developed. An approximate graphical deconvolution procedure for asymmetrical line profiles was described by Mijatović *et al.*[2] Then, in order to determine simultaneously the electron impact width, shift and ion broadening parameter, a fitting method was developed by Nikolić *et al.*[3] for the asymmetric Stark profiles of isolated and overlapping neutral atom lines. This paper follows to a certain extent the earlier work by Goly and Weniger[4] who determined widths, shifts, and ion broadening parameters for several C I and N I lines (for the latter, widths only) by a convolution procedure (Doppler and best fit Stark profile).

Generally speaking, this fitting method involves the computation of convolution integrals of Gaussian and of asymmetric Stark broadening profiles for a wide range of ion broadening and Debye shielding parameters. These have been tabulated, and the Stark widths may be derived from the known parameters. Applications were performed by Nikolić *et al.*[3] and by Schinköth *et al.*[5]

An iterative nonlinear deconvolution method was developed by Biraud and others.[6,7] The method utilizes the Fourier transform of the spectral distribution functions involved and its description is quite complex.[8] An application for the deconvolution of Si II lines was performed by Wollschläger *et al.*[9]

References for Appendix B

[1] J. T. Davies and J. M. Vaughan, Astrophys. J. **137**, 1302 (1963).
[2] Z. Mijatović, R. Kobilarov, B. T. Vujicić, D. Nikolić, and N. Konjević, J. Quant. Spectrosc. Radiat. Transf. **50**, 329 (1993).
[3] D. Nikolić, Z. Mijatović, R. Kobilarov, S. Djurović, and N. Konjević, *Spectral Line Shapes*, **10**, AIP Conf. Proc. 467, edited by R. M. Herman (AIP, Woodbury, NY, 1999), Vol. 10, pp. 191–192; 193–194; J. Quant. Spectrosc. Radiat. Transf. **70**, 67 (2001).
[4] A. Goly and S. Weniger, J. Quant. Spectrosc. Radiat. Transfer **36**, 147 (1986).
[5] D. Schinköth, M. Kock, and E. Schulz-Gulde, J. Quant. Spectrosc. Radiat. Transf. **64**, 635 (2000).
[6] Y. Biraud, Astron. Astrophys. **1**, 124 (1969).
[7] M. Depiesse, Y. Biraud, A. Lesage, and J. Richou, J. Quant. Spectrosc. Radiat. Transf. **54**, 539 (1995).
[8] P. A. Jansson, *Deconvolution of Images and Spectra*, 2nd ed. (Academic, San Diego, 1997).
[9] F. Wollschläger, J. Mitsching, D. Meiners, M. Depiesse, J. Richou, and A. Lesage, J. Quant. Spectrosc. Radiat. Transf. **58**, 135 (1997).

8. Tables of Stark Widths and Shifts

Aluminum

Al II

Ground state: $1s^2 2s^2 2p^6 3s^2\ ^1S_0$
Ionization energy: 18.829 eV = 151 862.7 cm^{-1}

Colon *et al.*[1] observed Al II line shapes side on in the plume of a laser produced plasma, obtained by ablation of aluminum in a nitrogen atmosphere. The plasma parameters were carefully chosen in order to achieve good experimental conditions for the homogeneity and the stability of the plasma. Self-absorption was found to be quite weak, even for the strong transition at 2816.18 Å. An Abel inversion procedure was used to determine the radial temperature distribution in the Al II emission volume. The line profiles were corrected for instrumental and Doppler broadening. The calculated, and experimentally confirmed, Stark width for the Al II 4663 Å transition was used to determine the electron density.

Reference

[1] C. Colon, G. Hatem, E. Verdugo, P. Ruis, and J. Campos, J. Appl. Phys. **73**, 4752 (1993).

Key data on experiments

Reference	Plasma source	Method of measurement: Electron density	Method of measurement: Temperature	Remarks
1	Laser-produced plasma	Known Stark width of Al II line	Boltzmann plot of Al II spectral lines	

Numerical results for Al II

No.	Transition array	Multiplet	Wavelength (Å)	Temperature (K)	Electron density (10^{17} cm^{-3})	w_m (Å)	w_m/w_{th}	d_m (Å)	d_m/d_{th}	Acc.	Reference
1	$3s-3p$	$^1S-^3P°$	2669.17	10 500	0.1	0.0062				C	1
2	$3s-3p$	$^1P°-^1D$	3900.68	10 500	0.1	0.010				C	1
3	$3p-3d$	$^1P°-^1D$	1990.53	10 500	0.1	0.044				C^+	1
4	$3p-4s$	$^1P°-^1S$	2816.18	10 500	0.1	0.0424				C^+	1
5	$3p^2-3s4f$	$^1D-^1F°$	2631.55	10 500	0.1	0.064				C	1
6	$4p-4d$	$^1P°-^1D$	5593.23	10 500	0.1	0.38				B	1

Aluminum

Al III

Ground state: $1s^2 2s^2 2p^6 3s\ ^2S_{1/2}$
Ionization energy: 28.45 eV = 229 445.71 cm^{-1}

Chan *et al.*[1] observed the widths of two Al III multiplets in a laser-produced plasma. Two laser beams at 1.054 μm are used to generate a plasma plume produced by vaporization of a thin Al film deposited on a glass slide. A laser probe at 0.527 μm measures simultaneously the electron density via polarization wave front interferometry and the plasma absorption. The electron temperature is obtained from absolute emission measurements combined with the optical absorption measurements. At the high densities ($N_e = 23-168 \times 10^{17}$ cm^{-3}) of this experiment, Stark broadening is the dominant broadening mechanism. Doppler and instrumental broadening are very small compared to the measured widths, and therefore the line profiles are not corrected. At the range of electron densities utilized, the authors observed the line profiles of the doublets either as resolved lines or as a single merged doublet ''line.'' Only the multiplet wavelengths are listed in the table, and it is assumed by the authors that the widths of all multiplet components are identical. Curve fits using Lorentzian functions were used to obtain the widths of the individual components.

The Al III Stark widths are in very good agreement with the semi classical calculations by Dimitrijević *et al.*[2] For the high electron densities and moderate temperatures of this experiment, strongly coupled plasma conditions were almost reached, but no significant deviations from the theoretical line widths were found.

References

[1] L. Y. Chan, A. N. Mostovych, and K. J. Kearney, J. Quant. Spectrosc. Radiat. Transf. **55**, 815 (1996).
[2] M. S. Dimitrijević, Z. Djurić, and A. A. Mihajlov, J. Phys. D **27**, 247 (1994).

Key data on experiments

Reference	Plasma source	Method of measurement: Electron density	Method of measurement: Temperature	Remarks
1	Laser produced and heated plasma	Polarization wave front interferometer at 527 nm	Absorption at 527 nm combined with absolute emission measurements	

Numerical results for Al III

No.	Transition array	Multiplet	Wavelength (Å)	Temperature (K)	Electron density (10^{17} cm^{-3})	w_m (Å)	w_m/w_{th}	d_m (Å)	d_m/d_{th}	Acc.	Reference
1	$3d-4p$	^{2}D–^{2}P°	3605.22	50 000	64	8.5	0.55			B$^+$	1
				50 000	97	25	1.00			B$^+$	1
				50 000	104	26.5	1.00			B$^+$	1
				50 000	119	29	0.97			A	1
				50 000	133	32	0.96			A	1
				50 000	167	34	0.84			A	1
2	$4s-4p$	^{2}S–^{2}P°	5705.30	50 000	23.5	18.5	0.89			B	1
				50 000	89	65	0.90			B$^+$	1
				50 000	97	67	0.85			B$^+$	1
				50 000	112	93	1.02			A	1
				50 000	121	81	0.82			A	1

Argon

Ar I

Ground state: $1s^2 2s^2 2p^6 3s^2 3p^6\ ^1S_0$

Ionization energy: 15.7596 eV = 127 109.70 cm^{-1}

Finding list

Wavelength (Å)	No.	Wavelength (Å)	No.	Wavelength (Å)	No.	Wavelength (Å)	No.
1048.22	2	4300.10	11	7030.25	28	7723.76	4
1066.66	1	4333.56	17	7067.22	6	7724.21	9
4044.42	13	4510.73	16	7068.74	28	7948.18	8
4158.59	12	6296.87	26	7107.48	28	8006.16	4
4164.18	12	6307.66	25	7125.82	29	8014.79	3
4181.88	15	6416.31	27	7147.04	6	8103.69	4
4190.71	11	6538.11	22	7206.98	29	8115.31	3
4191.03	14	6604.85	22	7272.94	7	8264.52	9
4200.67	11	6752.83	20	7372.12	21	8408.21	8
4251.18	10	6871.29	19	7383.98	6	8424.65	3
4259.36	18	6888.17	23	7503.87	9	8521.44	8
4266.29	12	6937.66	19	7514.65	5	8761.69	24
4272.17	12	6965.43	7	7635.11	4		

A fairly large number of Stark broadening studies were carried out for this spectrum,[1–11] the majority with steady-state, wall-stabilized arcs.[2–5,8,10,11]

In three arc experiments[3,8,11] and in another experiment with a plasma jet,[1] the plasmas were observed side on, and the Abel inversion process was applied to obtain the Stark parameters for specific local plasma conditions.

It was recognized in all experiments that Doppler and instrumental broadening contribute significantly to the linewidths, and standard deconvolution techniques were usually applied to the observed profiles to eliminate these contributions. However, Schinköth *et al.*[12] fitted generalized asymmetric line profile functions to the experimental profiles, according to the method given by Goly and Weniger.[13] Tests for possible self-absorption are mentioned in some papers, but in Refs. 5 and 10, optically thick conditions are deliberately generated to determine the Stark widths of the vacuum ultraviolet (VUV) resonance and some infrared lines with an equation-of-radiative-transfer model, utilizing best fits to the observed line shapes, especially for the far wings. In other papers, tests for optical thickness are not reported, but we estimate that such effects should be quite small, and not exceed a few percent.

In all experiments in which the observations were carried out end on, some uncertainties are introduced due to inhomogeneous end layers. These are estimated to be normally not larger than a few percent, but may be more for the pulsed arc configuration in Refs. 6 and 7, since the arc channel is expanded at its ends into wide open spaces.

The Stark shifts reported by Djurović *et al.*[8] were measured at the positions of the halfwidths. The theoretical comparison data are taken for the same conditions. We did not utilize the results of Badie *et al.*[3] for the 703 nm line, since they are not reported numerically but given in graphical representations that are not specifically correlated to both the plasma temperature and the electron density.

Schinköth *et al.*[12] observed 15 near infrared Ar I line shapes with a wall-stabilized arc end on and used a carbon arc for absolute calibration. Their values are in reasonable agreement with those of Jones *et al.*[13] and of Sohns and Kock,[5] but differ appreciably from those of Bakshi and Kearney.[1] Two of the three Stark width values in common with those of Musielok's[4] are close to the results of Schinköth *et al.*

References

[1] V. Bakshi and R. J. Kearney, J. Quant. Spectrosc. Radiat. Transf. **42**, 405 (1989).
[2] T. S. Basha and Z. A. Abdel-Aal, Acta Phys. Pol. A **75**, 565 (1989).
[3] J. M. Badie, E. Billou, and G. Vallbona, Rev. Phys. Appl. **25**, 527(1990).
[4] J. Musielok, Acta Phys. Pol. A **86**, 315 (1994).
[5] E. Sohns and M. Kock, J. Quant. Spectrosc. Radiat. Transf. **47**, 325 (1992).
[6] S. Djenize, Lj. Skuljan, and R. Konjević, J. Quant. Spectrosc. Radiat. Transf. **54**, 581 (1995).
[7] Lj. Skuljan, V. Milosavljević, A. Srećković, and S. Djenize, Bull. Astron. Belgrade **151**, 17 (1995).
[8] S. Djurović, Z. Mijatović, R. Kobilarov, and N. Konjević, J. Quant. Spectrosc. Radiat. Transf. **57**, 695 (1997).
[9] J. A. Aparicio, C. Perez, J. A. del Val, M. A. Gigosos, M. I. de la Rosa, and S. Mar, J. Phys. B **31**, 4909 (1998).
[10] J. P. Knauer and M. Kock, J. Quant. Spectrosc. Radiat. Transf. **56**, 563 (1996).
[11] D. Nikolić, S. Djurović, Z. Mijatović, R. Kobilarov, and N. Konjević, *Spectral Line Shapes*, AIP Proc. No. 467, edited by R. M. Herman (AIP, Woodbury, NY, 1999), Vol. 10, pp. 191–192; S. Djurović (private communication).
[12] D. Schinköth, M. Kock, and E. Schulz-Gulde, J. Quant. Spectrosc. Radiat. Transf. **64**, 635 (2000).
[13] D. W. Jones, K. Musiol, and W. L. Wiese, *Spectral Line Shapes*, edited by B. Wende (Gruyter, New York, 1983), Vol. 2, pp. 125–136.

Key data on experiments

Reference	Plasma source	Method of measurement		Remarks
		Electron density	Temperature	
1	Plasma jet	H_β Stark width	Plasma composition and Boltzmann plot of Ar I lines	
2	Wall-stabilized arc	Interferometry	Plasma composition	No details on electron density diagnostics
3	Wall-stabilized arc	H_β Stark width	Absolute intensities of three Ar I lines	
4	Wall-stabilized arc	H_β Stark width	Absolute line intensities of Ar I, Ar II, N I, and N II lines above 12 000 K and Boltzmann plot of Ar II lines	For a few lines, photographic recording is used
5, 10	Wall-stabilized arc	Radiative transfer model	Absolute intensity of Ar II optically thin 4806.2 Å line and argon continuum at 4450 Å	Line profiles measured under optically thick conditions
6, 7	Low-pressure pulsed arc	Laser interferometer at 6328 Å	Relative line intensities of Ar I and Ar II lines	Shot-to-shot scanning
8, 11	Wall-stabilized arc	H_β Stark width	Plasma composition	The experimental set up and operating conditions in Ref. 11 are very similar to those in Ref. 8; therefore, similar uncertainties are to be expected (no error estimates are provided in the extended abstract of a conference proceeding in Ref. 11)
9	Low-pressure pulsed arc	Laser interferometer at 6328 Å	Boltzmann plot of Ar II line intensities and ratio Ar I to Ar II line intensities	Multichannel detector used
10	Wall-stabilized arc	Radiative transfer model	Absolute intensity measurements of Ar I optically thick 8104 and 8115 Å lines and optically thin 4300 Å line	Line profiles measured under optically thick conditions
12	Wall-stabilized arc	Absolute intensity of continuum radiation at 4450 Å	Absolute intensity of an optically thin line	

Numerical results for Ar I

No.	Transition array	Multiplet	Wavelength (Å)	Temperature (K)	Electron density (10^{17} cm^{-3})	w_m (Å)	w_m/w_{th}	d_m (Å)	d_m/d_{th}	Acc.	Reference
1	$3p^6-4s$	^{1}S–^{2}[3/2]°	1066.66	12 500	1.0	0.014	1.17			B	5
				13 000	1.0	0.011	0.89			B	10
2	$3p^6-4s'$	^{1}S–^{2}[1/2]°	1048.22	12 500	1.0	0.013	1.16			B	5
				13 000	1.0	0.012	1.05			B	10
3	$4s-4p$	^{2}[3/2]°–^{2}[5/2]	8115.31	12 500	1.0	0.904	0.77	0.19	0.52	B,C	5
			8014.79	10 000	0.1	0.082				B^+	12
				12 500	1.0	0.834		0.21		B,C	5
			8424.65	10 000	0.1	0.079	0.94			A	12
				12 500	1.0	0.895	0.93	0.25	1.75	B,C	5
4		^{2}[3/2]°–^{2}[3/2]	8103.69	10 000	0.1	0.083	0.75			B^+	12
				12 500	1.0	0.802		0.17		B,C	5
			8006.16	10 000	0.1	0.087				B^+	12
				12 600	1.0	0.783		0.25		B,C	5
			7723.76	10 000	0.1	0.068				B^+	12
				12 500	1.0	0.706		0.18		B,C	5
			7635.11	10 000	0.1	0.074				B^+	12
				12 500	1.0	0.800		0.20		B,C	5
				13 000	0.33			0.21		B	6
5		^{2}[3/2]°–^{2}[1/2]	7514.65	10 000	0.1	0.074				B^+	12
				12 500	1.0	0.856		0.17		B,C	5
6	$4s-4p'$	^{2}[3/2]°–^{2}[3/2]	7383.98	10 000	0.1	0.071				A	12
				12 500	1.0	0.748		0.11		B,C	5
				13 000	0.33			0.12		B	6
				13 500–26 500	1.0	1.03		0.42		B^+,A	9
			7147.04	11 900	0.60	0.38				B	1
				13 200	1.2	0.70				B^+	4
				13 500–26 500	1.0	1.09		0.33		B^+,B^+	9
			7067.22	10 000	0.1	0.066				A	12
				13 000	0.33			0.09		B	6
				18000	0.66			0.16		B	6
				13 500–26 500	1.0	1.06		0.45		A,A	9
7		^{2}[3/2]°–^{2}[1/2]	7272.94	13 500–26 500	1.0	0.96		0.38		B^+,A	9
			6965.43	11 900	0.60	0.40				B	1
				13 000	0.33			0.10		B	6
				17000	0.55			0.18		B	6
				13 500–26 500	1.0	0.97		0.26		A,A	9
8	$4s'-4p'$	^{2}[1/2]°–^{2}[3/2]	8408.21	10 000	0.1	0.082	0.74			A	12
				12 500	1.0	1.047	0.82	0.19	0.52	B,C	5
			8521.44	10 000	0.1	0.102				B^+	12
				11 300	0.42	0.31				B	4
			7948.18	10 000	0.1	0.086	0.89			B^+	12
				11 900	0.60	0.58	0.90			B^+	1
				12 500	1.0	0.867	0.79	0.22	0.60	B,C	5
9		^{2}[1/2]°–^{2}[1/2]	8264.52	10 000	0.1	0.092				B^+	12
				11 300	0.42	0.38				B	4
				11 900	0.60	0.55				B^+	1
				12 500	1.0	0.998		0.24		B,C	5
			7724.21	10 000	0.1	0.082				B^+	12
				12 500	1.0	0.945		0.21		B,C	5
			7503.87	10 000	0.1	0.085				B^+	12
				11 900	0.60	0.70				B^+	1
				12 500	1.0	1.057		0.22		B,C	5
10	$4s-5p$	^{2}[3/2]°–^{2}[1/2]	4251.18	10 800	0.31	0.42				B^+	4
11		^{2}[3/2]°–^{2}[5/2]	4300.10	10 200	0.220	0.48				B^+	2
				10 430	0.315	0.62				B^+	2
				11 000	0.396	0.79				B^+	2
				12 080	0.690	1.33				B^+	2
				12 380	0.850	1.65				B^+	2
				12 980	1.080	2.09				B^+	2
				14 200	1.44	2.80				B^+	2
				10 800	0.31	0.62				B^+	4

Numerical results for Ar I—Continued

No.	Transition array	Multiplet	Wavelength (Å)	Temperature (K)	Electron density (10^{17} cm^{-3})	w_m (Å)	w_m/w_{th}	d_m (Å)	d_m/d_{th}	Acc.	Reference
				11 500	0.51	1.05				B^+	4
				12 600	0.99	1.80				B^+	4
				13 400	0.45	0.90				B^+	4
			4200.67	13 400	0.45	0.94	0.87			B^+	4
			4190.71	9 300	0.074	0.094	0.57	0.068	0.97	B,B	11
				9 400	0.083	0.111	0.63	0.977	0.96	B,B	11
				9 500	0.098	0.127	0.61	0.084	0.90	B,B	11
				9 700	0.120	0.157	0.61	0.104	0.91	B,B^+	11
				9 900	0.140	0.177	0.59	0.116	0.88	B,B^+	11
				10 050	0.160	0.210	0.61	0.138	0.92	B,B^+	11
				10 250	0.190	0.233	0.56	0.147	0.83	B^+,B^+	11
				10 400	0.215	0.266	0.56	0.173	0.87	B^+,B^+	11
				10 550	0.246	0.290	0.53	0.188	0.83	B^+,B^+	11
				10 700	0.270	0.305	0.51	0.198	0.80	B^+,B^+	11
				10 750	0.282	0.315	0.50	0.204	0.80	B^+,B^+	11
				10 800	0.290	0.320	0.50	0.207	0.79	B^+,B^+	11
12		$^2[3/2]°-{}^2[3/2]$	4272.17	9 800	0.14	0.28	0.96			B^+	4
				10 800	0.31	0.50	0.74			B^+	4
				11 500	0.51	1.00	0.88			B^+	4
				12 600	0.99	1.80	0.78			B^+	4
				13 400	0.45	0.91	0.86			B^+	4
				16 000	0.22			0.12	0.55	B	6
			4266.29	9 800	0.14	0.33				B^+	4
				10 800	0.31	0.60				B^+	4
				11 500	0.51	1.05				B^+	4
				12 600	0.99	2.40				B^+	4
			4164.18	9 800	0.14	0.30				B^+	4
				11 500	0.51	0.96				B^+	4
			4158.59	10 800	0.31	0.60				B^+	4
				11 500	0.51	1.05				B^+	4
				12 600	0.99	2.00				B^+	4
				13 400	0.45	1.07				B^+	4
				13 500–26 500	1.0	2.46		0.71		B^+,B^+	9
13	$4s-5p'$	$^2[3/2]°-{}^2[3/2]$	4044.42	9 800	0.14	0.30				B^+	4
				11 500	0.51	1.08				B^+	4
				13 400	0.45	0.95				B^+	4
14	$4s'-5p'$	$^2[1/2]°-{}^2[3/2]$	4191.03	9 300	0.074	0.105		0.070		B,B	11
				9 400	0.083	0.125		0.087		B,B	11
				9 500	0.098	0.138		0.094		B,B^+	11
				9 700	0.120	0.168		0.119		B,B^+	11
				9 900	0.140	0.206		0.135		B^+,B^+	11
				10 050	0.160	0.233		0.159		B^+,B^+	11
				10 250	0.190	0.261		0.172		B^+,B^+	11
				10 400	0.215	0.285		0.197		B^+,B^+	11
				10 550	0.246	0.325		0.217		B^+,B^+	11
				10 700	0.270	0.343		0.229		B^+,B^+	11
				10 750	0.282	0.354		0.236		B^+,B^+	11
				10 800	0.290	0.360		0.240		B^+,B^+	11
				10 800	0.31	0.71				B^+	4
				11 500	0.51	1.03				B^+	4
				12 600	0.99	1.90				B^+	4
				13 400	0.45	1.17				B^+	4
15		$^2[1/2]°-{}^2[1/2]$	4181.88	9 800	0.14	0.35				B^+	4
				11 500	0.51	1.18				B^+	4
				12 600	0.99	2.45				B^+	4
				13 400	0.45	1.19				B^+	4
16	$4s'-5p'$	$^2[1/2]°-{}^2[1/2]$	4510.73	10 800	0.31	0.73	0.60			B^+	4
				13 400	0.45	1.18	0.63			B^+	4
17	$4s'-5p'$	$^2[1/2]°-{}^2[3/2]$	4333.56	13 400	0.45	1.10				B^+	4
18		$^2[1/2]°-{}^2[1/2]$	4259.36	9 800	0.14	0.31	0.79			B^+	4
				10 800	0.31	0.70	0.77			B^+	4
				11 500	0.51	1.14	0.75			B^+	4
				12 600	0.99	2.00	0.65			B^+	4

Numerical results for Ar I—Continued

No.	Transition array	Multiplet	Wavelength (Å)	Temperature (K)	Electron density (10^{17} cm^{-3})	w_m (Å)	w_m/w_{th}	d_m (Å)	d_m/d_{th}	Acc.	Reference
				13 400	0.45	1.08	0.77			B^+	4
				8 900	0.047	0.10	0.81	0.06	0.85	B,B	8
				9 130	0.060	0.12	0.73	0.07	0.77	B,B	8
				9 260	0.070	0.14	0.70	0.08	0.75	B,B	8
				9 470	0.090	0.19	0.75	0.09	0.71	B,B^+	8
				9 680	0.105	0.24	0.80	0.12	0.77	B,B^+	8
				9 930	0.140	0.30	0.75	0.16	0.79	B^+,B^+	8
				10 120	0.170	0.35	0.73	0.19	0.75	B^+,B^+	8
				10 310	0.200	0.42	0.74	0.23	0.79	B^+,B^+	8
				10 540	0.230	0.49	0.71	0.25	0.73	B^+,A	8
				10 690	0.270	0.57	0.72	0.30	0.77	A,A	8
				10 890	0.310	0.62	0.68	0.34	0.75	A,A	8
				10 980	0.330	0.66	0.69	0.36	0.76	A,A	8
				11 040	0.340	0.70	0.70	0.37	0.75	A,A	8
				11 070	0.350	0.71	0.70	0.38	0.75	A,A	8
				13 000	0.38	0.97	0.83			B	7
				14 000	0.26			0.23	0.60	B	6
				15 000	0.14	0.31	0.70			B	7
				16 200	0.26	0.68	0.81			B	7
19	$4p-4d$	$^2[1/2]-^2[1/2]°$	6937.66	13 500–26 500	1.0	9.83				B^+	9
			6871.29	13 500–26 500	1.0	9.07		1.93		A,B^+	9
20		$^2[1/2]-^2[3/2]°$	6752.83	13 500–26 500	1.0	6.82	0.78–0.67	2.26	0.77–0.84	B^+,A	9
21		$^2[5/2]-^2[7/2]°$	7372.12	13 500–26 500	1.0	18.77	1.60–1.38	5.28	1.36–1.49	B,B	9
22	$4p-4d'$	$^2[5/2]-^2[5/2]°$	6538.11	10 750	0.29	3.00				B	4
			6604.85	10 750	0.29	3.00				B	4
23		$^2[3/2]-^2[3/2]°$	6888.17	13 500–26 500	1.0	17.68				B	9
24	$4p'-4d'$	$^2[1/2]-^2[3/2]°$	8761.69	11 300	0.42	6.00	1.01			B^+	4
				12 500	0.85	11.80	0.94			B^+	4
25	$4p-5d$	$^2[3/2]-^2[3/2]°$	6307.66	10 750	0.29	5.10				B^+	4
26	$4p'-5d'$	$^2[1/2]-^2[3/2]°$	6296.87	10 750	0.29	7.30	1.10			B	4
27	$4p-6s$	$^2[1/2]-^2[3/2]°$	6416.31	13 500–26 500	1.0	12.20		5.61		A,A	9
28		$^2[5/2]-^2[3/2]°$	7030.25	11 900	0.60	6.6	0.77			B^+	1
				13 500–26 500	1.0	15.78	1.06–0.90	6.09	0.85–0.88	A,A	9
			7107.48	10 750	0.29	3.20				B^+	4
			7068.74	13 500–26 500	1.0	16.63		2.30		A,B^+	9
29	$4p'-6s'$	$^2[3/2]-^2[1/2]°$	7125.82	10 750	0.29	3.80				B^+	4
			7206.98	11 900	0.60	7.0[b]	0.77			B^+	1
				10 750	0.29	4.00	0.95			B^+	4
				11 300	0.42	6.60	1.06			B^+	4
				12 500	0.85	14.70	1.12			B^+	4
				13 500–26 500	1.0	13.39	0.84–0.72	7.14	0.94–0.98	B^+,A	9

Argon

Ar II

Ground state: $1s^2 2s^2 2p^6 3s^2 3p^5\ ^2P^\circ_{3/2}$
Ionization energy: 27.630 eV = 222 848.2 cm^{-1}

Finding list

Wavelength (Å)	No.	Wavelength (Å)	No.	Wavelength (Å)	No.	Wavelength (Å)	No.
2544.68	46	3780.84	33	4228.16	19	4806.02	17
2844.13	26	3786.38	3	4229.87	69	4847.81	17
2847.82	26	3796.59	55	4237.22	29	4865.91	63
2891.61	27	3799.38	33	4255.60	60	4867.56	75
2942.89	27	3803.17	55	4266.53	18	4879.86	22
2955.39	37	3808.57	3	4275.16	62	4889.04	23
2979.05	27	3809.46	57	4277.53	29	4904.75	10
3000.44	37	3819.02	54	4282.90	18	4914.31	48
3014.48	37	3825.67	54	4297.96	79	4933.21	17
3033.51	27	3826.81	33	4300.65	11	4942.92	76
3093.40	42	3841.52	33	4309.24	86	4949.40	75
3139.02	32	3844.73	33	4331.20	18	4955.11	85
3169.67	32	3850.58	20	4348.06	18	4965.08	22
3181.04	32	3868.53	44	4352.20	1	4972.16	17
3212.52	32	3872.14	33	4362.07	13	5009.33	17
3236.81	41	3875.26	2	4371.33	1	5017.16	12
3243.69	32	3880.33	33	4375.95	25	5062.04	17
3249.80	32	3900.63	33	4379.67	18	5141.78	12
3273.32	39	3911.58	33	4383.75	24	5145.31	21
3281.71	32	3914.77	2	4385.06	67	5165.77	76
3293.64	41	3925.72	65	4400.10	1	5176.23	12
3307.23	41	3928.62	20	4400.99	1	5216.81	47
3350.92	51	3931.24	2	4420.91	1	5305.69	77
3376.44	51	3932.55	44	4426.00	18	5812.76	49
3388.53	45	3944.27	2	4430.19	18	5985.91	91
3464.13	38	3946.10	65	4431.00	1	6103.54	7
3476.75	31	3952.73	43	4433.84	83	6114.92	70
3509.78	31	3958.38	36	4445.85	84	6123.36	70
3514.39	31	3968.36	2	4460.56	1	6138.66	4
3535.32	31	3979.36	44	4474.76	15	6172.29	70
3559.51	38	3988.16	36	4481.81	13	6187.14	88
3561.03	50	3992.05	2	4490.98	13	6243.12	4
3565.03	35	4011.21	59	4498.54	90	6375.94	74
3576.62	34	4013.86	2	4530.55	16	6399.21	4
3581.61	34	4033.81	58	4535.49	64	6437.60	6
3582.35	34	4035.46	30	4545.05	23	6483.08	7
3588.44	34	4038.80	2	4563.74	80	6614.35	73
3622.14	57	4042.89	30	4579.35	25	6620.97	89
3637.03	87	4079.57	30	4589.90	28	6643.70	9
3639.83	53	4082.39	19	4598.76	15	6666.36	6
3655.28	40	4099.46	71	4609.57	28	6684.29	9
3660.44	52	4112.82	19	4611.24	79	6696.29	92
3718.21	56	4156.08	58	4637.23	28	6756.55	9
3720.43	57	4168.97	82	4657.90	23	6808.53	5
3724.52	56	4178.36	18	4682.28	10	6818.38	72
3729.31	20	4179.30	58	4703.36	81	6861.27	6
3737.89	56	4189.65	68	4710.82	10	6863.54	9
3763.50	33	4203.41	78	4726.87	22	6886.61	9
3765.27	57	4217.43	66	4735.90	17	7054.99	73
3766.12	14	4218.66	61	4764.86	23	7233.54	8
3770.52	57	4222.64	62	4792.09	75	7380.43	8

Four experiments were performed for numerous lines of this spectrum, two with steady-state plasma sources and two with pulsed sources. In all four cases, the optical depth for the investigated lines was checked either by comparing measured line intensity ratios within multiplets with known data,[1] or by using a mirror[2,4] arranged behind the plasma column, which by focusing the plasma onto itself essentially doubled the optical path length, or by analyzing the observed line shapes.[3]

Standard deconvolution procedures were used by all groups[1–4] to take into account and correct for the known contributions of instrumental and Doppler broadening to the measured Voigt-type profiles. The plasmas were observed end-on by three groups of authors,[1,2,4] and thus the effects of inhomogeneous end layers may be significant. This is especially so in the experiment of Djenize *et al.*[1] where large open spaces exist at the ends of the plasma channel and to a lesser degree in the work of Aparicio *et al.*[4] and of Dzierzega and Musiol.[2] The latter authors note that they reduced their plasma-end effects by using split electrodes, while the others did not discuss this problem. In the experiment by Pellerin *et al.*,[3] the observed plasma volume—viewed side on—is highly inhomogeneous, but it has a symmetric distribution around the arc axis, and thus local values of plasma temperature and electron density could be obtained by an Abel inversion process.

Djenize *et al.* employed a shot-to-shot scanning technique with their low-pressure pulsed arc, while Aparicio *et al.* recorded their line profiles in single shots with an optical multichannel analyzer, and Dzierzega and Musiol obtained the Stark profiles with a photodiode array detector.

Aparicio *et al.*[3] have presented their Stark width and shift data at a normalized electron density, but they have averaged them over the temperature range of their experiment, rather than listing them for specific temperature values. Their results are therefore not unambiguous. This is strongly reflected in some of the listed experiment/theory ratios, which show great variations. This occurs for certain transitions where the calculated shifts change sign in this temperature range and thus become extremely small in this process. We therefore strongly recommend that the presentation of averaged results should be avoided.

It should be noted that some Stark width results exhibit surprisingly large variations within multiplets, such as those in multiplet $3d\,^4\mathrm{D}-4p\,^4\mathrm{D}^\circ$ determined by Pellerin *et al.*[3] and Aparicio *et al.*[4]

References

[1] S. Djenize, M. Malesević, A. Srećković, M. Milosavljević, and J. Purić, J. Quant. Spectrosc. Radiat. Transf. **42**, 429 (1989).
[2] K. Dzierzega and K. Musiol, J. Quant. Spectrosc. Radiat. Transf. **52**, 747 (1994).
[3] S. Pellerin, K. Musiol, and J. Chapelle, J. Quant. Spectrosc. Radiat. Transf. **57**, 377 (1997).
[4] J. A. Aparicio, M. A. Gigosos, V. R. Gonzales, C. Perez, M. I. de la Rosa, and S. Mar, J. Phys. B **31**, 1029 (1998).

Key data on experiments

Reference	Plasma source	Method of measurement: Electron density	Method of measurement: Temperature	Remarks
1	Low-pressure pulsed arc	Laser interferometer at 6328 Å	Boltzmann plot of Ar II lines and ratio of Ar III to Ar II lines	
2	Wall-stabilized arc	H_β Stark width and continuum intensity	Boltzmann plot of Ar II lines	
3	Modified wall-stabilized arc	Plasma composition data and Stark width of the Ar I 6965.43 Å line	Larenz–Fowler–Milne method, Olsen–Richter graph and relative intensities of two Ar II lines	
4	Low-pressure pulsed arc	Laser interferometer at 6328 Å	Boltzmann plot of Ar II lines	

Numerical results for Ar II

No.	Transition array	Multiplet	Wavelength (Å)	Temperature (K)	Electron density (10^{17} cm^{-3})	w_m (Å)	w_m/w_{th}	d_m (Å)	d_m/d_{th}	Acc.	Reference
1	$3p^4(^3P)3d-3p^4(^3P)4p$	$^4D-^4P°$	4400.99	22 000	1.00	0.343	1.33			B	3
			4371.33	22 000	1.00	0.324	1.28			B	3
			4431.00	22 000	1.00	0.286	1.10			B	3
				18 400–26 500	1.00	0.313	1.17–1.23	0.080	0.95–1.03	B,A	4
			4400.10	22 000	1.00	0.307	1.19			B	3
			4352.20	22 000	1.00	0.350	1.39			B	3
			4460.56	22 000	1.00	0.266	1.01			B	3
				18 400–26 500	1.00	0.368	1.36–1.43	0.051	0.60–0.65	B,B^+	4
			4420.91	22 000	1.00	0.244	0.94			B	3
				18 400–26 500	1.00	0.338	1.27–1.33			C^+	4
2		$^4D-^4D°$	4013.86	10 880	2.03	0.467	0.93	0.090	0.48	B^+,C^+	2
				11 520	1.79	0.353	0.81	0.073	0.46	B^+,C	2
				12 200	0.74	0.224	1.28		0.14	B^+	2
				13 030	1.10	0.256	1.01			B^+	2
				13 880	1.39	0.267	0.85	0.056	0.48	B^+,D	2
				22 000	1.00	0.252	1.23			B	3
				18 400–26 500	1.00	0.215	1.02–1.08	0.019	0.25–0.27	B^+,B	4
				26 000	1.76	0.340	0.96	0.116	0.92	B,C^+	1
			3968.36	22 000	1.00	0.236	1.17			B	3
				18 400–26 500	1.00	0.294	1.42–1.51			B^+	4
			3914.77	22 000	1.00	0.207	1.06			B	3
				18 400–26 500	1.00	0.209	0.99–1.04			B^+	4
			3944.27	22 000	1.00	0.220	1.11			B	3
				18 400–26 500	1.00	0.240	1.13–1.20	0.045	0.58–0.63	B^+,B	4
			3875.26	22 000	1.00	0.192	1.00			B	3
				18 400–26 500	1.00	0.275	1.40–1.48	0.021	0.29–0.32	B^+,B	4
			4038.80	22 000	1.00	0.241	1.16			B	3
				18 400–26 500	1.00	0.299	1.40–1.48			B	4
			3992.05	22 000	1.00	0.219	1.08			B	3
				18 400–26 500	1.00	0.324	1.55–1.64			B^+	4
			3931.24	22 000	1.00	0.191	0.97			B	3
3		$^4D-^2D°$	3786.38	22 000	1.00	0.203				B	3
				18 400–26 500	1.00	0.237		0.034		B^+,B	4
			3808.57	22 000	1.00	0.187				B	3
4		$^4F-^2D°$	6243.12	18 400–26 500	1.00	0.603		0.065		B^+,B^+	4
			6138.66	18 400–26 500	1.00	0.586		0.070		B^+,A	4
			6399.21	18 400–26 500	1.00	0.495				B^+	4
5		$^2P-^2D°$	6808.53	22 000	1.00	0.753				B	3
6		$^2P-^2P°$	6861.27	18 400–26 500	1.00	0.626		0.140		B^+,A	4
			6666.36	18 400–26 500	1.00	0.624		0.166		B^+,A	4
			6437.60	18 400–26 500	1.00	0.650		0.331		B^+,B^+	4
7		$^2P-^2S°$	6483.08	18 400–26 500	1.00	0.652		0.167		B^+,A	4
			6103.54	22 000	1.00	0.653				B	3
				18 400–26 500	1.00	0.613		0.117		B^+,A	4
8		$^4P-^4S°$	7380.43	18 400–26 500	1.00	0.767		0.215		B^+,A	4
			7233.54	22 000	1.00	0.619				C^+	3
9		$^4F-^4D°$	6756.55	18 400–26 500	1.00	0.628		0.096		B^+,B^+	4
			6863.54	18 400–26 500	1.00	0.554		0.048		A,B^+	4
			6684.29	18 400–26 500	1.00	0.616		0.057		B^+,B^+	4
			6886.61	18 400–26 500	1.00	0.695		0.058		A,B^+	4
			6643.70	18 400–26 500	1.00	0.718				B^+	4
10	$3p^4(^3P)3d-3p^4(^1D)4p$	$^2F-^2F°$	4904.75	22 000	1.00	0.369				B	3
				18 400–26 500	1.00	0.389				B^+	4
			4682.28	22 000	1.00	0.292				C^+	3
			4710.82	22 000	1.00	0.319				B	3
11		$^2F-^2D°$	4300.65	22 000	1.00	0.392				B	3
				18 400–26 500	1.00	0.464				B^+	4
12		$^2D-^2F°$	5141.78	18 400–26 500	1.00	0.332				B^+	4
			5017.16	18 400–26 500	1.00	0.437				B	4
			5176.23	18 400–26 500	1.00	0.448				B^+	4

Numerical results for Ar II—Continued

No.	Transition array	Multiplet	Wavelength (Å)	Temperature (K)	Electron density (10^{17}cm^{-3})	w_m (Å)	w_m/w_{th}	d_m (Å)	d_m/d_{th}	Acc.	Reference
13		^{2}D–^{2}D°	4481.81	10 880	2.03	0.780				B$^+$	2
				11 520	1.79	0.477		0.018		B$^+$,D	2
				13 030	1.10	0.330				A	2
				13 880	1.39	0.428				B$^+$	2
				22 000	1.00	0.373				B	3
			4362.07	18 400–26 500	1.00	0.333				B$^+$	4
			4490.98	18 400–26 500	1.00	0.382				B$^+$	4
				22 000	1.00	0.395				B	3
14		^{2}P–^{2}P°	3766.12	18 400–26 500	1.00	1.014		−0.268		B$^+$,B	4
15		^{2}D–^{2}P°	4474.76	18 400–26500	1.00	1.286		0.300		B$^+$,B$^+$	4
				22 000	1.00	1.097				B	3
			4598.76	18 400–26 500	1.00	0.838		0.229		B$^+$,A	4
16		^{2}F–^{2}P°	4530.55	18 400–26 500	1.00	0.768		0.144		B$^+$,B$^+$	4
17	$3p^4(^3\mathrm{P})4s$–$3p^4(^3\mathrm{P})4p$	^{4}P–^{4}P°	4806.02	10 880	2.03	0.484	0.58	−0.077	0.44	B$^+$,C	2
				11 520	1.79	0.440	0.62	−0.077	0.52	B$^+$,C	2
				12 200	0.74	0.157	0.54			A	2
				13 030	1.10	0.232	0.55	−0.046	0.66	A,D	2
				13 880	1.39	0.305	0.58	−0.056	0.66	B$^+$,D	2
				22 000	1.00	0.323	0.94			B	3
				17 000–26 700	1.00	0.288	0.81–0.85	−0.050	1.46–94.6	B$^+$,B$^+$	4
			4933.21	22 000	1.00	0.322	0.88			B	3
				18 100–24 400	1.00	0.325	0.87–0.90	−0.076	2.52–11.84	B$^+$,B$^+$	4
			4972.16	22 000	1.00	0.349	0.94			B	3
				16 500–23 200	1.00	0.295	0.77–0.80	−0.054	1.36–5.30	B$^+$,B	4
			4735.90	10 880	2.03	0.641	0.80	−0.122	0.71	B$^+$,C$^+$	2
				11 520	1.79	0.509	0.74	−0.098	0.69	B$^+$,C	2
				12 200	0.74	0.226	0.81	−0.049	0.88	A,D	2
				13 030	1.10	0.306	0.75	−0.049	0.73	A,D	2
				13 880	1.39	0.356	0.71	−0.049	0.65	B$^+$,D	2
			4847.81	10 880	2.03	0.545	0.65	−0.140	0.78	B$^+$,B	2
				11 520	1.79	0.461	0.64	−0.140	0.94	B$^+$,B	2
				12 200	0.74	0.222	0.76	−0.074	1.38	A,C	2
				13 030	1.1	0.303	0.71	−0.075	1.06	A,C	2
				13 880	1.39	0.366	0.70	−0.090	1.14	B$^+$,C$^+$	2
				22 000	1.00	0.338	0.96			B	3
				17 000–26 700	1.00	0.296	0.82–0.86	−0.064	1.83–119.0	B$^+$,A	4
			5009.33	22 000	1.00	0.345	0.92			B	3
				16 500–23 200	1.00	0.287	0.68–0.77	−0.056	1.39–5.42	B$^+$,B$^+$	4
			5062.04	22 000	1.00	0.403	1.05			B	3
				16 500–23 200	1.00	0.324	0.81–0.85	−0.07	1.70–6.64	B$^+$,B$^+$	4
18		^{4}P–^{4}D°	4348.06	22 000	1.00	0.292	1.01			B	3
				20 900–31 800	1.00	0.239	0.82–0.88	−0.036	2.53–4.93	B$^+$,B	4
			4426.00	10 880	2.03	0.546	0.74	−0.089	0.58	B$^+$,C	2
				11 520	1.79	0.475	0.77	−0.062	0.50	B$^+$,D	2
				12 200	0.74	0.193	0.77			A	2
				13 030	1.10	0.294	0.81	−0.038	0.63	A,D	2
				13 880	1.39	0.340	0.76	−0.038	0.57	B$^+$,D	2
				22 000	1.00	0.305	1.02			B	3
				18 400–26 500	1.00			−0.049	2.09–103.6	B	4
			4430.19	22 000	1.00	0.284	0.96			B	3
				18 400–26 500	1.00			−0.021	0.89–44.3	B	4
			4266.53	22 000	1.00	0.320	1.15			B	3
				18 400–26 500	1.00	0.252	0.89–0.93	−0.025	1.15–56.9	B$^+$,B	4
			4331.20	22 000	1.00	0.338	1.18			B	3
				18 400–26 500	1.00			−0.021	0.93–46.4	B	4
			4379.67	10 880	2.09	0.457	0.63			B$^+$	2
				11 520	1.79	0.429	0.71	−0.042	0.35	B$^+$,D	2
				12 200	0.74	0.186	0.76			A	2
				13 030	1.10	0.284	0.80			A	2
				13 880	1.39	0.315	0.72			B$^+$	2

Numerical results for Ar II—Continued

No.	Transition array	Multiplet	Wavelength (Å)	Temperature (K)	Electron density (10^{17}cm^{-3})	w_m (Å)	w_m/w_{th}	d_m (Å)	d_m/d_{th}	Acc.	Reference
				22 000	1.00	0.316	1.07			B	3
			4178.36	22 000	1.00	0.320	1.20			B	3
			4282.90	22 000	1.00	0.252	0.90			B	3
				18 400–26 500	1.00	0.200	0.70–0.73	−0.035	1.48–79.1	B^+,B^+	4
19		^{4}P–^{2}D°	4082.39	18 400–26 500	1.00	0.338		−0.059		B^+,B^+	4
			4112.82	22 000	1.00	0.221				B	3
			4228.16	22 000	1.00	0.299				B	3
				18 400–26 500	1.00	0.331		−0.015		C^+,B	4
20		^{4}P–^{4}S°	3729.31	10 880	2.03	0.381				B^+	2
				11 520	1.79	0.310				B^+	2
				12 200	0.74	0.166				A	2
				13 030	1.10	0.190				A	2
				13 880	1.39	0.222				B^+	2
				22 000	1.00	0.229				B	3
			3850.58	10 880	2.03	0.486		−0.047		B^+,D	2
				11 520	1.79	0.328		−0.046		B^+,D	2
				12 200	0.74	0.186				A	2
				13 030	1.10	0.202				A	2
				13 880	1.39	0.268				B^+	2
				22 000	1.00	0.235				B	3
				18 400–26 500	1.00	0.257		−0.016		A,B	4
			3928.62	26 000	1.76	0.340				B	1
				10 880	2.03	0.504				B^+	2
				11 520	1.79	0.318				B^+	2
				12 200	0.74	0.180				A	2
				13 030	1.10	0.244				A	2
				22 000	1.00	0.233				B	3
				18 400–26 500	1.00	0.336				B^+	4
21		^{2}P–^{4}D°	5145.31	22 000	1.00	0.415				B	3
				18 400–26 500	1.00	0.223		−0.060		B^+,B^+	4
22		^{2}P–^{2}D°	4879.86	10 880	2.03	0.728		−0.152		B^+,B	2
				11 520	1.79	0.587		−0.124		B^+,B	2
				12 200	0.74	0.234		−0.050		A,D	2
				13 030	1.10	0.370		−0.050		A,D	2
				13 880	1.39	0.454		−0.062		B^+,C^+	2
				18 400–26 500	1.00			−0.030		B^+	4
			4965.08	10 880	2.03	0.764		−0.040		B^+,D	2
				11 520	1.79	0.587		−0.080		B^+,C	2
				12 200	0.74	0.285				A	2
				13 030	1.10	0.366		−0.040		A,D	2
				13 880	1.39	0.472		−0.054		B^+,D	2
				16 500–23 200	1.00	0.390		−0.056		B^+,B^+	4
			4726.87	10 880	2.03	0.741		−0.086		B^+,C^+	2
				11 520	1.79	0.594		−0.064		B^+,C	2
				12 200	0.74	0.184		−0.038		B^+,D	2
				13 030	1.10	0.356		−0.037		B^+,D	2
				22 000	1.00	0.393				B	3
				18 400–26 500	1.00			−0.045		B^+	4
23		^{2}P–^{2}P°	4545.05	10 880	2.03	0.614		−0.048		B^+,D	2
				11 520	1.79	0.504		−0.048		B^+,D	2
				12 200	0.74	0.252		−0.037		A,D	2
				13 030	1.10	0.320				A	2
				13 880	1.39	0.396		−0.032		B^+,D	2
				22 000	1.00	0.362				B	3
				18 400–26 500	1.00			−0.036		B^+	4
			4889.04	22 000	1.00	0.386				B	3
			4657.90	10 880	2.03	0.587		−0.080		B^+,C^+	2
				11 520	1.79	0.464		−0.063		B^+,C	2
				12 200	0.74	0.236		−0.049		A,D	2
				13 030	1.10	0.342		−.0037		A,D	2
				13 880	1.39	0.404		−0.063		B^+,D	2

Numerical results for Ar II—Continued

No.	Transition array	Multiplet	Wavelength (Å)	Temperature (K)	Electron density (10^{17}cm^{-3})	w_m (Å)	w_m/w_{th}	d_m (Å)	d_m/d_{th}	Acc.	Reference
				22 000	1.00	0.370				B	3
				17000–26 700	1.00	0.328		−0.041		B^+,B^+	4
			4764.86	10 880	2.03	0.750		−0.058		B^+,D	2
				11 520	1.79	0.496		−0.035		B^+,D	2
				12 200	0.74	0.226		−0.035		A,D	2
				13 030	1.10	0.346		−0.035		A,D	2
				13 880	1.39	0.426		−0.035		B^+,D	2
				22 000	1.00	0.384				B	3
				17 000–26 700	1.00	0.340		−0.035		B^+,B^+	4
24		^{2}P–^{4}S°	4383.75	18 400–26500	1.00	0.413		−0.056		B^+,B	4
25		^{2}P–^{2}S°	4375.95	22 000	1.00	0.244				C^+	3
			4579.35	10 880	2.03	0.688				B^+	2
				11 520	1.79	0.487				B^+	2
				12 200	0.74	0.184				B^+	2
				13 880	1.39	0.322				C^+	2
				16 500–23 200	1.00	0.322		−0.013		B^+,C^+	4
				22 000	1.00	0.363				B	3
26	$3p^4(^3P)4s'$–$3p^4(^1D)4p'$	^{2}P–^{2}D°	2844.13	26 000	1.76	0.258		−0.037		B,D	1
			2847.82	22 000	1.00	0.138				C^+	3
27		^{2}P–^{2}P°	2979.05	22 000	1.00	0.252				C^+	3
			2891.61	22 000	1.00	0.236				C^+	3
			3033.51	22 000	1.00	0.212				B	3
				26 000	1.76	0.320				B	1
			2942.89	22 000	1.00	0.202				C^+	3
				26 000	1.76	0.344		−0.037		B,D	1
28	$3p^4(^1D)4s'$–$3p^4(^1D)4p'$	^{2}D–^{2}F°	4609.57	10 880	2.03	0.491		−0.086		B^+,C^+	2
				11 520	1.79	0.466		−0.076		B^+,C	2
				12 200	0.74	0.214		−0.034		A,D	2
				13 030	1.10	0.269		−0.034		A,D	2
				13 880	1.39	0.362		−0.059		B^+,D	2
				22 000	1.00	0.340				B	3
				17 000–26 700	1.00	0.302		−0.039		B^+,B^+	4
			4589.90	10 880	2.03	0.533		−0.036		B^+,D	2
				11 520	1.79	0.459		−0.032		B^+,D	2
				12 200	0.74	0.259				A	2
				13 030	1,10	0.324				A	2
				13 880	1.39	390				B^+	2
				22 000	1.00	0.350				B	3
				16 500–23 200	1.00	0.298		−0.022		B^+,B	4
			4637.23	22 000	1.00	0.365				B	3
				18 400–26 500	1.00	0.366		−0.035		B,B^+	4
29		^{2}D–^{2}P°	4277.53	22 000	1.00	0.721				B	3
				26 000	1.76	0.852		0.153		B,B^+	1
			4237.22	18 400–26 500	1.00	0.579		0.137		B^+,A	4
30		^{2}D–^{2}D°	4042.89	22 000	1.00	0.277				B	3
				18 400–26 500	1.00	0.414		−0.060		B^+,A	4
			4079.57	18 400–26 500	1.00	0.429		−0.042		B^+,B^+	4
			4035.46	22 000	1.00	0.291				B	3
				18 400–26 500	1.00	0.367				B^+	4
31	$3p^4(^3P)4p$–$3p^4(^3P)4d$	^{4}P°–^{4}D	3514.39	22 000	1.00	0.460				C^+	3
			3535.32	22 000	1.00	0.520				C^+	3
			3476.75	22 000	1.00	0.354				C^+	3
				26 000	1.76	0.624		0.204		B,B^+	1
			3509.78	22 000	1.00	0.380				C^+	3
32		^{4}P°–^{4}P	3139.02	22 000	1.00	0.356	0.78			C^+	3
			3212.52	22 000	1.00	0.366	0.77			C^+	3
			3281.71	22 000	1.00	0.418	0.84			C^+	3
			3181.04	22 000	1.00	0.350	0.74			C^+	3

Numerical results for Ar II—Continued

No.	Transition array	Multiplet	Wavelength (Å)	Temperature (K)	Electron density (10^{17}cm^{-3})	w_m (Å)	w_m/w_{th}	d_m (Å)	d_m/d_{th}	Acc.	Reference
			3243.69	22 000	1.00	0.368	0.76			C^+	3
			3249.80	20 000, 26 000	1.0,1.76	0.362, 0.664	0.74,0.78			B	1
				22 000	1.00	0.366	0.75			B	3
			3169.67	22 000	1.00	0.356	0.77			B	3
				26 000	1.76	0.664	0.82	0.215	0.51	B,B^+	1
33		^{4}D°–^{4}D	3780.84	22 000	1.00	0.577	1.04			B	3
				26 000	1.76	0.816	0.85	0.154	0.31	B,B	1
				18 400–26 500	1.00	0.754	1.34–1.38	0.188	0.63–0.63	B^+,B	4
			3826.81	22 000	1.00	0.677	1.19			B	3
				18 400–26 500	1.00	0.643	1.12–1.15	0.188	0.62–0.64	B^+,B^+	4
			3872.14	22 000	1.00	0.535	0.92			B	3
				18 400–26 500	1.00	0.767	1.30–1.34	0.200	0.64–0.67	B^+,B^+	4
			3880.33	18 400–26 500	1.00	0.535	0.90–0.93	0.110	0.35–0.37	B^+,B^+	4
			3763.50	18 400–26 500	1.00	0.562	1.01–1.00	0.164	0.53–0.56	B^+,B^+	4
			3799.38	22 000	1.00	0.485	0.86			B	3
				18 400–26 500	1.00	0.569	1.00–1.03	0.207	0.69–0.72	B^+,B^+	4
			3841.52	22 000	1.00	0.444	0.77			B	3
				18 400–26 500	1.00	0.481	0.83–0.75	0.199	0.65–0.68	B^+,B^+	4
			3844.73	22 000	1.00	0.200	0.35			C^+	3
			3900.63	18 400–26 500	1.00	0.525	0.88–0.90	0.307	0.97–1.01	B^+,B^+	4
			3911.58	18 400–26 500	1.00	0.478	0.79–0.82	0.246	0.77–0.81	B^+,B^+	4
34		^{4}D°–^{4}F	3588.44	11 520	1.79	0.842		0.416		B^+,B^+	2
				13 030	1.10	0.540		0.227		A,B^+	2
				13 880	1.39	0.642		0.294		B^+,B^+	2
				22 000	1.00	0.596				B	3
				26 000	1.76	0.882		0.384		B,B^+	1
			3576.62	22 000	1.00	0.623				B	3
				18 400–26 500	1.00	1.180		0.567		C^+,C	4
				26 000	1.76	1.042		0.333		C^+,C	1
			3582.35	22 000	1.00	0.656				B	3
				18 400–26 500	1.00			0.507		B^+	4
			3581.61	22 000	1.00	0.513				B	3
35		^{4}D°–^{4}P	3565.03	22 000	1.00	0.570				C^+	3
				26 000	1.76	1.004		0.308		B,B^+	1
36		^{2}D°–^{4}D	3958.38	22 000	1.00	0.120				C^+	3
			3988.16	22 000	1.00	0.580				B	3
				18 400–26 500	1.00	0.682		0.341		B^+,B^+	4
37		^{2}D°–^{2}D	3000.44	22 000	1.00	0.880				C^+	3
			2955.39	22 000	1.00	0.696				C^+	3
			3014.48	22 000	1.00	0.698				C^+	3
38		^{2}D°–^{2}F	3559.51	22 000	1.00	0.677	1.01			B	3
			3464.13	22 000	1.00	0.585	0.91			C^+	3
				26 000	1.76	1.004	0.90	0.360	0.64	B,B^+	1
39		^{2}D°–^{2}P	3273.32	22 000	1.00	0.780				C^+	3
40		^{2}P°–^{2}F	3655.28	22 000	1.00	0.630				C^+	3
				18 400–26 500	1.00	0.855		0.174		B^+,B^+	4
41		^{2}P°–^{2}P	3307.23	26 000	1.76	1.326	0.60	0.308	0.35	B,B^+	1
			3293.64	26 000	1.76			0.230	0.26	B,B^+	1
			3236.81	22 000	1.00	0.756	0.60			C^+	3
42		^{2}P°–^{2}D	3093.40	22 000	1.00	0.697				C^+	3
43		^{4}S°–^{4}F	3952.73	22 000	1.00	0.589				C^+	3
				18 400–26 500	1.00	0.698		0.276		B^+,B^+	4
44		^{4}S°–^{4}P	3868.53	22 000	1.00	0.787	1.13			B	3
				26 000	1.76	1.154	0.95	0.359	0.59	B,B^+	1
				18 400–26 500	1.00	0.726	1.03–1.05	0.302	0.84–0.88	B,B^+	4
			3932.55	22 000	1.00	0.804	1.12			B	3
				18 400–26 500	1.00	0.857	1.18–1.20	0.258	0.69–0.73	B^+,B^+	4
			3979.36	22 000	1.00	0.795	1.08			B	3
				18 400–26 500	1.00	0.836	1.12–1.15	0.231	0.61–0.64	B^+,B^+	4

Numerical results for Ar II—Continued

No.	Transition array	Multiplet	Wavelength (Å)	Temperature (K)	Electron density (10^{17}cm^{-3})	w_m (Å)	w_m/w_{th}	d_m (Å)	d_m/d_{th}	Acc.	Reference
45		^{2}S°–^{2}P	3388.53	26 000	1.76	1.342		0.255		B,B$^+$	1
46	$3p^4(^3P)4p$–$3p^4(^1D)4d$	^{2}P°–^{2}P	2544.68	22 000	1.00	0.426				C$^+$	3
47	$3p^4(^1D)4p'$–$3p^4(^3P)4d'$	^{2}D°–^{2}D	5216.81	18 400–26 500	1.00	2.527				A	4
48		^{2}P°–^{2}D	4914.31	18 400–26 500	1.00			−0.707		B	4
49		^{2}D°–^{2}P	5812.76	18 400–26 500	1.00	2.911		0.799		B$^+$,B$^+$	4
50	$3p^4(^1D)4p'$–$3p^4(^1D)4d'$	^{2}F°–^{2}G	3561.03	22 000	1.00	0.639				B	3
51		^{2}F°–^{2}F	3376.44	22 000	1.00	0.668				C$^+$	3
				26 000	1.76	1.174		0.690		B,B$^+$	1
			3350.92	22 000	1.00	0.591				B	3
52		^{2}P°–^{2}P	3660.44	18 400–26 500	1.00	1.236		0.154		B$^+$,B$^+$	4
53		^{2}P°–^{2}D	3639.83	22 000	1.00	0.216				B	3
54		^{2}D°–^{2}P	3825.67	22 000	1.00	1.054				C$^+$	3
			3819.02	18 400–26 500	1.00	1.361				B$^+$	4
55		^{2}D°–^{2}D	3803.17	22 000	1.00	1.007				B	3
				18 400–26 500	1.00	1.134		0.375		B,B	4
				26 000	1.76	0.690		0.538		C,B	1
			3796.59	18 400–26 500	1.00	1.000		0.241		B$^+$,B$^+$	4
56		^{2}D°–^{2}F	3737.89	22 000	1.00	1.012				B	3
				18 400–26 500	1.00	1.126		0.222		A,B$^+$	4
				26 000	1.76	1.456		0.577		B,B$^+$	1
			3718.21	22 000	1.00	0.961				B	3
				18 400–26 500	1.00	0.932		0.231		B$^+$,B$^+$	4
			3724.52	18 400–26 500	1.00	1.144		0.147		B$^+$,B	4
57	$3p^4(^3P)4p$–$3p^4(^3P)5s$	^{4}P°–^{4}P	3765.27	18 400–26 500	1.00	0.742	1.10–1.12	0.182	0.51–0.53	B$^+$,B$^+$	4
			3720.43	22 000	1.00	0.616	0.94			C$^+$	3
				18 400–26 500	1.00	0.842	1.28–1.30	0.249	0.71–0.74	B$^+$,B$^+$	4
			3622.14	22 000	1.00	0.662	1.06			B	3
				18 400–26 500	1.00	0.802	1.28–1.30	0.298	0.90–0.94	B$^+$,B$^+$	4
			3809.46	22 000	1.00	0.746	1.08			B	3
				18 400–26 500	1.00	0.753	1.09–1.11	0.279	0.76–0.79	B$^+$,A	4
			3770.52	18 400–26 500	1.00	0.767	1.13–1.15	0.285	0.79–0.83	B$^+$,B$^+$	4
				26 000	1.76			0.498	0.82	B$^+$	1
58		^{4}D°–^{4}P	4033.81	22 000	1.00	0.830				B	3
				18 400–26 500	1.00	0.884		0.316		B$^+$,B$^+$	4
			4179.30	18 400–26 500	1.00	0.864		0.319		B$^+$,A	4
			4156.08	18 400–26 500	1.00	0.833		0.323		B$^+$,A	4
59		^{4}D°–^{2}P	4011.21	18 400–26 500	1.00	0.905		0.605		B$^+$,B$^+$	4
60		^{2}D°–^{4}P	4255.60	18 400–26 500	1.00			0.276		A	4
61		^{2}D°–^{2}P	4218.66	22 000	1.00	0.849	0.96			B	3
				18 400–26 500	1.00	0.903	1.02–1.03	0.314	0.65–0.67	A,A	4
				26 000	1.76			0.502	0.61	B$^+$	1
62		^{2}P°–^{2}P	4222.64	22 000	1.00	0.820				B	3
				18 400–26 500	1.00	0.903		0.314		A,A	4
				26 000	1.76			0.394		B$^+$	1
			4275.16	22 000	1.00	0.608				B	3
63		^{4}S°–^{4}P	4865.91	18 400–26 500	1.00	1.285		0.680		B$^+$,B$^+$	4
64		^{4}S°–^{2}P	4535.49	18 400–26 500	1.00	1.062		0.412		B$^+$,A	4
65	$3p^4(^1D)4p'$–$3p^4(^1D)5s'$	^{2}F°–^{2}D	3946.10	22 000	1.00	0.918				B	3
				18 400–26 500	1.00	0.811		0.332		B$^+$,B$^+$	4
			3925.72	22 000	1.00	0.785				B	3
				18 400–26 500	1.00	0.941		0.315		B$^+$,A	4
				26 000	1.76	1.454		0.498		B,B$^+$	1
66	$3p^4(^1S)4s''$–$3p^4(^3P)5p$	^{2}S–^{2}D°	4217.43	22 000	1.00	0.734				C$^+$	3
				18 400–26 500	1.00	1.008		0.036		B$^+$,C	4
67		^{2}S–^{4}D°	4385.06	18 400–26 500	1.00	0.969		0.129		B$^+$,A	4

Numerical results for Ar II—Continued

No.	Transition array	Multiplet	Wavelength (Å)	Temperature (K)	Electron density (10^{17}cm^{-3})	w_m (Å)	w_m/w_{th}	d_m (Å)	d_m/d_{th}	Acc.	Reference
68		^{2}S–^{4}S°	4189.65	18 400–26 500	1.00	1.041		0.224		B$^+$,B$^+$	4
69		^{2}S–^{2}S°	4229.87	18 400–26 500	1.00			−0.196		B	4
70	$3p^4(^1D)3d'$–$3p^4(^1D)4p'$	^{2}G–^{2}F°	6114.92	22 000	1.00	0.551				B	3
				18 400–26 500	1.00	0.347		0.027		B$^+$,B$^+$	4
			6123.36	22 000	1.00	0.574				B	3
			6172.29	18 400–26 500	1.00	0.477		0.062		B$^+$,A	4
71	$3p^4(^3P)4p$–$3p^4(^1D)3d'$	^{2}P°–^{2}S	4099.46	22 000	1.00	0.500				B	3
72		^{4}D°–^{2}D	6818.38	22 000	1.00	1.413				B	3
73		^{2}P°–^{2}P	6614.35	18 400–26 500	1.00	0.972				B$^+$	4
			7054.99	18 400–26 500	1.00	1.016		−0.018		B$^+$,B	4
74		^{2}D°–^{2}P	6375.94	18 400–26 500	1.00	1.092		−0.287		B$^+$,B$^+$	4
75	$3p^4(^3P)4p$–$3p^4(^1S)3d''$	^{2}D°–^{2}D	4792.09	22 000	1.00	0.422				B	3
				18 400–26 500	1.00	0.489				A	4
			4949.40	22 000	1.00	0.421				B	3
			4867.56	18 400–26 500	1.00	0.583		−0.295		B$^+$,B$^+$	4
76		^{2}P°–^{2}D	4942.92	22 000	1.00	0.462				B	3
				18 400–26 500	1.00	0.508		−0.045		B$^+$,B$^+$	4
			5165.77	18 400–26 500	1.00	0.445		−0.037		B$^+$,B$^+$	4
77		^{2}S°–^{2}D	5305.69	18 400–26 500	1.00	0.524		−0.043		A,B$^+$	4
78	$3p^4(^1D)3d'$–$3p^4(^3P_1)4f$	^{2}D–^{2}[4]°	4203.41	22 000	1.00	1.377				B	3
				18 400–26 500	1.00	1.082		0.209		B$^+$,A	4
79		^{2}D–^{2}[2]°	4297.96	22 000	1.00	1.351				B	3
				18 400–26 500	1.00	1.594		0.487		B$^+$,B$^+$	4
			4611.24	18 400–26 500	1.00			0.456		B$^+$	4
80		^{2}P–^{2}[3]°	4563.74	18 400–26 500	1.00	1.158		0.421		B$^+$,B$^+$	4
81		^{2}P–^{2}[2]°	4703.36	22 000	1.00	1.261				B	3
				18 400–26 500	1.00	1.438		0.440		B$^+$,A	4
82		^{2}D–^{2}[3]°	4168.97	18 400–26 500	1.00	1.165				B$^+$	4
83	$3p^4(^1D)3d'$–$3p^4(^3P_2)4f$	^{2}D–^{2}[3]°	4433.84	22 000	1.00	1.179				B	3
				18 400–26 500	1.00			0.210		A	4
84		^{2}D–^{2}[4]°	4445.85	22 000	1.00	0.895				B	3
				18 400–26 500	1.00	1.200		0.146		B$^+$,B$^+$	4
85		^{2}P–^{2}[2]°	4955.11	22 000	1.00	0.952				C$^+$	3
86	$3p^4(^1S)4s''$–$3p^4(^3P)5p$	^{2}S–^{2}P°	4309.24	22 000	1.00	0.638				B	3
87	$3p^4(^1D)4p'$–$3p^4(^3P)5d$	^{2}D°–^{4}F	3637.03	22 000	1.00	0.652				B	3
88	$3p^4(^1S)3d''$–$3p^4(^3P_1)4f$	^{2}D–^{2}[2]°	6187.14	18 400–26 500	1.00			0.577		A	4
89	$3p^4(^1S)3d''$–$3p^4(^3P_2)4f$	^{2}D–^{2}[2]°	6620.97	18 400–26 500	1.00	1.984		0.665		B$^+$,B$^+$	4
90	$3p^4(^1D)3d'$–$3p^4(^3P_0)4f$	^{2}P–^{2}[3]°	4498.54	18 400–26 500	1.00	1.308		0.290		B$^+$,B$^+$	4
91	$3p^4(^1S)3d''$–$3p^4(^3P_0)4f$	^{2}D–^{2}[3]°	5985.91	18 400–26 500	1.00	1.868		0.260		B$^+$,A	4
92	$3p^4(^1S)3d''$–$3p^4(^3P_2)4f$	^{2}D–^{2}[3]°	6696.29	18 400–26 500	1.00	1.883		0.581		B$^+$,B$^+$	4

Argon

Ar III

Ground state: $1s^2 2s^2 2p^6 3s^2 3p^4\ ^3P_2$
Ionization energy: 40.74 eV = 328 600 cm^{-1}

Low-pressure pulsed arcs in the end-on configuration were employed both by Kobilarov and Konjević[1] as well as by Djenize *et al.*,[2] and the line profiles were photoelectrically scanned with a shot-to-shot technique. Self-absorption was checked by comparing line intensity ratios within multiplets with those expected from line/space (LS) coupling. Optically thin conditions were obtained by gradually diluting the argon test gas with helium,[1] or by using a fixed gas mixture of Ar and He.[2] A standard deconvolution procedure was applied to the observed Voigt-type line profiles in order to eliminate the nonnegligible contributions of Doppler and instrumental broadening. The effects of the inhomogeneous plasma end layers were not discussed in either paper. They are estimated to be more significant in the work of Djenize *et al.*[2] since large open spaces are provided for the plasma regions near the electrodes.

References

[1] R. Kobilarov and N. Konjević, Phys. Rev. A **41**, 6023 (1990).
[2] S. Djenize, S. Bukvić, A. Srećković, and M. Platisa, J. Phys. B **29**, 429 (1996).

Key data on experiments

Reference	Plasma source	Method of measurement: Electron density	Method of measurement: Temperature	Remarks
1	Low-pressure pulsed arc	Stark width of the He II P_α line	Boltzmann plot of O III lines	
2	Low-pressure pulsed arc	Laser interferometer at 6328 Å	Boltzmann plot of Ar III lines, ratios of Ar IV to Ar III lines and Ar III to Ar II lines	

Numerical results for Ar III

No.	Transition array	Multiplet	Wavelength (Å)	Temperature (K)	Electron density (10^{17} cm^{-3})	w_m (Å)	w_m/w_{th}	d_m (Å)	d_m/d_{th}	Acc.	Reference
1	$3d^3 3d'' - 3p^3(^2P^\circ)4p''$	$^3P^\circ - ^3P$	3391.84	38 000	3.5	0.52				B	2
2	$3p^3 4s - ^3p^3(^4S^\circ)4p$	$^5S^\circ - ^5P$	3285.84	38 000	3.5	0.46				B^+	2
			3301.85	38 000	3.5	0.42				B^+	2
3		$^3S^\circ - ^3P$	3511.15	80 000	5.8	0.60				B^+	1
				110 000	10.0	0.90				B^+	1
				Δ(110 000–80 000)	Δ(10.0–5.8)			Δ(−0.06)		C	1
			3514.20	80 000	5.8	0.64				B^+	1
				110 000	10.0	0.94				B^+	1
				Δ(11 0000–80 000)	Δ(10.0–5.8)			Δ(−0.06)		C	1
4	$3p^3 4p - 3p^3(^4S^\circ)5s$	$^5P - ^5S^\circ$	2166.19	38 000	3.5	0.53				B	2
			2170.22	38 000	3.5	0.61				B	2
			2177.20	38 000	3.5	0.56				B	2
5	$3p^3 4s' - 3p^3(^2D^\circ)4p'$	$^3D^\circ - ^3D$	3480.50	38 000	3.5	0.54				B	2
			3499.67	80 000	5.8	0.53				B^+	1
				11 0000	10.0	0.78				B^+	1
				Δ(110 000–80 000)	Δ(10.0–5.8)			Δ(−0.05)		C	1
			3503.59	38 000	3.5	0.48				B	2
				80 000	5.8	0.54				B^+	1
				11 0000	10.0	0.78				B^+	1
				Δ(110 000–80 000)	Δ(10.0–5.8)			Δ(−0.04)		D	1
6		$^3D^\circ - ^3F$	3336.17	38 000	3.5	0.56				B^+	2
			3344.76	38 000	3.5	0.54				B^+	2
			3358.53	38 000	3.5	0.46				B^+	2
7		$^3D^\circ - ^3P$	2855.31	80 000	5.8	0.44				B^+	1
				11 0000	10.0	0.62				B^+	1
				Δ(110 000–80 000)	Δ(10.0–5.8)			Δ(−0.03)		D	1
			2884.21	80 000	5.8	0.45				B^+	1
				11 0000	10.0	0.66				B^+	1
				Δ(110 000–80 000)	Δ(10.0–5.8)			Δ(−0.03)		C	1
8	$3p^3 4p' - 3p^3(^2D^\circ)4d'$	$^3D - ^3P^\circ$	2168.28	38 000	3.5	0.69				B	2
9	$3p^3 4p' - 3p^3(^2D^\circ)5s'$	$^3D - ^3D^\circ$	2133.87	38 000	3.5	0.51				B	2

Argon

Ar IV

Ground state: $1s^2 2s^2 2p^6 3s^2 3p^3\ ^4S^\circ_{3/2}$
Ionization energy: 59.81 eV = 482 400 cm^{-1}

Hey *et al.*[1] injected argon along the axis of a gas-liner pinch discharge and observed the plasma-broadened line profiles on a single-shot basis side on with an optical multichannel analyzer. Argon was confined to the center part of the plasma which is fairly homogeneous. No cold boundary layers exist, since the argon plasma is surrounded by a hydrogen plasma of similar temperature. Self-absorption effects were found to be negligible from checks of intensity ratios of multiplet components against LS coupling ratios. The contributions of Doppler and instrumental broadening were taken into account.

Kobilarov and Konjević[2] employed a low-pressure pulsed arc in the end-on configuration, that scanned the line profiles stepwise with a spectrometer–photomultiplier setup on a shot-to-shot basis. Self-absorption was checked with the same procedure as that discussed above, and the contributions of Doppler and instrumental broadening were taken into account with a standard deconvolution procedure and subtracted. The effects of inhomogeneous plasma end layers were not discussed, but are estimated to be quite small.

The results of the two groups often do not overlap within their estimated uncertainties. We have thus increased our uncertainty estimates somewhat so that mutual consistency is obtained.

References

[1] J. D. Hey, A. Gawron, X. J. Xu, P. Breger, and H.-J. Kunze, J. Phys. B **23**, 241 (1990).
[2] R. Kobilarov and N. Konjević, Phys. Rev. A **41**, 6023 (1990).

Key data on experiments

Reference	Plasma source	Method of measurement: Electron density	Method of measurement: Temperature	Remarks
1	Gas-liner pinch	Stark width of the He II P_α line	Intensity ratios of two N III and N IV multiplets	
2	Low-pressure pulsed arc	Stark width of the He II P_α line	Relative intensities of O III lines	

Numerical results for Ar IV

No.	Transition array	Multiplet	Wavelength (Å)	Temperature (K)	Electron density (10^{17} cm^{-3})	w_m (Å)	w_m/w_{th}	d_m (Å)	d_m/d_{th}	Acc.	Reference
1	$3p^2 4s - 3p^2(^3P)4p$	$^4P - ^4D^\circ$	2809.44	80 000	5.8	0.32				B	2
				81 200	24	2.38				B	1
				11 0000	10.0	0.48				B	2
				Δ(110 000–80 000)	Δ(10.0–5.8)			Δ(−0.03)		C	2
			2788.96	80 000	5.8	0.34				B	2
				81 200	24	2.49				B	1
				11 0000	10.0	0.49				B	2
				Δ(110 000–80 000)	Δ(10.0–5.8)			Δ(−0.03)		C	2
			2776.26	81 200	24	2.17				B	1
			2797.11	81 2 00	24	2.38				B	1
			2830.25	80 000	5.8	0.34				B	2
				11 0000	10.0	0.51				B	2
				Δ(110 000–80 000)	Δ(10.0–5.8)			Δ(−0.03)		C	2
2		$^4P - ^4P^\circ$	2640.34	81 200	24	1.74				B^+	1
			2615.68	81 200	24	1.63				B^+	1
3		$^2P - ^2P^\circ$	2599.47	81 200	24	1.63				B^+	1
4		$^2D - ^2D^\circ$	2621.36	81 2 00	24	1.52				B^+	1
			2624.92	81 200	24	1.52				B^+	1
5	$3p^2 4s' - 3p^2(^1D)4p'$	$^2D - ^2F^\circ$	2757.92	80 000	5.8	0.35				B^+	2
				81 200	24	1.96				B^+	1
				11 0000	10.0	0.52				B^+	2
				Δ(110 000–80 000)	Δ(10.0–5.8)			Δ(−0.03)		C	2
			2784.47	81 200	24	2.28				B^+	1

Boron

B I

Ground state: $1s^2 2s^2 2p\ ^2P^\circ_{1/2}$
Ionization energy: 8.298 eV = 66 927.86 cm^{-1}

Djenize *et al.*[1] have observed three B I lines with a low-pressure pulsed arc end on, scanning the profiles on a shot-to-shot-basis. A sufficient amount of boron entered the plasma by erosion of the glass wall of the discharge tube. Effects of the inhomogeneous plasma end layers were not discussed. Self-absorption was assumed to be negligible due to the very low concentration of the emitting species. Instrumental and Doppler broadening were taken into account by a standard deconvolution procedure.

Reference

[1] S. Djenize, A. Srećković, J. Labat, and M. Platisa, Phys. Scr. **45**, 320 (1992).

Key data on experiments

Reference	Plasma source	Method of measurement: Electron density	Method of measurement: Temperature	Remarks
1	Low-pressure pulsed arc	Laser interferometer at 6328 Å	Boltzmann plot of relative intensities of O III lines	

Numerical results for B I

No.	Transition array	Multiplet	Wavelength (Å)	Temperature (K)	Electron density (10^{17} cm^{-3})	w_m (Å)	w_m/w_{th}	d_m (Å)	d_m/d_{th}	Acc.	Reference
1	$2s^2 2p - 2s 2p^2$	$^2P^\circ - ^2D$	2088.91	45 000	2.20	0.142				B	1
			2089.57	45 000	2.20	0.142				B	1
2	$2p - (^1S)3s$	$^2P^\circ - ^2S$	2497.73	50 000	1.66	0.064				B	1

Boron

B II

Ground state: $1s^2 2s^2\ ^1S_0$
Ionization energy: 25.155 eV = 202 887.4 cm^{-1}

Djenize *et al.*[1,2] have observed two B II line profiles with a low-pressure pulsed arc end on, using a shot-to-shot technique. Boron entered the plasma by erosion of the glass wall of the discharge tube. Effects of the inhomogeneous plasma end layers were not discussed. Self-absorption was assumed to be negligible due to the very low concentration of the emitting species in the plasma. Instrumental and Doppler broadening were taken into account by applying a standard deconvolution procedure.

Blagojević *et al.*[3] have measured the Stark widths of three other B II lines with a similar low-pressure pulsed arc, but they used a gas mixture of He and a few percent of BCl_3. They also employed a shot-to-shot scanning technique in the end-on configuration. Self-absorption was checked by diluting the BCl_3 part of the gas mixture until the ratios of line intensities in B II multiplets were within a few percent of the expected LS-coupling ratios. Instrumental and Doppler broadening were again taken into account by applying a standard deconvolution procedure.

References

[1] D. Djenize, A. Srećković, J. Labat, and M. Platisa, Phys. Scr. **45**, 320 (1992).
[2] S. Djenize, L. C. Popović, J. Labat, A. Srećković, and M. Platisa, Contrib. Plasma Phys. **33**, 193 (1993).
[3] B. Blagojević, M. V. Popović, N. Konjević, and M. S. Dimitrijević, J. Quant. Spectrosc. Radiat. Transf. **61**, 361 (1999).

Key data on experiments

Reference	Plasma source	Method of measurement: Electron density	Method of measurement: Temperature	Remarks
1, 2	Low-pressure pulsed arc	Laser interferometer at 6328 Å	Boltzmann plot of relative line intensities of O III lines	
3	Low-pressure pulsed arc	Stark width of the He II P_α line	Adopted from another experiment with similar gas mixture and same experimental conditions	

Numerical results for B II

No.	Transition array	Multiplet	Wavelength (Å)	Temperature (K)	Electron density (10^{17} cm^{-3})	w_m (Å)	w_m/w_{th}	d_m (Å)	d_m/d_{th}	Acc.	Reference
1	$2s2p-2p^2$	$^1P^\circ-{}^1D$	3451.29	50 000	1.66	0.180		−0.08		B,C$^+$	1, 2
2	$2s3s-(^2S)3p$	$^3S-{}^3P^\circ$	7030.20	65 000	0.21	0.149	0.63			B$^+$	3
			7031.90	65 000	0.21	0.149	0.63			B$^+$	3
			7032.54	65 000	0.21	0.149	0.63			B$^+$	3
3	$2s3p-2p3p$	$^1P^\circ-{}^1P$	2220.30	41 000	2.20	0.192				B$^+$	1, 2

Boron

B III

Ground state: $1s^2 2s\ ^2S_{1/2}$
Ionization energy: 37.931 eV = 305 931.1 cm^{-1}

Djenize *et al.*[1] have observed the profile of the $4f-5g$ transition with a low-pressure pulsed arc end on, using a shot-to-shot scanning technique. Boron entered the plasma by erosion of the glass wall of the discharge tube. Effects of the inhomogeneous plasma end layers were not discussed. Self-absorption was assumed to be negligible due to the very low concentration of the emitting species in the plasma. Instrumental and Doppler broadening were taken into account by applying a standard deconvolution procedure.

Blagojević *et al.*[3] have measured the Stark widths and shifts of two other B II lines with a similar low-pressure pulsed arc, but they used a gas mixture of He and a few percent of BCl_3. They also employed a shot-to-shot technique in the end-on configuration. Self-absorption was checked by diluting the BCl_3 part of the gas mixture until the ratios of line intensities in B II multiplets were within a few percent of the expected LS-coupling ratios. Instrumental and Doppler broadening were taken into account by applying a standard deconvolution procedure. Effects of the inhomogeneous plasma end layers were not discussed, but are estimated to be small for this type of discharge.

Glenzer and Kunze[2] measured the line profiles of the $2s$-$2p$ resonance transitions with a gas-liner pinch. This source has no cold boundary layer for the emitting ions, and the plasma column was checked for axial and radial homogeneity. Optically thin conditions were produced by using very small amounts of boron trifluoride as the test gas, and hydrogen as the driver gas. Instrumental and Doppler broadening were taken into account by fitting the observed line profiles to Voigt functions.

It should be noted that the results of Glenzer and Kunze's measurements agree very closely with semiclassical calculations,[4] but their Stark widths are about twice as large as those from five-state close-coupling quantum mechanical calculations.[5]

References

[1] S. Djenize, A. Srećković, J. Labat, and M. Platisa, Phys. Scr. **45**, 320 (1992).
[2] S. Glenzer and H.-J. Kunze, Phys. Rev. A **53**, 2225 (1996).
[3] B. Blagojević, M. V. Popović, N. Konjević, and M. S. Dimitrijević, J. Quant. Spectrosc. Radiat. Transf. **61**, 361 (1999).
[4] M. S. Dimitrijević and S. Sahal-Bréchot, Astron. Astrophys., Suppl. Ser. **119**, 369 (1996); Bull. Astron. Belgrade **153**, 101 (1996).
[5] M. J. Seaton, J. Phys. B **21**, 3033 (1988).

Key data on experiments

Reference	Plasma source	Method of measurement: Electron density	Method of measurement: Temperature	Remarks
1	Low-pressure pulsed arc	Laser interferometer at 6328 Å	Boltzmann plot of O III lines	
2	Gas-liner pinch	90° Thomson scattering	90° Thomson scattering	
3	Low-pressure pulsed arc	Stark width of the He II P_α line	Adopted from another experiment with similar gas mixture and same experimental conditions	

Numerical results for B III

No.	Transition array	Multiplet	Wavelength (Å)	Temperature (K)	Electron density (10^{17}cm^{-3})	w_m (Å)	w_m/w_{th}	d_m (Å)	d_m/d_{th}	Acc.	Reference
1	$2s-2p$	^{2}S–^{2}P°	2067.23	106 000	18.1	0.220	1.02			B	2
			2065.78	106 000	18.1	0.221	1.03			B	2
2	$3s-3p$	^{2}S–^{2}P°	7835.25	65 000	0.28	0.334	0.82			B	3
				72 400	0.58	0.602	0.74			B	3
				Δ(72 400–65 000)	Δ(0.58–0.28)			Δ(−0.03)	1.77	D	3
			7841.41	65 000	0.28	0.311	0.76			B	3
				72 400	0.58	0.626	0.76			B	3
				Δ(72 400–65 000)	Δ(0.58–0.28)			Δ(−0.03)	1.77	D	3
3	$4f-5g$	^{2}F°–^{2}G	4497.73	40 000	1.70	4.08				B	1

Bromine

Br I

Ground state: $1s^22s^22p^63s^23p^63d^{10}4s^24p^5\ ^2P^\circ_{3/2}$
Ionization energy: 11.8138 eV = 95 284.7 cm^{-1}

Djurović *et al.*[1] have observed the Br I 7938.68 Å line with a wall-stabilized arc end on. Doppler, instrumental, and van der Waals broadening were taken into account. The measured line width was compared with Sahal-Bréchot's semiclassical theory and with a simplified semiclassical approach by Dimitrijević and Konjević.[3] The agreement is much better in the latter case.

Baclawski *et al.*[2] also used a wall-stabilized arc end on to measure three Br I lines with an optical multichannel analyzer.

In both experiments, plasma homogeneity is achieved by limiting the bromine vapor and argon mixture to the center part of the arc column, well away from the electrode areas, which are operated in pure argon. Self-absorption is checked in Ref. 1 by placing a concave mirror with a light chopper behind the arc, thereby imaging the plasma on itself and thus doubling the optical pathlength. No mention of possible self-absorption problems or of competing line broadening mechanisms is made in Ref. 2 (however, this is just an extended abstract in conference proceedings, not followed up as yet by publication in a journal).

The result by Baclawski *et al.*[2] for the Br I 4441.74 Å line width is four times smaller than the earlier result of Bengtson.[4] For the Br I 4477.72 and 4472.61 Å lines, the values of Baclawski *et al.*[2] are in close agreement with those of earlier work by Djurović *et al.*[5]

References

[1] S. Djurović, N. Konjević, and M. S. Dimitrijević, Z. Phys. D **16**, 255 (1990).
[2] A. Baclawski, A. Goly, I. Ksiazek, and T. Wujec, *Spectral Line Shapes*, AIP Conf. Proc. 386, edited by M. Zoppi and L. Ulivi (AIP, Woodbury, NY, 1997), Vol. 9, pp. 307–308.
[3] M. S. Dimitrijević and N. Konjević, Astron. Astrophys. **163**, 297 (1986).
[4] R. D. Bengtson, University of Maryland Technical Note BN-559 (1968).
[5] S. Djurović, R. Konjević, M. Platisa, and N. Konjević, J. Phys. B **21**, 739 (1988).

Key data on experiments

Reference	Plasma source	Method of measurement: Electron density	Method of measurement: Temperature	Remarks
1	Wall-stabilized arc	H_β Stark width	Plasma composition data	
2	Wall-stabilized arc	Stark width of Ar I 4300 Å line	Boltzmann plots of Ar and Br lines	

Numerical results for Br I

No.	Transition array	Multiplet	Wavelength (Å)	Temperature (K)	Electron density (10^{17}cm^{-3})	w_m (Å)	w_m/w_{th}	d_m (Å)	d_m/d_{th}	Acc.	Reference
1	$4p^45s-4p^4(^3P_2)6p$	^{4}P–^{4}D°	4441.74	10 750	0.45	1.26		0.52		B^+,C^+	2
				11 530	0.70	1.70		1.19		B^+,B	2
			4477.72	10 750	0.45	1.49		0.78		B^+,C^+	2
				11 530	0.70	2.32		1.50		B^+,B	2
2	$4p^4(^3P_2)5s-4p^4(^1D_2)5p$	^{4}P–^{2}P°	4472.61	10 570	0.45	1.31		0.65		B^+,C^+	2
				11 530	0.70	2.00		1.33		B^+,B	2
3	$4p^4(^1D_2)5s-4p^4(^1D_2)5p$	^{2}D–^{2}D°	7938.68	9 600	0.28	0.98	2.59			A	1

Bromine

Br II

Ground state: $1s^2 2s^2 2p^6 3s^2 3p^6 3d^{10} 4s^2 4p^4\ ^3P_2$
Ionization energy: 21.81 eV = 175 870 cm^{-1}

Labat *et al.*[1] have observed seven Br II lines in a pulsed, low-pressure discharge on a shot-to-shot basis end on. The discharge was operated in nitrogen with an admixture of bromine vapor. The plasma homogeneity was checked by operating the discharge in tubes of various lengths. The lines were checked for self-absorption by plotting the measured Lorentzian fractions versus electron density. For all measured Br II lines, self-absorption was found to be negligible. The linewidths were corrected for Doppler and instrumental contributions.

Measured values were compared with those provided by the modified semiempirical formula of Dimitrijević and Konjević[2] (in a simplified version).

Except for the Br II 4704 and 4816 Å lines, for which the measured halfwidths were 3 and 1.7 times larger than the calculated ones, rather good agreement was found.

The analysis of the Stark parameters of two Br II lines shows that they follow predicted regularities within the experimental error.

References

[1] O. Labat, S. Djenize, J. Purić, J. M. Labat, and A. Srećković, J. Phys. B **24**, 1251 (1991).
[2] M. S. Dimitrijević and N. Konjević, Astron. Astrophys. **172**, 345 (1987).

Key data on experiments

Reference	Plasma source	Method of measurement: Electron density	Method of measurement: Temperature	Remarks
1	Low-pressure pulsed arc	Single wavelength laser interferometer at 6328 Å	Boltzmann slope of six N III lines	

Numerical results for Br II

No.	Transition array	Multiplet	Wavelength (Å)	Temperature (K)	Electron density (10^{17} cm^{-3})	w_m (Å)	w_m/w_{th}	d_m (Å)	d_m/d_{th}	Acc.	Reference
1	$5s-5p$	$^5S^\circ-{}^5P$	4704.85	36 000	1.0	0.76				B	1
			4816.70	36 000	1.0	0.52				B	1
2	$5s'-5p'$	$^1D^\circ-{}^1D$	4223.89	36 000	1.0	0.50				B	1
3		$^1D^\circ-{}^1F$	5332.05	36 000	1.0	0.52				B	1
4		$^3D^\circ-{}^3P$	4179.63	36 000	1.0	0.42				B	1
5		$^3D^\circ-{}^3D$	4928.79	36 000	1.0	0.46				B	1
			4930.66	36 000	1.0	0.38				B	1

Bromine

Br III

Ground state: $1s^2 2s^2 2p^6 3s^2 3p^6 3d^{10} 4s^2 4p^3\ ^4S^\circ_{3/2}$
Ionization energy: 35.9 eV = 289 529 cm^{-1}

Labat *et al.*[1] have observed four Br III lines in a pulsed, low-pressure discharge end-on, on a shot-to-shot basis. The homogeneity of the plasma was checked by operating the discharge in tubes of various lengths. The line shapes were corrected for self-absorption by plotting the measured Lorentzian fractions versus electron density. For all Be III lines measured, self-absorption was found to be negligible. The linewidths were corrected for Doppler and instrumental contributions. The measurements by Labat *et al.*[1] are the first for Br III.

Since the set of energy levels for Br III is rather incomplete, no calculations of Stark widths have been done for Br III lines. But an analysis of the Stark parameters of two Br II, four Br III and three Br IV lines shows that they follow, within experimental error, the regularity formula derived from the simplified modified semiempirical formula of Dimitrijević and Konjević.[2]

References

[1] O. Labat, S. Djenize, J. Purić, J. M. Labat and A. Srećković, J. Phys. B **24**, 1251 (1991).
[2] M. S. Dimitrijević and N. Konjević, Astron. Astrophys. **172**, 345 (1987).

Key data on experiments

Reference	Plasma source	Method of measurement: Electron density	Method of measurement: Temperature	Remarks
1	Low-pressure discharge	Laser interferometer at 6328 Å	Boltzmann slope of six N III lines	

Numerical results for Br III

No.	Transition array	Multiplet	Wavelength (Å)	Temperature (K)	Electron density (10^{17} cm^{-3})	w_m (Å)	w_m/w_{th}	d_m (Å)	d_m/d_{th}	Acc.	Reference
1	$4d-5p$	^{4}F–^{4}D°	3074.42	56 000	1.0	0.38				B	1
			2926.96	56 000	1.0	0.40				B	1
			2994.04	56 000	1.0	0.26				B	1
2		^{2}F–^{2}D°	3020.76	56 000	1.0	0.30				B	1

Bromine

Br IV

Ground state: $1s^2 2s^2 2p^6 3s^2 3p^6 3d^{10} 4s^2 4p^2\ ^3P_0$
Ionization energy: 47.31 eV = 381 600 cm^{-1}

Labat *et al.*[1] have observed three Br IV lines with a pulsed low-pressure discharge end-on, on a shot-to-shot basis. The homogeneity of the plasma and specifically the influence of cold boundary layers at the ends of the tube were checked by operating the discharge in tubes of two different lengths, and no effects on the line shapes were found. Also, for all Br IV lines measured, self-absorption was found to be negligible. The linewidths were corrected for Doppler and instrumental contributions.

No Stark width or shift measurements of Br IV have been done before. The three observed lines are from the same multiplet and possess similar wavelengths; thus the variations in the Stark widths are unusually large.

Reference

[1] O. Labat, S. Djenize, J. Purić, J. M. Labat, and A. Srećković, J. Phys. B **24**, 1251 (1991).

Key data on experiments

Reference	Plasma source	Method of measurement: Electron density	Method of measurement: Temperature	Remarks
1	Low-pressure pulsed arc	Laser interferometer at 6328 Å	Boltzmann plot of six N III lines	

Numerical results for Br IV

No.	Transition array	Multiplet	Wavelength (Å)	Temperature (K)	Electron density (10^{17} cm^{-3})	w_m (Å)	w_m/w_{th}	d_m (Å)	d_m/d_{th}	Acc.	Reference
1	$5s-5p$	^{3}P°–^{3}D	2907.71	56 000	1.0	0.44				B	1
			2820.87	56 000	1.0	0.28				B	1
			2842.88	56 000	1.0	0.30				B	1

Cadmium

Cd II

Ground state: $1s^2 2s^2 2p^6 3s^2 3p^6 3d^{10} 4s^2 4p^6 4d^{10} 5s\ ^2S_{1/2}$
Ionization energy: 16.908 eV = 136 374.4 cm^{-1}

Djenize *et al.*[1] have observed Cd II lines in a pulsed discharge end-on, on a shot-to-shot basis. Cadmium was deposited on the electrode surface and sputtered into argon–helium or SF_6 carrier gases. The intensities were reproducible within 18%. The effects of the inhomogeneous plasma end layers were not discussed. Self-absorption was assumed to be negligible due to the manner in which the element was introduced into the plasma.

The authors assumed that due to the large mass and the small concentration of emitters, Doppler, van der Waals and resonance broadening were negligible. The line profiles were corrected for the apparatus function (0.07 Å).

No line shifts were detected within their accuracy of measurement, i.e., within ±0.02 Å.

The Stark width measurements have been compared with different approaches of the semiempirical theory,[2,3] and the ratios of experimental to theoretical values cover the range from 2.28 to 0.55.

References

[1] S. Djenize, A. Srećković, J. Labat, R. Konjević, and L. Popović, Phys. Rev. A. **44**, 410 (1991).
[2] H. R. Griem, Phys. Rev. **165**, 258 (1968).
[3] M. S. Dimitrijević and N. Konjević, Astron. Astrophys. **172**, 345 (1987).

Key data on experiments

Reference	Plasma source	Method of measurement: Electron density	Method of measurement: Temperature	Remarks
1	Low-pressure pulsed discharge	Laser interferometer at 6328 Å	Boltzmann plot of five S II spectral lines	

Numerical results for Cd II

No.	Transition array	Multiplet	Wavelength (Å)	Temperature (K)	Electron density (10^{17} cm^{-3})	w_m (Å)	w_m/w_{th}	d_m (Å)	d_m/d_{th}	Acc.	Reference
1	$5s-5p$	$^2S-^2P°$	2144.41	23 000	1.23	0.056				C	1
				30 000	1.00	0.042				C	1
			2265.02	23 000	1.23	0.042				C	1
				30 000	1.00	0.040				C	1
2	$5p-5s$	$^2P°-^2D$	4415.63	23 000	1.23	0.236				B	1
				30 000	1.00	0.138				C	1
3	$5p-5d$	$^2P°-^2D$	2321.07	23 000	1.23	0.112				C	1
			2194.56	23 000	1.23	0.112				C	1
4	$5p-6s$	$^2P°-^2S$	2748.54	23 000	1.23	0.110				C	1

Calcium

Ca II

Ground state: $1s^2 2s^2 2p^6 3s^2 3p^6 4s\ ^2S_{1/2}$
Ionization energy: 11.872 eV = 95 751.87 cm^{-1}

Srećković and Djenize[1] have observed the Ca II 3933.67 Å resonance line with a low-pressure pulsed arc end on. Calcium salts were deposited on the inner walls of the discharge tube, and the discharge was modified to obtain a homogeneous distribution of calcium in the plasma, with nitrogen as the carrier gas. The authors assumed that under their discharge conditions the concentration of Ca II emitters is very small, so that self-absorption can be neglected. van der Waals and resonance broadening were found to be negligible. The intensities were found to be reproducible within ±15% during the shot-to-shot scan of the line profile. The effects of the inhomogeneous plasma end layers were not discussed.

Comparisons with calculations, especially with a quantum mechanical result, support the assumption of an optically thin plasma.

Reference

[1] A. Srećković and S. Djenize, Bull. Astron. Belgrade **148**, 7 (1993).

Key data on experiments

Reference	Plasma source	Method of measurement: Electron density	Method of measurement: Temperature	Remarks
1	Low-pressure pulsed arc	Stark broadening of the 3995 Å N II spectral line	Intensity ratios of N IV to N lII, and N III to N II lines	

Numerical results for Ca II

No.	Transition array	Multiplet	Wavelength (Å)	Temperature (K)	Electron density (10^{17} cm^{-3})	w_m (Å)	w_m/w_{th}	d_m (Å)	d_m/d_{th}	Acc.	Reference
1	$4s-4p$	$^2S-^2P°$	3933.67	43 000	1.76	0.286	0.73	−0.140	0.89	B,C	2

Carbon

C I

Ground state: $1s^2 2s^2 2p^2\ ^3P_0$
Ionization energy: 11.260 eV = 90 820.41 cm^{-1}

Perez *et al.*[1] and Mijatović *et al.*[3] measured the Stark widths and shifts of three $3s-4p$ singlet transitions. Perez *et al.* operated a pulsed discharge in mixtures of He and CO_2, with the amount of CO_2 kept so small that self-absorption was negligible. The line profiles were corrected for Doppler and instrumental broadening.

Sohns and Kock[2] determined the Stark widths of some strong vacuum ultraviolet lines—all resonance transitions—with a wall-stabilized arc under conditions where the lines are strongly self-reversed. They applied a model calculation based on the equation of radiative transfer to the measured line shapes, which recovered the Stark widths.

Mijatović *et al.*[3] observed C I Stark profiles with a wall-stabilized arc operated in argon with small admixtures of CO_2 and H_2 (for plasma diagnostics). The observations were done end on, and self-absorption was checked by placing a concave mirror with a light chopper behind the arc that imaged the plasma on itself and thus generated two optical pathlengths that differed essentially by a factor of 2. The observed line profiles were corrected for Doppler and instrumental broadening with a standard deconvolution program.

The results of Mijatović *et al.*[3] are in excellent agreement with an earlier experiment.[4] They also indicate that ion dynamic treatment of the ions[5] produces little or no improvement.

All Stark shifts reported in Ref. 3 were measured at the position of the halfwidth and were compared with the corresponding theoretical shifts.

References

[1] C. Perez, I. de la Rosa, A. M. de Frutos, and S. Mar, Phys. Rev. A **44**, 6948 (1991).
[2] E. Sohns and M. Kock, J. Quant. Spectrosc. Radiat. Transf. **47**, 335 (1992).
[3] Z. Mijatović, N. Konjević, R. Kobilarov, and S. Djurović, Phys. Rev. E **51**, 613 (1995); Publ. Obs. Astron. Belgrade No. 50, 91 (1995).
[4] D. W. Jones and W. L. Wiese, Phys. Rev. A **30**, 2602 (1984).
[5] J. Barnard, J. Cooper, and E. W. Smith, J. Quant. Spectrosc. Radiat. Transf. **14**, 1025 (1974).

Key data on experiments

Reference	Plasma source	Method of measurement: Electron density	Method of measurement: Temperature	Remarks
1	Low-pressure pulsed arc	Stark widths of the He I 6678.15 Å and H_α line	Boltzmann plot of relative intensities of C II lines	
2	Wall-stabilized arc	Plasma model calculation	Blackbody limited VUV lines	

Numerical results for C I

No.	Transition array	Multiplet	Wavelength (Å)	Temperature (K)	Electron density (10^{17} cm^{-3})	w_m (Å)	w_m/w_{th}	d_m (Å)	d_m/d_{th}	Acc.	Reference
1	$2p^2-2p3s$	^{3}P–^{3}P°	1657.01	12 500	1.0	0.042	1.08			B	2
			1657.38	12 500	1.0	0.042	1.08			B	2
			1656.93	12 500	1.0	0.042	1.08			B	2
2	$2s^22p^2-2s2p^3$	^{3}P–^{3}D°	1560.68	12 500	1.0	0.0047				C^+	2
			1561.34	12 500	1.0	0.0047				C^+	2
			1560.71	12 500	1.0	0.0047				C^+	2
3		^{3}P–^{3}P°	1329.12	12 500	1.0	0.039				B	2
			1329.09	12 500	1.0	0.039				B	2
			1329.10	12 500	1.0	0.039				B	2
4	$2p^2-2p3d$	^{3}P–^{3}D°	1277.55	12 500	1.0	0.115	1.68			B	2
			1277.72	12 500	1.0	0.115	1.68			B	2
			1277.51	12 500	1.0	0.115	1.68			B	2
5	$2p^2-2p4s$	^{3}P–^{1}P°	1276.48	12 500	1.0	0.113				B	2
			1276.75	12 500	1.0	0.113				B	2
6	$2p^2-2p3d$	^{3}P–^{3}P°	1261.00	12 500	1.0	0.107	0.94			B	2
			1260.93	12 500	1.0	0.107	0.94			B	2
			1261.12	12 500	1.0	0.107	0.94			B	2
7	$2p^2-2p3s$	^{1}P–^{1}P°	1930.90	12 500	1.0	0.059	1.21			B	2
8	$2p^2-2p3d$	^{1}D–^{3}D°	1467.88	12 500	1.0	0.154				B	2
			1468.41	12 500	1.0	0.154				B	2
9	$2p^2-2p4s$	^{1}D–^{1}P°	1467.40	12 500	1.0	0.140	0.82			B	2
10	$2p^2-2p3d$	^{1}D–^{1}F°	1463.34	12 500	1.0	0.099	1.12			B	2
11		^{1}D–^{1}P°	1459.03	12 500	1.0	0.119	1.32			B	2
12		^{1}S–^{1}P°	1751.83	12 500	1.0	0.178	1.37			B	2
13	$2p3s-2p(°)4p$	^{1}P°–^{1}P	5380.34	9 900	0.220	0.58	1.03	0.092	0.69	A,C	3
				10 300	0.285	0.77	1.04	0.081	0.61	A,C	3
				14 900–15 400	0.91–0.92	2.09–2.22	0.77–0.77			B	1
14		^{1}P°–^{1}D	5052.17	9 320	0.142			0.29	1.10	A	3
				9 670	0.185	0.67	0.99	0.37	1.07	A,A	3
				9 870	0.215	0.79	1.01	0.43	1.06	A,A	3
				9 890	0.220	0.81	1.00	0.43	1.03	A,A	3
				10 110	0.255	0.93	0.99	0.49	1.02	A,A	3
				10 280	0.285	1.06	0.99	0.55	1.01	A,A	3
				10 310	0.290	1.06	0.98	0.56	1.01	A,A	3
				14 900–15 400	0.90–0.94	2.80–3.09	0.75–0.78			B	1
15		^{1}P°–^{1}S	4932.05	9 890	0.220	1.05	0.81	0.59	0.82	A,A	3
				10 280	0.285	1.35	0.80	0.72	0.66	A,A	3
				14 900–15 400	0.89–0.95	3.84–4.55	0.66–0.72			B	1

Carbon

C II

Ground state: $1s^22s^22p\ ^2P^\circ_{1/2}$
Ionization energy: 24.383 eV = 196 664.7 cm^{-1}

Perez *et al.*[1] measured some Stark widths with a pulsed arc which was operated in mixtures of He and CO_2. The amount of CO_2 was kept so small that self-absorption was negligible. The line profiles were corrected for Doppler and instrumental broadening. It should be noted that one of the transitions they measured, at 4267.26 Å, actually consists of three very closely spaced lines, two stronger ones at 4267.26 Å and a weaker one at 4267.00 Å.

Djenize *et al.*[2] used a pulsed low-pressure arc end on to determine the Stark width and shift of the 6784 Å line. Possible self-absorption effects as well as the effects of the inhomogeneous plasma end layers were not discussed, but the measured profiles were corrected for instrumental and Doppler broadening.

Sarandaev and Salakhov[3] used a pulsed capillary discharge for their measurements, with carbon evaporated from the internal walls of the capillary. Self-absorption in the carbon lines was checked with a continuum source of known temperature and by comparisons against LS-coupling intensity ratios for lines within multiplets. No significant amounts of self-absorption were found. The line profiles were corrected for Doppler and instrumental broadening.

Blagojević *et al.*[4] observed some C II Stark profiles end on with a low-pressure pulsed arc using a shot-to-shot scanning technique. The discharge was operated in helium with a

small admixture of C_2H_2. This admixture was gradually diluted until the intensities of strong C II lines changed proportionally to the concentration, indicating the absence of self-absorption. Again, the observed profiles were corrected for instrumental and Doppler broadening.

Srećković *et al.*[5] observed several C II lines in a low-pressure pulsed arc end-on, on a shot-to-shot basis. The optical depth was checked by studying intensity ratios of C II lines within low-lying multiplets. A standard unfolding procedure was used to account for the contributions of Doppler and instrumental broadening. The results of Srećković *et al.*[5] for multiplets 2, 3, and 8 are in fairly good agreement with those of Refs. 1, 3, and 4.

References

[1] C. Perez, I. de la Rosa, A. M. de Frutos, and S. Mar, Phys. Rev. A **44**, 6948 (1991).
[2] S. Djenize, L. C. Popović, J. Labat, A. Srećković, and M. Platisa, Contrib. Plasma Phys. **33**, 103 (1993).
[3] E. V. Sarandaev and M. Kh. Salakhov, J. Quant. Spectrosc. Radiat. Transf. **54**, 827 (1995).
[4] B. Blagojević, M. V. Popović, and N. Konjević, Phys. Scr. **59**, 374 (1999).
[5] A. Srećković, V. Drincić, S. Bukvić, and S. Djenize, J. Phys. B **33**, 4873 (2000).

Key data on experiments

Reference	Plasma source	Method of measurement		Remarks
		Electron density	Temperature	
1	Low-pressure pulsed arc	Stark widths of the He I 6678.15 Å and hydrogen H_α line	Boltzmann plot of C II lines	
2	Low-pressure pulsed arc	Laser interferometer at 6328 Å	Relative line intensities of O III and O II lines assuming local thermal equilibrium (LTE)	No self-absorption test is reported
3	Pulsed capillary discharge	H_α Stark width	Ratio of line intensities of two Cu II lines	Photographic technique
4	Low-pressure pulsed arc	Stark width of the He II P_α line	Boltzmann plot of relative intensities of N II lines	
5	Low–pressure pulsed arc	Laser interferometer at 6328 Å	Boltzmann plot of O II and C II lines	

Numerical results for C II

No.	Transition array	Multiplet	Wavelength (Å)	Temperature (K)	Electron density (10^{17} cm^{-3})	w_m (Å)	w_m/w_{th}	d_m (Å)	d_m/d_{th}	Acc.	Reference
1	$2s2p^2-2s^23p$	^{2}S–^{2}P°	2836.71	17 800	1.96	0.530	1.73	0.079	0.69	B, B$^+$	5
				19 500	1.44	0.388	1.72			B	5
				20 300	1.25	0.364	1.88			B	5
			2837.60	17 800	1.96	0.456	1.50	0.090	0.79	B, B$^+$	5
				19 500	1.44	0.440	1.99			B	5
				20 300	1.25	0.426	2.20			B	5
2	$2s^23s-2s^23p$	^{2}S–^{2}P°	6578.05	17 100	0.25	0213	0.81			B$^+$	4
				17 500	0.23	0.200	083			B$^+$	4
				17 800	1.96	2.198	1.07	−0.11	0.16	B$^+$,B$^+$	5
				18 800	0.31	0.265	0.82			B$^+$	4
				19 500	1.44	1.128	0.75			B$^+$	5
				20 500	0.98	0.862	0.85			B$^+$	5
				20 000–30 000	0.80–1.35	0.70–1.57	0.84–1.15			C$^+$	1
				22 000	2.21	1.88	0.82	−0.11	0.14	C,D	3
				35 000	1.43	1.11	0.78	−0.14	0.31	C,D	3
			6582.88	17 100	0.25	0.227	0.87			B$^+$	4
				17 500	0.23	0.206	0.86			B$^+$	4
				17 800	1.96	2.145	1.04	−0.15	0.21	B$^+$,B$^+$	5
				18 800	0.31	0.265	0.82			B$^+$	4
				19 500	1.44	1.198	0.80			B$^+$	5
				20 500	0.98	0.860	0.85			B$^+$	5
				20 000–30 000	0.90–1.35	0.66–1.47	0.71–1.08			C$^+$	1
				22 000	2.21	1.81	0.81	−0.09	0.11	C,D	3
				35 000	1.43	1.11	0.79	−0.13	0.28	C,D	3
3	$2s^23p-2s^23d$	^{2}P°–^{2}D	7236.44	17 100	0.25	0.290	0.96			B$^+$	4
				17 100	0.31	0350	0.93			B$^+$	4
				18 800	0.31	0.353	0.95			B$^+$	4
			7231.33	17 100	0.25	0.298	0.97			B$^+$	4
				17 100	0.31	0.350	0.93			B$^+$	4
				17 800	1.96	2.220	0.94	−0.142	0.56	B$^+$,B$^+$	5
				18 800	0.31	0.338	0.91			B$^+$	4
				19 500	1.44	1.448	0.76			B$^+$	5
				20 500	0.98	0.936	0.80			B$^+$	5
			7236.19	17 800	1.96	2.034	0.87	−0.159	0.63	B$^+$,B$^+$	5
				19 500	1.44	1.188	0.69			B$^+$	5
				20 500	0.98	0.914	0.78			B$^+$	5
4	$2s^23p-2s^24s$	^{2}P°–^{2}S	3920.68	12 800–30 000	0.95–1.50	0.95–1.52	0.99–1.08			C$^+$	1
5	$2s^23d-2s^24f$	^{2}D–^{2}F°	4267.26	12 800–31 000	0.40–1.33	0.96–2.34	1.30–1.11			C	1
6	$2s2p(^3P°)3s-2s2p(^3P°)3p$	^{4}P°–^{4}D	6783.91	40 000	1.61	1.02	0.75	0.14	0.40	C,C	2
7		^{4}P°–^{4}S	5648.07	20 000–30000	1.10–1.35	0.53–071				C$^+$	1
8		^{4}P°–^{4}P	5151.08	18 300	1.82	0.899		0.093		B$^+$,B$^+$	5
				19 500	1.44	0.768				B$^+$	5
				20 500	0.98	0.616				B$^+$	5
			5145.16	18 300	1.82	0.790				B$^+$	5
				19 500	1.44	0.996				B$^+$	5
				20 500	0.98	0.801				B$^+$	5
				20 000–35 000	0.90–1.35	0.50–0.93				C$^+$	1
				20 000–35 000	0.90–1.35	0.44–0.74				C$^+$	1
			5143.49	18 300	1.82	1.194		0.147		B$^+$,B$^+$	5
				19 500	1.44	0.980				B$^+$	5
				20 500	0.98	0.860				B$^+$	5
				20 000–35 000	0.90–1.35	0.32–0.89				C$^+$	1

Carbon

C III

Ground state: $1s^2 2s^2\,{}^1S_0$
Ionization energy: 47.888 eV = 386 241.0 cm^{-1}

Istrefi[1] measured the Stark widths of two C III lines with a Z-pinch plasma end on, using a shot-to-shot scanning technique. The line profiles were checked for the absence of self-absorption and were deconvoluted by a standard procedure to account for the contributions from Doppler and instrumental broadening.

Blagojević *et al.*[2] used a low-pressure pulsed arc and employed a shot-to-shot scanning procedure to determine the Stark widths of some $3s-3p$ transitions. All observations were carried out in the end-on configuration.

Negligible self-absorption for the C III lines was achieved by diluting the C_2H_2 admixture to the helium carrier gas until the intensities of the strongest lines were linearly proportional to the gas admixture. The measured line shapes were corrected for Doppler and instrumental broadening with a standard deconvolution procedure.

Srećković *et al.*[3] observed a C III line in a linear low-pressure pulsed arc end-on, on a shot-to-shot basis. Self-absorption was estimated to be negligible, based on studies of intensity ratios of C II lines within low-lying multiplets. A standard unfolding procedure was used to account for the contributions of Doppler and instrumental broadening. The results of Srećković *et al.*[3] agree with those of Kusch.[4]

Blagojević *et al.*[5] measured the Stark widths of several C III transitions with a low-pressure pulsed arc end on with a shot-to-shot scanning technique. The optical thickness of the lines (and to some extent the homogeneity of the discharge) was tested with the introduction of a movable electrode, thus creating different plasma observation lengths. Self-absorption was minimized by optimizing the composition of the gas mixture and the total pressure. The contributions of instrumental and Doppler broadening were accounted for by applying a standard deconvolution procedure.

References

[1] L. Istrefi, Rev. Roum. Phys. **33**, 667 (1988).
[2] B. Blagojević, M. V. Popović, N. Konjević, and M. S. Dimitrijević, J. Quant. Spectrosc. Radiat. Transf. **61**, 361 (1999).
[3] A. Srećković, V. Drincić, S. Bukvić, and S. Djenize, J. Phys. B **33**, 4873 (2000).
[4] H. J. Kusch, Z. Astrophys. **67**, 64 (1967).
[5] B. Blagojević, M. V. Popović, and N. Konjević, J. Quant. Spectrosc. Radiat. Transf. **67**, 9 (2000).

Key data on experiments

Reference	Plasma source	Method of measurement: Electron density	Method of measurement: Temperature	Remarks
1	Low-pressure pulsed arc	Stark width of the He II P_α line	Boltzmann plot of N II lines	
2	Low-pressure pulsed arc	Stark width of the He II P_α line	Adopted from another experiment with similar experimental conditions where temperature is measured from the Boltzmann plot of N III lines	
3	Low-pressure pulsed arc	Laser interferometer at 6328 Å	Boltzmann plot of O II and C II lines	
5	Low-pressure pulsed arc	Stark width of the He II P_α line	Boltzmann plot of N II lines	

Numerical results for C III

No.	Transition array	Multiplet	Wavelength (Å)	Temperature (K)	Electron density (10^{17} cm^{-3})	w_m (Å)	w_m/w_{th}	d_m (Å)	d_m/d_{th}	Acc.	Reference
1	$2s2p-2p^2$	^{1}P°–^{1}D	2296.89	13 800	0.91	0.324				B	3
				15 700	1.45	0.400				B	3
				17 800	1.96	0.427		−0.001		B,C	3
				19 000	1.66	0.390				B	3
				20 300	1.25	0.386				B	3
2	$2s3s-2s3p$	^{3}S–^{3}P°	4647.42	18 800	0.31	0.162	0.98			B^+	5
				19 100	0.41	0.200	0.92			B^+	5
				19 500	0.39	0.188	0.91			B^+	5
				19 800	0.44	0.220	0.95			B^+	5
				65 000	0.28	0.083	0.90			B	2
				72 400	0.58	0.161	0.88			B^+	2
				78 300	0.76	0.219	0.93			B^+	2
			4650.25	18 800	0.31	0.161	0.97			B^+	5
				19 500	0.39	0.190	0.92			B^+	5
				19 800	0.44	0.222	0.96			B^+	5
				65 000	0.28	0.083	0.90			B	2
				72 400	0.58	0.170	0.93			B^+	2
				78 300	0.76	0.219	0.93			B^+	2
			4651.47	18 300	0.33	0.160				B^+	5
				18 800	0.31	0.166	1.00			B^+	5
				19 100	0.41	0.202	0.93			B^+	5
				19 500	0.39	0.194	0.94			B^+	5
				19 800	0.44	0.223	0.96			B^+	5
				65 000	0.28	0.083	0.90			B	2
				72 400	0.58	0.163	0.89			B^+	2
3	$2p3s-2p3p$	^{3}P°–^{3}P	4659.06	32 800	4.66	6.14				C^+	1
			4673.95	32 800	4.66	3.23				C^+	1

Carbon

C IV

Ground state: $1s^2 2s^2 S_{1/2}$
Ionization energy: 64.494 eV = 520 178.4 cm^{-1}

Glenzer *et al.*[1] employed a gas-liner pinch for their Stark width measurements, while Blagojević *et al.*[2] used a low-pressure pulsed arc. In both experiments, the strongest C IV lines were tested for possible self-absorption effects, but no indications were seen for the operating conditions selected. Also, the measured line shapes were fitted to Voigt functions, so that the contributions of Doppler and instrumental broadening could be subtracted.

Glenzer *et al.* observed side on and emphasized that the observed center part of their plasma is rather homogeneous, and that no cold boundary layers exist. Blagojević *et al.*, who observed end on, did not discuss the effect of cooler plasma-end layers in the electrodes. However, the triply ionized carbon atoms should recombine there rather quickly, and produce only very small plasma inhomogeneity effects.

The increments in shift measured by Blagojević *et al.* between the two electron densities indicated in the table are in the opposite direction from those predicted by theory.[3]

Srećković *et al.*[4] measured the Stark widths of two C IV lines of the same multiplet with a low-pressure pulsed arc end-on, on a shot-to-shot basis. Self-absorption was estimated to be negligible, based on studies of intensity ratios of C II lines within low-lying multiplets and the observation that the C IV concentration is much smaller than that of C II at the electron temperature of this experiment. A standard unfolding procedure was used to account for the contributions of Doppler and instrumental broadening. The results of Srećković *et al.*[4] exhibit considerable scatter, considering that the Stark widths are for lines from the same multiplet. The theoretical comparison data are from the semiclassical calculations of Dimitrijević *et al.*[3]

References

[1] S. Glenzer, N. I. Uzelac, and H.-J. Kunze, Phys. Rev. A **45**, 8795 (1992).
[2] B. Blagojević, M. V. Popović, N. Konjević, and M. S. Dimitrijević, J. Quant. Spectrosc. Radiat. Transf. **61**, 361 (1999).
[3] M. S. Dimitrijević, S. Sahal-Bréchot, and V. Bommier, Astron. Astrophys., Suppl. Ser. **89**, 581 (1991).
[4] A. Srećković, V. Drincić, S. Bukvić, and S. Djenize, J. Phys. B **33**, 4873 (2000).

Key data on experiments

Reference	Plasma source	Method of measurement: Electron density	Method of measurement: Temperature	Remarks
1	Gas-liner pinch	90° Thomson scattering	90° Thomson scattering	
2	Low-pressure pulsed arc	Stark width of the He II P_α line	Adopted from another experiment with a similar gas mixture and the same experimental conditions	
4	Low-pressure pulsed arc	Laser interferometer at 6328 Å	Boltzmann plot of O II and C II lines	

Numerical results for C IV

No.	Transition array	Multiplet	Wavelength (Å)	Temperature (K)	Electron density (10^{17} cm^{-3})	w_m (Å)	w_m/w_{th}	d_m (Å)	d_m/d_{th}	Acc.	Reference
1	$3s-3p$	^{2}S–^{2}P°	5801.31	15 700	1.45	1.138				B	4
				17 000	1.87	1.296				B	4
				17 800	1.96	1.317				B	4
				18 300	1.82	1.264				B	4
				19 000	1.66	1.196	0.80			B	4
				72 400	0.58	0.244	0.84			B$^+$	2
				78 300	0.76	0.313	0.84			B$^+$	2
				80 100	0.80	0.329	0.85			B$^+$	2
				Δ(80 100–72 400)	Δ(0.80–0.58)			Δ(0.03)		D	2
				81 300	15	6.7	0.92			B	1
				99 800	24	9.7	0.86			B$^+$	1
			5811.97	15 700	1.45	0.964				B	4
				17 000	1.87	1.154				B	4
				17 800	1.96	1.084		0.072		B,B	4
				18 300	1.82	1.074				B	4
				19 000	1.66	1.042	0.70			B	4
				19 500	1.44	0.762	0.59			B	4
				19 800	1.37	0.735	0.60			B	4
				20 300	1.25	0.694	0.62			B	4
				72 400	0.58	0.229	0.79			B$^+$	2
				78 300	0.76	0.304	0.82			B$^+$	2
				Δ(80 100–72 400)	Δ(0.80–0.58)			Δ(0.03)		D	2

Chlorine

Cl I

Ground state: $1s^2 2s^2 2p^6 3s^2 3p^5\ ^2P^\circ_{3/2}$
Ionization energy: 12.9676 eV = 104 590.7 cm^{-1}

Djurović *et al.*[1] have observed four Cl I lines with a wall-stabilized arc end on. The center part of the arc column was operated in argon with admixtures of CCl_2F_2 (10%) and H_2 (5%), while the electrode regions were run in pure argon. The optical depth was measured with a mirror arrangement which imaged the arc column on itself and thus doubled the pathlength. Doppler, instrumental, as well as van der Waals broadening were taken into account. The measured linewidths are two times larger than the calculated semiclassical values,[2,3] while the simplified semiclassical approach[4] provides agreement within 10%.

References

[1] S. Djurović, N. Konjević, and M. S. Dimitrijević, Z. Phys. D **16**, 255 (1990).
[2] S. Sahal-Bréchot, Astron. Astrophys. **1**, 91 (1969).
[3] S. Sahal-Bréchot, Astron. Astrophys. **2**, 322 (1969).
[4] M. S. Dimitrijević and N. Konjević, Astron. Astrophys. **163**, 297 (1986).

Key data on experiments

Reference	Plasma source	Method of measurement: Electron density	Method of measurement: Temperature	Remarks
1	Wall-stabilized arc	H_β Stark width	Plasma composition data	

Numerical results for Cl I

No.	Transition array	Multiplet	Wavelength (Å)	Temperature (K)	Electron density (10^{17} cm^{-3})	w_m (Å)	w_m/w_{th}	d_m (Å)	d_m/d_{th}	Acc.	Reference
1	$3p^4(^3P)4s-3p^4(^1D)4p$	$^2P-^2D°$	4491.03	9 800	0.315	0.25	2.19			A	1
			4623.94	9 800	0.315	0.28	2.32			A	1
2		$^2D-^2D°$	8084.51	9 400	0.220	0.54	2.0			B^+	1
			8085.56	9 400	0.220	0.54	2.0			B^+	1

Chlorine

Cl II

Ground state: $1s^22s^22p^63s^23p^4\,{}^3P_2$
Ionization energy: 23.814 eV = 192 070 cm^{-1}

Kobilarov and Konjević[1] have observed Cl II lines in a low-pressure pulsed arc on a shot-to-shot basis end on. A controlled quantity of the element of interest was diluted in helium in order to obtain optically thin conditions. Self-absorption was checked by comparing the line intensity ratios within multiplets with known values and by varying the plasma length. The line profiles were corrected for instrumental and Doppler broadening using a standard deconvolution procedure.

The results of Kobilarov and Konjević[1] have been compared with values obtained with the modified semiempirical formulas of Dimitrijević and Konjević[2] and of Dimitrijević and Krsljanin.[3]

The experiment-to-theory width ratios are 1.34 and the shift ratios are 1.59.

References

[1] R. Kobilarov and N. Konjević, Phys. Rev. A. **41**, 6023 (1990).
[2] M. S. Dimitrijević and N. Konjević, J. Quant. Spectrosc. Radiat. Transf. **24**, 451 (1980).
[3] M. S. Dimitrijević and V. Krsljanin, Astron. Astrophys. **165**, 269 (1986).

Key data on experiments

Reference	Plasma source	Method of measurement: Electron density	Method of measurement: Temperature	Remarks
1	Low-pressure pulsed arc	Laser interferometer at 6328 Å and Stark width of the Paschen-α He II line	Relative intensities of O II 4366.90 and 4369.31 Å lines and Boltzmann plot of O III 3754, 3707, 3703 and 4369 Å lines	

Numerical results for Cl II

No.	Transition array	Multiplet	Wavelength (Å)	Temperature (K)	Electron density (10^{17} cm^{-3})	w_m (Å)	w_m/w_{th}	d_m (Å)	d_m/d_{th}	Acc.	Reference
1	$4s'-4p'$	$^3D°-^3P$	4336.21	27 000	0.9	0.28		0.03		A, B	1
				31 000	1.4	0.41		0.03		A, B	1
			4343.63	27 000	0.9	0.28		0.03		A, B	1
				31 000	1.4	0.42		0.03		A, B	1

Chlorine

Cl III

Ground state: $1s^2 2s^2 2p^6 3s^2 3p^3\ {}^4S^{\circ}_{3/2}$
Ionization energy: 39.61 eV = 319 500 cm^{-1}

Kobilarov and Konjević[1] observed Cl III lines in a low-pressure pulsed arc on a shot-to-shot basis end on. A controlled quantity of chlorine was diluted in helium in order to obtain optically thin conditions. Self-absorption was checked by comparing measured line intensity ratios within multiplets with well-known data and by varying the plasma length. The line profiles were corrected for instrumental and Doppler broadening using a standard deconvolution procedure.

The measurements of Kobilarov and Konjević[1] have been compared with values obtained from the modified semiempirical formulas of Dimitrijević and Konjević[2] and of Dimitrijević and Krsljanin.[3] The experiment to-theory width ratios are typically 1.1 and the shift ratios are approximately 1.7.

References

[1] R. Kobilarov and N. Konjević, Phys. Rev. A **41**, 6023 (1990).
[2] M. S. Dimitrijević and N. Konjević, J. Quant. Spectrosc. Radiat. Transf. **24**, 451 (1980).
[3] M. S. Dimitrijević and V. Krsljanin, Astron. Astrophys. **165**, 269 (1986).

Key data on experiments

Reference	Plasma source	Method of measurement: Electron density	Method of measurement: Temperature	Remarks
1	Low-pressure pulsed arc	Laser interferometer at 6328 Å and Stark width of the Paschen-α He II line	Intensity ratio of two O II lines and Boltzmann plot of four O III lines	

Numerical results for Cl III

No.	Transition array	Multiplet	Wavelength (Å)	Temperature (K)	Electron density (10^{17} cm^{-3})	w_m (Å)	w_m/w_{th}	d_m (Å)	d_m/d_{th}	Acc.	Reference
1	$4s-4p$	$^4P-{}^4D^{\circ}$	3656.95	27 000	0.9	0.18		−0.02		B^+,C	1
				31 000	1.4	0.26		−0.02		A,C	1
			3705.45	27 000	0.9	0.16		−0.02		B^+,C	1
				31 000	1.4	0.24		−0.02		A,C	1
			3670.28	27 000	0.9	0.18		−0.02		B^+,C	1
				31 000	1.4	0.26		−0.02		A,C	1
2	$4s'-4p'$	$^2D-{}^2F^{\circ}$	3560.68	27 000	0.9	0.18		−0.02		B^+,C	1
				31 000	1.4	0.26		−0.02		A,C	1
			3530.03	27 000	0.9	0.18		−0.02		B^+,C	1
				31 000	1.4	0.27		−0.02		A,C	1

Copper

Cu I

Ground state: $1s^2 2s^2 2p^6 3s^2 3p^6 3d^{10} 4s\ {}^2S_{1/2}$
Ionization energy: 7.7264 eV = 62 317.60 cm^{-1}

Skuljan *et al.*[1] have photoelectrically observed the Cu I 3247 Å resonance line end on with a pulsed arc superimposed on a glow discharge. Copper was evaporated from the electrodes, and it was estimated that there is no self-absorption in the resonance line due to the very low concentration of copper atoms in the argon–helium plasma. A standard deconvolution procedure was used to account for other broadening mechanisms. Effects of the inhomogeneous plasma end layers were not discussed.

Reference

[1] L. Skuljan, S. Bukvić, and S. Djenize, Publ. Obs. Astron. Belgrade **50**, 127 (1995).

Key data on experiment

Reference	Plasma source	Method of measurement: Electron density	Method of measurement: Temperature	Remarks
1	Low-pressure pulsed arc, superimposed on a glow discharge	Laser interferometer at 6328 Å	Intensity ratio of Ar II 5009.0 Å and Ar I 6965.0 Å lines	

Numerical results for Cu I

No.	Transition array	Multiplet	Wavelength (Å)	Temperature (K)	Electron density (10^{17}cm^{-3})	w_m (Å)	w_m/w_{th}	d_m (Å)	d_m/d_{th}	Acc.	Reference
1	$4s-4p$	^{2}S–^{2}P°	3247.54	17000	0.66	0.095				B	1

Copper

Cu II

Ground state: $1s^2 2s^2 2p^6 3s^2 3p^6 3d^{10}\,{}^1S_0$
Ionization energy: 20.2924 eV = 163 669.2 cm^{-1}

A pulsed capillary discharge was used for the Cu II Stark width measurements by Fishman *et al.*[2] (The same data were already published in Ref. 1.) The cathode contained a small amount of copper in order to keep self-absorption to at most to a few percent. The Cu II lines were photographically observed side on, 0.5–1.0 mm from the end of the capillary. The electron density was measured to be constant over the radius, and the line profiles therefore do not vary over the transverse cross section. A pulsed continuum light source was used to check and correct optical depth effects.

The authors want to point out that the advantage of their source is that a high electron density can be reached: $1.8-2.0\times10^{18}$ cm^{-3}. At this density, Stark broadening is so dominant that all other causes of line broadening as well as instrumental broadening may be neglected. No previous data are available for comparison. It should be noted that the lines within the triplets show unusually large variations in their Stark widths.

References

[1] E. V. Sarandaev and M. Kh. Salakhov, Opt. Spectrosc. (USSR) **66**, 268 (1989).
[2] I. S. Fishman, E. V. Sarandaev, and M. Kh. Salakhov, J. Quant. Spectrosc. Radiat. Transf. **52**, 887 (1994).

Key data on experiments

Reference	Plasma source	Method of measurement: Electron density	Method of measurement: Temperature	Remarks
1	Pulsed capillary discharge	H_α Stark width	Intensity ratios of three pairs of Cu II lines	Photographic technique
2	Pulsed capillary discharge		Intensity ratio of two Cu II lines and source function of the Cu I 3247 Å line	Photographic technique

Numerical results for Cu II

No.	Transition array	Multiplet	Wavelength (Å)	Temperature (K)	Electron density (10^{17} cm^{-3})	w_m (Å)	w_m/w_{th}	d_m (Å)	d_m/d_{th}	Acc.	Reference
1	$4s-4p$	^{1}D–^{3}P°	2400.11	24 000	19.2	0.79				C^+	2
2	$4p-5s$	^{3}P°–^{3}D	2403.33	24 000	19.2	2.38				C^+	2
3		^{3}F°–^{3}D	2506.27	24 000	19.2	2.44				B	2
			2544.80	24 000	19.2	2.71				B	2
			2485.79	24 000	19.2	2.17				B	2
			2713.51	24 000	19.2	2.40				C^+	2
4		^{3}D°–^{3}D	2689.30	24 000	19.2	2.30				B	2
			2666.28	24 000	19.2	2.59				C^+	2
			2590.53	24 000	19.2	1.75				C	2
5		^{1}F°–^{3}D	2769.67	24 000	19.2	2.57				B	2
6		^{1}P°–^{3}D	2877.70	24 000	19.2	2.40				C	2

Fluorine

F I

Ground state: $1s^2 2s^2 2p^5\ ^2P^\circ_{3/2}$
Ionization energy: 17.4228 eV = 140 524.3 cm^{-1}

Djurović *et al.*[1] measured two $3s-3p$ transitions with a wall-stabilized arc end on. A concave mirror behind the arc (with a light chopper) imaged the light source onto itself and thus effectively doubled the optical path, allowing precise checks for self-absorption. The optical depth was made negligible with the appropriate composition of a gas mixture containing SF_6. Confining this gas mixture to the center part of the arc column completely avoided plasma inhomogeneity problems. The Stark profiles were obtained from the measured line shapes with a standard deconvolution procedure which accounts for the contributions of Doppler and instrumental broadening.

Hong and Fleurier[2] measured the Stark widths of several F I lines with a Z pinch in a He–SF_6 gas mixture side on. Self-absorption effects were estimated to be at a moderate level, and Abel inversions were performed to obtain the plasma conditions at the center of the discharge. Since the results were published as an extended abstract for a conference only, with important experimental details missing, the uncertainty estimates presented here are of an approximate nature.

References

[1] S. Djurović, N. Konjević, and M. S. Dimitrijević, Z. Phys. D **16**, 255 (1990).
[2] D. Hong and C. Fleurier, *Spectral Line Shapes*, edited by R. Stamm and B. Talin (Nova Science, Commack, NY, 1993), Vol. 7, pp. 123–124.

Key data on experiments

Reference	Plasma source	Method of measurement: Electron density	Method of measurement: Temperature	Remarks
1	Wall-stabilized arc	H_β Stark width	Plasma composition data	
2	*Z* pinch	Stark widths of the He I lines	Ratios of S II to F I lines	No details as to which He I lines are used; no details about temperature measurements

Numerical results for F I

No.	Transition array	Multiplet	Wavelength (Å)	Temperature (K)	Electron density (10^{17} cm^{-3})	w_m (Å)	w_m/w_{th}	d_m (Å)	d_m/d_{th}	Acc.	Reference
1	$2p^4 3s-2p^4(^3P)3p$	$^4P-^4P^\circ$	7398.65	23 500	1.9	0.68	0.88			B	2
			7482.72	23 500	1.9	0.73	0.95			B	2
			742565	23 500	1.9	0.65	0.84			B	2
			7552.24	23 500	1.9	0.74	0.96			B	2
2		$^4P-^4D^\circ$	6902.48	23 500	1.9	0.63	0.89			B	2
			6909.82	23 500	1.9	0.70	0.99			B	2
			6834.26	23 500	1.9	0.62	0.88			B	2
			6870.22	23 500	1.9	0.55	0.78			B	2
			6795.53	23 500	1.9	0.62	0.88			B	2
3		$^4P-^4S^\circ$	6239.65	23 500	1.9	0.60	0.83			B	2
			6348.51	23 500	1.9	0.71	0.98			B	2
4	$3s-(^1D)3p$	$^2D-^2F^\circ$	7309.03	10 000	0.27	0.25				B	1
			7314.30	10 000	0.27	0.26				B	1

Fluorine

F II

Ground state: $1s^2 2s^2 2p^4\ ^3P_2$
Ionization energy: 34.971 eV = 282 058.6 cm^{-1}

Djenize *et al.*[1] measured the Stark widths and shifts of eight F II lines with a low-pressure pulsed arc operated in SF_6 and observed end on, using a shot-to-shot scanning procedure. The optical depth of the lines was checked by comparing measured line intensity ratios within multiplets with LS-coupling ratios. Good agreement was found by these authors, indicating small self-absorption effects. The contributions of Doppler and instrumental broadening were eliminated by applying a standard deconvolution technique to the observed Voigt profiles. The Stark shifts were measured relative to unshifted lines emitted from the same plasma at late times of the discharge, at when the electron density is considerably smaller. No shifts were detected for the $3s'-3p'$ triplet and

singlet transitions within the precision of the measurements (0.02 Å). The effects of inhomogeneous plasma end layers were not discussed.

Blagojević *et al.*[2] measured the Stark widths of two multiplets with a low-pressure pulsed arc end on. The line profiles were recorded with a shot-to-shot scanning technique. Conditions with negligible line self-absorption were found by diluting the SF_6 admixture to helium until the strongest line intensities were strictly proportional to the concentration of SF_6. To recover the Stark widths from the measured Voigt profiles, produced by contributions from instrumental and Doppler broadening, a standard deconvolution procedure was used. The effects of inhomogeneous plasma end layers near and in the electrodes are not discussed, but are estimated to be quite small.

References

[1] S. Djenize, J. Labat, A. Srećković, O. Labat, M. Platisa, and J. Purić, Phys. Scr. **44**, 148 (1991).
[2] B. Blagojević, M. V. Popović, and N. Konjević, Phys. Scr. **59**, 374 (1999).

Key data on experiments

Reference	Plasma source	Method of measurement: Electron density	Method of measurement: Temperature	Remarks
1	Low-pressure pulsed arc	Laser interferometer at 6328 Å	Boltzmann plot of F II lines and intensity ratios of F III to F II lines	
2	Low-pressure pulsed arc	Stark width of the He II P_α line	Boltzmann plot of N II lines	

Numerical results for F II

No.	Transition array	Multiplet	Wavelength (Å)	Temperature (K)	Electron density (10^{17} cm^{-3})	w_m (Å)	w_m/w_{th}	d_m (Å)	d_m/d_{th}	Acc.	Reference
1	$2p^3 3s - 2p^3(^4S°)3p$	$^5S° - ^5P$	3847.09	33 000	1.15	0.248	1.16			B^+	1
				45 000	1.90	0.348		0.06		B^+,C	1
			3849.99	33 000	1.15	0.224	1.04			B^+	1
				45 000	1.90	0.348		0.06		B^+,C	1
2		$^3S° - ^3P$	4024.73	16 300	0.31	0.065	0.84			B^+	2
				17 100	0.25	0.048	0.78			B^+	2
				17 500	0.23	0.048	0.85			B^+	2
				18 800	0.31	0.060	0.79			B^+	2
				19 500	0.39	0.076	0.80			B^+	2
			4025.50	16 300	0.31	0.063	0.82			B^+	2
				17 100	0.25	0.051	0.81			B^+	2
				17 500	0.23	0.050	0.89			B^+	2
				18 800	0.31	0.059	0.78			B^+	2
				19 500	0.39	0.076	0.80			B^+	2
3	$2p^3 3s' - 2p^3(^2D°)3p'$	$^3D° - ^3D$	4109.16	33 000	1.15	0.162				B^+	1
				45 000	1.90	0.296				B^+	1
			4119.21	45 000	1.90	0.250				B^+	1
4		$^3D° - ^3P$	3541.77	33 000	1.15	0.230				B^+	1
				45 000	1.90	0.354				B^+	1
5		$^1D° - ^1F$	4299.17	33 000	1.15	0.212				B^+	1
				45 000	1.90	0.360				B^+	1
6		$^1D° - ^1D$	3202.76	45 000	1.90	0.250				B^+	1
7	$2p^3 3p - 2p^3(^4S°)3d$	$^5P - ^5D°$	3505.63	33 000	1.15	0.276	1.17			B^+	1
				45 000	1.90	0.522		0.08		B^+,C^+	1
8		$^3P - ^3D°$	4103.09	17 100	0.25	0.060	0.79			B^+	2
			4103.53	17 100	0.25	0.063	0.82			B^+	2

Fluorine

F III

Ground state: $1s^2 2s^2 2p^3\ ^4S^\circ_{3/2}$
Ionization energy: 62.708 eV = 505 777 cm^{-1}

Djenize *et al.*[1] measured the Stark width and shift of a F III line in SF_6 with a low-pressure pulsed arc end on using a shot-to-shot scanning procedure. The optical depth of the line was checked by comparing the measured line intensity ratios within two strong F II multiplets with LS-coupling ratios. Good agreement was found, indicating minimal self-absorption effects. The contributions of Doppler and instrumental broadening were eliminated by applying a standard deconvolution technique to the observed Voigt profile. The Stark shift was measured relative to unshifted lines emitted from the same plasma at late times of the discharge the time

when the electron density is considerably smaller. No shift was detected for the F III line within the precision of the measurements (0.02 Å). The effects of inhomogeneous plasma end layers were not discussed.

Blagojević *et al.*[2] measured the Stark widths and shifts of several F III transitions with a low-pressure pulsed arc end on with a shot-to-shot scanning technique. The optical thickness of the lines (and to some degree the homogeneity of the discharge) was tested by the introduction of a movable electrode, thus creating different plasma lengths. Self-absorption was minimized by optimizing the composition of the gas mixture and the total pressure. The contributions of instrumental and Doppler broadening were accounted for by applying a standard deconvolution procedure.

References

[1] S. Djenize, J. Labat, A. Srećković, O. Labat, M. Platisa, and J. Purić, Phys. Scr. **44**, 148 (1991).
[2] B. Blagojević, M. V. Popović, and N. Konjević, J. Quant. Spectrosc. Radiat. Transf. **67**, 9 (2000).

Key data on experiments

Reference	Plasma source	Method of measurement: Electron density	Method of measurement: Temperature	Remarks
1	Low-pressure pulsed arc	Laser interferometer at 6328 Å	Boltzmann plot of F II lines and intensity ratios of F III to F II lines	
2	Low-pressure pulsed arc	Stark width of the He II P_α line	Boltzmann plot of N II lines	

Numerical results for F III

No.	Transition array	Multiplet	Wavelength (Å)	Temperature (K)	Electron density (10^{17} cm^{-3})	w_m (Å)	w_m/w_{th}	d_m (Å)	d_m/d_{th}	Acc.	Reference
1	$3s-3p$	^{2}P–^{2}D°	3174.13	33 400	0.64	0.082				B$^+$	2
				39 700	0.83	0.092				B$^+$	2
				46 000	1.05	0.122				B$^+$	2
			3174.73	39 700	0.83	0.096				B$^+$	2
				46 000	1.05	0.144				B$^+$	2
2	$3p-3d$	^{2}D°–^{2}F	2833.96	39 700	0.57	0.054				B$^+$	2
			2835.61	39 700	0.57	0.057				B$^+$	2
3	$2p^2 3p'-2p^2(^1\mathrm{D})3d'$	^{2}P°–^{2}P	3154.39	33 000	1.15	0.112				B$^+$	1
				45 000	1.90	0.202				B$^+$	1

Fluorine

F IV

Ground state: $1s^2 2s^2 2p^2\ ^3\mathrm{P}_0$
Ionization energy: 87.140 eV = 702 830 cm^{-1}

Uzelac *et al.*[1] measured the Stark width of a $3s-3p$ transition with a gas-liner pinch side on. The F IV ions, obtained from a 10% mixture of SF_6 in hydrogen, were concentrated in the center part of the discharge where the plasma is rather homogeneous. Thus, no cold boundary layers exist. The plasma reproducibility was checked by monitoring the continuum radiation. Intensity ratios of multiplet components were checked and found to adhere to LS-coupling ratios, thus showing that no appreciable self-absorption was present. The contributions of Doppler and instrumental broadening were taken into account with a deconvolution procedure based on the fitting of the observed Voigt profile.

References

[1] N. I. Uzelac, S. Glenzer, N. Konjević, J. D. Hey, and H.-J. Kunze, Phys. Rev. E **47**, 3623 (1993).

Key data on experiments

Reference	Plasma source	Method of measurement: Electron density	Method of measurement: Temperature	Remarks
1	Gas-liner pinch	90° Thomson scattering	90° Thomson scattering	

Numerical results for F IV

No.	Transition array	Multiplet	Wavelength (Å)	Temperature (K)	Electron density (10^{17} cm^{-3})	w_m (Å)	w_m/w_{th}	d_m (Å)	d_m/d_{th}	Acc.	Reference
1	$2p3s-2p(^2P°)3p$	$^3P°-^3D$	2820.74	110 000	13.6	0.64				B^+	1
				122 000	9.4	0.50				B^+	1
				167 000	15.7	0.72				B^+	1

Fluorine

F V

Ground state: $1s^22s^22p\,^2P^\circ_{1/2}$
Ionization energy: 114.24 eV = 921 430 cm^{-1}

Uzelac *et al.*[1] and Glenzer *et al.*[2] measured the Stark widths of $3s-3p$ and $3p-3d$ transitions with a gas-liner pinch side on. The fluorine ions, obtained from a 10% mixture of SF_6 in hydrogen for the test gas, were concentrated in the center part of the discharge where the hydrogen plasma is rather homogeneous, as was experimentally checked. It is a special feature of the gas-liner pinch that cold boundary layers for the test ions are essentially absent. The plasma reproducibility was checked by monitoring the continuum radiation, and intensity ratios of multiplet components were found to adhere to LS-coupling ratios, showing that no appreciable self-absorption was present. The contributions of Doppler and instrumental broadening were taken into account with a deconvolution procedure based on the fitting of the observed Voigt profiles.

Blagojević *et al.*[3] measured the Stark widths of two transitions with a low-pressure pulsed arc end on with a shot-to-shot scanning technique. The optical thickness of the lines (and to some degree the homogeneity of the discharge) was tested by the introduction of a movable electrode, which created different plasma lengths for observation. Self-absorption was minimized by optimizing the composition of the gas mixture and the total pressure. The observed line profiles were fitted to Voigt functions, so that the contributions of instrumental and Doppler broadening could be subtracted.

Some experimental results could be compared with the improved semiclassical calculations of Blagojević *et al.*[3]

References

[1] N. I. Uzelac, S. Glenzer, N. Konjević, J. D. Hey, and H.-J. Kunze, Phys. Rev. E **47**, 3623 (1993).
[2] S. Glenzer, J. D. Hey, and H.-J. Kunze, J. Phys. B **27**, 413 (1994).
[3] B. Blagojević, M. V. Popović, N. Konjević, and M. S. Dimitrijević, Phys. Rev. E **54**, 743 (1996).

Key data on experiments

Reference	Plasma source	Method of measurement: Electron density	Method of measurement: Temperature	Remarks
1, 2	Gas-liner pinch	90° Thomson scattering	90° Thomson scattering	
3	Low-pressure pulsed arc	Stark width of the He II P_α line	Boltzmann plots of the relative intensities of the F VI and F V lines	

Numerical results for F V

No.	Transition array	Multiplet	Wavelength (Å)	Temperature (K)	Electron density (10^{17} cm^{-3})	w_m (Å)	w_m/w_{th}	d_m (Å)	d_m/d_{th}	Acc.	Reference
1	$3s-(^1S)3p$	$^2S-^2P°$	2450.63	71 200	2.54	0.116	1.04			B^+	3
				294 800	37.7	1.53	1.66			B	2
2	$3p-(^1S)3d$	$^2P°-^2D$	2703.96	71 200	2.54	0.134	1.01			B^+	3
				135 800	25.9	0.97	1.02			C^+	2
3	$2s2p3s-2s2p(^3P°)3p$	$^4P°-^4D$	2702.30	135 800	25.9	0.97				C^+	2
				167 000	15.7	0.71				B	1

Fluorine

F VII

Ground state: $1s^2 2s\ ^2S_{1/2}$
Ionization energy: 185.186 eV = 1 493 629 cm^{-1}

Glenzer *et al.*[1] measured the Stark widths of the two components of the $3s$-$3p$ doublet with a gas-liner pinch. They observed side on the center part of the discharge where the plasma is rather homogeneous and a cold boundary layer is essentially absent. The two multiplet components yielded the same value for the Stark width and had an intensity ratio of 2:1 in accordance with LS coupling, thus confirming that the line emission was optically thin under the selected plasma conditions. The contributions from Doppler and instrumental broadening, both about 15% of the overall linewidths, were taken into account.

Good agreement was obtained with the semiclassical calculations of Dimitrijević and Sahal-Bréchot,[2] as shown in the table below.

References

[1] S. Glenzer, N. I. Uzelac, and H.-J. Kunze, *Spectral Line Shapes*, edited by R. Stamm and B. Talin (Nova Science, Commack, NY 1993), Vol. 7, pp. 119-120.
[2] M. S. Dimitrijević and S. Sahal-Bréchot, Astron. Astrophys., Suppl. Ser. **101**, 587 (1993).

Key data on experiments

Reference	Plasma source	Method of measurement: Electron density	Method of measurement: Temperature	Remarks
1	Gas-liner pinch	90° Thomson scattering	90° Thomson scattering	

Numerical results for F VII

No.	Transition array	Multiplet	Wavelength (Å)	Temperature (K)	Electron density (10^{17} cm^{-3})	w_m (Å)	w_m/w_{th}	d_m (Å)	d_m/d_{th}	Acc.	Reference
1	$3s-(^1S)3p$	$^2S-^2P°$	3246.56	167 100	15.7	0.87	1.06			B^+	1
				192 600	21.0	1.11	1.09			B^+	1
				214 700	29.2	1.49	1.11			B^+	1
			3276.99	167 100	15.7	0.87	1.08			B^+	1
				192 600	21.0	1.11	1.11			B^+	1
				214 700	29.2	1.49	1.14			B^+	1

Helium

He I

Ground state: $1s^2\ ^1S_0$
Ionization energy: 24.5874 eV = 198 310.68 cm^{-1}

Eight experiments with pulsed plasma sources[1–8] were performed for prominent lines of this spectrum. The optical depth for the center parts of the lines was checked either by variation of the discharge length,[3–5] including the doubling of the optical path by a mirror arrangement, or by the dilution of the helium component of the plasma.[8] Guimerans *et al.*[1] calculated the optical depth at the line centers for the conditions of their experiment. Other authors[2,6] simply stated that they had addressed the self-absorption problem, but did not provide any details.

The contributions to the measured line widths by mechanisms other than Stark broadening, mainly instrumental and Doppler broadening, were discussed by all authors and were either taken care of by standard deconvolution techniques or found to be negligible for the higher electron densities. The effects of inhomogeneous plasma end layers have not been discussed much. They were expected to be of significance in the pulsed low-pressure arc experiment of Djenize *et al.*[7] because their arc channel is expanded into wide open spaces at both ends. Smaller uncertainties due to these effects may be also introduced in some of the other experiments[3,4,5,8] whereas this is not a problem in the work of Vujićić *et al.*[2] (side-on observations) and of Büscher *et al.*[6] (no cold boundary layers in their source). About half of the authors use shot-to-shot scanning techniques, while others use optical multichannel analyzers which provide complete line profiles in each shot.

For the theoretical comparison data, the quasistatic approximation was always used. As pointed out in Refs. 3 and 8, ion dynamic corrections will improve the agreement.

It should finally be noted that some data contained in Ref. 6 were not tabulated since they were obtained in the range of nonideal plasma conditions. Also, the shifts reported in Ref. 8 were measured at the position of the halfwidth and were compared with the corresponding theoretical shifts.

References

[1] Y. Guimerans, E. J. Iglesias, D. Mandelbaum, and A. Sanchez, J. Quant. Spectrosc. Radiat. Transf. **42**, 39 (1989).

[2] B. T. Vujićić, S. Djurović, and J. Halenka, Z. Phys. D **11**, 119 (1989); S. Djurović (private communication).
[3] R. Kobilarov, N. Konjević, and M. V. Popović, Phys. Rev. A **40**, 3871 (1989).
[4] C. Perez, I. de la Rosa, A. M. de Frutos, and S. Mar, Phys. Rev. A **44**, 6785 (1991).
[5] C. Perez, J. A. Aparicio, I. de la Rosa, S. Mar, and M. A. Gigosos, Phys. Rev. E **51**, 3764 (1995).
[6] S. Büscher, S. Glenzer, Th. Wrubel, and H.-J. Kunze, J. Quant. Spectrosc. Radiat. Transf. **54**, 73 (1995).
[7] S. Djenize, Lj. Skuljan, and R. Konjević, J. Quant. Spectrosc. Radiat. Transf. **54**, 581 (1995).
[8] Z. Mijatović, N. Konjević, M. Ivković, and R. Kobilarov, Phys. Rev. E **51**, 4891 (1995).

Key data on experiments

Reference	Plasma source	Method of measurement: Electron density	Method of measurement: Temperature	Remarks
1	Low-pressure pulsed arc	Stark width and shape of the He I 4471 Å line	Line-to-continuum ratio at two wavelengths	
2	Laser-produced plasma	Stark widths of the He I 3889 and 5016 Å lines	Line-to-continuum ratio at two wavelengths	
3	Low-pressure pulsed arc	Laser interferometer at 6328 Å	Intensity ratio of O II impurity lines	
4	Low-pressure pulsed arc	Twyman–Green interferometer at five wavelengths	Intensity ratio of He II to He I lines and line intensity model	
5	Low-pressure pulsed arc	Twyman–Green interferometer at two wavelengths	Boltzmann plot of He I lines	
6	Gas-liner pinch	90° Thomson scattering	90° Thomson scattering	
7	Low-pressure pulsed arc	Laser interferometer at 6328 Å	Intensity ratios of Ar II to Ar I and He II to He I lines	
8	Low-pressure pulsed arc	CO_2 laser interferometer at 10.6 μm	H_γ line-to-continuum ratio	

Numerical results for He I

No.	Transition array	Multiplet	Wavelength (Å)	Temperature (K)	Electron density (10^{17} cm^{-3})	w_m (Å)	w_m/w_{th}	d_m (Å)	d_m/d_{th}	Acc.	Reference
1	$1s2s-1s2p$	$^1S°-^1P$	20581.30	24 400	0.077	1.18	1.38			B	1
				25 500	0,091	1.18	1.15			B	1
				25 500	0.099	1.14	1.02			B	1
2	$1s2s-1s3p$	$^1S°-^1P$	5015.68	19 000	0.200	1.76	1.04			B^+	4
				19 100	0.235	1.89	0.94			B^+	4
				19 200	0.269	2.00	0.90			B^+	4
				21 400	0.034	0.27	1.03	−0.09	1.10	A,B^+	8
				22 100	0.288	2.11	0.86			B^+	4
				22 700	0.045	0.38	1.09	−0.12	1.09	A,B^+	8
				23 600	0.059	0.47	1.02	−0.15	1.08	A,B^+	8
				30 150	0.323	2.37	0.87			A	4
				35 550	0.469	2.64	0.88			A	4
				36 450	0.646	4.40	0.79			A	4
				39 600	0.401	2.97	0.89			A	4
				40 950	0.626	3.96	0.74			A	4
				41 100	0.451	3.42	0.91			A	4
				41 350	0.556	3.98	0.85			A	4
				41 850	0.515	3.78	0.88			A	4
				42 050	0.488	3.72	0.91			A	4
				40 000	0.090			−0.08	0.44	B	7
3		$^3S-^3P°$	3888.65	31000	0.54	1.24	0.86			B^+	3
				32 000	0.19	0.46	0.93			B^+	3
				35 000	0.85	1.98	0.86			A	3
				35 500	0.35	0.87	0.94			B^+	3
				Δ(35 000–31 000)	Δ(0.85–0.54)			Δ(0.19)	0.89	B	3
				Δ(35 500–32 000)	Δ(0.35 –0.19)			Δ(0.11)	1.10	C^+	3
				36 000	0.61	1.51	0.92			B^+	3
				39 000	0.11			0.04	0.75	B	7
				40 000	0.28			0.11	0.76	B^+	7
				42 000	0.98	2.50	0.94			A	3
				Δ(42 000–36 000)	Δ(0.98–0.61)			Δ(0.30)	1.20	B^+	3
4	$1s2s-1s4p$	$^3S-^3P°$	3187.74	21 400	0.034	0.26	0.98	0.10	1.38	B^+,B^+	8
				22 700	0.045	0.32	0.91	0.13	1.34	A,B^+	8
				23 600	0.059	0.43	0.93	0.17	1.31	A,A	8
5	$1s2p-1s3s$	$^1P°-^1S$	7281.35	16 000–25 000	0.10–1.43	0.71–13.0	0.83–0.96	0.47–5.72	1.14–0.97	B^+,B^+	5
				40 000	0.060			0.16	0.77	B	7
6		$^3P°-^3S$	7065.19	21 400	0.034	0.17	0.98	0.11	1.27	B^+,B^+	8
				22 700	0.045	0.22	0.96	0.14	1.21	B^+,A	8
				23 600	0.059	0.29	0.95	0.19	1.24	A,A	8
7	$1s2p-1s3d$	$^1P°-^1D$	6678.15	19 000	0.200	1.75	0.99			B^+	4
				19 100	0.235	2.02	0.97			B^+	4
				19 200	0.269	2.26	0.98			B^+	4
				19 300	0.025	0.22	1.11	0.09	1.23	B^+,B^+	8
				21 400	0.034	0.32	1.17	0.13	1.29	B^+,B^+	8
				22 100	0.288	2.27	0.89			B^+	4
				22 700	0.045	0.43	1.17	0.16	1.24	A,A	8
				23 600	0.059	0.57	1.17	0.23	1.23	A,A	8
				26 700	0.71	6.2	0.97			B^+	2
				27 600	0.81	6.8	0.92			B^+	2
				28 700	0.915	7.6	0.91			B^+	2
				30 100	0.97	8.0	0.90			B^+	2
				30 150	0.323	2.31	0.82			A	4
				32 500	1.06	8.4	0.86			B^+	2
				34 800	1.23	8.8	0.77			B^+	2
				35 300	1.62	11.5	0.76			B^+	2
				35 550	0.469	2.62	0.84			A	4
				36 450	0.646	4.24	0.73			A	4
				39 600	0.401	2.83	0.82			A	4
				40 950	0.626	4.07	0.73			A	4

Numerical results for He I—Continued

No.	Transition array	Multiplet	Wavelength (Å)	Temperature (K)	Electron density (10^{17} cm^{-3})	w_m (Å)	w_m/w_{th}	d_m (Å)	d_m/d_{th}	Acc.	Reference
				41 350	0.556	3.92	0.80			A	4
				41 850	0.515	3.78	0.84			A	4
				42 050	0.488	3.55	0.84			A	4
				40 000	0.090			0.20	0.87	B^+	7
8		$^3P^\circ - ^3D$	5875.62	31 000	0.54	2.00	0.93			B^+	3
				35 000	0.85	3.18	0.93			A	3
				Δ(35 000–31 000)	Δ(0.85–0.54)			Δ(−0.17)	1.26	C^+	3
				36 000	0.61	2.45	1.01			A	3
				42 000	0.98	3.95	1.00			A	3
				Δ(42 000–36 000)	Δ(0.98–0.61)			Δ(−0.28)	1.63	B^+	3
				44 600	4.9	20.5	1.02	−0.94	0.63	B,B	6
9	$1s2p-1s4s$	$^3P^\circ - ^3S$	4713.15	19000	0.200	1.78	0.89			B^+	4
				19 100	0.235	2.05	0.87			B^+	4
				19 200	0.269	2.17	0.83			A	4
				22 100	0.288	2.66	0.90			A	4
				30 150	0.323	2.95	0.86			A	4
				35 550	0.469	3.62	0.94			A	4
				36 450	0.646	6.67	0.94			A	4
				39 600	0.401	4.06	0.93			A	4
				40 950	0.626	6.22	0.90			A	4
				41 100	0.451	4.66	0.95			A	4
				41 350	0.556	5.51	0.90			A	4
				41 850	0.515	5.05	0.97			A	4
				42 050	0.488	4.41	0.82			A	4
				19 300	0.025	0.23	0.94	0.15	1.23	A,B^+	8
				21 400	0.034	0.31	0.92	0.20	1.23	A,A	8
				22 700	0.045	0.41	0.92	0.27	1.25	A,A	8
				23 600	0.059	0.54	0.91	0.34	1.22	A,A	8

Iodine

I I

Ground state:
$1s^2 2s^2 2p^6 3s^2 3p^6 3d^{10} 4s^2 4p^6 4d^{10} 5s^2 5p^5\ ^2P^\circ_{3/2}$
Ionization energy: 10.4513 eV = 84 295.4 cm^{-1}

Djurović *et al.*[1,2] have observed several iodine lines with a wall-stabilized arc end on. The arc was operated in argon, and the center part, which was utilized for measurement of the line profiles, was supplied with an admixture of 5% I–H to the argon gas. A mirror, plus a light chopper, was placed behind the arc to check for possible self-absorption via doubling the pathlength. Doppler, instrumental, as well as van der Waals broadening were taken in account. The line profiles were photoelectrically recorded with a spectrometer of 0.1 Å resolution and were digitized.

No other measurements are available for comparison, but some results given in Ref. 1 have already been published in our 1990 critical review.[3]

In Ref. 1, semiempirical calculations are cited,[4,5] which provide average experiment-to-theory ratios of 0.60 and 0.71, respectively, for the widths. In Ref. 2, it was shown that of semiclassical and simplified semi-classical calculations[5,6] the simplified version provides better agreement with the experiment. Studies of regularities and similarities for the Stark widths and shifts of analogous transitions of halogens were also performed,[1,2] and the regular behavior expected was found.

References

[1] S. Djurović and N. Konjević, Z. Phys. D **11**, 113 (1989).
[2] S. Djurović, N. Konjević, and M. S. Dimitrijević, Z. Phys. D **16**, 255 (1990).
[3] N. Konjević and W. L. Wiese, J. Phys. Chem. Ref. Data **19**, 1307 (1990).
[4] S. A. Freudenstein and J. Cooper, Astrophys. J. **224**, 1079 (1978).
[5] M. S. Dimitrijević and N. Konjević, Astron. Astrophys. **163**, 297 (1986).
[6] S. Sahal-Bréchot, Astron. Astrophys. **1**, 91 (1969).

Key data on experiments

Reference	Plasma source	Method of measurement: Electron density	Method of measurement: Temperature	Remarks
1	Wall-stabilized arc	H_β Stark width	Plasma composition data	

Numerical results for I I

No.	Transition array	Multiplet	Wavelength (Å)	Temperature (K)	Electron density (10^{17} cm^{-3})	w_m (Å)	w_m/w_{th}	d_m (Å)	d_m/d_{th}	Acc.	Reference
1	$6s-6p$	^{4}P–^{4}P°	8043.74	9 300	0.21	0.74				A	1
				9 400	0.23			0.24		A	1
2		^{4}P–^{4}D°	5586.36	9 400	0.23	0.40				A	1
			5764.33	9 400	0.23	0.37				A	1
3		^{2}P–^{4}D°	6082.43	9 300	0.21			0.09		B	1
				9 400	0.23	0.44				A	1
			6293.98	9 400	0.23	0.41				A	1
4		^{4}P–^{2}P°	5427.06	9 400	0.23	0.38				A	1
5		^{2}P–^{2}P°	5894.03	9 200	0.18			0.10		B	1
				9 400	0.23	0.43				A	1
6		^{2}P–^{2}S°	6359.16	9 300	0.22	0.40				A	1
7	$6s-7p$	^{4}P–^{4}D°	4862.32	9 400	0.23	1.30				A	1
				9 400	0.22			0.49		B$^+$	1
8		^{2}P–^{2}D°	5234.57	9 200	0.18			0.45		A	1
				9 400	0.23	1.39				A	1
9		^{4}P–^{4}S°	4896.75	9 400	0.23	1.20				A	1
10		^{4}P–^{4}P°	4916.94	9 200	0.18			0.45		A	1
				9 400	0.23	1.26				A	1
11		^{2}P–^{4}P°	5119.29	9 200	0.18			0.60		A	1
				9 400	0.23	1.57				A	1
			5204.15	9 200	0.18			0.60		B$^+$	1
				9 400	0.23	1.57				A	1
12	$6s-8p$	^{4}P–^{4}D°	4102.23	9 400	0.23	0.29	3.42			A	2
13	$6s'-8p$	^{2}D–^{4}D°	7700.20	9 300	0.20	1.47	2.50			A	2
14	⋯	⋯	7305.43	9 300	0.20	1.43	2.40			B$^+$	2
15	⋯	⋯	7087.76	9 400	0.22	1.69	2.57			B$^+$	2

Iodine

I II

Ground state:
$1s^2 2s^2 2p^6 3s^2 3p^6 3d^{10} 4s^2 4p^6 4d^{10} 5s^2 5p^4\ ^3P_2$
Ionization energy: 19.131 eV = 154 304 cm^{-1}

Labat *et al.*[1] have observed three I II lines in a linear pulsed discharge end-on, on a shot-to-shot basis. The plasma is assumed to be homogeneous, but the effects of inhomogeneous end layers were not discussed. The driving gas is nitrogen at a pressure of 130 Pa, and iodine vapor was added at partial pressures of between 13 and 43 Pa. The iodine pressure was kept very low to reduce self-absorption.

The linewidths were corrected for Doppler and instrumental contributions. No other measurements are available for comparison.

Fair agreement was found with data calculated according to the simplified semiempirical formula of Dimitrijević and Konjević.[2]

References

[1] O. Labat, S. Djenize, J. Labat, J. Purić, and A. Srećković, Phys. Lett. A. **143**, 455 (1990).
[2] M. S. Dimitrijević and N. Konjević, Astron. Astrophys. **172**, 345 (1987).

Key data on experiments

Reference	Plasma source	Method of measurement: Electron density	Method of measurement: Temperature	Remarks
1	Low-pressure pulsed arc	Laser interferometer at 6328 Å	Boltzmann plot of six spectral lines of doubly ionized nitrogen	

Numerical results for I II

No.	Transition array	Multiplet	Wavelength (Å)	Temperature (K)	Electron density (10^{17} cm^{-3})	w_m (Å)	w_m/w_{th}	d_m (Å)	d_m/d_{th}	Acc.	Reference
1	$6s-6p$	$^5S^\circ-{}^5P$	5161.20	64 000	1	0.44				B	1
2		$^3S^\circ-{}^3P$	5625.69	64 000	1	0.78				B	1
3	$6s'-6p'$	$^3D^\circ-{}^3F$	5345.15	64 000	1	1.02				B	1

Iodine

I III

Ground state: $1s^22s^22p^63s^23p^63d^{10}4s^24p^64d^{10}5s^25p^3\,{}^4S^\circ_{3/2}$
Ionization energy: 33.0 eV = 266 000 cm^{-1}

Labat *et al.*[1] have observed three I III lines in a low-pressure pulsed discharge end-on, on a shot-to-shot basis. The plasma was assumed to be homogeneous, but the effects of the inhomogeneous end layers were not discussed. The driver gas was nitrogen at a pressure of 130 Pa, and iodine vapor was added at partial pressures of between 13 and 43 Pa. The iodine pressure was kept at a minimum to minimize self-absorption. The linewidths were corrected for Doppler and instrumental contributions.

No other measurements are available for comparison, and no theoretical comparison data exist.

Reference

[1] O. Labat, S. Djenize. J. Labat, J. Purić, and A. Srećković, Phys. Lett. A. **143**, 455 (1990).

Key data on experiments

Reference	Plasma source	Method of measurement: Electron density	Method of measurement: Temperature	Remarks
1	Low-pressure pulsed arc	Laser interferometer at 6328 Å	Boltzmann plot of six spectral lines of doubly ionized nitrogen	

Numerical results for I III

No.	Transition array	Multiplet	Wavelength (Å)	Temperature (K)	Electron density (10^{17} cm^{-3})	w_m (Å)	w_m/w_{th}	d_m (Å)	d_m/d_{th}	Acc.	Reference
1	[a]	[a]	3963.16	64 000	1.0	0.38				B	1
2	[a]	[a]	3613.81	64 000	1.0	0.38				B	1
3	[a]	[a]	3153.88	64 000	1.0	0.30				B	1

[a]Lines are not spectroscopically classified.

Iron

Fe I

Ground state: $1s^22s^22p^63s^23p^63d^64s^2\,{}^5D_4$
Ionization energy: 7.9024 eV = 63 737.1 cm^{-1}

Lesage *et al.*[1] measured the Stark widths of several Fe I lines with a shock tube under various plasma conditions. The optical thickness of the lines was tested by varying the density of the emitters in neon carrier gas and by looking for variations of the intensity ratios of lines within multiplets. A carbon arc was also used to compare line maxima with blackbody intensities at the same temperature and wavelength. The observed linewidths were corrected for other possible causes of line broadening in order to obtain the Stark widths. The plasma temperature was varied over a

range of 6600–10 250 K, and this showed a significant increase of the Stark widths with the temperature. For the Fe I 5383 Å line the results agree, within the error bars, with Freudenstein's[4] results, done for a narrower range of temperature. They also agree with Freudenstein's and Freudenstein and Cooper's simple theoretical formula[4,5] for the lower temperatures.

de Frutos *et al.*[2] have measured six Fe I Stark widths with a laser-generated plasma. The lines were checked for self-absorption effects, and the profiles were corrected for instrumental broadening. Stark-shift values are reported for the first time for these lines. The authors did not state the accuracy of their measurements.

Skuljan *et al.*[3] have photoelectrically observed two Fe I Stark widths in a low-pressure arc initiated by a glow discharge. Iron was evaporated from the electrodes. The very low concentration of emitters minimizes self-absorption effects for the Fe I lines in the argon–helium plasma, which is observed end on.

References

[1] A. Lesage, J. L. Lebrun, and J. Richou, Astrophys. J. **360**, 737 (1990); (private communication).
[2] A. M. de Frutos, A. Pueyo, L. Sabatier, R. Fabbro, and J. M. Orza, *Spectral Line Shapes* (Nova Science, Commack, NY, 1993), Vol. 7, p. 143.
[3] L. J. Skuljan, S. Bukvić, A. Srećković, and S. Djenize, Bull. Astron. Belgrade **152**, 17 (1995).
[4] S. Freudenstein, Ph.D. thesis, University of Colorado, 1997.
[5] S. Freudenstein and J. Cooper, Astron. Astrophys. **71**, 283 (1979).

Key data on experiments

Reference	Plasma source	Method of measurement: Electron density	Method of measurement: Temperature	Remarks
1	Shock tube	He–Ne laser interferometer at 3.39 μm	Fe I line intensity ratios	
2	Continuous CO_2 laser	Known Stark width of the Fe I 5383 Å line	Intensity ratio of two Fe I lines	
3	Low-pressure pulsed arc	He–Ne laser interferometer at 6328 Å	Intensity ratio of Ar II to Ar I lines	

Numerical results for Fe I

No.	Transition array	Multiplet	Wavelength (Å)	Temperature (K)	Electron density (10^{17} cm^{-3})	w_m (Å)	w_m/w_{th}	d_m (Å)	d_m/d_{th}	Acc.	Reference
1	$3d^74s-3d^74p$	a^5F–y^3D°	3245.97	13 000	0.38	0.262				B	3
2	$3d^64s4p-3d^64s5s$	z^7D°–e^7D	4260.47	6 000	0.10	0.11		0.051		C,B	2
3	$3d^64s4p-3d^64s4d$	z^7D°–f^5D	3239.46	13 000	0.38	0.357				B	3
4	$3d^64s4p-3d^64s5s$	z^5D°–e^5D	5393.17	6 000	0.10	0.09		0.050		B,B	2
5	$3d^74p-3d^74d$	z^5G°–e^5H	5383.37	6 000	0.100	0.212		−0.03		B,C	2
				6 600	0.04	0.032				D	1
				6 700	0.04	0.028				D	1
				7 400	0.04	0.046				C	1
				8 145	0.115	0.1373				B^+	1
				8 200	0.08	0.096				C	1
				8 400	0.25	0.360				C	1
				8 697	0.19	0.2763				A	1
				8 942	0.216	0.4144				B	1
				9 000	1.0	1.30				C	1
				9 025	0.282	0.3876				A	1
				9 097	0.26	0.2689				C	1
				9 200	0.83	0.96				C	1
				9 339	0.325	0.5605				A	1
				9 385	0.376	0.6298				B^+	1
				9 417	0.4	0.533				B^+	1
				9 500	1.07	1.5				D	1
				9 737	0.55	0.6325				D	1

Numerical results for Fe I—Continued

No.	Transition array	Multiplet	Wavelength (Å)	Temperature (K)	Electron density (10^{17} cm^{-3})	w_m (Å)	w_m/w_{th}	d_m (Å)	d_m/d_{th}	Acc.	Reference
				9 839	0.434	1.1305				C^+	1
				9 860	0.66	0.94				D	1
				9 900	0.50	0.66				D	1
				10 190	0.58	1.1686				A	1
				10 250	0.66	1.1678				A	1
				10 273	0.53	0.6491				C	1
				10 484	0.595	1.1903				A	1
				11 970	0.112	0.3167				A	1
				12 291	0.165	0.4364				B	1
				12 305	0.15	0.3673				A	1
				12 760	0.231	0.6824				A	1
				12 910	0.254	0.6334				A	1
				13 019	0.282	0.7879				A	1
				13 274	0.420	1.229				A	1
				13 305	0.388	0.808				C^+	1
				13 385	0.376	1.013				A	1
				13 449	0.43	1.242				A	1
				14 074	0.537	1.4693				A	1
			5424.07	6 000	0.100	0.28		−0.07		B,C^+	2
			5369.96	7 400	0.04	0.02				C	1
				8 200	0.08	0.10				C	1
				8 400	0.25	0.34				B	1
				9 000	1.00	0.96				B	1
				9 200	0.83	0.84				C	1
				9 500	1.07	1.12				D	1
				9 860	0.66	0.76				D	1
				9 900	0.50	0.60				D	1
			5367.47	7 400	0.04	0.024				C	1
				8 200	0.08	0.12				C	1
				8 400	0.25	0.40				B	1
				9 000	1.00	1.34				B	1
				9 200	0.83	1.26				C	1
				9 500	1.07	1.36				D	1
				9 900	0.66	1.08				D	1
				9 900	0.50	0.92				D	1
6	$z^3G°-e^3H$		5415.20	6 000	0.10	0.28		−0.064		B,B	2
				7 400	0.04	0.06				C	1
				8 200	0.08	0.164				C	1
				8 400	0.25	0.48				B	1
				9 000	1.00	1.42				B	1
				9 200	0.83	1.46				C	1
				9 400	0.50	0.92				D	1
				9 500	1.07	1.80				D	1
				9 900	0.66	1.12				D	1
			5410.91	6 000	0.10	0.21		−0.053		B,B	2
				7 400	0.04	0.06				C	1
				8 200	0.08	0.12				C	1
				8 400	0.25	0.40				B	1
				9 000	1.00	1.60				B	1
				9 400	0.50	0.84				D	1
				9 500	1.07	1.90				D	1
				9 900	0.66	0.92				D	1
7	$z^5G°-f^5G$		5404.12	7 400	0.04	0.034				C	1
				8 200	0.08	0.13				C	1
				8 400	0.25	0.36				B	1
				9 000	1.00	1.08				B	1
				9 200	0.83	1.22				C	1
				9 400	0.50	0.76				D	1
				9 500	1.07	1.30				D	1
				9 900	0.66	0.86				D	1

Iron

Fe II

Ground state: $1s^2 2s^2 2p^6 3s^2 3p^6 3d^6 4s\ ^6\mathrm{D}_{9/2}$
Ionization energy: 16.1879 eV = 130 563 cm^{-1}

Purić *et al.*[1] have photoelectrically observed two multiplets of Fe II in a low-pressure pulsed arc discharge end on with a shot-to-shot scanning technique. Iron is evaporated from the electrodes. The amount of Fe II ions released was estimated to be small enough not to cause any self-absorption. The effects of inhomogeneous plasma end layers were not discussed. The line profiles were corrected for instrumental and Doppler broadening. van der Waals broadening is smaller by more than an order of magnitude compared to the above mentioned effects and was neglected. The ion contribution is negligible under these conditions. The experimental data were compared to values obtained from trend analysis. The agreement between measured and predicted values is within 40%.

We have reduced the accuracies estimated for the 2598.37 and 2373.74 Å lines, since their measured halfwidths differ considerably from all other halfwidth data within the respective multiplets. The measured widths are compared with those obtained from the semiclassical calculations by Dimitrijević.[2]

References

[1] J. Purić, S. Djenize, A. Srećković, S. Bukvić, S. Pivalica, and J. Labat, Astron. Astrophys., Suppl. Ser. **102**, 607 (1993).
[2] M. S. Dimitrijević, Astron. Astrophys., Suppl. Ser. **111**, 565 (1995).

Key data on experiments

Reference	Plasma source	Method of measurement: Electron density	Method of measurement: Temperature	Remarks
1	Low-pressure pulsed arc	Laser interferometer at 6328 Å	Ratios of S III to S II line intensities	

Numerical results for Fe II

No.	Transition array	Multiplet	Wavelength (Å)	Temperature (K)	Electron density (10^{17} cm^{-3})	w_m (Å)	w_m/w_{th}	d_m (Å)	d_m/d_{th}	Acc.	Reference
1	$3d^6(^5\mathrm{D})4s-3d^6(^5\mathrm{D})4p$	$a^6\mathrm{D}-z^6\mathrm{D}^\circ$	2598.37	28 000	1.06	0.044	0.67			C	1
				29 000	1.64	0.058	0.58			B	1
				30 000	1.95	0.070	0.60			B	1
			2607.09	29 000	1.27	0.058	0.75			B	1
				29 000	1.64	0.076	0.76			B	1
				30 000	1.95	0.100	0.85			B	1
			2611.87	28 000	1.06	0.072	1.09			B	1
				29 000	1.64	0.090	0.90			B	1
				30 000	1.95	0.096	0.82			B	1
			2613.82	28 000	1.06	0.044	0.67			B	1
				29 000	1.64	0.072	0.72			B	1
				30 000	1.95	0.088	0.75			B	1
			2617.62	28 000	1.06	0.050	0.76			B	1
				29 000	1.64	0.072	0.72			B	1
				30 000	1.95	0.084	0.72			B	1
2		$a^6\mathrm{D}-z^6\mathrm{F}^\circ$	2373.74	28 000	1.06	0.062	1.09			C	1
			2382.04	28 000	1.06	0.048	0.84			B	1
				29 000	1.64	0.080	0.93			B	1
				30 000	1.95	0.090	0.89			B	1
			2388.63	28 000	1.06	0.044	0.77			B	1
				30 000	1.95	0.076	0.75			B	1
			2404.43	27 000	0.63	0.030	0.88			B	1
			2404.89	28 000	1.06	0.042	0.74			B	1
				29 000	1.64	0.066	0.77			B	1
				30 000	1.95	0.081	0.85			B	1
			2406.60	28 000	1.06	0.038	0.67			B	1
				30 000	1.95	0.080	0.79			B	1
			2410.52	28 000	1.06	0.042	0.74			B	1
			2410.07	28 000	1.06	0.040	0.70			B	1
			2413.31	29 000	1.64	0.068	0.79			B	1
				30 000	1.95	0.094	0.93			B	1

Krypton
Kr I

Ground state: $1s^2 2s^2 2p^6 3s^2 3p^6 3d^{10} 4s^2 4p^6\ {}^1S_0$
Ionization energy: 13.9996 eV = 112 914.35 cm^{-1}

Uzelac and Konjević[1] have used a linear flash tube of variable plasma observation length to record a Kr I line end on. This feature enabled them to take self-absorption of the line profile accurately into account. Doppler and van der Waals broadening were found to be negligible under their experimental conditions, and instrumental broadening was taken into account. Their measured Kr I 5870.9 Å linewidth is less than half the value calculated with a simple semiclassical formula,[2] but is in agreement with the experimental results of Vitel and Skowronek[3] in the small overlapping region (see Fig. 1 in Ref. 1). The measured Stark shifts of Uzelac and Konjević[1] are about 35% smaller than calculated values.[2]

Lesage *et al.*[4] have measured several Kr I lines emitted from a shock-heated plasma photographically. Small amounts of krypton and hydrogen were added to the neon carrier gas. The linewidths were corrected for self-absorption, Doppler, van der Waals and instrumental broadening.

The result for the Stark width of the Kr I 5570.3 Å line lies between earlier results of Klein and Meiners[5] and of Brandt *et al.*[6]

Knauer and Kock[7] observed two Kr I resonance lines with a wall-stabilized arc end on. The arc was operated in pure krypton at atmospheric pressure. The lines thus have large optical depths and are strongly self-reversed due to absorption in the cool electrode regions. Therefore a radiative transfer model was developed and tailored to the experimental conditions. C_4 Stark constants were obtained, utilizing known transition probabilities. The C_4 constants were converted to Stark widths for a temperature of 13000 K, close to the mean value of the measured arc temperatures.

Schinköth *et al.*[8] have observed 12 near-infrared Kr I line shapes with a wall-stabilized arc end on. Their observations were done for optically thin conditions, which were achieved by utilizing another gas as the principal carrier gas and by keeping the krypton admixture under 10%. The experimental line profiles were corrected for Doppler and instrumental broadening by applying a fitting procedure by Goly and Weniger,[9] which allows the treatment of weakly asymmetric profiles. The widths of given by Schinköth *et al.* are smaller by factors of 1.5–2.5 than those reported by Ernst *et al.*[10] Undetected self-absorption in Ref. 10 may be partly responsible for these systematic differences.

References

[1] N. I. Uzelac and N. Konjević, J. Phys. B **22**, 2517 (1989).
[2] M. S. Dimitrijević and N. Konjević, Astron. Astrophys. **163**, 297 (1986).
[3] Y. Vitel and M. Skowronek, J. Phys. B **20**, 6493 (1987).
[4] A. Lesage, D. Abadie, and M. H. Miller, Phys. Rev. A **40**, 1367 (1989).
[5] P. Klein and D. Meiners, J. Quant. Spectrosc. Radiat. Transf. **17**, 197 (1977).
[6] T. Brandt, V. Helbig, and K. P. Nick, *The Physics of Ionized Gases, SPIG 1980* (contributions) (Boris Kidric Institute of Nuclear Sciences, Beograd, Yugoslavia, 1980), p. 208.
[7] J. P. Knauer and M. Kock, J. Quant. Spectrosc. Radiat. Transf. **56**, 563 (1996).
[8] D. Schinköth, M. Kock, and E. Schulz-Gulde, J. Quant. Spectrosc. Radiat. Transf. **64**, 635 (1999).
[9] A. Goly and S. Weniger, J. Quant. Spectrosc. Radiat. Transf. **36**, 147 (1986).
[10] W. E. Ernst, B.-H. Müller, and T. Zaengel, Physica C (Amsterdam) **93**, 414 (1978).

Key data on experiments

Reference	Plasma source	Method of measurement: Electron density	Method of measurement: Temperature	Remarks
1	Linear flash tube	Stark width of H_α	Ratio of Kr I and Kr II lines	
4	Diaphragm shock tube	Stark width of H_β	Equations for shock wave compressed and heated plasma	
7	Wall-stabilized arc	Derived from temperature using the LTE model	Kr I 8509 Å optically thick and Kr I 4502 Å optically thin lines and continuum radiation	
8	Wall-stabilized arc	Emission coefficient for continuum radiation of rare gases	Total line emission coefficient of Ar II 4806 Å and Kr II 4577 Å lines	

Numerical results for Kr I

No.	Transition array	Multiplet	Wavelength (Å)	Temperature (K)	Electron density (10^{17} cm^{-3})	w_m (Å)	w_m/w_{th}	d_m (Å)	d_m/d_{th}	Acc.	Reference
1	$4p^6-4p^5 5s$	^{1}S–[1/2]°	1164.87	13 000	1.0	0.0202				B^+	7
2		^{1}S–[3/2]°	1235.84	13 000	1.0	0.0182				B^+	7
3	$5s-5p$	[3/2]°–[1/2]	7587.41	10 000	0.1	0.10				B	8
4		[3/2]°–[3/2]	7601.54	10 000	0.1	0.086				B	8
			7694.54	10 000	0.1	0.08				B	8
			8190.05	10 000	0.1	0.086				B	8
			8298.11	10 000	0.1	0.09				B	8
5		[3/2]°–[5/2]	8104.36	10 000	0.1	0.113				B	8
			8112.90	10 000	0.1	0.10				B	8
			8776.75	10 000	0.1	0.093				B	8
6	$5s-5p'$	[3/2]°–[1/2]	5570.29	11 000	1.0	0.86				B^+	4
7		[3/2]°–[3/2]	5870.91	11 500	4.5	3.0		1.0		B^+,B	1
				11 650	6.4	4.3		1.3		B^+,B	1
				11 900	7.6	5.2		1.6		B^+,B	1
				12 500	8.7	6.0		1.9		B^+,B	1
				12 750	10.2	6.8		1.9		B^+,B	1
8	$5s-6p$	[3/2]°–[3/2]	4273.97	11 000	1.0	2.75				B^+	4
			4463.69	11 000	1.0	2.63				B^+	4
9	$5s'-5p'$	[1/2]°–[1/2]	7685.24	10 000	0.1	0.093				B	8
			7854.82	10 000	0.1	0.090				B	8
10		[1/2]°–[3/2]	8059.50	10 000	0.1	0.083				B	8
			8263.24	10 000	0.1	0.105				B	8

Krypton

Kr II

Ground state: $1s^2 2s^2 2p^6 3s^2 3p^6 3d^{10} 4s^2 4p^5\ ^2P^\circ_{3/2}$
Ionization energy: 24.360 eV = 196 474.8 cm^{-1}

Finding list

Wavelength (Å)	No.	Wavelength (Å)	No.	Wavelength (Å)	No.	Wavelength (Å)	No.
3651.02	16	3906.18	21	4268.81	17	4633.89	9
3718.02	19	3920.08	12	4292.92	2	4658.88	1
3718.60	14	3921.68	20	4300.49	8	4739.00	1
3728.04	15	3994.84	4	4322.98	22	4762.44	7
3735.78	13	4057.04	10	4355.48	2	4765.74	2
3741.64	19	4065.13	11	4431.69	2	4811.76	2
3744.80	13	4088.34	11	4436.81	3	4825.18	8
3778.05	13	4098.73	4	4475.01	10	4832.08	1
3783.09	13	4109.25	11	4577.21	9	4846.61	6
3875.44	18	4145.12	5	4615.29	6		
3894.71	12	4250.58	7	4619.17	7		

Uzelac and Konjević[1] have used a linear flash tube of variable plasma observation length to record three Kr II lines end on. The variable-length feature enabled them to take self-absorption of the line profiles accurately into account. A small amount of hydrogen (3%) was added to the low-pressure krypton gas to measure the electron density via the H_α profile. Doppler and van der Waals broadening were found to be negligible under these experimental conditions, and instrumental broadening was taken into account.

Lesage *et al.*[2] have measured several Kr II lines emitted from a shock-heated plasma photographically. Small amounts of krypton and hydrogen were added to the neon carrier gas. The linewidths were corrected for self-absorption, Doppler, van der Waals, and instrumental broadening.

Bertuccelli and Di Rocco[3] have measured a fairly large number of Kr II line widths using a low-pressure pulsed capillary discharge and a shot-to-shot technique, observing end on. Competing broadening mechanisms were found to be negligible, but instrumental broadening was taken into account.

Di Rocco *et al.*[4] measured line shifts for some Kr II lines. But they did not provide any information on the plasma conditions. Thus, their results are not tabulated.

Milosavljević *et al.*[5] have measured several Kr II lines in a low-pressure pulsed arc end on in pure krypton. Line profiles were recorded on a shot-to-shot basis. The optical depth was checked by measuring the relative intensities of Kr II lines within the $5s\,^4\mathrm{P}-5p\,^4\mathrm{P}^\circ$ multiplet and by comparing them with well-known intensity data. Agreement was obtained within the estimated uncertainties, thus indicating little or no self-absorption. The line profiles were corrected for instrumental and Doppler broadening.

Comparisons with earlier experimental data listed in our previous reviews are not conclusive since they are all suspected of systematic errors.

The Stark widths measured by Milosavljević *et al.*[5] are smaller than those in Refs. 1–3, often by about factors of 2. On the other hand, the data in Ref. 5 are in satisfactory agreement with those calculated by Popović and Dimitrijević[6] with the modified semiempirical approach. Milosavljević *et al.*[5] also measured Stark shifts and found that the shifts for the lines of multiplet Nos. 2 and 6, as well as the lines at 4619.17 and 4577.21 Å were essentially zero.

References

[1] N. I. Uzelac and N. Konjević, J. Phys. B **22**, 2517 (1989).
[2] A. Lesage, D. Abadie, and M. H. Miller, Phys. Rev. A **40**, 1367 (1989).
[3] G. Bertuccelli and H. O. Di Rocco, Phys. Scr. **44**, 138 (1991).
[4] H. O. Di Rocco, G. Bertuccelli, J. Reyna Almandos, F. Bredice, and M. Gallardo, J. Quant. Spectrosc. Radiat. Transf. **41**, 161 (1989).
[5] V. Milosavljević, S. Djenize, M. S. Dimitrijević, and L. C. Popović, Phys. Rev. E **62**, 4137 (2000).
[6] L. C. Popović and M. S. Dimitrijević, Astron. Astrophys., Suppl. Ser. **127**, 295 (1998).

Key data on experiments

Reference	Plasma source	Method of measurement: Electron density	Method of measurement: Temperature	Remarks
1	Flash tube	Stark width of H_α	Intensity ratio of Kr II to Kr I line	
2	Diaphragm shock tube	Stark width of H_β	H_β and Ne I 5852 Å line intensities and line-reversal technique	Photographic technique
3	Low-pressure pulsed capillary discharge	Known experimental Stark widths of five Kr II lines	Saha relation and measurements of electrical conductivity	
5	Low-pressure pulsed arc	6328 Å laser interferometer	Intensity ratio of Kr II to Kr I lines	

Numerical results for Kr II

No.	Transition array	Multiplet	Wavelength (Å)	Temperature (K)	Electron density (10^{17} cm^{-3})	w_m (Å)	w_m/w_{th}	d_m (Å)	d_m/d_{th}	Acc.	Reference
1	$5s-5p$	$^4\mathrm{P}-^4\mathrm{P}^\circ$	4739.00	11 000	1.0	0.49				B	2
				11 500	4.5	1.8				B^+	1
				11 650	6.4	2.6				B^+	1
				11 900	7.6	3.1				B^+	1
				12 500	8.7	3.4				B^+	1
				12 750	10.2	4.0				B^+	1
				14 500	0.265	0.120				C^+	3
				17 000	1.65	0.338		−0.014		C^+,C^+	5
			4658.88	11 000	1.0	0.45				B	2
				11 500	4.5	1.8				B^+	1
				11 650	6.4	2.6				B^+	1
				11 900	7.6	3.0				B^+	1
				12 500	8.7	3.5				B^+	1
				12 750	10.2	4.0				B^+	1
				14 500	0.265	0.104				C^+	3
				17 000	1.65	0.399		−0.010		B,C^+	5
			4832.08	14 500	0.265	0.103				C^+	3
				17 000	1.65	0.429		−0.014		B,C^+	5
2		$^4\mathrm{P}-^4\mathrm{D}^\circ$	4355.48	11 000	1.0	0.39				B^+	2
				11 500	4.5	1.7				B^+	1
				11 650	6.4	2.5				B^+	1
				11 900	7.6	2.9				B^+	1
				12 500	8.7	3.4				B^+	1
				12 750	10.2	3.9				B^+	1
				14 500	0.265	0.121				C^+	3
				17 000	1.65	0.378				C^+	5
			4765.74	11 000	1.0	0.51				B	2
				14 500	0.265	0.112				C^+	3

Numerical results for Kr II—Continued

No.	Transition array	Multiplet	Wavelength (Å)	Temperature (K)	Electron density (10^{17} cm^{-3})	w_m (Å)	w_m/w_{th}	d_m (Å)	d_m/d_{th}	Acc.	Reference
				17 000	1.65	0.454				C	5
			4292.92	11 000	1.0	0.30				B	2
				14 500	0.265	0.101				C^+	3
			4811.76	14 500	0.265	0.081				C^+	3
			4431.69	11 000	1.0	0.31				B^+	2
				14 500	0.265	0.098				C^+	3
3		$^4P-^2P°$	4436.81	14 500	0.265	0.083				C^+	3
4		$^4P-^2D°$	3994.84	14 500	0.265	0.086				C^+	3
			4098.73	14 500	0.265	0.084				C^+	3
5		$^4P-^4S°$	4145.12	14 500	0.265	0.079				C^+	3
6		$^2P-^2P°$	4846.61	14 500	0.265	0.096				C^+	3
				17 000	1.65	0.426				B^+	5
			4615.29	14 500	0.265	0.089				C^+	3
				17 000	1.65	0.454				C	5
7		$^2P-^2D°$	4250.58	14 500	0.265	0.081				C^+	3
			4762.44	14 500	0.265	0.097				C^+	3
			4619.17	11 000	1.0	0.54				B	2
				14 500	0.265	0.117				C^+	3
				17 000	1.65	0.305				C	5
8		$^2P-^4S°$	4300.49	14 500	0.265	0.081				C^+	3
			4825.18	14 500	0.265	0.102				C^+	3
9	$5s'-5p'$	$^2D-^2F°$	4633.89	14 500	0.265	0.100				C^+	3
				17 000	1.65	0.391		−0.018		C^+,C^+	5
			4577.21	14 500	0.265	0.104				C^+	3
				17 000	1.65	0.449				B	5
10		$^2D-^2P°$	4475.01	17 000	1.65	0.512		−0.017		C^+,C^+	5
			4057.04	14 500	0.265	0.117				C^+	3
11		$^2D-^2D°$	4088.34	14 500	0.265	0.098				C^+	3
				17 000	1.65	0.274		−0.017		C^+,C^+	5
			4065.13	14 500	0.265	0.117				C^+	3
			4109.25	14 500	0.265	0.104				C^+	3
12	$5p-5d$	$^4D°-^4D$	3894.71	14 500	0.265	0.092				C^+	3
			3920.08	14 500	0.265	0.097				C^+	3
13		$^4D°-^4F$	3783.09	14 500	0.265	0.104				C^+	3
				17 000	1.65	0.879				B^+	5
			3778.05	17 000	1.65	0.848		0.090		B^+,B^+	5
			3744.80	14 500	0.265	0.138				C^+	3
			3735.78	14 500	0.265	0.100				C^+	3
14		$^4D°-^4P$	3718.60	14 500	0.265	0.124				C^+	3
15		$^2P°-^2P$	3728.04	14 500	0.265	0.086				C^+	3
16		$^2P°-^4P$	3651.02	14 500	0.265	0.114				C^+	3
17		$^4S°-^4F$	4268.81	14 500	0.265	0.129				C^+	3
18		$^4S°-^4P$	3875.44	14 500	0.265	0.129				C^+	3
19	$5p'-5d'$	$^2F°-^2G$	3718.02	14 500	0.265	0.089				C^+	3
			3741.64	14 500	0.265	0.110				C^+	3
20		$^2D°-^2P$	3921.68	14 500	0.265	0.178				C^+	3
21		$^2D°-^2F$	3906.18	14 500	0.265	0.111				C^+	3
22	$5s''-5p''$	$^2S-^2P°$	4322.98	14 500	0.265	0.097				C^+	3

Krypton

Kr III

Ground state: $1s^2 2s^2 2p^6 3s^2 3p^6 3d^{10} 4s^2 4p^4\ ^3P_2$
Ionization energy: 36.95 eV = 298 020 cm^{-1}

Ahmad *et al.*[1] have observed Kr III line profiles in a gas-liner pinch side on. This source produces a homogeneous and optically thin volume of plasma without the usual cold boundary layers. The test gas was 1% krypton or less in hydrogen. Stark widths were measured for three lines of the $5s\ ^5S°-5p\ ^5P$ multiplet. The observed line shapes were fitted to Voigt functions, so that the contributions of Doppler and instrumental broadening could be subtracted. They were compared with simplified semiclassical calculations by Hey and Breger.[2,3] The calculated widths systematically underestimate the experimental results, which is, according to Ref. 1, probably due to incomplete knowledge of the Kr III energy levels.

Di Rocco *et al.*[4] have measured line shifts for several Kr

III lines. But since they did not provide any information on the plasma conditions, their results are not tabulated.

Milosavljević *et al.*[5] have measured several Kr III lines in a low-pressure pulsed arc end on in pure krypton. Line profiles were recorded on a shot-to-shot basis. No optical depth check was made for this spectrum, but a test was made for Kr II lines under similar conditions (see Kr II). The line profiles were corrected for instrumental and Doppler broadening.

The results of Milosavljević *et al.*[5] are in agreement with earlier ones of Konjević and Pittman[6] at similar temperatures. Simplified semiempirical calculations by Dimitrijević and Konjević[7] provide values in good agreement with the experimental values of Refs. 5 and 6.

References

[1] I. Ahmad, S. Büscher, Th. Wrubel, and H.-J. Kunze, Phys. Rev. E **58**, 6524 (1998).
[2] J. D. Hey and P. Breger, J. Quant. Spectrosc. Radiat. Transf. **24**, 349 (1980).
[3] J. D. Hey and P. Breger, J. Quant. Spectrosc. Radiat. Transf. **24**, 427 (1980).
[4] H. O. Di Rocco, G. Bertuccelli, J. Reyna Almandos, F. Bredice, and M. Gallardo, J. Quant. Spectrosc. Radiat. Transf. **41**, 161 (1989).
[5] V. Milosavljević, S. Djenize, M. S. Dimitrijević, and L. C. Popović, Phys. Rev. E **62**, 4137 (2000).
[6] N. Konjević and T. L. Pittman, J. Quant. Spectrosc. Radiat. Transf. **37**, 311 (1987).
[7] M. S. Dimitrijević and N. Konjević, Astron. Astrophys. **172**, 345 (1987).

Key data on experiments

Reference	Plasma source	Method of measurement: Electron density	Method of measurement: Temperature	Remarks
1	Gas-liner pinch	90° Thomson scattering	90° Thomson scattering	
5	Low-pressure pulsed arc	Laser interferometer at 6328 Å	Intensity ratios of Kr II to Kr I lines	

Numerical results for Kr III

No.	Transition array	Multiplet	Wavelength (Å)	Temperature (K)	Electron density (10^{17} cm^{-3})	w_m (Å)	w_m/w_{th}	d_m (Å)	d_m/d_{th}	Acc.	Reference
1	$5s-5p$	$^5S°-^5P$	3351.93	17 000	1.65	0.308		0.032		B,C$^+$	5
				37 100	5.3	1.14				B	1
				42 900	6.5	1.15				B	1
				42 600	6.6	1.22				C$^+$	1
				40 600	7.1	1.14				C$^+$	1
				49 900	10.2	1.41				B	1
				56 900	11.6	1.81				B	1
				61 500	13.9	1.76				B	1
			3325.75	17 000	1.65	0.290		0.031		B,C$^+$	5
				37 100	5.3	1.14				B	1
				42 900	6.5	1.15				B	1
				42 600	6.6	1.22				C$^+$	1
				40 600	7.1	1.14				C$^+$	1
				49 900	10.2	1.41				B	1
				56 900	11.6	1.81				B	1
				61 500	13.9	1.76				B	1
			3245.69	17 000	1.65	0.300		0.026		B,C$^+$	5
				37 100	5.3	1.14				B	1
				42 900	6.5	1.15				B	1
				42 600	6.6	1.22				C$^+$	1
				40 600	7.1	1.14				C$^+$	1
				49 900	10.2	1.41				B	1
				56 900	11.6	1.81				B	1
				61 500	13.9	1.76				B	1
2		$^3S°-^3P$	3507.42	17 000	1.65	0.328		0.020		B,C$^+$	5
3	$5s'-5p'$	$^3D°-^3F$	3439.46	17 000	1.65	0.306		0.021		B,C$^+$	5
			3264.81	17 000	1.65	0.214		0.015		B,C	5
4		$^3D°-^3D$	3268.48	17 000	1.65	0.261				B	5
5		$^3D°-^3P$	3024.45	17 000	1.65	0.280		0.011		B,D	5
6	$5s''-5p''$	$^3P°-^3D$	3374.96	17 000	1.65	0.480		0.013		B,C	5
7		$^3P°-^3P$	3046.93	17 000	1.65	0.395				B	5
8	$4d''-5p''$	$^3P°-^3D$	3022.30	17 000	1.65	0.455				B	5

Lead

Pb I

Ground state: $1s^2 2s^2 2p^6 3s^2 3p^6 3d^{10} 4s^2 4p^6 4d^{10} 4f^{14} 5s^2 5p^6 5d^{10} 6s^2 6p^2\ ^3P_0$
Ionization energy: 7.4167 eV = 59 819.7 cm^{-1}

A pulsed capillary discharge was used for the Pb I Stark parameter measurements by Sarandaev and Salakhov[1] and by Fishman *et al.*[2] Small amounts of lead were contained in a metallic cathode, so that self-absorption was kept to a few percent. A pulsed continuum light source was used to correct optical depth effects. The Pb I resonance line at 2833 Å was the only line which needed to be corrected. The Pb I lines were observed side on, about 0.5 mm–1.0 mm from the end of the capillary. The electron density was measured to be approximately constant and the line profiles therefore do not vary over the transverse cross section. The authors pointed out that an advantage of their source is the high electron density it can reach (2.0×10^{18} cm^{-3}) which is 10 times higher than that previously obtained by Miller *et al.*[3] for the same kind of measurements. At these densities, Stark broadening is so dominant that all other causes of line broadening as well as instrumental broadening may be neglected. The line profiles were recorded photographically. In Ref. 2, the electron and ion contributions were derived separately using Eqs. (4.90) and (4.41) of Ref. 4, but in the present table only the total widths are shown.

References

[1] E. V. Sarandaev and M. Kh. Salakhov, Opt. Spectrosc. (USSR) **66**, 268 (1989).
[2] I. S. Fishman, E. V. Sarandaev, and M. Kh. Salakhov, J. Quant. Spectrosc. Radiat. Transf. **52**, 887 (1994).
[3] M. H. Miller, R. D. Bengtson and J. M. Lindsay, Phys. Rev. A **20**, 1997 (1979).
[4] H. R. Griem, *Plasma Spectroscopy* (McGraw–Hill, New York, 1964), p. 452.

Key data on experiments

Reference	Plasma source	Method of measurement: Electron density	Method of measurement: Temperature	Remarks
1	Pulsed capillary discharge	H_α Stark width	Intensity ratios of three pairs of Cu II lines	Photographic technique
2	Pulsed capillary discharge	H_α Stark width	Intensity ratios of Cu II lines and Cu I 3247 Å line source function	Photographic technique

Numerical results for Pb I

No.	Transition array	Multiplet	Wavelength (Å)	Temperature (K)	Electron density (10^{17} cm^{-3})	w_m (Å)	w_m/w_{th}	d_m (Å)	d_m/d_{th}	Acc.	Reference
1	$6p-6d$	$^3P-^3D°$	2614.18	24 000	1.0	0.209		−0.021		B^+,B^+	1
2		$^3P-^3F°$	2801.99	24 000	1.0	0.274		−0.017		B^+,B^+	1
			2873.32	24 000	1.0	0.200		0.007		C,C^+	1
3	$6p-7s$	$^3P-^3P°$	2663.61	24 000	1.0	0.081		0.049		C^+,B^+	1
			4057.81	24 000	11.0	1.76		1.21		B^+,B^+	2
			3639.57	24 000	11.0	1.43		1.03		B^+,B^+	2
			3683.46	24 000	11.0	1.43		1.03		B^+,B^+	2
			2833.06	24 000	1.0	0.077		0.062		C^+,B^+	1
4		$^1D-^3P°$	3739.94	24 000	11.0	1.54		1.03		C^+,B^+	2

Lead

Pb II

Ground state: $1s^2 2s^2 2p^6 3s^2 3p^6 3d^{10} 4s^2 4p^6 4d^{10} 4f^{14} 5s^2 5p^6 5d^{10} 6s^2 6p\ ^2P^{\circ}_{1/2}$
Ionization energy: 15.0322 eV = 121 243 cm^{-1}

Djenize *et al.*[1] have observed Pb II lines in a pulsed discharge end-on, on a shot-to-shot basis. The plasma conditions were reproducible within 6%–8%. Plasma homogeneity was assumed, but not experimentally tested. Self-absorption was assumed to be negligible due to the manner in which the lead was introduced into the plasma. The linewidths were corrected for Doppler and instrumental contributions. An earlier result by Miller *et al.*[3] for the Pb II 4386 Å line is 3.5 times larger than that of Djenize *et al.* There is no line in common with the measurements by Purić *et al.*[4] Comparisons with Griem's[5] semiempirical formula and its modified version yield ratios of 0.88 and 0.96, respectively, between measured and calculated values for the 2203.5 Å resonance line.

Fishman *et al.*[2] have photographically observed Pb II lines with a high-density pulsed capillary discharge side on. Radial electron density measurements based on the Abel inversion technique confirmed the homogeneity of their plasma. Self-absorption for the lines under study was measured and found to be rather small, not exceeding 15%.

At the high electron density of their capillary discharge, the Stark widths of the investigated Pb II lines were so large ($\approx$10 Å) that all other types of broadening as well as the instrumental width (of the order 0.1 Å) could be neglected.

The results of Fishman *et al.*[2] disagree strongly with earlier shock-tube data by Miller *et al.*[3] Fishman *et al.* speculated that significant self-absorption in the earlier work is the cause of this discrepancy. For the Pb II 4245 Å line, good agreement is obtained with the results of Purić *et al.*[4]

Nevertheless, rather conservative uncertainty estimates have been applied to the tabulated data, since the results of Refs. 1 and 2 for the only line where they overlap, the 4386 Å line, differ by more than a factor of 2.

References

[1] S. Djenize, A. Srećković, J. Labat, R. Konjević, and M. Brnović, Z. Phys. D **24**, 1 (1992).
[2] I. S. Fishman, E. V. Sarandaev, and M. Kh. Salakhov, J. Quant. Spectrosc. Radiat. Transf. **52**, 887 (1994).
[3] M. H. Miller, R. D. Bengtson, and J. M. Lindsay, Phys. Rev. A **20**, 1997 (1979).
[4] J. Purić, M. Cuk, and I. S. Lakicević, Phys. Rev. A **32**, 1106 (1985).
[5] H. R. Griem, Phys. Rev. **165**, 258 (1968).

Key data on experiments

Reference	Plasma source	Method of measurement: Electron density	Method of measurement: Temperature	Remarks
1	Low-pressure pulsed arc	Laser interferometer at 6328 Å and known Stark widths of S III and S II lines	Intensity ratio of S III and S II lines	
2	Pulsed capillary discharge	H_α Stark width	Relative intensities of two Cu II lines and source function of Cu I 3247 Å line	Photographic technique

Numerical results for Pb II

No.	Transition array	Multiplet	Wavelength (Å)	Temperature (K)	Electron density (10^{17} cm^{-3})	w_m (Å)	w_m/w_{th}	d_m (Å)	d_m/d_{th}	Acc.	Reference
1	$6p-7s$	$^2P^{\circ}-{}^2S$	2203.53	28 000	1.90	0.094				C^+	1
2	$6d-5f$	$^2D-{}^2F^{\circ}$	4244.92	24 000	11.0	8.25				C^+	2
			4386.46	24 000	11.0	7.70				C^+	2
				27 000	1.62	0.510		0.151		C^+,C^+	1
3	$7s-7p$	$^2S-{}^2P^{\circ}$	6660.20	24 000	11.0	9.90				C^+	2

Mercury

Hg II

Ground state: $1s^2 2s^2 2p^6 3s^2 3p^6 3d^{10} 4s^2 4p^6 4d^{10} 4f^{14} 5s^2 5p^6 5d^{10} 6s\ ^2S_{1/2}$
Ionization energy: 18.751 eV = 151 280 cm^{-1}

Djenize *et al.*[1] have observed Hg II lines in a pulsed discharge end-on, on a shot by shot basis. The plasma conditions were reproducible within 6%–8%. The plasma was assumed to be homogeneous, but the effects of the inhomogeneous end layers were not discussed. The driving gas was nitrogen at 390 Pa. Self-absorption was assumed to be negligible due to the method by which the mercury was introduced into the plasma. The linewidths were corrected for Doppler and instrumental contributions.

Earlier, Murakawa[2] had performed a measurement at a much lower temperature (6500 K) which produced a Stark width for the Hg II 3984.0 Å line which is approximately two times larger.

The Stark widths for the Hg II 2262 and 2224 Å lines measured by Djenize *et al.*[1] are two times larger than those calculated with semiempirical approximations,[3,4] but for Hg II 6150 Å the reverse is found.

References

[1] S. Djenize, A. Srećković, J. Labat, R. Konjević, and M. Brnović, Z. Phys. D **24**, 1 (1992).
[2] K. Murakawa, Phys. Rev. **146**, 135 (1966).
[3] H. R. Griem, Phys. Rev. **165**, 258 (1968).
[4] M. S. Dimitrijević and N. Konjević, Astron. Astrophys. **172**, 345 (1987).

Key data on experiments

Reference	Plasma source	Method of measurement: Electron density	Method of measurement: Temperature	Remarks
1	Low-pressure pulsed arc	Laser interferometer at 6328 Å and known Stark width of the N III 4200 Å line	Intensity ratios of N IV to N III lines, and N III to N II lines	

Numerical results for Hg II

No.	Transition array	Multiplet	Wavelength (Å)	Temperature (K)	Electron density (10^{17} cm^{-3})	w_m (Å)	w_m/w_{th}	d_m (Å)	d_m/d_{th}	Acc.	Reference
1	$6s^2-6s6p$	$^2D-^2P°$	2262.22	42 000	1.33	0.124		−0.03		B, D	1
2	$6s^2-5d6p$	$^2D-^2P°$	3983.93	48 000	1.37	0.192				B	1
3	$6p-6d$	$^2P°-^2D$	2224.71	42 000	1.33	0.190		−0.06		B, C	1
4	$6d-9p$	$^2D-^2P°$	3264.06	42 000	1.33	1.250		−0.05		C, C	1
5	$7s-7p$	$^2S-^2P°$	6149.50	48 000	1.37	0.690		−0.21		B, B	1

Mercury

Hg III

Ground state: $1s^2 2s^2 2p^6 3s^2 3p^6 3d^{10} 4s^2 4p^6 4d^{10} 4f^{14} 5s^2 5p^6 5d^{10}\ ^1S_0$
Ionization energy: 34.2 eV = 276 000 cm^{-1}

Djenize *et al.*[1] have observed the Hg III line at 2354 Å in a low-pressure pulsed discharge end-on, on a shot-to-shot basis. The plasma reproducibility was 6%–8%. The plasma was assumed to be homogeneous, but the effects of the inhomogeneous end layers were not discussed. The driving gas was nitrogen at 390 Pa. Self-absorption was assumed to be negligible due to the method by which the mercury is introduced into the plasma.

The linewidths were corrected for Doppler and instrumental contributions.

The measured linewidth is about two times larger than the width calculated according to semiempirical approximations.[2,3]

References

[1] S. Djenize, A. Srećković, J. Labat, R. Konjević, and M. Brnović, Z. Phys. D **24**, 1 (1992).
[2] H. R. Griem, Phys. Rev. **165**, 258 (1968).
[3] M. S. Dimitrijević and N. Konjević, Astron. Astrophys. **172**, 345 (1987).

Key data on experiments

Reference	Plasma source	Method of measurement: Electron density	Method of measurement: Temperature	Remarks
1	Low-pressure pulsed arc	Laser interferometer at 6328 Å and known Stark width of the N III 4200 Å line	Intensity ratios of N IV to N III lines, and N III to N II lines	

Numerical results for Hg III

No.	Transition array	Multiplet	Wavelength (Å)	Temperature (K)	Electron density (10^{17} cm^{-3})	w_m (Å)	w_m/w_{th}	d_m (Å)	d_m/d_{th}	Acc.	Reference
1	$6s-6p$	$^1D-^3P°$	2354.23	48 000	1.37	0.070				C^+	1

Neon

Ne I

Ground state: $1s^2 2s^2 2p^6\ ^1S_0$
Ionization energy: 21.5646 eV = 173 930.17 cm^{-1}

Finding list

Wavelength (Å)	No.	Wavelength (Å)	No.	Wavelength (Å)	No.	Wavelength (Å)	No.
5852.49	10	6182.15	19	6678.28	9	7488.87	11
5881.90	5	6217.28	3	6717.04	9	7535.77	13
5944.83	4	6266.50	9	6929.47	7	7544.04	13
5975.53	4	6304.79	3	7024.05	7	8136.41	17
6030.00	5	6334.43	2	7032.41	1	8300.33	15
6074.34	1	6382.99	3	7051.29	16	8365.75	14
6096.16	4	6402.25	2	7173.94	8	8377.61	12
6128.45	4	6506.53	2	7245.17	1	8418.43	15
6143.06	3	6532.88	7	7438.90	6	8495.36	12
6163.59	10	6598.95	10	7472.44	11	8591.26	18

Döhrn and Helbig[1] used a wall-stabilized arc end on and scanned the line profiles photoelectrically. The optical depth was found to be negligible. Instrumental, Doppler and neutral particle (van der Waals) broadening were taken into account and subtracted. Effects of the inhomogeneous plasma end layers were not discussed, and no estimates of errors were provided for the measured Stark widths and shifts. del Val *et al.*[2] employed a pulsed arc end on and a spectrometer equipped with an optical multichannel analyzer. Self-absorption was checked with a mirror arrangement in which the optical pathlength was doubled, and this effect was found to be almost negligible. The observed profiles were fitted to Voigt functions, and the Doppler and instrumental broadening contributions, obtained from measurements, were taken into account using a standard deconvolution procedure. The van der Waals pressure broadening contribution was estimated to be very small and was neglected. Effects of inhomogeneous end layers were not discussed.

The experiment/theory ratios are generally significantly better for the widths than for the shifts.

References

[1] A. Döhrn and V. Helbig, Phys. Rev. E **53**, 6581 (1996).
[2] J. A. del Val, J. A. Aparicio, and S. Mar, Astrophys. J. **513**, 535 (1999).

Key data on experiments

Reference	Plasma source	Method of measurement: Electron density	Method of measurement: Temperature	Remarks
1	Wall-stabilized arc	Two-wavelength Michelson interferometer	Plasma composition data	
2	Low-pressure pulsed arc	Twyman–Green interferometer at 4880 Å and H_α Stark width	Boltzmann plot of Ne I lines	The source of transition probabilities used for temperature measurements is not known

Numerical results for Ne I

No.	Transition array	Multiplet	Wavelength (Å)	Temperature (K)	Electron density (10^{17} cm^{-3})	w_m (Å)	w_m/w_{th}	d_m (Å)	d_m/d_{th}	Acc.	Reference
1	$2p^5(^2P^\circ_{3/2})3s-2p^5(^2P^\circ_{3/2})3p$	$^2[3/2]^\circ-^2[1/2]$	7032.41	18 000	1.0	0.45	0.89	0.074	1.09	B^+,B^+	2
			7245.17	18 000	1.0	0.48	0.87	0.077	1.92	B^+,B^+	2
			6074.34	18 000	1.0	0.63		0.142		B^+,B^+	2
2		$^2[3/2]^\circ-^2[5/2]$	6402.25	18 000	1.0	0.47	0.93	0.170	0.98	C,B^+	2
			6334.43	18 000	1.0	0.41		0.136		B^+,A	2
			6506.53	18 000	1.0	0.47	0.89	0.155	0.89	B,B^+	2
3		$^2[3/2]^\circ-^2[3/2]$	6217.28	18 000	1.0	0.43		0.156		B^+,B^+	2
			6143.06	18 000	1.0	0.42		0.171		B^+,B^+	2
			6382.99	18 000	1.0	0.44		0.152		B,A	2
			6304.79	18 000	1.0	0.52		0.168		B^+,A	2
4	$2p^5(^2P^\circ_{3/2})3s-2p^5(^2P^\circ_{1/2})3p$	$^2[3/2]^\circ-^2[3/2]$	5975.53	18 000	1.0	0.55		0.133		B^+,B^+	2
			5944.83	10 000	0.10	0.034	0.94	0.016	0.90	B^+	1
				18 000	1.0	0.43	0.94	0.134	0.71	B,B^+	2
			6128.45	18 000	1.0	0.38		0.154		C^+,B	2
			6096.16	10 000	0.10	0.037	0.98	0.015	0.85	B^+	1
				18 000	1.0	0.44	0.91	0.138	0.74	B^+,B^+	2
5		$^2[3/2]^\circ-^2[1/2]$	5881.90	10 000	0.10	0.029		0.015		B^+	1
			6030.00	18 000	1.0	0.51		0.150		B,B^+	2
6	$2p^5(^2P^\circ_{3/2})3s-2p^5(^2P^\circ_{3/2})3p$	$^2[1/2]^\circ-^2[1/2]$	7438.90	18 000	1.0	0.49		0.070		B^+,B	2
7		$^2[1/2]^\circ-^2[3/2]$	6532.88	18 000	1.0	0.50	0.90	0.160	0.80	B^+,A	2
			6929.47	18 000	1.0	0.54	0.84	0.183	1.34	B^+,B^+	2
			7024.05	18 000	1.0	0.55		0.156		B^+,B	2
8		$^2[1/2]^\circ-^2[5/2]$	7173.94	18 000	1.0	0.58		0.134		B^+,B^+	2
9	$2p^5(^2P^\circ_{1/2})3s-2p^5(^2P^\circ_{1/2})3p$	$^2[1/2]^\circ-^2[3/2]$	6266.50	18 000	1.0	0.45	0.88	0.150	0.77	B,B^+	2
			6717.04	18 000	1.0	0.57		0.164		B^+,B^+	2
			6678.28	10 000	0.10	0.047	1.09	0.019	1.41	B^+	1
10		$^2[1/2]^\circ-^2[1/2]$	6163.59	18 000	1.0	0.45		0.147		B^+,B^+	2
			6598.95	18 000	1.0	0.51		0.160		B^+,B^+	2
			5852.49	10 000	0.10	0.054		0.029		B^+	1
11	$2p^5(^2P^\circ_{3/2})3p-2p^5(^2P^\circ_{3/2})3d$	$^2[1/2]-^2[3/2]^\circ$	7488.87	18 000	1.0	4.02	0.81	1.75	0.77	B^+,A	2
			7472.44	18 000	1.0	5.59		1.83		B^+,B^+	2
12		$^2[5/2]-^2[7/2]^\circ$	8377.61	18 000	1.0	4.83	0.91	1.97	0.80	B^+,A	2

Numerical results for Ne I—Continued

No.	Transition array	Multiplet	Wavelength (Å)	Temperature (K)	Electron density (10^{17} cm^{-3})	w_m (Å)	w_m/w_{th}	d_m (Å)	d_m/d_{th}	Acc.	Reference
			8495.36	18 000	1.0	4.80	0.90	2.19	0.86	B^+,B^+	2
13		$^2[1/2]-^2[1/2]^\circ$	7535.77	18 000	1.0	3.31		1.57		B^+,B^+	2
			7544.04	18 000	1.0	4.31		1.60		B^+,A	2
14		$^2[5/2]-^2[3/2]^\circ$	8365.75	18 000	1.0	4.73		2.16		B,B	2
15		$^2[5/2]-^2[5/2]^\circ$	8300.33	18 000	1.0	4.83		2.11		B^+,B^+	2
			8418.43	18 000	1.0	2.97		1.88		B^+,B^+	2
16	$2p^5(^2P^\circ_{3/2})3p-2p^5(^2P^\circ_{1/2})3d$	$^2[1/2]-^2[3/2]^\circ$	7051.29	18 000	1.0	4.56		1.46		C^+,B^+	2
17		$^2[3/2]-^2[5/2]^\circ$	8136.41	18 000	1.0	5.22		1.91		B^+,B^+	2
18	$2p^5(^2P^\circ_{1/2})3p-2p^5(^2P^\circ_{1/2})3d$	$^2[3/2]-^2[5/2]^0$	8591.26	18 000	1.0	3.49		2.29		B^+,B^+	2
19	$2p^5(^2P^\circ_{3/2})3p-2p^5(^2P^\circ_{3/2})5s$	$^2[5/2]-^2[3/2]^\circ$	6182.15	18 000	1.0	6.16		3.93		C^+,D	2

Neon

Ne II

Ground state: $1s^22s^22p^5\ ^2P^\circ_{3/2}$
Ionization energy: 40.963 eV = 330 391.0 cm^{-1}

Finding list

Wavelength (Å)	No.	Wavelength (Å)	No.	Wavelength (Å)	No.	Wavelength (Å)	No.
3323.73	6	3459.32	30	3713.08	4	4365.64	43
3329.16	7	3477.65	8	3721.82	21	4369.86	41
3334.84	2	3479.52	32	3727.11	4	4377.95	50
3344.40	2	3480.73	32	3734.94	1	4379.50	40
3345.45	27	3481.93	5	3744.63	22	4384.08	45
3345.83	27	3503.58	14	3751.24	1	4385.06	43
3355.02	2	3537.98	29	3753.78	19	4391.94	40
3357.82	7	3542.24	29	3766.26	1	4397.94	40
3360.60	2	3542.85	18	3777.13	1	4428.52	43
3362.94	7	3546.21	13	3799.96	20	4430.90	40
3367.22	10	3557.80	5	3818.42	20	4446.46	40
3371.80	11	3561.20	17	3829.75	20	4456.95	46
3374.06	7	3565.83	18	3942.26	3	4468.91	46
3377.16	25	3568.50	26	4062.90	38	4471.52	50
3378.22	6	3571.23	15	4098.77	38	4475.22	50
3388.42	10	3574.61	26	4133.65	38	4498.94	49
3392.80	6	3590.45	15	4150.67	38	4508.21	52
3404.82	31	3594.16	18	4217.07	35	4511.37	51
3406.95	31	3612.33	12	4219.76	37	4522.66	52
3413.15	28	3628.04	23	4221.09	34	4553.16	39
3416.91	8	3632.68	16	4231.53	35	4569.01	53
3417.69	9	3643.93	4	4233.85	36	4580.35	54
3428.69	25	3644.86	23	4239.91	34	4588.13	52
3438.93	28	3659.89	16	4242.21	33	4612.89	49
3440.75	28	3664.07	1	4250.65	35	4615.98	51
3441.98	24	3679.82	23	4257.80	34	4627.85	55
3443.71	25	3694.21	1	4290.40	42	4634.73	51
3453.07	8	3697.12	23	4322.26	48		
3454.77	30	3701.78	22	4339.78	47		
3456.61	14	3709.62	1	4341.42	44		

Uzelac *et al.*[1] measured the Stark widths of several $3s-3p$ and $3p-3d$ transitions with a gas-liner pinch side on. Neon was injected along the axis of the discharge and was concentrated in the center part where the plasma is fairly homogeneous. No cold boundary layers exist for the neon test gas since it is surrounded by a hydrogen plasma of similar temperature, the ''driver gas,'' with which it gets mixed. The plasma reproducibility was checked by monitoring the continuum radiation, and intensity ratios of multiplet components were checked and found to adhere to LS-coupling ratios, indicating that no appreciable self-absorption was present. The observed line profiles were fitted to Voigt functions, so that the contributions of (the known) Doppler and measured apparatus profiles could be taken into account and

subtracted. Blagojević *et al.*[2] measured the Stark widths of two multiplets with a low-pressure pulsed arc end on, using a shot-to-shot scanning technique. They checked for self-absorption and diluted the admixture of neon to the helium carrier gas until they achieved optically thin conditions. The contributions from instrumental and Doppler broadening were eliminated by a standard deconvolution technique. The effects of inhomogeneous plasma end layers near and in the electrodes are not discussed, but are estimated to be small.

del Val *et al.*[3] measured a large number of Ne II lines in a modified[4] pulsed arc end on. The authors used the well-known mirror technique to check for self-absorption and found it to be negligible. A computerized procedure was used to extract the Lorentzian Stark component from the observed profile, using a standard deconvolution procedure. A comparison of their results with earlier experimental data and with Griems's semiclassical calculations shows fairly large discrepancies, up to a factor of 2 in some cases, which remain unresolved. Also, unexpectedly, the Stark widths measured by del Val *et al.*[3] for different transitions originating from the identical upper level, or for component lines within multiplets, often vary widely. Because of this highly irregular behavior, we have applied more conservative uncertainty estimates than the authors.

References

[1] N. I. Uzelac, S. Glenzer, N. Konjević, J. D. Hey, and H.-J. Kunze, Phys. Rev. E **47**, 3623 (1993).
[2] B. Blagojević, M. V. Popović, and N. Konjević, Phys. Scr. **59**, 374 (1999).
[3] J. A. del Val, J. A. Aparicio, and S. Mar, Astrophys. J. **536**, 998 (2000).
[4] J. A. Aparicio, M. A. Gigosos, V. R. Gonzalez, C. Perez, M. I. de la Rosa, and S. Mar, J. Phys. B **31**, 1029 (1998).

Key data on experiments

Reference	Plasma source	Method of measurement: Electron density	Method of measurement: Temperature	Remarks
1	Gas-liner pinch	90° Thomson scattering	90° Thomson scattering	
2	Low-pressure pulsed arc	Stark width of the He II P_α line	Boltzmann plot of N II lines	
3	Low-pressure pulsed arc	Laser interferometer at 4579 and 5140 Å and H_α Stark width	Boltzmann plot of Ne II and O II lines	

Numerical results for Ne II

No.	Transition array	Multiplet	Wavelength (Å)	Temperature (K)	Electron density (10^{17} cm^{-3})	w_m (Å)	w_m/w_{th}	d_m (Å)	d_m/d_{th}	Acc.	Reference
1	$2p^4(^3P)3s-2p^4(^3P)3p$	$^4P-^4P°$	3709.62	40 000	1.0	0.15	1.2			B	3
			3751.24	40 000	1.0	0.12	1.0			B	3
			3664.07	40 000	1.0	0.15	1.3			B	3
			3734.94	40 000	1.0	0.10	0.8			B	3
			3777.13	40 000	1.0	0.14	1.1			B	3
			3694.21	40 000	1.0	0.23	1.8			B	3
			3766.26	40 000	1.0	0.13	1.0			B	3
2		$^4P-^4D°$	3334.84	40 000	1.0	0.28	2.5			B	3
				73 000	19.0	1.20				B^+	1
				82 000	26.8	1.66				B^+	1
			3360.60	40 000	1.0	0.18	1.6			B	3
				73 000	19.0	1.00				B	1
				82 000	26.8	1.29				B	1
			3344.40	40 000	1.0	0.20				B	3
			3355.02	40 000	1.0	0.25	2.2			C^+	3
3		$^2P-^4D°$	3942.26	40 000	1.0	0.12				C^+	3
4		$^2P-^2D°$	3713.08	17 500	0.23	0.040	1.10			B^+	2
				18 800	0.31	0.055	1.06			B^+	2
				19 500	0.39	0.071	1.03			B^+	2
				40 000	1.0	0.29	2.0			B	3
			3727.11	17 500	0.23	0.042	1.08			B^+	2
				18 800	0.31	0.053	1.03			B^+	2
				19 500	0.39	0.070	1.08			B^+	2
				40 000	1.0	0.23	1.6			B	3
			3643.93	40 000	1.0	0.13	0.9			B	3
5		$^2P-^2S°$	3481.93	40 000	1.0	0.15				B	3
			3557.80	40 000	1.0	0.10				B	3
6		$^2P-^2P°$	3323.73	73 000	19.0	1.46				B	1
			3378.22	40 000	1.0	0.15				B	3

Numerical results for Ne II—Continued

No.	Transition array	Multiplet	Wavelength (Å)	Temperature (K)	Electron density (10^{17} cm^{-3})	w_m (Å)	w_m/w_{th}	d_m (Å)	d_m/d_{th}	Acc.	Reference
				73 000	19.0	1.55				B	1
				82 000	26.8	1.51				B	1
			3392.80	40 000	1.0	0.21				B	3
7	$2p^4(^3P)3p-2p^4(^3P)3d$	$^4D^\circ-^4D$	3362.94	40 000	1.0	0.19				B	3
			3374.06	40 000	1.0	0.16				B	3
			3357.82	40 000	1.0	0.20				B	3
			3329.16	40 000	1.0	0.19				B	3
8		$^2D^\circ-^2D$	3453.07	40 000	1.0	0.19				B	3
			3416.91	40 000	1.0	0.27				C^+	3
			3477.65	40 000	1.0	0.16				C^+	3
9		$^2D^\circ-^4F$	3417.69	17 500	0.23	0.044	1.07			B^+	2
				18 800	0.31	0.060	1.09			B^+	2
				19 500	0.39	0.071	1.13			B^+	2
				40 000	1.0	0.31	2.0			B	3
10		$^2D^\circ-^2F$	3388.42	40 000	1.0	0.28				B	3
				73 000	19.0	2.16				B	1
				82 000	26.8	2.19				B	1
			3367.22	40 000	1.0	0.26				B	3
				73 000	19.0	1.84				B^+	1
11		$^2D^\circ-^4P$	3371.80	40 000	1.0	0.24				B	3
12		$^2S^\circ-^2D$	3612.33	40 000	1.0	0.20				B	3
13		$^2S^\circ-^4P$	3546.21	40 000	1.0	0.16				B	3
14		$^2S^\circ-^2P$	3456.61	40 000	1.0	0.23	1.3			B	3
			3503.58	40 000	1.0	0.19	1.1			B	3
15		$^4S^\circ-^4F$	3571.23	40 000	1.0	0.19				B	3
			3590.45	40 000	1.0	0.20				B	3
16		$^4S^\circ-^2D$	3632.68	40 000	1.0	0.17				B	3
			3659.89	40 000	1.0	0.10				C^+	3
17		$^4S^\circ-^2F$	3561.20	40 000	1.0	0.20				B	3
18		$^4S^\circ-^4P$	3594.16	40 000	1.0	0.20	1.0			B	3
			3565.83	40 000	1.0	0.20	1.1			B	3
			3542.85	40 000	1.0	0.27	1.5			B	3
19		$^2P^\circ-^4F$	3753.78	40 000	1.0	0.20				B	3
20		$^2P^\circ-^2D$	3799.96	40 000	1.0	0.19				B	3
			3818.42	40 000	1.0	0.22				B	3
			3829.75	40 000	1.0	0.23				B	3
21		$^2P^\circ-^2F$	3721.82	40 000	1.0	0.17				B	3
22		$^2P^\circ-^4P$	3744.63	40 000	1.0	0.21				B	3
			3701.78	40 000	1.0	0.25				B	3
23		$^2P^\circ-^2P$	3679.82	40 000	1.0	0.14				C^+	3
			3697.12	40 000	1.0	0.28				C^+	3
			3628.04	40 000	1.0	0.22				B	3
			3644.86	40 000	1.0	0.23				B	3
24	$2p^4(^3P)3p-2p^4(^3P)4s$	$^4S^\circ-^4P$	3441.98	40 000	1.0	0.17				B	3
25		$^2P^\circ-^2P$	3377.16	40 000	1.0	0.46				B	3
			3428.69	40 000	1.0	0.42				B	3
			3443.71	40 000	1.0	0.56				B	3
26	$2p^4(^1D)3s-2p^4(^1D)3p$	$^2D-^2F^\circ$	3574.61	40 000	1.0	0.16				B	3
			3568.50	40 000	1.0	0.16				B	3
27		$^2D-^2P^\circ$	3345.45	40 000	1.0	0.16				B	3
			3345.83	40 000	1.0	0.21				B	3
28	$2p^4(^1D)3p-2p^4(^1D)3d$	$^2P^\circ-^2P$	3413.15	40 000	1.0	0.22				B	3
			3440.75	40 000	1.0	0.24				B	3
			3438.93	40 000	1.0	0.27				B	3
29		$^2D^\circ-^2P$	3537.98	40 000	1.0	0.23				B	3
			3542.24	40 000	1.0	0.20				B	3
30		$^2D^\circ-^2D$	3454.77	40 000	1.0	0.22				B	3
			3459.32	40 000	1.0	0.21				B	3
31		$^2D^\circ-^2F$	3404.82	40 000	1.0	0.20				B	3
			3406.95	40 000	1.0	0.23				B	3
32	$2p^4(^1S)3s-2p^4(^1S)3p$	$^2S-^2P^\circ$	3479.52	40 000	1.0	0.40				B	3
			3480.73	40 000	1.0	0.36				B	3
33	$2p^4(^3P)3d-2p^4(^3P)4f$	$^4D-^2[1]^\circ$	4242.21	40 000	1.0	1.99				B^+	3

Numerical results for Ne II—Continued

No.	Transition array	Multiplet	Wavelength (Å)	Temperature (K)	Electron density (10^{17} cm^{-3})	w_m (Å)	w_m/w_{th}	d_m (Å)	d_m/d_{th}	Acc.	Reference
34		$^4D-^2[2]°$	4221.09	40 000	1.0	1.68				B^+	3
			4239.91	40 000	1.0	1.62				B^+	3
			4257.80	40 000	1.0	1.87				B^+	3
35		$^4D^2-[3]°$	4217.07	40 000	1.0	1.99				B^+	3
			4231.53	40 000	1.0	1.74				B^+	3
			4250.65	40 000	1.0	1.83				B^+	3
36		$^4D-^2[4]°$	4233.85	40 000	1.0	1.65				B^+	3
37		$^4D-^4D°$	4219.76	40 000	1.0	1.54				B^+	3
38		$^4D-^4F°$	4133.65	40 000	1.0	1.43				B^+	3
			4150.67	40 000	1.0	1.82				B^+	3
			4062.90	40 000	1.0	1.34				B^+	3
			4098.77	40 000	1.0	1.94				B^+	3
39		$^4F-^4D°$	4553.16	40 000	1.0	1.92				B^+	3
40		$^4F-^4F°$	4430.90	40 000	1.0	2.08				B^+	3
			4446.46	40 000	1.0	1.81				B^+	3
			4379.50	40 000	1.0	1.64				B^+	3
			4397.94	40 000	1.0	1.67				B^+	3
			4391.94	40 000	1.0	1.62				B^+	3
41		$^4F-^2[3]°$	4369.86	40 000	1.0	1.87				B^+	3
42		$^4F^2-[6]°$	4290.40	40 000	1.0	1.68				B^+	3
43		$^2F-^2[3]°$	4385.06	40 000	1.0	1.58				B^+	3
			4365.64	40 000	1.0	1.45				B^+	3
			4428.52	40 000	1.0	2.08				B^+	3
44		$^2F-^4F°$	4341.42	40 000	1.0	2.55				B^+	3
45		$^2F-^4G°$	4384.08	40 000	1.0	1.93				B^+	3
46		$^2D-^4D°$	4456.95	40 000	1.0	2.04				B^+	3
			4468.91	40 000	1.0	1.86				B^+	3
47		$^2D-^4F°$	4339.78	40 000	1.0	1.95				B^+	3
48		$^2D-^4G°$	4322.26	40 000	1.0	1.90				B^+	3
49		$^4P-^4D°$	4498.94	40 000	1.0	1.83				B^+	3
			4612.89	40 000	1.0	3.37				B^+	3
50		$^4P-^4F°$	4475.22	40 000	1.0	1.79				B^+	3
			4377.95	40 000	1.0	1.74				B^+	3
			4471.52	40 000	1.0	2.01				B^+	3
51		$^2P-^4D°$	4615.98	40 000	1.0	2.16				B^+	3
			4634.73	40 000	1.0	1.73				B^+	3
			4511.37	40 000	1.0	1.84				B^+	3
52		$^2P-^4F°$	4508.21	40 000	1.0	2.40				B^+	3
			4588.13	40 000	1.0	1.98				B^+	3
			4522.66	40 000	1.0	1.76				B^+	3
53		$^2P-^4G°$	4569.01	40 000	1.0	1.92				B^+	3
54	$2p^4(^3P)4s-2p^4(^3P)4f$	$^4P-^4F°$	4580.35	40 000	1.0	2.03				B^+	3
55		$^4P-^4G°$	4627.85	40 000	1.0	1.96				B^+	3

Neon

Ne III

Ground state: $1s^2 2s^2 2p^4\ ^3P_2$
Ionization energy: 63.46 eV = 511 800 cm^{-1}

Uzelac *et al.*[1] measured the Stark widths of several $3s-3p$ and $3p-3d$ transitions with a gas-liner pinch side on. Neon was injected along the axis of the discharge and was concentrated in the center part where the plasma is fairly homogeneous. No cold boundary layers exist for the neon test gas since it is surrounded by a hydrogen plasma of similar temperature, the ''driver gas,'' with which it gets mixed. The plasma reproducibility was checked by monitoring the continuum radiation, and intensity ratios of multiplet components were checked and found to adhere to LS-coupling ratios, indicating that no appreciable self-absorption was present. The observed line profiles were fitted to Voigt functions, so that the contributions of the (known) Doppler and measured apparatus profiles could be taken into account and subtracted.

Blagojević *et al.*[2] measured the Stark widths of several Ne III transitions with a low-pressure pulsed arc end on with a shot-to-shot scanning technique. The optical thickness of the lines (and to some degree the homogeneity of the discharge)

was tested by the introduction of a movable electrode, thus creating different plasma observation lengths. Self-absorption was minimized by optimizing the composition of the gas mixture and the total pressure. The contributions of instrumental and Doppler broadening were accounted for by applying a standard deconvolution procedure.

References

[1] N. I. Uzelac, S. Glenzer, N. Konjević, J. D. Hey, and H.-J. Kunze, Phys. Rev. E **47**, 3623 (1993).
[2] B. Blagojević, M. V. Popović, and N. Konjević, J. Quant. Spectrosc. Radiat. Transf. **67**, 9 (2000).

Key data on experiments

Reference	Plasma source	Method of measurement: Electron density	Method of measurement: Temperature	Remarks
1	Gas-liner pinch	90° Thomson scattering	90° Thomson scattering	
2	Low-pressure pulsed arc	Stark width of the He II P_α line	Boltzmann plot of N II lines	

Numerical results for Ne III

No.	Transition array	Multiplet	Wavelength (Å)	Temperature (K)	Electron density (10^{17} cm^{-3})	w_m (Å)	w_m/w_{th}	d_m (Å)	d_m/d_{th}	Acc.	Reference
1	$2p^3(^4S°)3s-2p^3(^4S°)3p$	$^5S°-^5P$	2590.04	85 000	27.2	0.93				B	1
			2593.60	85 000	27.2	1.00				B	1
2		$^3S°-^3P$	2677.90	46 000	1.05	0.065				B$^+$	2
				85 000	27.2	1.14				B$^+$	1
			2678.64	46 000	1.05	0.068				B$^+$	2
3	$2p^3(^4S°)3p-2p^3(^4S°)3d$	$^3P-^3D°$	2412.73	33 400	0.64	0.045				B$^+$	2
			2412.97	33 400	0.64	0.047				B$^+$	2
4	$2p^3 3s'-2p^3(^2D°)3p'$	$^3D°-^3D$	2777.63	85 000	27.2	1.04				B$^+$	1
5		$^3D°-^3F$	2610.03	85 000	27.2	1.06				B	1
6		$^1D°-^1F$	2866.72	85 000	27.2	1.23				B$^+$	1
7	$2p^3 3p'-2p^3(^2D°)3d'$	$^1F-^1G°$	2273.58	85 000	27.2	0.78				B$^+$	1
8	$2p^3 3s''-2p^3(^2P°)3p''$	$^1P°-^1D$	2473.39	85 000	27.2	0.90				B$^+$	1
9	$2p^3 3p''-2p^3(^2P°)3d''$	$^1D-^1F°$	2507.04	85 000	27.2	1.07				B	1

Neon

Ne IV

Ground state: $1s^2 2s^2 2p^3\ ^4S^\circ_{3/2}$
Ionization energy: 97.12 eV = 783 300 cm^{-1}

Uzelac *et al.*[1] measured the Stark widths of two $3s-3p$ multiplets with a gas-liner pinch side on. Neon was injected along the axis of the discharge and was concentrated in the center part where the plasma is fairly homogeneous. No cold boundary layers exist for the neon test gas, since it is surrounded by a hydrogen plasma of similar temperature, the driver gas, with which it gets mixed. The plasma reproducibility was checked by monitoring the continuum radiation, and intensity ratios of multiplet components were checked and found to adhere to LS-coupling ratios, indicating that no appreciable self-absorption was present. The observed line profiles were fitted to Voigt functions, so that the contributions of Doppler and instrumental broadening, both determined from measurements, could be taken into account and subtracted.

References

[1] N. I. Uzelac, S. Glenzer, N. Konjević, J. D. Hey, and H.-J. Kunze, Phys. Rev. E **47**, 3623 (1993).

Key data on experiments

Reference	Plasma source	Method of measurement: Electron density	Method of measurement: Temperature	Remarks
1	Gas-liner pinch	90° Thomson scattering	90° Thomson scattering	

Numerical results for Ne IV

No.	Transition array	Multiplet	Wavelength (Å)	Temperature (K)	Electron density (10^{17} cm^{-3})	w_m (Å)	w_m/w_{th}	d_m (Å)	d_m/d_{th}	Acc.	Reference
1	$2p^2 3s - 2p^2(^3P)3p$	$^4P - ^4D^\circ$	2352.52	85 000	27.2	0.79				B^+	1
			2357.96	85 000	27.2	0.80				B^+	1
2	$2p^2 3s' - 2p^2(^1D)3p'$	$^2D - ^2F^\circ$	2285.79	85 000	27.2	0.76				B^+	1
			2293.49	85 000	27.2	0.70				B	1

Neon

Ne V

Ground state: $1s^2 2s^2 2p^2\ ^3P_0$
Ionization energy: 126.22 eV = 1 018 000 cm^{-1}

Uzelac *et al.*[1] measured the Stark widths of a $3s-3p$ multiplet with a gas-liner pinch side on. Neon was injected along the axis of the discharge and was concentrated in the center part where the plasma is fairly homogeneous. No cold boundary layers exist for the neon test gas since it is surrounded by a hydrogen plasma of similar temperature, the driver gas, with which it gets mixed. The plasma reproducibility was checked by monitoring the continuum radiation, and the intensity ratios of the multiplet components were checked and found to adhere to LS-coupling ratios, indicating that no appreciable self-absorption was present. The observed line profiles were fitted to Voigt functions, so that the contributions of Doppler and instrumental broadening, both determined from measurements, could be taken into account and subtracted.

References

[1] N. I. Uzelac, S. Glenzer, N. Konjević, J. D. Hey, and H.-J. Kunze, Phys. Rev. E **47**, 3623 (1993).

Key data on experiments

Reference	Plasma source	Method of measurement: Electron density	Method of measurement: Temperature	Remarks
1	Gas-liner pinch	90° Thomson scattering	90° Thomson scattering	

Numerical results for Ne V

No.	Transition array	Multiplet	Wavelength (Å)	Temperature (K)	Electron density (10^{17} cm^{-3})	w_m (Å)	w_m/w_{th}	d_m (Å)	d_m/d_{th}	Acc.	Reference
1	$2p3s - 2p(^2P^\circ)3p$	$^3P^\circ - ^3D$	2265.71	298 000	28.5	0.64				B^+	1

Neon

Ne VI

Ground state: $1s^2 2s^2 2p\ ^2P^\circ_{1/2}$
Ionization energy: 157.93 eV = 1 273 800 cm^{-1}

Uzelac *et al.*[1] and Glenzer *et al.*[2] measured the Stark widths of two multiplets with a gas-liner pinch side on. Neon was injected along the axis of the discharge and was concentrated in the center part where the plasma is fairly homogeneous. No cold boundary layers exist for the neon test gas since it is surrounded by a hydrogen plasma of similar temperature, the driver gas, with which it gets mixed. The Stark profiles were observed with an optical multichannel analyzer, and the plasma reproducibility was checked by monitoring the continuum radiation. The intensity ratios of multiplet components were checked and found to adhere to LS-coupling ratios, indicating that no appreciable self-absorption was present. The observed line profiles were fitted to Voigt functions, so that the contributions of Doppler and instrumental broadening, both determined from appropriate measurements, could be taken into account and subtracted.

References

[1] N. I. Uzelac, S. Glenzer, N. Konjević, J. D. Hey, and H.-J. Kunze, Phys. Rev. E **47**, 3623 (1993).
[2] S. Glenzer, J. D. Hey, and H.-J. Kunze, J. Phys. B **27**, 413 (1994).

Key data on experiments

Reference	Plasma source	Method of measurement: Electron density	Method of measurement: Temperature	Remarks
1, 2	Gas-liner pinch	90° Thomson scattering	90° Thomson scattering	

Numerical results for Ne VI

No.	Transition array	Multiplet	Wavelength (Å)	Temperature (K)	Electron density (10^{17} cm^{-3})	w_m (Å)	w_m/w_{th}	d_m (Å)	d_m/d_{th}	Acc.	Reference
1	$2s2p3s-2s2p(^3P°)3p$	$^4P°-^4D$	2253.22	156 700	44.4	0.98				B^+	2
				291 000	20.5	0.57				B^+	1
				298 000	28.5	0.72				B^+	1
2	$3p-(^1S)3d$	$^2P°-^2D$	2229.0	156 700	44.4	0.84				B^+	2

Neon

Ne VII

Ground state: $1s^2 2s^2\ ^1S_0$
Ionization energy: 207.28 eV = 1 671 792 cm^{-1}

Wrubel *et al.*[1,2] measured the profiles of the $3s-3p$ transitions of this Be-like ion with a gas-liner pinch. Neon was injected along the axis of the discharge and was confined to the center part where the plasma was found to be nearly homogeneous. No cold boundary layers exist for the neon plasma since it is surrounded by a hydrogen plasma of similar temperature, the driver gas, with which it gets mixed. The Stark profiles were observed side on with a spectrometer equipped with an optical multichannel analyzer. The intensity ratios of the triplet lines were measured and found to adhere to the LS-coupling ratios, indicating the absence of self-absorption. The observed line profiles were fitted to Voigt functions with a least-squares procedure, so that the contributions of the measured instrumental broadening and Doppler profile could be taken into account and subtracted.

References

[1] Th. Wrubel, S. Glenzer, S. Büscher, H.-J. Kunze, and S. Alexiou, Astron. Astrophys. **307**, 1023 (1996).
[2] Th. Wrubel, I. Ahmad, S. Büscher, H.-J. Kunze, and S. H. Glenzer, Phys. Rev. E **57**, 5972 (1998).

Key data on experiments

Reference	Plasma source	Method of measurement: Electron density	Method of measurement: Temperature	Remarks
1, 2	Gas-liner pinch	90° Thomson scattering	90° Thomson scattering	

Numerical results for Ne VII

No.	Transition array	Multiplet	Wavelength (Å)	Temperature (K)	Electron density (10^{17} cm^{-3})	w_m (Å)	w_m/w_{th}	d_m (Å)	d_m/d_{th}	Acc.	Reference
1	$2s3s-2s(^2S)3p$	$^3S-^3P°$	1981.97	238 000	30	0.45				B^+	1, 2
			1992.06	238 000	30	0.45				B	1
			1997.35	238 000	30	0.45				C^+	1
2		$^1S-^1P°$	3643.6	220 500	35	1.76				B^+	1, 2

Neon

Ne VIII

Ground state: $1s^2 2s\ ^2S_{1/2}$
Ionization energy: 239.099 eV = 1 928 462 cm^{-1}

Glenzer *et al.*[1] measured the Stark width of the stronger component of the $3s-3p$ doublet with a gas-liner pinch. They observed the center part of their pinch discharge side on, where the plasma is rather homogeneous and where no cold boundary layers exist. The possiblity of self-absorption was tested by measuring the intensity ratio of the two multiplet components, which was found to be 2:1 in agreement with the LS-coupling value, thus indicating optically thin conditions. The measured line shapes were fitted to Voigt functions, so that the contributions of Doppler and instrumental broadening could be subtracted.

The experimental results were compared to semiclassical calculations by Dimitrijević and Sahal-Bréchot.[2]

References

[1] S. Glenzer, N. I. Uzelac, and H.-J. Kunze, Phys. Rev. A **45**, 8795 (1992).
[2] M. S. Dimitrijević and S. Sahal-Bréchot, Bull. Astron. Belgrade **148**, 29 (1993).

Key data on experiments

Reference	Plasma source	Method of measurement: Electron density	Method of measurement: Temperature	Remarks
1	Gas-liner pinch	90° Thomson scattering	90° Thomson scattering	

Numerical results for Ne VIII

No.	Transition array	Multiplet	Wavelength (Å)	Temperature (K)	Electron density (10^{17} cm^{-3})	w_m (Å)	w_m/w_{th}	d_m (Å)	d_m/d_{th}	Acc.	Reference
1	$3s-3p$	$^2S-^2P°$	2820.7	344 700	28	1.2	1.61			B^+	1
				493 200	32	1.2	1.68			B^+	1

Nickel

Ni I

Ground state: $1s^2 2s^2 2p^6 3s^2 3p^6 3d^8 4s^2\ ^3F_4$
Ionization energy: 7.6398 eV = 61 619 cm^{-1}

Three experiments[1–3] were carried out with a low-pressure pulsed arc discharge. The observations were done in the end-on mode on a shot-to-shot basis. Using numerical estimates, self-absorption was neglected due to the very low concentration of emitting atoms. The effects of the inhomogeneous plasma end layers were not discussed. The line profiles were corrected for Doppler and instrumental broadening. Satisfactory agreement was found between the measured widths of the Ni I 3461 and 3414 Å lines[3] and those calculated in Ref. 3 using a simplified semiclassical method of Freudenstein and Cooper.[4] These lines are transitions between lower excited levels. But for the Ni I 3446 and 3619 Å lines, the measured values are two to three times larger than the calculated ones.

References

[1] Lj. Skuljan, S. Bukvić, A. Srećković, and S. Djenize, Bull. Astron. Belgrade **152**, 17 (1995).
[2] A. Srećković, S. Bukvić, and S. Djenize, Publ. Obs. Astron. Belgrade **53**, 147 (1996).
[3] S. Djenize, Lj. Skuljan, J. Labat, S. Bukvić, and R. Konjević, Astron. Astrophys., Suppl. Ser. **105**, 115 (1994).
[4] S. Freudenstein and J. Cooper, Astron., Astrophys. **71**, 283 (1979).

Key data on experiments

Reference	Plasma source	Method of measurement: Electron density	Method of measurement: Temperature	Remarks
1, 3	Low-pressure pulsed arc	He–Ne laser interferometer at 6328 Å	Intensity ratio of Ar II 5009 Å and Ar I 6965 Å spectral lines	
2	Low-pressure pulsed arc	He–Ne laser interferometer at 6328 Å	Intensity ratios of N IV 3479 Å, N III 3939 Å and N II 3990 Å spectral lines	

Numerical results for Ni I

No.	Transition array	Multiplet	Wavelength (Å)	Temperature (K)	Electron density (10^{17} cm^{-3})	w_m (Å)	w_m/w_{th}	d_m (Å)	d_m/d_{th}	Acc.	Reference
1	$3d^9 4s - 3d^8 4s 4p$	a^3D–z^5F°	3461.66	18 000	0.66	0.050		0.013		B,C	3
2	$3d^9 4s - 3d^9 4p$	a^3D–z^3F°	3414.76	13 000	0.38	0.029		0.016		C^+,C	3
3		a^3D–z^3D°	3446.26	18 000	0.66	0.170				B	3
4		a^3D–z^1F°	3243.05	17 000	0.55	0.197				B	1
5		a^1D–z^3P°	3973.55	46 000	2.4	0.550		0.029		B,C	2
				47 000	3.0	0.692		0.029		B,C	2
				47 000	3.6	0.700		0.056		B,C	2
				47 000	4.2	0.781		0.072		B, C	2
6		a^1D–z^1F°	3619.39	13 000	0.36	0.072				C^+	3

Nickel

Ni II

Ground state: $1s^2 2s^2 2p^6 3s^2 3p^6 3d^9\ ^2D_{5/2}$
Ionization energy: 18.169 eV = 146 541.56 cm^{-1}

Djenize *et al.*[1] have observed two Ni II lines in a low-pressure pulsed arc end-on, on a shot-to-shot basis. The plasma was assumed to be homogeneous, but the effects of the inhomogeneous end layers were not discussed. Self-absorption was assumed to be negligible due to the very low concentration of emitting atoms, and this was checked by numerical estimates. The line profiles were corrected for Doppler and apparatus contributions. Measured widths were compared with the values calculated with Griems semiempirical formula[2] and with the modified semiempirical formula of Dimitrijević and Konjević.[3]

The calculated values are 3.2 to 4.4 times smaller than the measured ones. Semiclassical calculations done by Dimitrijević[4] reduce the disagreement to factors of 1.7 and 1.5, respectively.

References

[1] S. Djenize, Lj. Skuljan, J. Labat, S. Bukvić, and R. Konjević, Astron. Astrophys., Suppl. Ser. **105**, 115 (1994).
[2] H. R. Griem, Phys. Rev. **165**, 258 (1968).
[3] M. S. Dimitrijević and N. Konjević, Astron. Astrophys. **172**, 345 (1987).
[4] M. S. Dimitrijević, Astron. Astrophys., Suppl. Ser. **114**, 171 (1995).

Key data on experiments

Reference	Plasma source	Method of measurement: Electron density	Method of measurement: Temperature	Remarks
1	Low-pressure pulsed arc	He–Ne laser interferometer at 6328 Å	Intensity ratio of the Ar II 5009 Å and Ar I 6965 Å lines	

Numerical results for Ni II

No.	Transition array	Multiplet	Wavelength (Å)	Temperature (K)	Electron density (10^{17} cm^{-3})	w_m (Å)	w_m/w_{th}	d_m (Å)	d_m/d_{th}	Acc.	Reference
1	$3d^8 4s - 3d^8 4p$	a^4F–z^4G°	2264.46	17 000	0.55	0.056	1.7	0.022		B,C	1
			2270.21	17 000	0.55	0.050	1.5			B	1

Nitrogen

N I

Ground state: $1s^2 2s^2 2p^3\ ^4S^\circ_{3/2}$
Ionization energy: 14.5341 eV = 117 225.4 cm^{-1}

Jones *et al.*[1] measured the Stark widths and ion broadening parameters for five N I lines with a wall-stabilized arc end on. (Their paper, published in 1987, was inadvertently omitted from our last review.) A gas mixture of argon with a small amount of nitrogen was admitted into the center part of the arc column and was kept from entering the inhomogeneous electrode regions by an appropriate gas flow arrangement. Self-absorption was checked with a concave mirror and light chopper behind the arc, which focused the source back into itself and thus effectively doubled the optical pathlength. The observed linewidths were corrected for Doppler and instrumental broadening.

The results for the Stark widths agree usually within ±10% with earlier experiments. Ion broadening parameters were also determined and are in fair agreement (±25%) with calculated values.

Sohns and Kock[2] determined the Stark widths of some strong vacuum ultraviolet lines—all resonance transitions—with a wall-stabilized arc under plasma conditions where the lines are strongly self-reversed. They applied a model calculation based on the equation of radiative transfer to the measured line shapes, from which the Stark widths were recovered.

References

[1] D. W. Jones, G. Pichler, and W. L. Wiese, Phys. Rev. A **35**, 2585 (1987).
[2] E. Sohns and M. Kock, J. Quant. Spectrosc. Radiat. Transf. **47**, 335 (1992).

Key data on experiments

Reference	Plasma source	Method of measurement: Electron density	Method of measurement: Temperature	Remarks
1	Wall-stabilized arc	H_β Stark width	Plasma composition data	
2	Wall-stabilized arc	Plasma model calculation	Blackbody limited VUV lines	Line profiles measured under optically thick conditions

Numerical results for N I

No.	Transition array	Multiplet	Wavelength (Å)	Temperature (K)	Electron density (10^{17} cm^{-3})	w_m (Å)	w_m/w_{th}	d_m (Å)	d_m/d_{th}	Acc.	Reference
1	$2p^3-2p^2(^3P)3s$	$^4S°-^4P$	1199.55	12 500	1.0	0.0068	0.44			C^+	2
			1200.22	12 500	1.0	0.0068	0.44			C^+	2
			1200.71	12 500	1.0	0.0068	0.44			C^+	2
2		$^2D°-^2P$	1492.63	12 500	1.0	0.025	0.89			B	2
			1494.68	12 500	1.0	0.025	0.89			B	2
			1492.82	12 500	1.0	0.025	0.89			B	2
3	$2p^3-2p^2(^1D)3s$	$^2D°-^2D$	1243.18	12 500	1.0	0.038	2.20			B	2
			1243.31	12 500	1.0	0.038	2.20			B	2
			1243.17	12 500	1.0	0.038	2.20			B	2
4	$2p^3-2p^2(^3P)4s$	$^2D°-^2P$	1176.51	12 500	1.0	0.072	0.62			B	2
			1177.69	12 500	1.0	0.072	0.62			B	2
			1176.63	12 500	1.0	0.072	0.62			B	2
5	$2p^3-2p^2(^3P)3s$	$^2P°-^2P$	1742.73	12 500	1.0	0.035	0.92			B	2
			1745.25	12 500	1.0	0.035	0.92			B	2
			1745.26	12 500	1.0	0.035	0.92			B	2
			1742.72	12 500	1.0	0.035	0.92			B	2
6	$2p^3-2p^2(^1D)3s$	$^2P°-^2D$	1411.95	12 500	1.0	0.055	2.44			B	2
			1411.93	12 500	1.0	0.055	2.44			B	2
			1411.94	12 500	1.0	0.055	2.44			B	2
7	$2p^3-2p^2(^3P)4s$	$^2P°-^2P$	1326.57	12 500	1.0	0.094	0.63			B	2
			1327.92	12 500	1.0	0.094	0.63			B	2
			1326.56	12 500	1.0	0.094	0.63			B	2
8	$2p^3-2p^2(^3P)3d$	$^2P°-^4D$	1312.87	12 500	1.0	0.137				B	2
			1313.07	12 500	1.0	0.137				B	2
9	$2p^3-2p^2(^3P)3d$	$^2P°-^2P$	1319.68	12 500	1.0	0.079	1.07			B	2
			1319.00	12 500	1.0	0.079	1.07			B	2
			1319.67	12 500	1.0	0.079	1.07			B	2
10		$^2P°-^2F$	1316.29	12 500	1.0	0.136	1.72			B	2
11		$^2P°-^4P$	1316.04	12 500	1.0	0.137				B	2
			1315.43	12 500	1.0	0.137				B	2
12		$^2P°-^2D$	1310.54	12 500	1.0	0.078	0.87			B	2
			1310.94	12 500	1.0	0.078	0.87			B	2
			1310.95	12 500	1.0	0.078	0.87			B	2
13	$2p^23s-2p^2(^3P)4p$	$^4P-^4S°$	4151.48	12 100	0.717	1.13	0.85			A	1
			4143.43	12 100	0.717	1.17	0.88			A	1
14		$^2P-^2S°$	4935.12	12 100	0.717	1.55	0.93			A	1
15	$2p^2(^3P)3s-2p^2(^1D)3p$	$^2P-^2D°$	4109.95	12 100	0.717	5.49				A	1
			4099.94	12 100	0.717	5.35				A	1

Nitrogen

N II

Ground state: $1s^2 2s^2 2p^2\ ^3P_0$
Ionization energy: 29.601 eV = 238 750.5 cm^{-1}

Finding list

Wavelength (Å)	No.	Wavelength (Å)	No.	Wavelength (Å)	No.	Wavelength (Å)	No.
3829.80	21	4447.03	12	5005.15	14	5666.63	3
3838.37	21	4507.56	17	5007.33	18	5676.02	3
3842.19	21	4530.41	44	5016.38	14	5679.56	3
3847.40	21	4552.53	44	5023.05	32	5686.21	3
3855.10	21	4564.76	11	5025.66	14	5710.77	3
3856.06	21	4601.48	5	5045.10	4	5730.66	3
3919.00	13	4607.15	5	5073.59	8	5927.81	19
3955.85	6	4613.87	5	5183.20	36	5931.78	19
3995.00	10	4621.39	5	5186.21	36	5940.24	19
4026.07	38	4630.54	5	5190.38	34	5941.65	19
4035.08	38	4643.09	5	5313.42	35	5952.39	19
4041.31	38	4654.53	9	5340.21	35	5954.28	30
4043.53	38	4694.64	45	5351.23	35	6150.75	23
4056.90	38	4774.24	16	5452.07	20	6167.75	23
4073.04	37	4779.72	16	5454.22	20	6170.16	23
4076.91	37	4781.19	16	5462.58	20	6173.31	23
4082.27	37	4788.14	16	5475.29	25	6340.58	27
4087.30	37	4793.65	16	5478.09	20	6346.86	27
4098.87	28	4803.29	16	5480.05	20	6379.62	2
4131.78	40	4810.30	16	5495.65	20	6482.05	7
4133.67	33	4860.17	15	5526.23	31	6504.61	26
4145.77	33	4895.12	1	5530.24	31	6610.56	22
4171.61	39	4987.36	18	5535.38	31	6629.79	24
4176.16	39	4991.24	32	5540.06	31	6809.98	29
4179.67	42	4994.37	18	5543.47	31	6834.09	29
4241.78	41	5001.13	14	5551.92	31		
4442.02	43	5001.47	14	5552.68	31		

Istrefi[1] measured the Stark widths of six N II lines with a *Z* pinch end on, using a shot-to-shot scanning technique. The line profiles were checked for the absence of self-absorption and were deconvoluted by a standard procedure to eliminate contributions from instrumental and Doppler broadening.

The experiments by Djenize *et al.*,[2] by Milosavljević and Djenize[4,5] and by Milosavljević *et al.*[7] were all done with a low-pressure pulsed arc in either the original or a modified version. The observations were always carried out in the end-on configuration, and the line profiles were scanned stepwise with a shot-to-shot technique. Self-absorption was checked by measuring line-intensity ratios within multiplets and by comparing with LS-coupling ratios. If significant self-absorption was present, it was minimized by the appropriate dilution of the nitrogen admixture. Instrumental and Doppler broadening were accounted for by applying a standard deconvolution technique, but the effects of the inhomogeneous plasma end layers were not discussed.

Perez *et al.*[3] measured the Stark widths of a fairly large number of N II lines with a pulsed discharge. However, their preliminary paper, an extended abstract of a conference presentation, provides no details of their experiment.

Mar *et al.*[8] measured more than 100 Stark widths and 47 shifts of N II lines with a pulsed discharge observed end on. Self-absorption was minimized by an appropriate choice of the helium-nitrogen mixture and total pressure. A mirror is employed to detect self-absorption and to reconstruct spectral profiles when necessary. A check was done of the possible influence of boundary layers, and they were found to be negligible. Instrumental and Doppler broadening were accounted for by applying a standard deconvolution technique.

Blagojević *et al.*[6] measured the Stark widths of two multiplets with a low-pressure pulsed arc end on, using a shot-to-shot scanning technique. They checked for self-absorption and diluted the admixture of nitrogen to the helium carrier gas until they achieved optically thin conditions. The contributions from instrumental and Doppler broadening were eliminated by a standard deconvolution technique.

References

[1] L. Istrefi, Rev. Roum. Phys. **33**, 667 (1988).
[2] S. Djenize, A. Srećković, and J. Labat, Astron. Astrophys. **253**, 632 (1992).
[3] C. Perez, I. de la Rosa, M. A. Gigosos, J. A. Aparicio, and S. Mar, *Spectral Line Shapes*, AIP Conf. Proc. 386, edited by M. Zoppi and L. Ulivi (AIP, Woodbury, NY 1997), pp. 153–154.
[4] V. Milosavljević and S. Djenize, Bull. Astron. Belgrade **156**, 43 (1997).
[5] V. Milosavljević and S. Djenize, Astron. Astrophys., Suppl. Ser. **128**, 197 (1998); Publ. Astron. Obs. Belgrade No. **61**, 115 (1998).
[6] B. Blagojević, M. V. Popović, and N. Konjević, Phys. Scr. **59**, 374 (1999).
[7] V. Milosavljević, R. Konjević, and S. Djenize, Astron. Astrophys., Suppl. Ser. **135**, 565 (1999).
[8] S. Mar, J. A. Aparicio, M. I. de la Rosa, J. A. del Val, M. A. Gigosos, V. R. Gonzalez, and C. Perez, J. Phys. B **33**, 1169 (2000).

Key data on experiments

Reference	Plasma source	Method of measurement: Electron density	Method of measurement: Temperature	Remarks
1	Low-pressure pulsed arc	Stark width of the He II P_α line	Boltzmann plot of N II lines	
2	Low-pressure pulsed arc	Laser interferometer at 6328 Å	Boltzmann plot of N II lines	
3	Pulsed arc	Two-wavelength Twyman–Green interferometer	Boltzmann plot of N II lines	
4,5	Low-pressure pulsed arc	Laser interferometer at 6328 Å	Intensity ratios of N IV to N III and N III to N II lines	
6	Low-pressure pulsed arc	Stark width of the He II P_α line	Boltzmann plot of relative intensities of N II lines	
7	Low-pressure pulsed arc	Laser interferometer at 6328 Å	Ratios of N III to N II line intensities	
8	Pulsed arc	Two-wavelength Twyman–Green interferometer and He I 4713 Å Stark parameter	Boltzmann plot of N II lines and N II/N I intensity ratio	

Numerical results for N II

No.	Transition array	Multiplet	Wavelength (Å)	Temperature (K)	Electron density (10^{17} cm^{-3})	w_m (Å)	w_m/w_{th}	d_m (Å)	d_m/d_{th}	Acc.	Reference
1	$2s2p^3-2s^22p3p$	^{1}D°–^{1}P	4895.12	28 000	1.0	0.456		0.132		A,A	8
				31 000	1.60	0.436				B$^+$	2
2	$2p3s-2p3p$	^{3}P°–^{1}P	6379.62	28 000	1.0	0.640				A	8
3		^{3}P°–^{3}D	5679.56	5 000–8 000	1.0	0.54	0.57–0.65			B	3
				17 000	0.17	0.070	0.63			B$^+$	6
				17 500	0.23	0.099	0.66			B$^+$	6
				18 800	0.31	0.120	0.59			B$^+$	6
				28 000	1.0	0.430	0.68	−0.031	0.13	A,B$^+$	8
				31 000	1.60	0.688	0.70			B$^+$	2
				54 000	2.8	0.760		−0.01		B$^+$,D	5
			5666.63	5 000–8 000	1.0	0.47	0.49–0.57			B	3
				28 000	1.0	0.425	0.67	−0.034	0.14	A,B$^+$	8
				31 000	1.60	0.648	0.67			B$^+$	2
				54 000	2.8	0.750		−0.01		B$^+$,D	5
			5676.02	5 000–8 000	1.0	0.51	0.54–0.62			B	3
				16 300	0.31	0.134	0.65			B$^+$	6
				17 500	0.23	0.094	0.62			B$^+$	6
				18 800	0.31	0.120	0.59			B$^+$	6
				28 000	1.0	0.452	0.72	−0.028	0.11	A,B$^+$	8
				31 000	1.60	0.648	0.66			B$^+$	2
				54 000	2.8	0.680		−0.01		B$^+$,D	5
			5686.21	5 000–8 000	1.0	0.49	0.52–0.59			B	3
				28 000	1.0	0.475	0.75	−0.031	0.13	A,B$^+$	8
				31 000	1.60	0.606	0.62			B$^+$	2
				54 000	2.8	0.650		−0.01		B$^+$,D	5
			5710.77	5 000–8 000	1.0	0.47	0.49-0.57			B	3
				28 000	1.0	0.455	0.72	−0.033	0.14	A,B$^+$	8
			5730.66	28 000	1.0	0.601	0.94			C$^+$	8
4		^{3}P°–^{3}S	5045.10	5 000–8 000	1.0	0.32				B	3
				28 000	1.0	0.380		−0.023		A,B$^+$	8
				31 000	1.60	0.452		0.002		B$^+$,D	2
5		^{3}P°–^{3}P	4630.54	5 000–8 000	1.0	0.38				B	3

Numerical results for N II–Continued

No.	Transition array	Multiplet	Wavelength (Å)	Temperature (K)	Electron density (10^{17} cm^{-3})	w_m (Å)	w_m/w_{th}	d_m (Å)	d_m/d_{th}	Acc.	Reference
				28 000	1.0	0.326		0.007		A,B	8
				30 000	0.75	0.20				B^+	7
				33 000	1.15	0.30				B^+	7
				35 000	1.30	0.32				B^+	7
				38 000	1.45	0.36				B^+	7
				54 000	2.8	0.500		0.02		B^+,D	5
			4613.87	5 000–8 000	1.0	0.30				B	3
				28 000	1.0	0.294		0.013		B^+,B^+	8
				31 000	1.60	0.422		0.045		B^+,C	2
			4643.09	5 000–8 000	1.0	0.35				B	3
				28 000	1.0	0.329		0.022		A,B	8
				54 000	2.8	0.520		0.06		B^+,C	5
			4621.39	5 000–8 000	1.0	0.35				B	3
				28 000	1.0	0.314				A	8
			4601.48	5 000–8 000	1.0	0.38				B	3
				28 000	1.0	0.354				A	8
			4607.15	5 000–8 000	1.0	0.35				B	3
				28 000	1.0	0.357		0.005		A,D	8
6		^{3}P°–^{1}D	3955.85	28 000	1.0	0.277		0.047		A,B^+	8
				31 000	1.60	0.350				B^+	2
7		^{1}P°–^{1}P	6482.05	5 000–8 000	1.0	0.63				B	3
				28 000	1.0	0.676		0.013		A,B	8
8		^{1}P°–^{3}S	5073.59	28 000	1.0	0.300				B^+	8
9		^{1}P°–^{3}P	4654.53	28 000	1.0	0.343				A	8
10		^{1}P°–^{1}D	3995.00	5 000–8 000	1.0	0.28				B	3
				28 000	1.0	0.272		0.038		A,B^+	8
				31 000	1.60	0.580		0.045		B^+,C	2
				32 800	4.66	1.38				B	1
				54 000	2.8	0.540		0.06		B^+,C	5
11	$2p3p-2p3d$	^{1}P–^{3}F°	4564.76	28 000	1.0	0.492				A	8
12		^{1}P–^{1}D°	4447.03	5 000–8 000	1.0	0.35				B	3
				28 000	1.0	0.387				A	8
				31 000	1.60	0.512		0.036		B^+,C	2
				32 800	4.66	1.83				B	1
13		^{1}P–^{1}P°	3919.00	28 000	1.0	0.354		0.028		B^+,B^+	8
14		^{3}D–^{3}F°	5005.15	5 000–8 000	1.0	0.37				B	3
				17 100	0.25	0.071	0.62			B^+	6
				17 500	0.23	0.064	0.61			B^+	6
				18 800	0.31	0.083	0.59			B^+	6
				28 000	1.0	0.353	0.80			B	8
			5001.47	17 100	0.25	0.068	0.59			B^+	6
				17 500	0.23	0.066	063			B^+	6
				18 800	0.31	0.086	0.61			B^+	6
			5001.13	17 100	0.25	0.065	0.57			B^+	6
				17 500	0.23	0.068	0.65			B^+	6
				18 800	0.31	0.083	0.59			B^+	6
			5016.38	28 000	1.0	0.424	0.96			A	8
			5025.66	28 000	1.0	0.439	0.99	0.019	0.35	A,B	8
15		^{3}D–^{1}D°	4860.17	28 000	1.0	0.306				C^+	8
16		^{3}D–^{3}D°	4803.29	5 000–8 000	1.0	0.36				B	3
				28 000	1.0	0.372		0.022		B^+,B^+	8
				31 000	1.60	0.418		0.056		B^+,C	2
				32 800	4.66	1.36				B	1
			4788.14	5 000–8 000	1.0	0.37				B	3
				28 000	1.0	0.408		0.016		A,B	8
			4779.72	28 000	1.0	0.427		0.009		A,B	8
			4810.30	28 000	1.0	0.394				A	8
			4793.65	28 000	1.0	0.402				B^+	8
			4781.19	28 000	1.0	0.438				B^+	8
			4774.24	28 000	1.0	0.377				A	8
17		^{3}D–^{3}P°	4507.56	28 000	1.0	0.569				B^+	8
18		^{3}S–^{3}P°	4987.36	28 000	1.0	0.498	1.02			B^+	8
			5007.33	28 000	1.0	0.463	0.95	0.017	[a]	A,B	8
			4994.37	5 000–8 000	1.0	0.45	0.64-0.73			B	3
				28 000	1.0	0.441	0.84			A	8

Numerical results for N II–Continued

No.	Transition array	Multiplet	Wavelength (Å)	Temperature (K)	Electron density (10^{17} cm^{-3})	w_m (Å)	w_m/w_{th}	d_m (Å)	d_m/d_{th}	Acc.	Reference
19		^{3}P–^{3}D°	5941.65	5 000–8 000	1.0	0.50	0.51-0.59			B	3
				28 000	1.0	0.582	0.93	−0.020	[a]	A,B$^+$	8
				54 000	2.8	0.520				B$^+$	5
			5931.78	5 000–8 000	1.0	0.56	0.58-0.66			B	3
				28 000	1.0	0.593	0.95			A	8
			5927.81	5 000–8 000	1.0	0.57	0.58-0.68			B	3
				28 000	1.0	0.607	0.97			A	8
			5952.39	5 000–8 000	1.0	0.58	0.60-0.69			B	3
				28 000	1.0	0.652		−0.024	[a]	A,B	8
			5940.24	5 000–8 000	1.0	0.60	0.62-0.71			B	3
				28 000	1.0	0.647	1.03	−0.029	[a]	A,B$^+$	8
20		^{3}P–^{3}P°	5452.07	28 000	1.0	0.481				B$^+$	8
			5454.22	28 000	1.0	0.487				B$^+$	8
			5462.58	28 000	1.0	0.498		0.045		A,B$^+$	8
			5478.09	28 000	1.0	0.572				A	8
			5480.05	28 000	1.0	0.582		0.036		B$^+$,B$^+$	8
			5495.65	28 000	1.0	0.553		0.029		A,B$^+$	8
21	$2p3p-2p4s$	^{3}P–^{3}P°	3855.10	28 000	1.0	0.784	1.03			B$^+$	8
			3842.19	28 000	1.0	0.813	1.07	0.379	1.63	B$^+$,B$^+$	8
			3847.40	28 000	1.0	0.883	1.16	0.322	1.38	A,B$^+$	8
			3856.06	28 000	1.0	0.749	0.98	0.444	1.91	B,B$^+$	8
			3829.80	28 000	1.0	0.856	1.12	0.557	2.39	B,B$^+$	8
			3838.37	28 000	1.0	0.805	1.06	0.356	1.53	A,A	8
22	$2p3p-2p3d$	^{1}D–^{1}F°	6610.56	5 000–8 000	1.0	0.79				B	3
				28 000	1.0	0.813		−0.062		A,B$^+$	8
23	$2p3d-2p4p$	^{3}F°–^{3}D	6170.16	28 000	1.0	1.907	0.96			B$^+$	8
			6150.75	28 000	1.0	1.757	0.88			B$^+$	8
			6173.31	28 000	1.0	1.793	0.90	0.553	0.77	B$^+$,A	8
			6167.75	28 000	1.0	1.999	1.00	0.535	0.74	A,A	8
24		^{1}D°–^{1}P	6629.79	28 000	1.0	1.865				B$^+$	8
25		^{1}D°–^{1}D	5475.29	28 000	1.0	1.163				C	8
26		^{3}D°–^{3}D	6504.61	28 000	1.0	2.381		0.710		B$^+$,B$^+$	8
27		^{3}D°–^{3}P	6346.86	28 000	1.0	2.181	1.19			B$^+$	8
			6340.58	28 000	1.0	2.014	1.10	0.327	0.37	B$^+$,B$^+$	8
28	$2s^22p3d-2s2p^2(^4P)3s$	^{3}D°–^{3}P	4098.87	32 800	4.66	1.70				B	1
29	$2p3d-2p4p$	^{3}P°–^{3}S	6809.98	28 000	1.0	2.491	1.18	0.719	0.71	A,B$^+$	8
			6834.09	28 000	1.0	2.531	1.20			B$^+$	8
30		^{1}P°–^{1}S	5954.28	28 000	1.0			0.805		B$^+$	8
31	$2s2p^23s-2s2p^2(^4P)3p$	^{5}P–^{5}D°	5535.38	5 000–8 000	1.0	0.42				B	3
				28 000	1.0	0.433				B$^+$	8
			5526.23	28 000	1.0	0.464				B$^+$	8
			5540.06	28 000	1.0	0.410				B	8
			5543.47	28 000	1.0	0.410				B	8
			5552.68	28 000	1.0	0.288				C$^+$	8
			5530.24	28 000	1.0	0.409		−0.030		A,B$^+$	8
			5551.92	28 000	1.0	0.404				B$^+$	8
32		^{5}P–^{5}P°	4991.24	28 000	1.0	0.244		−0.042		D,B$^+$	8
			5023.05	28 000	1.0	0.369				A	8
33		^{5}P–^{5}S°	4133.67	28 000	1.0	0.317				B$^+$	8
			4145.77	28 000	1.0	0.235				B$^+$	8
34	$2s2p^23p-2s2p^23d$	^{5}D°–^{5}F	5190.38	28 000	1.0	0.438				A	8
35		^{5}P°–^{5}P	5351.23	28 000	1.0	0.534				B	8
			5313.42	28 000	1.0	0.444				B	8
			5340.21	28 000	1.0			0.289		A	8
36		^{5}P°–^{5}D	5183.20	28 000	1.0	0.482				C	8
			5186.21	28 000	1.0	0.489				B$^+$	8
37	$3d-4f$	^{3}F°[5/2]	4076.91	28 000	1.0	1.509				B$^+$	8
			4087.30	28 000	1.0	1.467				A	8
			4073.04	28 000	1.0	1.65				B	8
			4082.27	28 000	1.0	1.61		−0.212		B,A	8
38	$3d-4f'$	^{3}F°–[7/2]	4035.08	28 000	1.0	1.275		−0.066		A,B$^+$	8
				54 000	2.8	0.57		−0.028		B$^+$,D	4

Numerical results for N II–Continued

No.	Transition array	Multiplet	Wavelength (Å)	Temperature (K)	Electron density (10^{17} cm^{-3})	w_m (Å)	w_m/w_{th}	d_m (Å)	d_m/d_{th}	Acc.	Reference
			4043.53	28 000	1.0	1.65				B^+	8
			4056.90	28 000	1.0	1.843				B^+	8
			4041.31	5 000–8 000	1.0	1.09	0.63–0.70			B	3
				28 000	1.0	1.28	1.04	−0.079	0.20	B^+,B^+	8
				31 000	1.60	1.440	0.75	−0.134	0.22	B^+,B	2
				32 800	4.66	3.41	0.61			B	1
				54 000	2.8	0.59		−0.042		B^+,C	4
			4026.07	28 000	1.0	1.86				B^+	8
				31 000	1.60	1.926		−0.114		B^+,B	2
				32 800	4.66	4.95				B	1
39	$3d-4f$	^{1}D°–[5/2]	4176.16	28 000	1.0	1.60				B^+	8
			4171.61	28 000	1.0	1.53				B^+	8
40	$3d-4f'$	^{1}D°–[7/2]	4131.78	28 000	1.0	1.57				C^+	8
41	$3d-4f$	^{3}D°–[5/2]	4241.78	28 000	1.0	1.526				B^+	8
				31 000	1.60	1.512		−0.085		B^+,C	2
42	$3d-4f'$	^{3}D°–[5/2]	4179.67	28 000	1.0	1.95				C^+	8
43		^{3}P°–[5/2]	4442.02	28 000	1.0	2.533	1.35			B^+	8
44		^{1}F°–[7/2]	4552.53	28 000	1.0	2.05		−0.156		B^+,B^+	8
				54 000	2.8	2.56				B^+	4
			4530.41	28 000	1.0	2.252		−0.157		A,B^+	8
				31 000	1.60	2.000		−0.17		B^+,B	2
45		^{1}P°–[5/2]	4694.64	28 000	1.0	2.633		−0.336		A,B^+	8

[a]Theory predicts a shift in the opposite direction.

Nitrogen

N III

Ground state: $1s^2 2s^2 2p\ ^2P^\circ_{1/2}$
Ionization energy: 47.449 eV = 382 704 cm^{-1}

Djenize *et al.*,[1] Milosavljević and Djenize,[4] and Djenize and Milosavljević[5] used a low-pressure pulsed arc in the end-on configuration to determine Stark widths and shifts of several N III lines with a shot-to-shot scanning technique. The plasma conditions were reproducible within ±8%, as indicated from monitoring of a N III transition. Self-absorption in the line centers was checked by comparing measured line intensity ratios in multiplets with LS-coupling ratios, and it was minimized by the choice of appropriate gas mixtures. The contributions of Doppler and instrumental broadening to the measured linewidths were subtracted by employing a standard deconvolution technique. However, the effects of the inhomogeneous plasma end layers were not discussed. Djenize and Milosavljević[5] determined that for all their measured lines no Stark shifts were detected within their experimental uncertainty of ±0.015 Å.

Glenzer *et al.*[2] measured several Stark widths with a gas-liner pinch side on. They operated the pinch under conditions where the discharge was highly reproducible and homogeneous, and where the nitrogen test gas was sufficiently diluted so that self-absorption became negligible, as checked from the intensity ratios in multiplets where LS-coupling prevails.

Blagojević *et al.*[3,6] measured the Stark widths and shifts of several $3s-3p$ and $3p-3d$ transitions with a low-pressure pulsed arc end on with a shot-to-shot scanning technique. The optical thickness of the lines (and to some degree the homogeneity of the discharge) was tested by the introduction of a movable electrode, thus creating different plasma observation lengths. Self-absorption was minimized by optimizing the composition of the gas mixture and the total pressure. The contributions of instrumental and Doppler broadening were accounted for by applying a standard deconvolution procedure.

References

[1] S. Djenize, L. C. Popović, J. Labat, A. Srećković, and M. Platisa, Contrib. Plasma Phys. **33**, 193 (1993).
[2] S. Glenzer, J. D. Hey, and H.-J. Kunze, J. Phys. B **27**, 413 (1994).
[3] B. Blagojević, M. V. Popović, N. Konjević, and M. S. Dimitrijević, Phys. Rev. E **54**, 743 (1996).
[4] V. Milosavljević and S. Djenize, Astron. Astrophys., Suppl. Ser. **128**, 197 (1998).
[5] S. Djenize and V. Milosavljević, Astron. Astrophys., Suppl. Ser. **131**, 355 (1998).
[6] B. Blagojević, M. V. Popović, and N. Konjević, J. Quant. Spectrosc. Radiat. Transf. **67**, 9 (2000).

Key data on experiments

Reference	Plasma source	Method of measurement: Electron density	Method of measurement: Temperature	Remarks
1, 4	Low-pressure pulsed arc	Laser interferometer at 6328 Å	Intensity ratios of N IV to N III and N III to N II lines	
2	Gas-liner pinch	90° Thomson scattering	90° Thomson scattering	
3	Low-pressure pulsed arc	Stark width of the He II P_α line	Boltzmann plot of N III lines and intensity ratios of N IV and N III lines	
5	Low-pressure pulsed arc	Laser interferometer at 6328 Å	Intensity ratios of N IV to N III lines and N III to N II lines and ratio of He II P_α to He I 5876 Å lines	
6	Low-pressure pulsed arc	Stark width of the He II P_α line	Boltzmann plot of N II lines	

Numerical results for N III

No.	Transition array	Multiplet	Wavelength (Å)	Temperature (K)	Electron density (10^{17} cm^{-3})	w_m (Å)	w_m/w_{th}	d_m (Å)	d_m/d_{th}	Acc.	Reference
1	$3s-(^1S)3p$	$^2S-^2P^\circ$	4097.36	17 500	0.23	0.083	0.98			B^+	6
				18 800	0.31	0.100	0.92			B^+	6
				19 500	0.39	0.116	0.86			B^+	6
				30 000	0.75	0.26	1.22			B^+	5
				33 000	1.15	0.40	1.27			B^+	5
				33 000	1.38	0.345	0.92			B^+	3
				35000	1.30	0.42	1.21			B^+	5
				36 100	1.71	0.423	0.93			B^+	3
				37 900	1.11	0.262	0.92			B^+	3
				39 000	1.45	0.48	1.29			B^+	5
				39 600	2.64	0.587	0.88			B^+	3
				44 300	2.52	0.557	0.91			B^+	3
				Δ(44 300–33 000)	Δ(2.52–1.38)			Δ(−0.04)	5.6	C	3
				54 000	2.80	0.69	1.10			B^+	5
				87 000	7.1	1.71	1.27			B^+	2
				96 300	10.1	2.25	1.20			B^+	2
			4103.39	17 500	0.23	0.080	0.95			B^+	6
				18 300	0.33	0.114	0.97			B^+	6
				18 800	0.31	0.105	0.96			B^+	6
				19 100	0.41	0.126	0.88			B^+	6
				19 500	0.39	0.118	0.88			B^+	6
				30 000	0.75	0.26	1.23			B^+	5
				33 000	1.15	0.38	1.21			B^+	5
				33 000	1.38	0.343	0.92			B^+	3
				35 000	1.30	0.42	1.21			B^+	5
				36 100	1.71	0.400	0.90			B^+	3
				37 900	1.11	0.279	0.98			B^+	3
				39 000	1.45	0.46	1.24			B^+	5
				39 600	2.64	0.587	0.88			B^+	3
				44 300	2.52	0.557	0.91			B^+	3
				Δ(44 300–33 000)	Δ(2.52–1.38)			Δ(−0.04)	5.6	C	3
				54 000	2.80	0.72	1.15			B^+	5
2	$3p-(^1S)3d$	$^2P^\circ-^2D$	4634.13	17 500	0.23	0.104	0.99			B^+	6
				18 300	0.33	0.145	0.99			B^+	6
				18 800	0.31	0.131	0.96			B^+	6
				19 100	0.41	0.168	0.94			B^+	6
				19 500	0.39	0.156	0.93			B^+	6
				33 000	1.38	0.470	1.00			B^+	3
				33 000	1.15	0.42	1.06			B^+	5
				35 000	1.30	0.46	1.06			B^+	5
				36 100	1.71	0.553	0.97			B^+	3
				37 900	1.11	0.352	0.98			B^+	3
				39 000	1.45	0.52	1.12			B^+	5
				39 600	2.54	0.793	0.95			B^+	3

Numerical results for N III—Continued

No.	Transition array	Multiplet	Wavelength (Å)	Temperature (K)	Electron density (10^{17} cm^{-3})	w_m (Å)	w_m/w_{th}	d_m (Å)	d_m/d_{th}	Acc.	Reference
				44 300	2.52	0.766	1.00			B^+	3
				Δ(44 300–33 000)	Δ(2.52–1.38)			Δ(−0.04)	5.4	C	3
				54 000	2.80	0.58	0.74			B^+	5
			4640.64	17 500	0.23	0.102	0.97			B^+	6
				18 300	0.33	0.148	1.00			B^+	6
				18 800	0.31	0.130	0.96			B^+	6
				19 100	0.41	0.169	0.95			B^+	6
				19 500	0.39	0.160	0.95			B^+	6
				33 000	1.38	0.443	0.95			B^+	3
				33 000	1.15	0.38	0.96			B^+	5
				35 000	1.30	0.42	0.96			B^+	5
				36 100	1.71	0.526	0.94			B^+	3
				37 900	1.11	0.352	0.98			B^+	3
				39 000	1.45	0.54	1.16			B^+	5
				39 600	2.64	0.795	0.95			B^+	3
				44 300	2.52	0.746	0.97			B^+	3
				Δ(44 300–33 000)	Δ(2.52–1.38)			Δ(−0.03)	4.1	D	3
				54 000	2.80	0.54	0.69			B^+	5
				91 700	5.8	0.96	0.71			B^+	2
3	$3d-(^1S)4p$	$^2D-^2P°$	2247.95	52 000	2.45	0.46		−0.09		B^+,C^+	1
4	$2s2p3s-2s2p(^3P°)3p$	$^4P°-^4D$	4514.85	54 000	2.8	0.460		−0.01		B,D	4
				99 800	10.2	1.90				B	2
			4510.96	54 000	2.8	0.360		−0.01		B,D	4
5	$2s2p3p-2s2p(^3P°)3d$	$^2P-^2D°$	3938.51	54 000	2.8	0.340		−0.03		B,D	4
6		$^2P-^2P°$	2983.64	54 000	2.8	0.400		−0.01		B,D	4
7		$^4D-^4F°$	4867.17	54 000	2.8	0.520		−0.02		B,D	4
			4861.27	54 000	2.8	0.580		−0.02		B,D	4
8		$^4S-^4P°$	4546.36	54 000	2.8	0.510		−0.05		B,D	4

Nitrogen

N IV

Ground state: $1s^2 2s^2\ ^1S_0$
Ionization energy: 77.474 eV = 624 866 cm^{-1}

Wrubel *et al.*[1] measured the Stark widths of some $3s-3p$ triplet and singlet transitions utilizing a gas-liner pinch. N IV ions were confined to the homogeneous center of a hydrogen plasma column, and cool boundary layers were absent. The optical thickness of the lines was checked by comparing the line intensity ratios within the triplet with LS-coupling ratios. Agreement within 2% was found, indicating the absence of self-absorption. The observed line profiles were fitted to Voigt functions, so that the contributions of Doppler and apparatus broadening could be taken into account and subtracted.

Milosavljević and Djenize[2] used a low-pressure pulsed arc for their end-on observations. The line profiles were recorded stepwise with a shot-to-shot technique. Self-absorption was checked and minimized by measuring line-intensity ratios within multiplets of N II and N III and by comparing them with LS-coupling ratios. It is seen from their Fig. 1, however, that for the $3s-3p$ triplet of N IV departures from LS-coupling ratios amount to about 20%, indicating some residual self-absorption. Instrumental and Doppler broadening were accounted for by applying a standard deconvolution technique, but the effects of the inhomogeneous plasma end layers were not discussed.

Blagojević *et al.*[3] measured the Stark widths of the $3s-3p$ triplet lines with a low-pressure pulsed arc end on, using a shot-to-shot scanning technique to record the line profiles. They checked for self-absorption effects by diluting the nitrogen gas in helium until they obtained within a few percent the LS-coupling ratios for the line intensities in the triplet. The contributions from instrumental and Doppler broadening were accounted for by a standard deconvolution technique.

References

[1] T. Wrubel, I. Ahmad, S. Büscher, H.-J. Kunze, and S. H. Glenzer, Phys. Rev. E **57**, 5972 (1998).
[2] V. Milosavljević and S. Djenize, Astron. Astrophys., Suppl. Ser. **128**, 197 (1998).
[3] B. Blagojević, M. V. Popović, N. Konjević, and M. S. Dimitrijević, J. Quant. Spectrosc. Radiat. Transf. **61**, 361 (1999).

Key data on experiments

Reference	Plasma source	Method of measurement: Electron density	Method of measurement: Temperature	Remarks
1	Gas-liner pinch	90° Thomson scattering	90° Thomson scattering	
2	Low-pressure pulsed arc	Laser interferometer at 6328 Å	Intensity ratios of N IV to N III and N III to N II lines	
3	Low-pressure pulsed arc	Stark width of the He II P_α line	Boltzmann plot of N III lines and intensity ratios of N IV to N III lines	

Numerical results for N IV

No.	Transition array	Multiplet	Wavelength (Å)	Temperature (K)	Electron density (10^{17} cm^{-3})	w_m (Å)	w_m/w_{th}	d_m (Å)	d_m/d_{th}	Acc.	Reference
1	$2s3s-2s(^2S)3p$	$^3S-^3P°$	3478.72	54 000	2.8	0.410	0.99	0.01		B^+,D	2
				72 400	0.86	0.122	1.12			B^+	3
				78 300	0.99	0.136	1.11			B^+	3
				80 100	1.13	0.148	1.07			B^+	3
				80 700	1.21	0.153	1.03			B^+	3
				81 200	5.8	0.84	1.19			B^+	1
				82 300	1.33	0.172	1.06			B^+	3
				Δ(82 300–72 400)	Δ(1.33–0.86)			Δ(0.04)		C	3
				96 300	8.1	1.10	1.15			B^+	1
				98 600	15.8	1.46	0.79			A	1
				101 000	19.4	1.72	0.76			A	1
				104 400	10.6	1.11	0.90			B^+	1
			3483.00	54 000	2.8	0.330	0.80	0.01		B^+,D	2
				72 400	0.86	0.122	1.12			B^+	3
				78 300	0.99	0.136	1.11			B^+	3
				80 100	1.13	0.150	1.08			B^+	3
				80 700	1.21	0.150	1.01			B^+	3
				81 200	5.8	0.84	1.19			B^+	1
				82 300	1.33	0.174	1.08			B^+	3
				Δ(82 300–72 400)	Δ(1.33–0.86)			Δ(0.03)		C	3
				96 300	8.1	1.10	1.15			B^+	1
				98 600	15.8	1.46	0.79			A	1
				101 000	19.4	1.72	0.76			A	1
				104 400	10.6	1.11	0.90			B^+	1
			3484.93	54 000	2.8	0.400	0.96	0.01		B^+,D	2
				72 400	0.86	0.122	1.12			B^+	3
				78 300	0.99	0.146	1..19			B^+	3
				81 100	1.13	0.146	1.05			B^+	3
				81 200	5.8	0.84	1.19			B^+	1
				96 300	8.1	1.10	1.15			B^+	1
				98 600	15.8	1.46	0.79			A	1
				101 000	19.4	1.72	0.76			A	1
				104 400	10.6	1.11	0.90			B^+	1
2		$^1S-^1P°$	6380.75	71 900	6.5	2.53				A	1
				81 200	4.6	1.73				B^+	1
3	$2s3p-2s(^2S)3d$	$^1P°-^1D$	4057.76	54 000	2.8	0.410		0.07		B^+,C^+	2
4	$2p3s-2p(^3P°)3p$	$^1P°-^1D$	3747.54	54 000	2.8	0.500		0.03		B^+,D	2

Nitrogen

N V

Ground state: $1s^2 2s^2 S_{1/2}$
Ionization energy: 97.890 eV = 789 537.2 cm^{-1}

Glenzer *et al.*[1] employed a gas-liner pinch for their Stark width measurements, while Blagojević *et al.*[2] used a low-pressure pulsed arc. In both experiments, the strongest N V lines were tested for possible self-absorption effects, but no indications were seen for the selected operating conditions. Also, the measured line shapes were corrected for Doppler and instrumental broadening with a standard deconvolution procedure.

Glenzer *et al.* observed side on and emphasized that their plasma is homogeneous, and that no cold boundary layers exist. Blagojević *et al.*, who observed end on, did not discuss the effect of cooler plasma-end layers in the electrodes. However, the four-times ionized nitrogen atoms should recombine there rather quickly, and produce only very small plasma inhomogeneity effects.

The increments in shift measured by Blagojević *et al.* between the two electron densities indicated in the table are in the opposite direction from those predicted by theory.[3]

References

[1] S. Glenzer, N. I. Uzelac, and H.-J. Kunze, Phys. Rev. A **45**, 8795 (1992).
[2] B. Blagojević, M. V. Popović, N. Konjević, and M. S. Dimitrijević, J. Quant. Spectrosc. Radiat. Transf. **61**, 361 (1999).
[3] M. S. Dimitrijević and S. Sahal-Bréchot, Astron. Astrophys., Suppl. Ser. **95**, 109 (1992).

Key data on experiments

Reference	Plasma source	Method of measurement: Electron density	Method of measurement: Temperature	Remarks
1	Gas-liner pinch	90° Thomson scattering	90° Thomson scattering	
2	Low-pressure pulsed arc	Stark width of the He II P_α line	Boltzmann plot of N III lines and intensity ratios of N IV to N III lines	

Numerical results for N V

No.	Transition array	Multiplet	Wavelength (Å)	Temperature (K)	Electron density (10^{17} cm^{-3})	w_m (Å)	w_m/w_{th}	d_m (Å)	d_m/d_{th}	Acc.	Reference
1	$3s-3p$	$^2S-^2P°$	4603.74	72 400	0.86	0.186	0.90			B^+	2
				78 300	0.99	0.204	0.89			B^+	2
				80 100	1.13	0.231	0.89			B^+	2
				80 700	1.21	0.249	0.90			B^+	2
				Δ(80 700–72 400)	Δ(1.21–0.86)			Δ(0.04)		D	2
				82 300	1.33	0.282	0.94			B^+	2
				173 000	12	2.2	1.09			B^+	1
				217 000	16	2.7	1.10			B	1
				253 000	20	3.4	1.16			B	1
				277 000	23	3.8	1.16			B^+	1
			4619.97	72 400	0.86	0.186	0.90			B^+	2
				78 300	0.99	0.204	0.89			B^+	2
				80 100	1.13	0.231	0.89			B^+	2
				80 700	1.21	0.249	0.90			B^+	2
				Δ(80 700–72 400)	Δ(1.21–0.86)			Δ(0.03)		D	2
				82 300	1.33	0.282	0.94			B^+	2

Oxygen

O I

Ground state: $1s^2 2s^2 2p^4\ ^3P_2$
Ionization energy: 13.6181 eV = 109 837.34 cm^{-1}

Sohns and Kock[1] determined the Stark widths of three resonance lines with a wall-stabilized arc source under conditions where the lines are strongly self-reversed. They applied a model calculation to the measured line shapes, based on the equation of radiative transfer, and obtained the Stark widths for the condition where an optimum fit occurs.

Mijatović *et al.*[2] measured the Stark broadening parameters of the $3s-4p$ triplet (consisting of three very-closely spaced, unresolvable lines) with a wall-stabilized arc which was operated in argon with admixtures of O_2 and H_2 (the latter for plasma diagnostics). The plasma was observed end

on, and tests for possible self-absorption were performed by placing a concave mirror with a light chopper behind the arc, thus imaging the plasma on itself and generating two optical pathlengths that differed essentially by a factor of 2. The observed profile was corrected for Doppler and instrumental broadening. The results are consistent with earlier experimental work and are in fair agreement with semiclassical theory.

All Stark shifts were measured at the position of the half-width, and were compared with the corresponding theoretical shifts.

References

[1] E. Sohns and M. Kock, J. Quant. Spectrosc. Radiat. Transf. **47**, 335 (1992).
[2] Z. Mijatović, N. Konjević, R. Kobilarov, and S. Djurović, Phys. Rev. E **51**, 613 (1995).

Key data on experiments

Reference	Plasma source	Method of measurement: Electron density	Method of measurement: Temperature	Remarks
1	Wall-stabilized arc	Plasma model calculation	Blackbody limited VUV lines	Line profiles measured under optically thick conditions
2	Wall-stabilized arc	H_β Stark width	Plasma composition data	

Numerical results for O I

No.	Transition array	Multiplet	Wavelength (Å)	Temperature (K)	Electron density (10^{17} cm^{-3})	w_m (Å)	w_m/w_{th}	d_m (Å)	d_m/d_{th}	Acc.	Reference
1	$2p^4-2p^3(^4S°)3s$	$^3P-^3S°$	1302.17	12 500	1.0	0.0233	1.29			C^+	1
			1304.86	12 500	1.0	0.0233	1.29			C^+	1
			1306.03	12 500	1.0	0.0233	1.29			C^+	1
2	$2p^3 3s-2p^3(^4S°)4p$	$^3S°-^3P$	4368.2	10 600	0.240	0.51	1.29	0.10	1.17	A	2
				10 980	0.312	0.67	1.28	0.13	1.17	A	2

Oxygen

O II

Ground state: $1s^2 2s^2 2p^3\ ^4S^\circ_{3/2}$
Ionization energy: 35.1211 eV = 283 270.9 cm^{-1}

Finding list

Wavelength (Å)	No.	Wavelength (Å)	No.	Wavelength (Å)	No.	Wavelength (Å)	No.
3270.86	23	4104.99	10	4327.46	24	4596.18	7
3289.98	12	4110.79	10	4336.86	2	4638.86	1
3470.67	16	4112.02	11	4345.56	2	4641.81	1
3729.22	28	4119.22	10	4347.21	8	4649.13	1
3739.76	18	4121.46	9	4349.43	2	4650.84	1
3749.48	3	4132.90	9	4351.26	8	4705.35	14
3802.98	21	4146.09	33	4366.89	2	4710.01	13
3954.36	5	4153.30	9	4395.93	15	4860.97	26
4072.15	6	4156.53	9	4414.90	4	4871.52	26
4075.86	6	4294.78	30	4416.97	4	4890.86	17
4078.84	6	4303.82	29	4448.19	22	4924.53	17
4085.11	6	4317.14	2	4477.88	32	4955.71	20
4089.27	31	4319.63	2	4590.97	7	5206.65	19
4092.93	6	4319.87	27	4595.96	7	6895.10	25

Djenize *et al.*[1,2] measured Stark widths and shifts with a low-pressure pulsed arc end on by scanning the line profiles with a shot-to-shot technique. The plasma was reproducible within 6%, as monitored by the intensity of an O II line. The optical depth of the lines was checked by measuring the component intensities in multiplets and comparing them with reference data. Differences of 12%–22% indicated, according to the authors, small self-absorption effects. The measured profiles contained significant contributions due to Doppler and instrumental broadening, which were eliminated with a standard deconvolution technique. The plasma tube had extended openings in the electrode regions (see Fig. 1 of Ref. 2), but end effects from these areas were not discussed.

Blagojević *et al.*[3] measured the Stark widths of two prominent $3s-3p$ and $3p-3d$ doublets with a low-pressure pulsed arc. Recordings of the line shapes were performed with a shot-to-shot procedure in the end-on configuration. Negligible self-absorption in the lines was achieved by diluting O_2 in helium until the intensities of the strongest O II lines became strictly proportional to the O_2 concentration. The measured line profiles were corrected for the contributions from Doppler and instrumental broadening with a standard deconvolution technique. Effects from inhomogeneous plasma end layers were not discussed, but are estimated to be small for the rapidly recombining O^+ ions.

del Val *et al.*[4] determined the Stark widths of 32 O II lines with a low-pressure pulsed arc end on in neon. They added only traces of oxygen to make self-absorption completely negligible. This was experimentally ascertained with a path-doubling mirror arrangement. The (known) widths from Doppler and instrumental broadening were eliminated by fitting the lines to Voigt profiles and by extracting the Lorentzian component, which yields the Stark width. Effects from inhomogeneous plasma end layers were not discussed, but are estimated to be small. The Stark widths measured for different lines within multiplets 6–10 show unusually large variations.

References

[1] S. Djenize, A. Srećković, J. Labat, and M. Platisa, Z. Phys. D **21**, 295 (1991).
[2] S. Djenize, V. Milosavljević, and A. Srećković, J. Quant. Spectrosc. Radiat. Transf. **59**, 71 (1998).
[3] B. Blagojević, M. V. Popović, and N. Konjević, Phys. Scr. **59**, 374 (1999).
[4] J. A. del Val, J. A. Aparicio, V. Gonzales, and S. Mar, Astron. Astrophys., Suppl. Ser. **140**, 171 (1999).

Key data on experiments

Reference	Plasma source	Method of measurement: Electron density	Method of measurement: Temperature	Remarks
1	Low-pressure pulsed arc	Laser interferometer at 6328 Å	Boltzmann plot of O II lines	
2	Low-pressure pulsed arc	Laser interferometer at 6328 Å	Intensity ratios of N IV to N III and N III to N II lines	
3	Low-pressure pulsed arc	Stark width of the He II P_α line	Boltzmann plot of N II lines	
4	Low-pressure pulsed arc	Twyman–Green interferometer at two wavelengths of argon ion laser and H_α Stark width	Boltzmann plot of O II and Ne II lines	Source of transition probabilities for temperature measurements not given

Numerical results for O II

No.	Transition array	Multiplet	Wavelength (Å)	Temperature (K)	Electron density (10^{17} cm^{-3})	w_m (Å)	w_m/w_{th}	d_m (Å)	d_m/d_{th}	Acc.	Reference
1	$2p^2(^3P)3s-2p^2(^3P)3p$	$^4P-^4D°$	4649.13	40 000	1.0	0.209	0.67			B^+	4
			4641.81	40 000	1.0	0.223	0.71			C^+	4
				54 000	2.8	0.62		0.03		B^+,D	2
			4638.86	40 000	1.0	0.220	0.70			B^+	4
				54 000	2.8	0.64		0.05		B^+,C	2
			4650.84	40 000	1.0	0.225	0.71			B^+	4
2		$^4P-^4P°$	4349.43	40 000	1.0	0.253	1.16			C	4
			4336.86	40 000	1.0	0.202	0.93			C^+	4
			4366.89	40 000	1.0	0.248	1.13			C^+	4
			4345.56	40 000	1.0	0.258	1.19			B^+	4
			4319.63	40 000	1.0	0.261	1.20			B	4
			4317.14	40 000	1.0	0.256	1.18			B	4
3		$^4P-^4S°$	3749.48	54 000	2.8	0.38				B^+	2
4		$^2P-^2D°$	4414.90	18 800	0.31	0.087	0.93			B^+	3
				19 100	0.41	0.113	0.91			B^+	3
				19 500	0.46	0.133	0.96			B^+	3
				19 500	0.39	0.110	0.94			B^+	3
				19 800	0.44	0.125	0.95			B^+	3

Numerical results for O II—Continued

No.	Transition array	Multiplet	Wavelength (Å)	Temperature (K)	Electron density (10^{17} cm^{-3})	w_m (Å)	w_m/w_{th}	d_m (Å)	d_m/d_{th}	Acc.	Reference
				19 900	0.47	0.135	0.96			B^+	3
			4416.97	18 800	0.31	0.086	0.92			B^+	3
				19 100	0.41	0.121	0.98			B^+	3
				19 500	0.46	0.130	0.94			B^+	3
				19 500	0.39	0.109	0.93			B^+	3
				19 800	0.44	0.124	0.94			B^+	3
				19 900	0.47	0.132	0.94			B^+	3
5		^{2}P–^{2}P°	3954.36	54 000	2.8	0.54				B^+	2
6	$2p^2(^3\mathrm{P})3p-2p^2(^3\mathrm{P})3d$	^{4}D°–^{4}F	4075.86	40 000	1.0	0.197	0.76			B^+	4
			4072.15	40 000	1.0	0.239	0.92			B^+	4
			4092.93	40 000	1.0	0.213	0.83			B^+	4
			4085.11	40 000	1.0	0.252	0.98			C^+	4
			4078.84	40 000	1.0	0.200	0.78			B	4
7	$2p^2(^1\mathrm{D})3s-2p^2(^1\mathrm{D})3p$	^{2}D–^{2}F°	4590.97	40 000	1.0	0.223				C^+	4
			4596.18	40 000	1.0	0.272				B^+	4
				54 000	2.8	0.42				B^+	2
			4595.96	54 000	2.8	0.38				B^+	2
8		^{2}D–^{2}D°	4351.26	40 000	1.0	0.225				C^+	4
			4347.21	40 000	1.0	0.311				C^+	4
9	$2p^2(^3\mathrm{P})3p-2p^2(^3\mathrm{P})3d$	^{4}P°–^{4}P	4121.46	40 000	1.0	0.242	0.94			C^+	4
			4156.53	40 000	1.0	0.329	1.26			C^+	4
			4153.30	40 000	1.0	0.293	1.13			B^+	4
			4132.90	40 000	1.0	0.299	1.15			C^+	4
10		^{4}P°–^{4}D	4119.22	40 000	1.0	0.248	0.90			C^+	4
			4104.99	54 000	2.8	0.82		0.03		B^+,D	2
			4110.79	40 000	1.0	0.219	0.81			B	4
11		^{4}P°–^{2}F	4112.02	40 000	1.0	0.343				B	4
12	$2p^2(^3\mathrm{P})3p-2p^2(^3\mathrm{P})4s$	^{4}P°–^{4}P	3289.98	60 000	0.81	0.344		0.08		B^+,C	1
13	$2p^2(^3\mathrm{P})3p-2p^2(^3\mathrm{P})3d$	^{2}D°–^{4}D	4710.01	60 000	0.81	0.240		0.02		B^+,D	1
14		^{2}D°–^{2}F	4705.35	18 800	0.31	0.115	0.91			B^+	3
				19 100	0.41	0.170	1.02			B^+	3
				19 500	0.46	0.195	1.05			B^+	3
				19 500	0.39	0.146	0.93			B^+	3
				19 800	0.44	0.174	0.98			B^+	3
				19 900	0.47	0.189	1.00			B^+	3
				60 000	0.7	0.240		0.02		B^+,D	1
15		^{2}D°–^{2}D	4395.93	60 000	0.81	0.254		−0.02		B^+,D	1
16	$2p^2(^3\mathrm{P})3p-2p^2(^3\mathrm{P})4s$	^{2}D°–^{2}P	3470.67	54 000	2.8	1.00		0.09		B^+,C^+	2
17	$2p^2(^3\mathrm{P})3p-2p^2(^3\mathrm{P})3d$	^{4}S°–^{4}P	4890.86	54 000	2.8	0.94				B^+	2
			4924.53	60 000	0.81	0.232				B^+	1
18	$2p^2(^3\mathrm{P})3p-2p^2(^3\mathrm{P})4s$	^{4}S°–^{4}P	3739.76	60 000	0.81	0.426		0.12		B^+,B	1
19	$2p^2(^3\mathrm{P})3p-2p^2(^3\mathrm{P})3d$	^{2}P°–^{2}P	5206.65	60 000	0.81	0.362		0.04		B^+,D	1
20		^{2}P°–^{2}D	4955.71	60 000	0.81	0.328				B^+	1
21	$2p^2(^3\mathrm{P})3p-2p^2(^3\mathrm{P})4s$	^{2}P°–^{2}P	3802.98	60 000	0.81	0.418		0.08		B^+,C	1
22	$2p^2(^1\mathrm{D})3p-2p^2(^1\mathrm{D})3d$	^{2}F°–^{2}F	4448.19	40 000	1.0	0.343				B	4
23	$2p^2(^1\mathrm{D})3p-2p^2(^1\mathrm{D})4s$	^{2}F°–^{2}D	3270.86	60 000	0.81			0.02		B^+,D	1
24	$2p^2(^1\mathrm{D})3p-2p^2(^1\mathrm{D})3d$	^{2}D°–^{2}D	4327.46	40 000	1.0	0.382				B	4
25	$2p^2(^3\mathrm{P})3d-2p^2(^3\mathrm{P})4p$	^{4}F–^{4}D°	6895.10	60 000	0.81	0.976				B^+	1
26	$2p^2(^1\mathrm{D})3p-2p^2(^1\mathrm{D})3d$	^{2}P°–^{2}D	4860.97	60 000	0.81	0.284				B^+	1
			4871.52	60 000	0.81	0.284		0.04		B^+,D	1
27		^{2}P°–^{2}S	4319.87	60 000	0.81	0.208		0.02		B^+,D	1
28	$2p^2(^1\mathrm{D})3p-2p^2(^1\mathrm{D})4s$	^{2}P°–^{2}D	3729.22	60 000	0.81	0.132		−0.02		B^+,D	1
29	$2p^2(^3\mathrm{P})3d-2p^2(^3\mathrm{P})4f$D	^{4}P–^{2}[3]°	4303.82	40 000	1.0	1.186				B	4
				60 000	0.81	0.774				B^+	1
30		^{4}P–^{2}[2]°	4294.78	60 000	0.81	0.774				B^+	1
31	$2p^2(^3\mathrm{P})3d-2p^2(^3\mathrm{P})4fG$	^{4}F–^{2}[5]°	4089.27	40 000	1.0	1.009				B	4
				60 000	0.81	0.538				B^+	1
32		^{2}P–^{2}[3]°	4477.88	40 000	1.0	1.27				B	4
33	$2p^3(^5\mathrm{S}°)3p-2p^3(^5\mathrm{S}°)3d$	^{6}P–^{6}D°	4146.09	40 000	1.0	0.432				B^+	4

Oxygen

O III

Ground state: $1s^2 2s^2 2p^2\ ^3P_0$
Ionization energy: 54.936 eV = 443 086 cm^{-1}

Blagojević *et al.*[1] measured the Stark widths with a low-pressure pulsed arc end on with a shot-to-shot scanning technique. The optical depth for the strongest lines was checked by measuring intensity ratios within multiplets and comparing them with LS-coupling ratios. Agreement within 3% was achieved by appropriate dilution of O_2 in the gas mixture. The contributions of instrumental and Doppler broadening were accounted for by applying a standard deconvolution procedure.

Reference

[1] B. Blagojević, M. V. Popović, and N. Konjević, J. Quant. Spectrosc. Radiat. Transf. **67**, 9 (2000).

Key data on experiments

Reference	Plasma source	Method of measurement: Electron density	Method of measurement: Temperature	Remarks
1	Low-pressure pulsed arc	Stark width of the He II P_α line	Boltzmann plot of N II lines	

Numerical results for O III

No.	Transition array	Multiplet	Wavelength (Å)	Temperature (K)	Electron density (10^{17} cm^{-3})	w_m (Å)	w_m/w_{th}	d_m (Å)	d_m/d_{th}	Acc.	Reference
1	$2p3s-2p(^2P°)3p$	$^3P°-^3D$	3759.80	18 300	0.33	0.067				B^+	1
				19 100	0.41	0.083				B^+	1
				19 500	0.46	0.097				B^+	1
				19 900	0.47	0.098				B^+	1
			3754.70	18 300	0.33	0.075				B^+	1
				19 100	0.41	0.081				B^+	1
				19 500	0.46	0.104				B^+	1
				19 900	0.47	0.091				B^+	1
2	$2p3p-2p(^2P°)3d$	$^3D-^3F°$	3265.46	26 000	0.32	0.045				B^+	1
				33 400	0.64	0.081				B^+	1
				39 700	0.83	0.100				B^+	1
				46 000	1.05	0.134				B^+	1
			3260.98	26 000	0.32	0.047				B^+	1
				39 700	0.83	0.100				B^+	1
			3267.31	39 700	0.83	0.103				B^+	1

Oxygen

O IV

Ground state: $1s^2 2s^2 2p\ ^2P^\circ_{1/2}$
Ionization energy: 77.416 eV = 624 382.0 cm^{-1}

Glenzer *et al.*[1] measured the Stark widths of the $3s-3p$ and $3p-3d$ doublets with a gas-liner pinch side on. They operated the discharge for conditions where the plasma was highly reproducible and where the homogeneity of the plasma in the center of the column was of the order of ±10%. By diluting the test gas, plasma conditions were found where self-absorption in the investigated lines was negligible. Also, a cold boundary layer of test gas ions was absent. The contributions of Doppler and instrumental broadening were taken into account by fitting the lines to Voigt functions.

Blagojević *et al.*[2,3] measured the Stark widths and shifts of the same transitions with a low-pressure pulsed arc end on with a shot-to-shot scanning technique. The optical depth for the strongest lines was checked by measuring intensity ratios within multiplets and comparing them with LS-coupling ratios. Agreement within 3% was achieved by appropriate dilution of O_2 in the gas mixture. The contributions of instrumental and Doppler broadening were accounted for by applying a standard deconvolution procedure.

The experimental results have been compared with improved semiclassical calculations of Blagojević *et al.*,[3] which include perturbations from energy levels with different parent terms. The agreement of the rather different experimental approaches by Glenzer *et al.*[1] and Blagojević *et al.*[2,3] with the calculated results is consistently good.

References

[1] S. Glenzer, J. D. Hey, and H.-J. Kunze, J. Phys. B **27**, 413 (1994).
[2] B. Blagojević, M. V. Popović, N. Konjević, and M. S. Dimitrijević, Phys. Rev. E **50**, 2986 (1994).
[3] B. Blagojević, M. V. Popović, N. Konjević, and M. S. Dimitrijević, Phys. Rev. E **54**, 743 (1996).

Key data on experiments

Reference	Plasma source	Method of measurement: Electron density	Method of measurement: Temperature	Remarks
1	Gas-liner pinch	90° Thomson scattering	90° Thomson scattering	
2, 3	Low-pressure pulsed arc	Stark width of the He II P_α line	Boltzmann plot of N III lines and ratios of N IV to N III lines	

Numerical results for O IV

No.	Transition array	Multiplet	Wavelength (Å)	Temperature (K)	Electron density (10^{17} cm^{-3})	w_m (Å)	w_m/w_{th}	d_m (Å)	d_m/d_{th}	Acc.	Reference
1	$3s-(^1S)3p$	$^2S-^2P^\circ$	3063.43	50 800	4.92	0.596	1.01			B^+	2
				54 500	5.6	0.62	0.95			B	1
				62 600	2.06	0.220	0.98			B^+	2
				85 000	5.38	0.525	1.02			B^+	2
				85 100	4.14	0.403	1.02			B^+	2
				87 000	10.3	0.96	0.98			C^+	1
				93 600	5.07	0.479	1.02			B^+	2
				Δ(87 600–62 600)	Δ(5.07–2.06)			Δ(0.03)	1.4	D	3
				98 600	9.9	0.98	1.09			B^+	1
				119 500	16.3	1.28	0.93			B^+	1
				131 800	6.45	0.501	0.95			B^+	2
			3071.60	50 800	4.92	0.599	1.01			B^+	2
				62 600	2.06	0.220	0.98			B^+	2
				85 000	5.38	0.524	1.02			B^+	2
				85 100	4.14	0.397	1.00			B^+	2
				87 600	5.07	0.465	0.99			B^+	2
				Δ(87 600–62 600)	Δ(5.07–2.06)			Δ(0.03)	1.4	D	3
				131 800	6.45	0.478	0.91			B^+	2
2	$3p-(^1S)3d$	$^2P^\circ-^2D$	3403.52	50 800	4.92	0.622	1.14			B^+	2
				62 600	2.06	0.235	1.16			B^+	2
				85 000	5.38	0.563	1.22			B^+	2
				85 100	4.14	0.416	1.17			B^+	2
				87 600	5.07	0.486	1.15			B^+	2
				Δ(87 600–62 600)	Δ(5.07–2.06)			Δ(0.03)	1.5	D	3
				131 800	6.45	0.521	1.08			B^+	2
			3411.69	50 800	4.92	0.596	1.09			B^+	2
				62 600	2.06	0.235	1.16			B^+	2
				76 600	10.1	1.00	1.11			B^+	1
				85 000	5.38	0.558	1.20			B^+	2
				85 100	4.14	0.445	1.25			B^+	2
				87 600	5.07	0.495	1.16			B^+	2
				Δ(93 600–62 600)	Δ(5.07–2.06)			Δ(0.03)	1.5	D	3
				131 800	6.45	0.534	1.11			B^+	2
3	$2s2p3s-2s2p(^3P^\circ)3p$	$^4P^\circ-^4D$	3390.19	76 600	10.1	0.87				B	1

Oxygen

O V

Ground state: $1s^2 2s^2\,{}^1S_0$
Ionization energy: 113.899 eV = 918 657 cm^{-1}

Wrubel *et al.*[1] measured the Stark width of the $3s-3p$ singlet transition utilizing a gas-liner pinch. O V ions were confined to the homogeneous center of a hydrogen plasma column, and cool boundary layers were absent. The optical thickness for this transition was estimated to be negligible under the experimental conditions, since the analogous triplet transition of N IV under very similar conditions was found to be optically thin. Doppler and apparatus broadening were taken into account with a deconvolution procedure.

Blagojević *et al.*[2] measured the Stark widths of two $3s-3p$ triplet lines with a low-pressure pulsed arc end on, using a shot-to-shot scanning technique for recording the line profiles. They checked for self-absorption effects by diluting the oxygen gas in helium until they obtained within a few percent the LS-coupling ratios for the line intensities in the triplet. The contributions from instrumental and Doppler broadening were accounted for by a standard deconvolution technique. Very good agreement is obtained with the semiclassical calculations of Dimitrijević and Sahal-Bréchot.[3]

References

[1] Th. Wrubel, I. Ahmad, S. Büscher, H.-J. Kunze, and S. H. Glenzer, Phys. Rev. E **57**, 5972 (1998).
[2] B. Blagojević, M. V. Popović, N. Konjević, and M. S. Dimitrijević, J. Quant. Spectrosc. Radiat. Transf. **61**, 361 (1999).
[3] M. S. Dimitrijević and S. Sahal-Bréchot, Bull. Astron. Belgrade **150**, 95 (1994).

Key data on experiments

Reference	Plasma source	Method of measurement: Electron density	Method of measurement: Temperature	Remarks
1	Gas-liner pinch	90° Thomson scattering	90° Thomson scattering	
2	Low-pressure pulsed arc	Stark width of the He II P_α line	Boltzmann plot of O IV lines	

Numerical results for O V

No.	Transition array	Multiplet	Wavelength (Å)	Temperature (K)	Electron density (10^{17} cm^{-3})	w_m (Å)	w_m/w_{th}	d_m (Å)	d_m/d_{th}	Acc.	Reference
1	$2s3s-2s(^2S)3p$	${}^3S-{}^3P°$	2786.99	54 600	0.95	0.077	1.05			B^+	2
				61 900	1.38	0.102	1.00			B^+	2
				65 500	1.09	0.073	0.93			B^+	2
				79 700	1.41	0.100	1.09			B^+	2
				88 700	1.57	0.105	1.10			B^+	2
				91 600	1.68	0.102	1.02			B^+	2
				93 300	1.54	0.105	1.15			B^+	2
				Δ(93 300−61 900)	Δ(1.54−1.38)			Δ(−0.02)		D	2
			2789.85	61 900	1.38	0.098	0.96			B^+	2
				79 700	1.42	0.098	1.06			B^+	2
				88 700	1.57	0.105	1.10			B^+	2
				91 600	1.68	0.108	1.08			B^+	2
				Δ(93 300−61 900)	Δ(1.54−1.38)			Δ(−0.015)		D	2
2		${}^1S-{}^1P°$	5114.06	90 500	10.8	1.85				B	1
				108 000	12.0	2.01				A	1
				167 000	17.2	2.16				B^+	1
				217 000	23.6	2.85				B^+	1

Oxygen

O VI

Ground state: $1s^2 2s\,{}^2S_{1/2}$
Ionization energy: 138.119 eV = 1 114 008 cm^{-1}

Glenzer *et al.*[1] employed a gas-liner pinch for their Stark width measurements, while Blagojević *et al.*[2] used a low-pressure pulsed arc. In both experiments, the O VI lines were tested for possible self-absorption effects by checking the intensity ratio of the multiplet components against the expected 2:1 ratio predicted by LS coupling. Optically thin conditions were obtained for the selected operating conditions. Also, the measured line shapes were fitted to Voigt functions, so that the contributions of Doppler and instrumental broadening could be subtracted.

Glenzer *et al.* observed side on and emphasized that their plasma is homogeneous, and that no cold boundary layers exist. Blagojević *et al.*, who observed end on, did not discuss

the effect of cooler plasma-end layers in the electrodes. However, the O^{+5} ions should recombine there rather quickly, and produce only very small plasma inhomogeneity effects.

The experimental results have been compared with semiclassical calculations of Dimitrijević and Sahal-Bréchot.[3]

References

[1] S. Glenzer, N. I. Uzelac, and H.-J. Kunze, Phys. Rev. A **45**, 8795 (1992).
[2] B. Blagojević, M. V. Popović, N. Konjević, and M. S. Dimitrijević, J. Quant. Spectrosc. Radiat. Transf. **61**, 361 (1999).
[3] M. S. Dimitrijević and S. Sahal-Bréchot, Astron. Astrophys., Suppl. Ser. **93**, 359 (1992); (private communication).

Key data on experiments

Reference	Plasma source	Method of measurement: Electron density	Method of measurement: Temperature	Remarks
1	Gas-liner pinch	90° Thomson scattering	90° Thomson scattering	
2	Low-pressure pulsed arc	Stark width of the He II P_α line	Boltzmann plot of relative intensities of O IV lines	

Numerical results for O VI

No.	Transition array	Multiplet	Wavelength (Å)	Temperature (K)	Electron density (10^{17} cm^{-3})	w_m (Å)	w_m/w_{th}	d_m (Å)	d_m/d_{th}	Acc.	Reference
1	$3s-3p$	$^2S-^2P°$	3811.35	61 900	1.38	0.178	1.01			B^+	2
				65 500	1.09	0.136	1.00			B^+	2
				79 700	1.42	0.171	1.05			B^+	2
				Δ(79 700–65 500)	Δ(1.42–1.09)			Δ(−0.03)		D	2
				96 300	10	1.0	0.92			B	1
				133 400	13	1.4	1.11			C^+	1
				181 000	21	1.8	1.01			B	1
				203 100	24	2.1	1.07			B^+	1
			3834.24	61 900	1.38	0.176	1.00			B^+	2
				65 500	1.09	0.132	0.97			B^+	2
				79 700	1.42	0.178	1.09			B^+	2
				Δ(79 700–65 500)	Δ(1.42–1.09)			Δ(−0.03)		D	2

Silicon

Si I

Ground state: $1s^2 2s^2 2p^6 3s^2 3p^2\ ^3P_0$
Ionization energy: 8.1517 eV = 65 748 cm^{-1}

Srećković *et al.*[1,2] have observed the Stark widths and shifts of five Si I lines with a pulsed discharge and a shot-to-shot technique end on. The plasma was reproducible within ±6%. The geometry of the quartz glass tube was modified in order to reduce the amount of silicon evaporated from the walls. The carrier gas was an argon–helium mixture. The optical depth was checked by measuring intensity ratios of lines within the $3p^2\ ^3P-3p4s\ ^3P°$ multiplet and comparing them with known data. Disagreement was only of the order of 10%, but the lines are of similar strength, and thus this test is rather insensitive. The effects of the inhomogeneous plasma end layers were not discussed.

A standard deconvolution procedure was used to unfold the Stark widths from instrumental and Doppler broadening. van der Waals and resonance broadening were estimated to be negligible.

The measured values were compared with the results of Purić *et al.*[3] and Griem's semiclassical approximation.[4] The data of Srećković *et al.*[2] are in much better agreement with calculated values than those of Purić *et al.*[3] The shifts are in good agreement with previous measurements and with the theoretical values.

References

[1] A. Srećković, S. Bukvić, and S. Djenize, Publ. Astron. Obs. Belgrade **57**, 117 (1997).
[2] A. Srećković, S. Bukvić, and S. Djenize, Phys. Scr. **57**, 225 (1998).
[3] J. Purić, J. Djenize, S. Labat, and Lj. Ćirković, Z. Phys. **267**, 71 (1974).
[4] H. R. Griem, *Spectral Line Broadening by Plasmas* (Academic, New York, 1974).

Key data on experiments

Reference	Plasma source	Method of measurement: Electron density	Method of measurement: Temperature	Remarks
1, 2	Low-pressure pulsed arc	Laser interferometer at 6328 Å	Intensity ratios of Ar III to Ar II spectral lines	

Numerical results for Si I

No.	Transition array	Multiplet	Wavelength (Å)	Temperature (K)	Electron density (10^{17} cm^{-3})	w_m (Å)	w_m/w_{th}	d_m (Å)	d_m/d_{th}	Acc.	Reference
1	$3s^2 3p^2 - 3s 3p^3$	^{3}P–^{3}D°	2207.98	28 500	1.9	0.78		0.10		C$^+$,B	1
2	$3p^2 - 3p 4s$	^{3}P–^{3}P°	2506.90	28 500	1.9	0.70	1.65	0.14	1.08	C$^+$,B	2
			2524.12	28 500	1.9	0.72	1.64	0.12	0.91	C$^+$,B	2
			2528.50	28 500	1.9	0.68	1.66	0.13	1.06	C$^+$,B	2
3		^{1}D–^{1}P°	2881.58	28 500	1.9	0.54	0.89	0.20	1.12	B$^+$,B	2

Silicon

Si II

Ground state: $1s^2 2s^2 2p^6 3s^2 3p\ ^2P^\circ_{1/2}$
Ionization energy: 16.346 eV = 131 838.4 cm^{-1}

Pérez *et al.*[1,2] have measured Si II line widths in a pulsed discharge end on. A SiH_4–He gas mixture was used in order to obtain a homogeneous distribution of silicon in the discharge tube. The experimental conditions were chosen to minimize self-absorption, but the authors have not provided details. An intensified diode array detector was used to record the Si II lines. The profiles were corrected for instrumental and Doppler broadening, using a computerized procedure. Comparisons with other experimental and theoretical data show considerable differences, in some cases approaching factors of 2.

Wollschläger *et al.*[3] have measured some Stark widths and shifts with a diaphragm shock tube side on in the reflected shock wave. Neon with a small admixture (0.05%–0.25%) of tetramethylsilane served as the test gas and ensured good plasma homogeneity. Effects of the thin boundary layers are neglected. The optical depth was determined via the absolute plasma radiance at the wavelengths of the lines, and the line profiles were corrected for self-absorption. The Stark profiles were also unfolded from the contributions of instrumental and Doppler broadening.

The Stark widths were compared with previous data. They are in good agreement with the measurements of Konjević *et al.*,[4] Purić and co-workers,[5–7] and Lesage *et al.*[8] Earlier values measured by Lesage *et al.*[9] and by Chiang and Griem[10] are larger by about a factor of 2. Optical depth and inhomogeneity problems, mentioned in Ref. 8, could explain these larger line widthvalues. The experimental results by Wollschläger *et al.*[3] do not agree with Griem's[11] theoretical widths, but are in good agreement with those of Lesage *et al.*,[9] where the specific situation of the particular transition is taken into account. Line shifts disagree with the earlier measurements of Lesage *et al.*[9] and of Purić *et al.*[5] but agree with their later[8] measurements. Agreement is found with Griem's predictions,[11] but not with those of Lesage *et al.*[9] However, as pointed out by Hey,[12] configuration mixing may explain the difference between the values calculated.

References

[1] C. Pérez, M. I. de la Rosa, A. M. de Frutos, V. R. Gonzalez, and S. Mar, Ann. Phys. (Paris) **15**, 115 (1990).
[2] C. Pérez, I. de la Rosa, A. M. de Frutos, and S. Mar, Phys. Rev. E **47**, 756 (1993).
[3] F. Wollschläger, J. Mitsching, D. Meiners, M. Depiesse, J. Richou, and A. Lesage, J. Quant. Spectrosc. Radiat. Transf. **58**, 135 (1997).
[4] N. Konjević, J. Purić, L. J. Ćirković, and J. Labat, J. Phys. B **3**, 999 (1970).
[5] J. Purić, S. Djenize, J. Labat, and L. J. Ćirković, Z. Phys. **267**, 71 (1974).
[6] J. Purić, S. Djenize, J. Labat, L. J. Ćirković, and I. Lakicević, *Proc. VIIIth Summer School on Phys. Ionized Gases*, Dubrovnik (1976).
[7] J. Purić, A. Lesage, and V. Knezević, *Physics of Ionized Gases, Contributed Papers* (edited by R. K. Janev (Institute of Physics, Beograd, Yugoslavia, 1978), pp. 237–240.
[8] A. Lesage, B. A. Rathore, I. S. Lakicević, and J. Purić, Phys. Rev. A **28**, 2264 (1983).
[9] A. Lesage, S. Sahal-Bréchot, and M. H. Miller, Phys. Rev. A **16**, 1617 (1977).
[10] T. Chiang and H. R. Griem, Phys. Rev. A **18**, 1169 (1978).
[11] H. R. Griem, *Spectral Line Broadening by Plasmas* (Academic, New York, 1974).
[12] J. D. Hey, J. Quant. Spectrosc. Radiat. Transf. **18**, 425 (1977).

Key data on experiments

Reference	Plasma source	Method of measurement: Electron density	Method of measurement: Temperature	Remarks
1, 2	Pulsed arc	Interferometrically calibrated He I 6678 and 5016 Å linewidths	Boltzmann plot and intensity ratios of Si II lines	No proof given of self-absorption, no error bar
3	Gas-driven shock tube	Michelson interferometer at 4880 and 6328 Å	Absolute intensity of Ne I line at $\lambda = 5852$ Å	

Numerical results for Si II

No.	Transition array	Multiplet	Wavelength (Å)	Temperature (K)	Electron density (10^{17} cm^{-3})	w_m (Å)	w_m/w_{th}	d_m (Å)	d_m/d_{th}	Acc.	Reference
1	$3p-4p$	^{2}D–^{2}P°	3856.02	12 000	1.0	0.59	0.56			A	3
				12 100	1.0	0.51	0.48			B$^+$	3
				12 500	1.0	0.50	0.47			B$^+$	3
				12 600	1.0	0.60	0.57			A	3
				13 000	1.0			−0.08	0.17	D	3
				13 400	1.0	0.58	0.55			A	3
				13 500	1.0	0.58	0.55			A	3
				13 600	1.0	0.53	0.50			A	3
				14 000	1.0	0.60	0.57			A	3
				14 300	1.0	0.53	0.50			A	3
				14 300	1.0	0.51	0.48			A	3
			3862.60	12 000	1.0	0.63	0.59			B$^+$	3
				12 100	1.0	0.56	0.53			A	3
				12 500	1.0	0.60	0.57			A	3
				13 000	1.0			−0.16	0.35	D	3
				13 100	1.0	0.61	0.57			A	3
				13 400	1.0	0.53	0.50			A$^+$	3
				13 500	1.0	0.57	0.54			A	3
				13 600	1.0	0.60	0.57			A	3
				14 000	1.0	0.53	0.50			A	3
				14 300	1.0	0.61	0.57			A	3
				14 300	1.0	0.51	0.48			A	3
			3853.66	12 000	1.0	0.57	0.53			B$^+$	3
				12 100	1.0	0.54	0.51			A	3
				12 500	1.0	0.55	0.52			B$^+$	3
				13 400	1.0	0.57	0.54			B$^+$	3
2	$3d-4f$	^{2}D–^{2}F°	4130.89	13 900	0.565	1.43	1.8			C	2
				16 400	0.662	1.47	1.7			C	2
				31 500	0.919	1.91	1.7			C	2
			4128.07	13 900	0.565	1.29	1.63			C	2
				16 400	0.662	1.31	1.52			C	2
3	$4s-4p$	^{2}S–^{2}P°	6371.36	13 900	0.565	1.22	1.00			B	2
				16 400	0.662	1.23	0.95			B	2
				31 500	0.919	1.29	0.75			B	2
				35 000	0.98	1.26	0.69			B	1
			6347.10	13 900	0.565	1.20	0.99			B	2
				16 400	0.662	1.25	0.96			B	2
				31 500	0.919	1.22	0.72			B	2
				35 000	0.98	1.20	0.66			B	1
4	$4p-4d$	^{2}P°–^{2}D	5055.98	13 900	0.565	1.80	1.09			B$^+$	2
				16 400	0.662	2.04	1.1			B$^+$	2
				31 500	0.919	2.08	0.86			B$^+$	2
				35 000	0.98	2.01	0.78			B$^+$	1
			5041.03	13 900	0.565	1.40	0.85			B$^+$	2
				16 400	0.662	1.64	0.88			B$^+$	2
				31 500	0.919	2.05	0.84			B$^+$	2
				35 000	0.98	2.25	0.87			B$^+$	1
5	$4d-5f$	^{2}D–^{2}F°	4621.72	13 900	0.565	1.30	0.65			B$^+$	2
				16 400	0.662	1.13	0.49			B$^+$	2
				31 500	0.919	1.04	0.53			B$^+$	2

Silicon

Si III

Ground state: $1s^2 2s^2 2p^6 3s^2\ ^1S_0$
Ionization energy: 33.493 eV = 270 139.3 cm^{-1}

Djenize *et al.*[1] have observed 10 Si III lines with a low-pressure pulsed discharge on a shot-to-shot basis end on. Silicon was introduced into the plasma as an impurity by sputtering from the Pyrex walls of the discharge tube. The optical depth was checked by measuring the intensity ratios of lines within Si III multiplets and comparing them with known data. Optically thin conditions were found. The effects of inhomogeneous plasma end layers were not discussed. Stark profiles were unfolded from apparatus and Doppler broadening using a standard deconvolution procedure.

Comparisons with Griem's[2] simplified semiclassical formula and with different semiempirical approaches[3,4] were done for two Si III multiplets. For the Si III 3806.8 Å line the agreement is good, but for the 3241.6 Å line the calculated values are too large by a factor of 2.

Taking into account the calculated variation of the Stark parameters of the Si III lines versus temperature, the Stark width given by Djenize *et al.*[1] for the Si III 3806.5 Å line is almost two times larger than the values measured previously by Platisa *et al.*[5] and by Kusch and Schroder.[6] For the 3241.6 Å line, the agreement with Platisa *et al.*[5] is within mutual uncertainty estimates.

Gonzalez *et al.*[7] observed Si III lines with a low-pressure pulsed arc end on, on a shot-to-shot basis. Axial homogeneity and cylindrical symmetry were checked, and self-absorption tests and corrections were performed by doubling the plasma pathlength, using a concave mirror in the extension of the arc axis. The line profiles were corrected for apparatus and Doppler broadening.

The results of Gonzalez *et al.*[7] are about 30%–45% larger than those of Kusch and Schröder,[6] but are consistent with those of Djenize *et al.*[1] for the 3806 Å line. The width data of Puric *et al.*[8] for the 4552 Å line are, about 30% lower, and for the 4567 Å line they are, by about the same amount, higher than the values of Gonzalez *et al.*, provided the calculated temperature dependence of all these lines is accurate. With the same assumption, one may state that the results of Platisa *et al.*[5] are about 70% lower and 20% higher for the two above cited lines, respectively. For the lines of multiplet No. 9, there is agreement with the Stark widths given by Djenize *et al.*[1] within mutual error limits, and the same holds for the data of Kusch and Schröder[6] for the 5739 Å line.

For the $4p\ ^3P^\circ - 4d\ ^3D$ multiplet, the values of Gonzalez *et al.* agree with Griem's semiclassical formula and with the approximate semiclassical calculations done by Dimitrijević.[9] For lines of the $4s\ ^3S - 4p\ ^3P^\circ$ multiplet, the values of Gonzalez *et al.* agree with the approximate semiclassical and with the modified semiempirical calculations.

References

[1] S. Djenize, A. Srećković, J. Labat, J. Purić, and M. Plastisa, J. Phys. B **25**, 785 (1992).
[2] H. R. Griem, *Spectral Line Broadening by Plasmas* (Plenum, New York, 1974).
[3] M. S. Dimitrijević and N. Konjević, *Spectral Line Shapes*, edited by B. Wende (de Gruyter, New York, 1981), pp. 211–239.
[4] M. S. Dimitrijević, S. Sahal-Bréchot, and V. Bommier, Astron. Astrophys., Suppl. Ser. **89**, 591 (1991).
[5] M. Platisa, M. S. Dimitrijević, M. Popović, and N. Konjević, J. Phys. B **10**, 2997 (1977).
[6] H. J. Kusch and K. Schröder, Astron. Astrophys. **116**, 255 (1982).
[7] V. R. Gonzalez, J. A. Aparicio, J. A. del Val, and S. Mar, Astron. Astrophys. **363**, 1177 (2000).
[8] J. Purić, S. Djenize, J. Labat, and Lj. Ćirković, Z. Phys. **267**, 71 (1974).
[9] M. S. Dimitrijević, Astron. Astrophys. **127**, 68 (1983).

Key data on experiments

Reference	Plasma source	Method of measurement: Electron density	Method of measurement: Temperature	Remarks
1	Low-pressure pulsed arc	Laser interferometer at 6328 Å and Stark widths of S III and O III lines	Boltzmann slope of nine O III lines and intensity ratio of S III to S II lines	
7	Low-pressure pulsed arc	He–Ne and Ar^+ laser interferometers at 6328 and 4880 Å and Stark widths of He I and H_α lines	Boltzmann slope of Si II and He I lines; Si III/Si II intensity ratios; absolute intensities of He I lines	

Numerical results for Si III

No.	Transition array	Multiplet	Wavelength (Å)	Temperature (K)	Electron density (10^{17} cm^{-3})	w_m (Å)	w_m/w_{th}	d_m (Å)	d_m/d_{th}	Acc.	Reference
1	$3s3p-3p^2$	^{1}P°–^{1}D	2541.82	48 000	2.6	0.296				B	1
				49 000	1.4	0.180				B	1
				50 000	1.7	0.204				B	1
				64 000	3.0	0.292				B	1
2	$3d-4p$	^{3}D–^{3}P°	3096.83	48 000	2.6	0.290				B	1
				49 000	1.4	0.168				B	1
				50 000	1.7	0.194				B	1
3	$4s-4p$	^{3}S–^{3}P°	4552.62	19 000	1.0	0.53		−0.10		A,B	7
			4567.84	19 000	1.0	0.50		−0.08		A,B	7
			4574.76	19 000	1.0	0.50		−0.09		A,B	7
4	$4s-4p$	^{1}S–^{1}P°	5739.73	19 000	1.0	0.87		−0.16		B^+,C^+	7
5	$4p-4d$	^{3}P°–^{3}D	3806.54	19 000	1.0	0.69		0.42		B,B	7
				48 000	2.6	1.18				B	1
				49 000	1.4	0.73				B	1
				50 000	1.7	0.99				B	1
			3796.12	19 000	1.0	0.68		0.43		B^+,B^+	7
			3791.40	19 000	1.0	0.68		0.39		B,B	7
6	$4p-5s$	^{3}P°–^{3}S	3241.62	48 000	2.6	0.73				B	1
				49 000	1.4	0.456				B	1
				50 000	1.7	0.54				B	1
7	$4d-5p$	^{3}D–^{3}P°	7462.50	19 000	1.0	5.20				D	7
			7465.99	19 000	1.0	6.47				C^+	7
8	$4d-5f$	^{1}D–^{1}F°	4716.65	48 000	2.6	2.77				B	1
				49 000	1.4	1.32				B	1
				50 000	1.7	1.62				B	1
9	$4f-5g$	^{1}F°–^{1}G	3924.47	48 000	2.6	1.63				B	1
				49 000	1.4	0.92				B	1
				50 000	1.7	1.11				B	1
10	$4f-5g$	^{3}F°–^{3}G	4813.33	19 000	1.0	3.98		−0.98		C^+,D	7
				48 000	2.6	4.38				B	1
				49 000	1.4	2.74				B	1
				50 000	1.7	2.92				B	1
			4819.71	19 000	1.0	4.25		−0.98		B,D	7
				48 000	2.6	4.38					
				49 000	1.4	2.55					
				50 000	1.7	2.92					
			4828.96	19 000	1.0	4.05		−0.98		A,D	7
				48 000	2.6	4.38				B	1
				49 000	1.4	2.74				B	1
				50 000	1.7	3.07				B	1
11	$3d'-4p'$	^{3}D°–^{3}P	3258.66	48 000	2.6	0.214				B	1
				49 000	1.4	0.174				B	1
				50 000	1.7	0.202				B	1
				64 000	3.0	0.180				B	1

Silicon

Si IV

Ground state: $1s^2 2s^2 2p^6 3s\ ^2S_{1/2}$
Ionization energy: 45.142 eV = 364 093.1 cm^{-1}

Djenize *et al.*[1] have observed seven Si IV lines with a pulsed discharge on a shot-to-shot basis end on. The discharge was operated in a mixture of oxygen and SF_6, and silicon was introduced into the plasma as an impurity, sputtered from the Pyrex walls of the discharge tube. The optical depth at the line centers was checked by utilizing the known line intensity ratios of lines within a Si III multiplet. No self-absorption was detected. The effects of the inhomogeneous plasma end layers were not discussed. Profiles are unfolded from apparatus and Doppler broadening using a standard deconvolution procedure. van der Waals and resonance broadening are neglected.

Comparisons with the simplified semiclassical formula[2] and with different semiempirical approaches[3,4] were carried out in Ref. 1. For the values measured earlier by Platisa *et al.*,[5] agreement was found within the error bars. As always, we have compared with the results of semiclassical theory, taken here from Ref. 4. It is seen that the agreement is generally not good.

References

[1] S. Djenize, A. Srećković, J. Labat, J. Purić, and M. Platisa, J. Phys. B **25**, 785 (1992).
[2] H. R. Griem, *Spectral Line Broadening by Plasmas* (Academic, New York, 1974).
[3] M. S. Dimitrijević and N. Konjević, *Spectral Line Shapes*, edited by B. Wende (de Gruyter, New York, 1981), pp. 211–239.
[4] M. S. Dimitrijević, S. Sahal-Bréchot, and V. Bommier, Astron. Astrophys., Suppl. Ser. **89**, 591 (1991).
[5] M. Platisa, M. S. Dimitrijević, M. Popović, and N. Konjević, J. Phys. B **10**, 2997 (1977).

Key data on experiments

Reference	Plasma source	Method of measurement: Electron density	Method of measurement: Temperature	Remarks
1	Low-pressure pulsed arc	Laser interferometer at 6328 Å and Stark widths of S III and O III lines	Boltzmann plot of O III lines and intensity ratios of S III to S II lines	

Numerical results for Si IV

No.	Transition array	Multiplet	Wavelength (Å)	Temperature (K)	Electron density (10^{17} cm^{-3})	w_m (Å)	w_m/w_{th}	d_m (Å)	d_m/d_{th}	Acc.	Reference
1	$4s-4p$	^{2}S–^{2}P°	4088.85	29 000	1.6	0.436	0.62			B	1
				30 000	1.8	0.576	0.74			B	1
				31 000	2.7	0.770	0.66			B	1
				32 000	2.3	0.730	0.75			B	1
2	$4p-4d$	^{2}P°–^{2}D	3149.56	48 000	2.6	0.656	0.93			B	1
				49 000	1.4	0.308	0.81			B	1
				50 000	1.7	0.374	0.82			B	1
				64 000	3.0	0.652	0.90			B	1
			3165.71	29 000	1.6	0.340	0.62			B	1
				30 000	1.8	0.382	0.63			B	1
				31 000	2.7	0.660	0.72			B	1
				32 000	2.3	0.504	0.67			B	1
3	$4p-5s$	^{2}P°–^{2}S	2120.18	29 000	1.6	0.194	0.65			B	1
			2127.47	29 000	1.6	0.194	0.65			B	1
4	$4d-5p$	^{2}D–^{2}P°	3762.44	29 000	1.6	0.578	0.50			B	1
				30 000	1.8	0.618	0.48			B	1
				31 000	2.7	1.000	0.52			B	1
				32 000	2.3	0.924	0.57			B	1
			3773.15	29 000	1.6	0.460	0.40			B	1

Sodium

Na I

Ground state: $1s^22s^22p^63s\ ^2S_{1/2}$
Ionization energy: 5.1391 eV = 41 449.6 cm^{-1}

Djenize *et al.*[1] have measured the Stark widths of three Na I lines with a pulsed discharge on a shot-to-shot basis end on. The discharge was operated in oxygen, and sodium was evaporated from the Pyrex glass walls of the discharge vessel, which contained Na_2O as an impurity. The investigated spectral line intensities were reproducible within ±10%. No experimental check of the optical depth was mentioned, but the authors estimated that self-absorption is small, due to the low concentration of Na atoms in the plasma. Deconvolution was done via the conventional procedure. When comparisons are possible, the measured values are 20% lower than Griems semiclassical calculations[2] and 25% lower than the calculations of Mazure and Nollez[3] with the model microfield method, but they are 13% higher than the semiclassical calculations of Dimitrijević and Sahal-Bréchot.[4]

Srećković *et al.*[5] have measured the shifts of the Na I resonance lines with the same source as Djenize *et al.*[1] Oxygen, nitrogen, and argon have been used as carrier gases.

The measured shifts are in very good agreement with the calculations of Griem[2] and Mazure and Nollez,[3] as well as with previous measurements of Purić *et al.*[6] But the semiclassical calculations of Dimitrijević and Sahal-Bréchot[4] produce results that are 40% higher.

References

[1] S. Djenize, A. Srećković, J. Labat, and M. Platisa, Phys. Scr. **45**, 320 (1992).
[2] H. R. Griem, *Spectral Line Broadening by Plasmas* (Academic, New York, 1974).
[3] A. Mazure and G. Nollez, Z. Naturforsch., Teil A **33**, 1575 (1978).
[4] M. S. Dimitrijević and S. Sahal-Bréchot, J. Quant. Spectrosc. Radiat. Transf. **34**, 149 (1985).
[5] A. Srećković, S. Djenize, and S. Bukvić, Phys. Scr. **53**, 54 (1996).
[6] J. Purić, J. Labat, S. Djenize, Lj. Cirković, and I. Lakicević, Phys. Lett. A **56A**, 83 (1976).

Key data on experiments

Reference	Plasma source	Method of measurement: Electron density	Method of measurement: Temperature	Remarks
1	Low-pressure pulsed arc	Laser interferometer at 6328 Å and Stark width of the O III 3759 Å line	Boltzmann slope of nine O III lines and intensity ratio of O III to O II spectral lines	
5	Low-pressure pulsed arc	Laser interferometer at 6328 Å and Stark widths of O III, N IV, N III, and N II lines	Intensity ratios of Ar IV to Ar III, N IV to N III and O III to O II spectral lines	

Numerical results for Na I

No.	Transition array	Multiplet	Wavelength (Å)	Temperature (K)	Electron density (10^{17} cm^{-3})	w_m (Å)	w_m/w_{th}	d_m (Å)	d_m/d_{th}	Acc.	Reference
1	$3s-3p$	^{2}S–^{2}P°	5889.95	38 000	3.50			0.38	0.98	B$^+$	5
				47 000	1.23			0.15	1.15	B	5
				48 000	2.55	1.26	0.81			B	1
				48 000	2.55			0.22	0.81	B	5
				49 000	1.80			0.15	0.80	B	5
			5895.92	38 000	3.50			0.41	1.06	B$^+$	5
				47 000	1.23			0.13	1.00	B	5
				48 000	2.55	1.24	0.80			B	1
				48 000	2.55			0.22	0.81	B	5
				49 000	1.80			0.18	0.80	B	5
2	$3s-3d$	^{2}S–^{2}D	3426.86	48 000	2.55	0.76				B	1

Sulfur

S II

Ground state: $1s^2 2s^2 2p^6 3s^2 3p^3\ ^4S^\circ_{3/2}$
Ionization energy: 23.33 eV = 188 200 cm^{-1}

Hong and Fleurier[1] have observed some S II line widths with a Z-pinch plasma side-on. The Abel inversion process was used to obtain line shapes emitted by a homogeneous plasma volume. The measured Stark widths are smaller than those of Bridges and Wiese[2] and Miller[3] except for the S II 5429 Å line, where the result agrees with Miller.

Djenize *et al.*[4] measured S II Stark widths with a pulsed discharge end-on, on a shot-to-shot basis. The line widths were corrected for instrumental and Doppler contributions, while van der Waals and resonance broadening were neglected. The effects of the inhomogeneous plasma end-layers were not discussed. Comparisons with previous measurements are possible for the S II 4524 Å line only, for which very good agreement is found with the value by Mar *et al.*[5]

Kobilarov and Konjević[6] observed two S II lines in a low-pressure pulsed discharge end-on, on a shot-to-shot basis. The test gas mixture was 10% SF_6 in helium, which minimized self-absorption.

The optical depth was checked by comparing measured intensity ratios within multiplets to values obtained from LS-coupling rules. Instrumental and Doppler broadening were taken into account. The S II line widths by Kobilarov and Konjević[6] are in agreement with those of Bridges and Wiese,[2] while the values by Mar *et al.*[5] are somewhat smaller.

References

[1] D. Hong and C. Fleurier, *Spectral Line Shapes*, edited by R. Stamm and B. Talin (Nova Science, Commack, NY, 1993), Vol. 7, pp. 123–124.
[2] J. M. Bridges and W. L. Wiese, Phys. Rev. **159**, 31 (1967).
[3] M. H. Miller, Technical Note BN-550, University of Maryland (1968).
[4] S. Djenize, A. Srećković, M. Plastisa, R. Konjević, J. Labat, and J. Purić, Phys. Rev. A **42**, 2379 (1990).
[5] S. Mar, A. Czernichowski, and J. Chapelle, J. Phys. D **19**, 43 (1986).
[6] R. Kobilarov and N. Konjević, Phys. Rev. A **41**, 6023 (1990).

Key data on experiments

Reference	Plasma source	Method of measurement: Electron density	Method of measurement: Temperature	Remarks
1	Z-pinch plasma	Helium Stark profiles	S II and F I line intensity ratios	
4	Low-pressure pulsed arc	Laser interferometer at 6328 Å	Boltzmann plot of six S II lines	
6	Low-pressure pulsed arc	Laser interferometer at 6328 Å and He II 4685 Å widths	Intensity ratio of two O II lines	

Numerical results for S II

No.	Transition array	Multiplet	Wavelength (Å)	Temperature (K)	Electron density (10^{17} cm^{-3})	w_m (Å)	w_m/w_{th}	d_m (Å)	d_m/d_{th}	Acc.	Reference
1	$3p^2 3d - 3p^2(^3P)4p$	$^4F - ^4D°$	5606.15	23 500	1.0	0.38				B^+	1
			5660.00	23 500	1.0	0.42				B^+	1
			5578.87	23 500	1.0	0.45				B	1
2		$^4D - ^4P°$	6305.48	23 500	1.0	1.01				B^+	1
3		$^2F - ^2D°$	6312.69	23 500	1.0	0.84				B^+	1
4	$3p^2 4s - 3p^2(^3P)4p$	$^4P - ^4D°$	5453.86	28 500	0.7	0.31		−0.04		A,C^+	6
				32 600	1.1	0.46		−0.04		A,C^+	6
			5428.66	23 500	1.0	0.46				B^+	1
			5509.71	23 500	1.0	0.40				B^+	1
			5473.61	23 500	1.0	0.45				B^+	1
				28 500	0.7	0.31		−0.04		A,C^+	6
				32 600	1.1	0.46		−0.04		A,C^+	6
			5564.96	23 500	1.0	0.40				B^+	1
5		$^2P - ^2D°$	5647.02	27 000	0.67	0.316				B^+	4
				34 000	1.02	0.396				B^+	4
				40 000	2.08			−0.06		B	4
6	$3p^2 4s' - 3p^2(^1D)4p'$	$^2D - ^2F°$	5320.72	23 500	1.0	0.36				B^+	1
			5345.71	23 500	1.0	0.41				B^+	1
7		$^2D - ^2P°$	4524.94	27 000	0.67	0.372		−0.04		B^+,C^+	4
				34 000	1.02	0.532				B^+	4
8	$3p^2 4p - 3p^2(^3P)4d$	$^4D° - ^4F$	4162.67	27 000	0.67	0.416		−0.04		B^+,C^+	4
				34 000	1.02	0.536				B^+	4
9		$^4D° - ^4D$	4028.75	27 000	0.67	0.376		0.06		B^+,B	4
				34 000	1.02	0.496				B^+	4
10		$^4P° - ^4D$	4267.76	27 000	0.67	0.458		0.04		B^+,C^+	4
11		$^4P° - ^4P$	3892.29	27 000	0.67	0.420				B^+	4
12		$^2D° - ^2P$	3616.77	27 000	0.67	0.440		0.05		B^+,C^+	4
				34 000	1.02	0.542				B^+	4
13		$^4S° - ^4P$	4032.77	27 000	0.67			0.08		B	4
				34 000	1.02	0.614				B^+	4

Sulfur

S III

Ground state: $1s^2 2s^2 2p^6 3s^2 3p^2\ ^3P_0$
Ionization energy: 34.83 eV = 280 900 cm^{-1}

A pulsed discharge was used by Djenize *et al.*[1] and Dimitrijević *et al.*[2] to observe Stark-broadened line profiles of S III end-on, on a shot-to-shot basis. The test gas was pure SO_2 at 170–400 Pa, and the plasma reproducibility was ±8%. The optical depth was checked via line intensity ratios within multiplets. Compared to theoretical ratios, they differed by less than ±6%. The linewidths were corrected for instrumental and Doppler contributions. van der Waals and resonance broadening were found to be negligible. The effects of inhomogeneous plasma end layers were not discussed.

Calculated values obtained with a modification of the simplified semiclassical approach and the modified semiempirical approach agree better with the experimental results of Dimitrijević *et al.*[2] than those calculated by the authors of Ref. 2 with a simplified semiclassical formula.

The Stark width of the S III 4332 Å line, measured by Djenize *et al.*,[1] agrees better with the modified versions of the semiempirical and the semiclassical formulas than with the original formulas. Very good agreement was found with the measured value given by Platisa *et al.*[3]

References

[1] S. Djenize, A. Srećković, M. Plastisa, R. Konjević, J. Labat, and J. Purić, Phys. Rev. A **42**, 2379 (1990).
[2] M. S. Dimitrijević, S. Djenize, A. Srećković, and M. Platisa, Phys. Scr. **53**, 545 (1996).
[3] M. Platisa, M. Popović, M. S. Dimitrijević, and N. Konjević, J. Quant. Spectrosc. Radiat. Transf. **22**, 333 (1979).

Key data on experiments

Reference	Plasma source	Method of measurement: Electron density	Method of measurement: Temperature	Remarks
1	Low-pressure pulsed arc	Laser interferometer at 6328 Å	Boltzmann plot of six S II spectral lines	
2	Low-pressure pulsed arc	Laser interferometer at 6328 Å	Ratio of S III to S II lines	

Numerical results for S III

No.	Transition array	Multiplet	Wavelength (Å)	Temperature (K)	Electron density (10^{17} cm^{-3})	w_m (Å)	w_m/w_{th}	d_m (Å)	d_m/d_{th}	Acc.	Reference
1	$3p4s-3p4p$	^{3}P°–^{3}D	4332.71	40 000	2.08	0.428		0.04		B,C	1
2	$3p4p-3p5s$	^{3}D–^{3}P°	2508.15	40 000	2.1	0.402				B	2
			2499.08	40 000	2.1	0.360				B	2
3		^{3}S–^{3}P°	2785.49	40 000	2.1	0.380				B	2

Tin

Sn I

Ground state:
$1s^2 2s^2 2p^6 3s^2 3p^6 3d^{10} 4s^2 4p^6 4d^{10} 5s^2 5p^2\ ^3P_0$
Ionization energy: 7.3439 eV = 59 232.5 cm^{-1}

Djenize *et al.*[1] have observed the Stark widths of three Sn I lines in a pulsed discharge end-on, on a shot-to-shot basis. The line intensities were reproducible within ±13%. The plasma was assumed to be homogeneous, but the effects of the inhomogeneous plasma end layers were not discussed. Self-absorption was assumed to be negligible due to the way the tin was introduced into the plasma. The linewidths were corrected for Doppler and instrumental contributions, but van der Waals and resonance broadening were neglected. The measured Stark widths are half as large as the semiclassically calculated Stark widths, according to the work of Dimitrijević and Konjević.[3]

Martinez and Blanco[2] observed Sn I lines with a laser-produced plasma and recorded the line profiles with a multichannel analyzer. A tin target of 99.94% purity was placed in argon at a pressure of 800 Pa. The authors mentioned but did not demonstrate the homogeneity of their plasma. Narrow lines, emitted by a hollow cathode lamp, were used to obtain the instrumental resolution (0.3 Å).

The optical depth was checked from the intensity ratios of lines within multiplets observed at different concentrations in the plasma and from calculations applied to the strongest Sn II lines. The line profiles were analyzed by a standard deconvolution method.

The Stark width of the 4526 Å line measured by Martinez and Blanco[2] is in close agreement with that of Miller *et al.*[4] No calculated values are available for comparison.

References

[1] S. Djenize, A. Srećković, J. Labat, R. Konjević, and M. Brnović, Z. Phys. D **24**, 1 (1992).
[2] B. Martinez and F. Blanco, J. Phys. B **32**, 241 (1999).
[3] M. S. Dimitrijević and N. Konjević, Astron. Astrophys. **163**, 297 (1986).
[4] M. H. Miller, R. A. Roig, and R. D. Bengtson, Phys. Rev. A **20**, 499 (1979).

Key data on experiments

Reference	Plasma source	Method of measurement: Electron density	Method of measurement: Temperature	Remarks
1	Low-pressure pulsed arc	Stark width of the 3995 Å N II spectral line	Intensity ratios of N IV to N III lines and N III to N II lines	
2	Laser-produced plasma	Stark widths of 3 Sn II lines	Boltzmann plot of Sn II lines	

Numerical results for Sn I

No.	Transition array	Multiplet	Wavelength (Å)	Temperature (K)	Electron density (10^{17} cm^{-3})	w_m (Å)	w_m/w_{th}	d_m (Å)	d_m/d_{th}	Acc.	Reference
1	$5p^2-6s$	^{3}P–^{3}P°	2839.99	43 000	1.76	0.264				C	1
			2863.32	43 000	1.76	0.22				D	1
			3034.12	43 000	1.76	0.26				D	1
2	$6s-5p^2$	^{1}P°–^{1}S	4524.74	10 000	0.10	0.06				D^+	2
3		^{3}P°–^{3}P	3175.05	10 000	0.10	0.05				D^+	2
4		^{1}P°–^{1}D	3262.34	10 000	0.10	0.04				D^+	2

Tin

Sn II

Ground state:
$1s^2 2s^2 2p^6 3s^2 3p^6 3d^{10} 4s^2 4p^6 4d^{10} 5s^2 5p\ ^2P_{1/2}$
Ionization energy: 14.632 eV = 118 017.0 cm^{-1}

Martinez and Blanco[1] have observed Sn II lines with a laser-produced plasma and recorded their data with a multichannel analyzer. A tin target of 99.94% purity was placed in a 600 Pa argon atmosphere. The authors mentioned, but did not provide supporting evidence, that the observed plasma volume was nearly homogeneous in both temperature and electron density. A hollow cathode lamp emitting narrow lines was used to obtain the instrumental broadening profile.

The optical depth of the Sn lines was checked by observing the intensity ratios of lines within multiplets at different concentrations of tin and by ascertaining that these ratios remain constant. Corrections were made for other causes of line broadening.

The experimental width parameters agree within their error bars with those of Purić *et al.*[2] Also, the measurement of the shift of Purić *et al.*[2] for the 6845.4 Å line agrees within 10% with calculations of Martinez and Blanco.[1] For the $6p-7s$, $6p-8s$, $6s-6p$, and $5d-7p$ transitions, the measured widths agree with calculated widths based on the semiempirical formula of Griem[3] within the estimated uncertainties, but for the $6p-6d$, $6p-7d$, $5d-4f$, and $5d-5f$ transitions disagreement in the 35%–60% range is encountered.

Djenize *et al.*[4] have observed Sn II lines in a low-pressure pulsed arc end-on, on a shot-to-shot basis. Tin was sputtered from the electrode into a SF_6 carrier gas at a pressure of 130 Pa.

Self-absorption was assumed to be negligible due to the way the tin is introduced into the plasma. The linewidths were corrected for Doppler and instrumental contributions, but van der Waals and resonance broadening were neglected. Djenize *et al.*[4] did not provide uncertainties for their linewidth and shift measurements. Also, the effects of the inhomogeneous plasma end layers were not discussed. Their linewidths, compared with those of Miller *et al.*,[5] are, after correction due to different temperatures, found to be four times smaller. The Sn II 6844 Å linewidth value measured by Purić *et al.*[2] is, after similar temperature correction, found to be 2.5 times smaller. A comparison of the Stark shift for the Sn II 6844 Å line leads to a value 3.2 times smaller than that given in Ref. 2.

References

[1] B. Martinez and F. Blanco, J. Phys. B **32**, 241 (1999).
[2] J. Purić, M. Cuk, and I. S. Lakicević, Phys. Rev. A **32**, 1106 (1985).
[3] H. R. Griem, Phys. Rev. **165**, 258 (1968).
[4] S. Djenize, A. Srećković, and J. Labat, Z. Phys. D **17**, 85 (1990).
[5] M. H. Miller, R. A. Roig, and R. D. Bengtson, Phys. Rev. A **20**, 499 (1979).

Key data on experiments

Reference	Plasma source	Method of measurement		Remarks
		Electron density	Temperature	
1	Laser-produced plasma	Known Stark widths of several Sn II lines	Boltzmann plot of four Sn II lines	Stark width data used for N_e measurement are not very accurate
4	Low-pressure pulsed arc	Laser interferometer at 6328 Å	Boltzmann plot of eight F II lines; ratio of a F III line to the eight F II lines	

Numerical results for Sn II

No.	Transition array	Multiplet	Wavelength (Å)	Temperature (K)	Electron density (10^{17} cm^{-3})	w_m (Å)	w_m/w_{th}	d_m (Å)	d_m/d_{th}	Acc.	Reference
1	$6s-6p$	^{2}S–^{2}P°	6453.50	10 000	0.10	0.28				C	1
				33 000	0.96	0.496		−0.13		B, C$^+$	4
			6844.05	10 000	0.10	0.40				C	1
				33 000	0.96	0.652		−0.18		B,C$^+$	4
2	$5p^2-4f$	^{2}D–^{2}F°	3351.97	33 000	0.96	0.250		0.05		B,C	4
			3283.21	33 000	0.96	0.214		0.05		B,C	4
3	$5d-4f$	^{2}D–^{2}F°	5799.18	10 000	0.10	0.34				C	1
				33 000	0.96	0.656		0.16		B,C$^+$	4
			5588.92	10 000	0.10	0.38				C	1
				33 000	0.96	0.770		0.10		B,C$^+$	4
			5797.20	10 000	0.10	0.36				C	1
4	$5d-7p$	^{2}D–^{2}P°	4877.22	10 000	0.10	0.44				C	1
			4944.31	10 000	0.10	0.40				C	1
5	$5d-5f$	^{2}D–^{2}F°	3537.57	10 000	0.10	0.36				C	1
			3620.54	10 000	0.10	0.38				C	1
6	$6p-7s$	^{2}P°–^{2}S	6761.45	10 000	0.10	0.50				C	1
7	$6p-6d$	^{2}P°–^{2}D	5332.36	10 000	0.10	0.60				C	1
			5596.20	10 000	0.10	0.46				C	1
			5561.95	10 000	0.10	0.52				C	1
8	$6p-8s$	^{2}P°–^{2}S	3715.23	10 000	0.10	0.36				C	1
			3841.44	10 000	0.10	0.34				C	1
9	$6p-7d$	^{2}P°–^{2}D	3472.46	10 000	0.10	0.42				C	1
			3582.39	10 000	0.10	0.36				C	1
			3575.45	10 000	0.10	0.46				C	1
10	$6p-8d$	^{2}P°–^{2}D	2994.44	10 000	0.10	0.86				C	1

Xenon

Xe I

Ground state: $1s^22s^22p^63s^23p^63d^{10}4s^24p^64d^{10}5s^25p^6\ ^1S_0$
Ionization energy: 12.130 eV = 97 833.81 cm^{-1}

Konjević and Uzelac[1] have used a flash tube of variable plasma length to observe the Xe I 4734 Å line end on. The variable-length feature enabled them to precisely take self-absorption in the line profile into account. Care was taken to observe under quasistationary conditions. The Xe I 4734 Å line shifts measured by Konjević and Uzelac agree very well with calculations by Dimitrijević and Konjević,[2] as well as with earlier measurements by Klein and Meiners[3] and Truong Bach *et al.*,[4] done at much lower electron densities.

References

[1] N. Konjević and N. I. Uzelac, J. Quant. Spectrosc. Radiat. Transf. **44**, 61 (1990)
[2] M. S. Dimitrijević and N. Konjević, Astron. Astrophys. **163**, 297 (1986).
[3] P. Klein and D. Meiners, J. Quant. Spectrosc. Radiat. Transf. **17**, 197 (1977).
[4] Truong Bach, J. Richou, A. Lesage, and M. H. Miller, Phys. Rev. A **24**, 2550 (1981).

Key data on experiments

Reference	Plasma source	Method of measurement: Electron density	Method of measurement: Temperature	Remarks
1	Flash tube	Laser interferometer at 6328 Å and 3.39 μm	Analysis of measurements of current density through flash lamp and from initial Xe pressure in the source	

Numerical results for Xe I

No.	Transition array	Multiplet	Wavelength (Å)	Temperature (K)	Electron density (10^{17} cm^{-3})	w_m (Å)	w_m/w_{th}	d_m (Å)	d_m/d_{th}	Acc.	Reference
1	$6s-6p'$	[3/2]°–[3/2]	4734.15	⋯	3.7			0.8		B$^+$	1
				⋯	5.2			1.5		B$^+$	1
				12 500	9.0			2.1		A	1
				13 000	11.0			2.7		A	1

Xenon

Xe II

Ground state: $1s^2 2s^2 2p^6 3s^2 3p^6 3d^{10} 4s^2 4p^6 4d^{10} 5s^2 5p^5\ ^2P^\circ_{3/2}$
Ionization energy: 21.21 eV = 171 068.4 cm^{-1}

Finding list

Wavelength (Å)	No.	Wavelength (Å)	No.	Wavelength (Å)	No.	Wavelength (Å)	No.
4180.10	29	4769.05	21	5125.70	32	5531.07	6
4215.60	3	4787.77	27	5184.48	33	5667.56	8
4269.84	10	4818.02	8	5191.37	10	5699.61	26
4321.82	10	4844.33	2	5260.44	17	5719.61	4
4330.52	35	4862.45	30	5261.95	33	5726.91	38
4414.84	41	4876.50	25	5292.22	1	5751.03	20
4448.13	39	4883.53	10	5309.27	12	5758.65	31
4524.21	11	4887.30	13	5313.87	36	5776.39	19
4532.49	22	4890.09	2	5339.33	1	5905.13	16
4585.48	37	4919.66	15	5368.07	18	5945.53	9
4592.05	42	4921.48	13	5372.39	3	5976.46	1
4603.03	3	4972.71	24	5419.15	2	6036.20	5
4615.50	23	4988.77	15	5438.96	14	6051.15	7
4651.94	12	4991.17	40	5460.38	4	6097.59	5
4668.49	28	5044.92	34	5472.61	6		

Lesage *et al.*[1] have measured Xe II lines emitted by a shock-heated plasma photographically. Small amounts of xenon and hydrogen were added to the neon carrier gas. The linewidths were corrected for Doppler, van der Waals and instrumental broadening, and checks for self-absorption as well as pertinent corrections were made.

Konjević and Uzelać[2] have used a flash tube of variable plasma length to observe a few Xe II lines end on. This feature enabled them to take self-absorption in the profiles into account. Care was taken to observe under quasistationary conditions.

Bertuccelli *et al.*[3,4] have measured the Stark widths of 30 Xe II lines with a high-current pinch discharge end on with a shot-to-shot technique. Competing broadening mechanisms were found to be negligible, and instrumental broadening was taken into account.

Gigosos *et al.*[5] have measured numerous Xe II linewidths and shifts with a pulsed discharge end on. Care was taken to minimize the inhomogeneity of the plasma. Small quantities of xenon were added to the helium carrier gas. A mirror–lens system was used to check self-absorption, and no indications of it were found. A vidicon and intensified diode array detectors were used to record the He I and the Xe II lines. The profiles were corrected for instrumental broadening.

References

[1] A. Lesage, D. Abadie, and M. H. Miller, Phys. Rev. **40**, 1367 (1989).
[2] N. Konjević and N. I. Uzelać, J. Quant. Spectrosc. Radiat. Transf. **44**, 61 (1990).
[3] D. Bertucelli, G. Bertuccelli, and H. O. Di Rocco, Phys Scr. **43**, 469 (1991).
[4] D. Bertucelli, G. Bertuccelli, and H. O. Di Rocco, Rev. Sci. Instrum. **62**, 966 (1991).
[5] M. A. Gigosos, S. Mar, C. Perez, and I. de la Rosa, Phys. Rev. E. **49**, 1575 (1994).

Key data on experiments

Reference	Plasma source	Method of measurement: Electron density	Method of measurement: Temperature	Remarks
1	Diaphragm shock tube	H_β Stark width	Intensity of Ne I 5852 Å and H_β lines and line-reversal technique	Photographic technique
2	Flash tube	Laser interferometry at 6328 Å and 3.39 μm	Measurement of the current density through the flash lamp and from the initial Xe pressure of the lamp	
3	*Z* pinch	Stark widths of three Xe II lines with well-known parameters	Saha equation and measurement of conductivity	
4	*Z* pinch	The same as in Ref. 3	Saha equation and measurement of conductivity	
5	Pulsed arc	Laser interferometer at 6328 Å and He I 5016 Å Stark width	Boltzmann plot of Xe II lines	

Numerical results for Xe II

No.	Transition array	Multiplet	Wavelength (Å)	Temperature (K)	Electron density (10^{17} cm^{-3})	w_m (Å)	w_m/w_{th}	d_m (Å)	d_m/d_{th}	Acc.	Reference
1	$6s-6p$	[2]–[2]°	5339.33	11 000	1.0	0.64				B	1
				13 000	11.0	6.5				A	2
				14 400	0.69	0.427				B	5
				15 000	1.0			−0.08		C$^+$	5
				20 600	0.20	0.150				D	4
			5292.22	11 000	1.0	0.79				B	1
				13 000	11.0	6.5				A	2
				14 300	0.66	0.501				B	5
				15 000	1.0			−0.07		C$^+$	5
				20 600	0.20	0.210				D	4
			5976.46	14 500	0.26	0.186				D	3
				14 500	0.70	0.450				B	5
				15 000	1.0			−0.09		C$^+$	5
				20 600	0.20	0.173				D	4
2		[2]–[3]°	4890.09	14 300	0.64	0.337				B	5
				14 500	0.26	0.124				B	3
				15 000	1.0			−0.06		C$^+$	5
				20 600	0.20	0.137				C	4
			4844.33	11 000	1.0	0.72				B	1
				12 500	9.0	5.0				A	2
				13 000	11.0	5.9				A	2
				14 100	0.60	0.466				B	5
				15 000	1.0			−0.03		C$^+$	5
				20 600	0.20	0.226				D$^+$	4
			5419.15	12 500	9.0	6.0				A	2
				13 000	11.0	7.5				A	2
				14 300	0.65	0.545				B	5
				15 000	1.0			−0.06		C$^+$	5
				20 600	0.20	0.210				D$^+$	4
3		[2]–[1]°	5372.39	11 000	1.0	0.65				B	1
				14 500	0.26	0.156				B	3
				14 500	0.70	0.408				B	5
				20 600	0.20	0.128				C	4
			4215.60	14 500	0.26	0.116				B	3
				20 600	0.20	0.109				C	4
			4603.03	11 000	1.0	0.65				B	1
				14 500	0.26	0.152				B	3
				14 600	0.73	0.420				B	5
				20 600	0.20	0.171				C	4
4	$5d-6p$	[2]–[3]°	5460.38	14 400	0.67	0.437				B$^+$	5
				14 500	0.26	0.143				B	3
				15 000	1.0			0.11		B	5
			5719.61	10 000	0.26	0.124				B	3
5		[2]–[2]°	6097.59	14 500	0.26	0.156				B	3
			6036.20	11 000	1.0	0.75				B	1
				14 500	0.26	0.146				B	3
				14 600	0.73	0.536				B	5
				15 000	1.0			0.12		B	5
6		[3]–[3]°	5531.07	11 000	1.0	0.63				B	1
				14 500	0.26	0.128				B	3
			5472.61	11 000	1.0	0.82				B	1
				14 600	0.73	0.430				B	5
				15 000	1.0			0.09		C$^+$	5
7		[3]–[2]°	6051.15	11 000	1.0	0.75				B	1
				14 600	0.73	0.554				B	5
				15 000	1.0			0.08		C$^+$	5
8		[2]–[1]°	5667.56	11 000	1.0	0.61				B	1
				14 500	0.26	0.116				B	3
			4818.02	14 500	0.26	0.109				B	3
9		[1]–[1]°	5945.53	14 500	0.26	0.141				B	3
10	$6s-6p$	[0]–[1]°	5191.37	14 500	0.26	0.140				B	3
				20 600	0.20	0.165				C	4
			4883.53	14 300	0.63	0.325				B$^+$	5
				14 500	0.26	0.129				B	3
				15 000	1.0			−0.14		B	5
				20 600	0.20	0.163				C	4

Numerical results for Xe II—Continued

No.	Transition array	Multiplet	Wavelength (Å)	Temperature (K)	Electron density (10^{17} cm^{-3})	w_m (Å)	w_m/w_{th}	d_m (Å)	d_m/d_{th}	Acc.	Reference
			4269.84	20 600	0.20	0.101				C	4
			4321.82	20 600	0.20	0.103				C	4
11		[0]–[2]°	4524.21	11 000	1.0	0.74				B	1
				14 500	0.26	0.121				B	3
				20 600	0.20	0.116				C	4
12		[1]–[1]°	5309.27	14 400	0.67	0.394				B^+	5
				15 000	1.0			−0.06		C^+	5
				20 600	0.20	0.113				C	9
			4651.94	20 600	0.20	0.137				C	4
13		[1]–[2]°	4921.48	11 000	1.0	0.56				B	1
				14 500	0.26	0.148				C	3
				14 500	0.70	0.372				B^+	5
				15 000	1.0			−0.04		C^+	5
				20 600	0.20	0.150				D	4
			4887.30	14 300	0.64	0.353				B^+	5
				14 500	0.26	0.119				B	3
				20 600	0.20	0.128				C	4
14		[1]–[0]°	5438.96	11 000	1.0	0.54				B	1
				14 300	0.66	0.404				B^+	5
				14 500	0.26	0.154				B	3
				15 000	1.0			−0.07		C^+	5
				20 600	0.20	0.150				C	4
15	$5d-6p$	[1]–[1]°	4988.77	14 500	0.26	0.129				B	3
				14 500	0.70	0.778				B^+	5
				15 000	1.0			0.29		B	5
			4919.66	14 500	0.26	0.113				B	3
				14 600	0.74	0.472				B^+	5
				20 600	0.20	0.116				C	4
16		[1]–[0]°	5905.13	14 500	0.26	0.146				B	3
17		[1]–[2]°	5260.44	14 500	0.26	0.138				B	3
				14 700	0.75	0.525				B^+	5
				15 000	1.0			0.02		C	5
				20 600	0.20	0.105				C	4
18		[0]–[1]°	5368.07	14 500	0.26	0.126				B	3
				14 800	0.79	0.473				B^+	5
19		[0]–[2]°	5776.39	14 500	0.26	0.143				B	3
20	$6s-6p$	[1]–[1]°	5751.03	14 500	0.26	0.198				B	3
21	$5d-6p$	[1]–[3]°	4769.05	14 500	0.26	0.102				B	3
22		[2]–[3]°	4532.49	11 000	1.0	0.55				B	1
				20 600	0.20	0.120				C	4
23		[2]–[1]°	4615.50	14 900	0.81	0.775				B^+	5
24	$6s-6p$	[2]–[1]°	4972.71	14 500	0.26	0.119				B	3
25		[2]–[3]°	4876.50	14 300	0.63	0.301				B^+	5
				15 000	1.0			−0.09		C^+	5
				20 600	0.20	0.143				D	4
26	$5d-6p$	[2]–[3°	5699.61	14 500	0.26	0.130				B	3
27		[2]–[2]°	4787.77	14 500	0.26	0.124				B	3
28		[2]–[1]°	4668.49	14 500	0.26	0.109				B	3
				20 600	0.20	0.135				C	4
29	$6p-6d$	[2]°–[2]	4180.10	11 000	1.0	1.16				B	1
30	$6p-7s$	[2]°–[2]	4862.45	14 300	0.63	1.030				B^+	5
				15 000	1.0			0.57		B^+	5
31	$5d-6p$	[2]–[3]°	5758.65	14 500	0.26	0.159				B	3
				20 600	0.20	0.150				C	4
32		[2]–[2]°	5125.70	20 600	0.20	0.113				C	4
33	$6s-6p$	[2]–[2]°	5261.95	14 500	0.26	0.147				B	3
				14 700	0.75	0.367				B^+	5
				20 600	0.20	0.128				C	4
			5184.48	20 600	0.20	0.098				C	4
34		[2]–[1]°	5044.92	14 500	0.26	0.168				B	3
				20 600	0.20	0.128				C	4
35	$6p-6d$	[3]°–[4]	4330.52	11 000	1.0	1.32				B	1
				14 700	0.77	1.282				B	5
				15 000	1.0			0.68		B	5
36	$6p-7s$	[3]°–[2]	5313.87	14 400	0.67	1.288				B^+	5
				15 000	1.0			1.08		A	5
37	$6p-6d$	[3]°–[3]	4585.48	11 000	1.0	1.32				B	1
				14 900	0.81	1.266				B^+	5

Numerical results for Xe II—Continued

No.	Transition array	Multiplet	Wavelength (Å)	Temperature (K)	Electron density (10^{17} cm^{-3})	w_m (Å)	w_m/w_{th}	d_m (Å)	d_m/d_{th}	Acc.	Reference
				15 000	1.0			0.82		B$^+$	5
38	$5d-6p$	[3]–[2]°	5726.91	14 500	0.26	0.161				B	3
39	$6p-6d$	[2]°–[3]	4448.13	11 000	1.0	1.32				B	1
40	$6p-7s$	[1]°–[2]	4991.17	14 800	0.88	2.881				B$^+$	5
				15 000	1.0			2.03		A	5
41	$6p-6d$	[3]°–[4]	4414.84	11 000	1.0	0.44				B	1
				20 600	0.20	0.128				C	4
42		[2]°–[3]	4592.05	14 700	0.75	1.895				B$^+$	5
				15 000	1.0			0.85		B$^+$	5

Xenon

Xe III

Ground state: $1s^2 2s^2 2p^6 3s^2 3p^6 3d^{10} 4s^2 4p^6 4d^{10} 5s^2 5p^4\ ^3P_2$
Ionization energy: 32.123 eV = 259 089 cm^{-1}

Finding list

Wavelength (Å)	No.	Wavelength (Å)	No.	Wavelength (Å)	No.	Wavelength (Å)	No.
2984.58	113	3236.84	5	3544.86	84	3950.59	8
2985.53	68	3240.47	91	3552.12	26	3965.45	34
2986.11	112	3242.86	5	3562.22	89	3969.91	99
2992.89	66	3244.13	123	3562.99	95	3985.96	88
2994.67	101	3246.85	45	3579.70	20	3992.85	39
2997.50	114	3256.25	75	3583.65	30	4028.56	37
3001.52	115	3267.05	85	3591.98	6	4043.23	71
3004.26	66	3268.98	7	3601.87	3	4050.07	11
3009.03	60	3276.39	23	3607.02	32	4060.45	92
3014.59	109	3278.44	73	3615.86	34	4078.70	96
3020.33	76	3280.50	63	3618.86	69	4109.08	17
3023.83	2	3284.64	93	3620.00	83	4132.40	58
3026.52	4	3295.94	24	3623.13	17	4145.74	27
3042.04	126	3304.05	57	3624.06	8	4152.04	98
3054.48	49	3306.80	57	3632.14	70	4176.53	30
3065.19	50	3314.26	111	3636.02	81	4194.87	41
3080.42	119	3314.87	56	3640.99	19	4209.58	71
3083.53	10	3331.65	23	3644.14	56	4213.99	44
3090.00	80	3339.50	61	3653.09	9	4216.71	14
3091.05	13	3340.06	50	3654.61	34	4240.24	64
3099.87	67	3340.37	82	3676.63	11	4272.58	46
3102.36	117	3340.67	35	3689.83	47	4285.89	41
3102.69	67	3344.93	110	3708.15	86	4309.32	44
3103.47	21	3357.99	22	3721.03	103	4387.47	51
3114.41	105	3362.77	116	3745.71	53	4413.06	82
3120.52	118	3370.65	59	3757.98	97	4417.97	82
3124.95	72	3379.03	62	3765.85	70	4434.17	28
3138.28	122	3384.10	1	3768.93	125	4503.41	100
3141.63	104	3390.64	90	3772.53	94	4537.38	28
3150.97	15	3403.91	79	3776.32	71	4641.40	127
3151.83	25	3435.74	116	3781.00	11	4657.78	40
3153.00	21	3444.24	16	3791.67	31	4673.67	42
3153.44	106	3454.27	43	3802.98	120	4683.55	12
3164.47	29	3467.22	48	3841.53	20	4712.58	55
3177.11	108	3468.22	7	3841.87	38	4743.87	52
3184.27	107	3494.51	83	3861.04	24	4748.94	102
3185.21	124	3494.82	54	3877.82	33	4794.49	27
3196.25	18	3501.65	121	3880.46	16	4869.40	36
3196.51	4	3509.77	76	3884.99	6	4927.51	57
3222.99	118	3522.80	5	3903.67	9	5524.33	78
3227.16	74	3539.94	77	3915.31	65		
3235.73	87	3542.35	32	3922.55	8		

Iriarte *et al.*[1] and Romeo y Bidegain *et al.*[2] applied a pinch discharge to observe a fairly large number of Xe III line profiles end-on, on a shot-to-shot basis with a photomultiplier. No check of self-absorption was reported, except that xenon was kept at a low (0.06 mbar) pressure. The observed line profiles were corrected for Doppler and instrumental broadening.

Di Rocco *et al.*[3] have measured line shifts of some Xe III lines. Since they did not provide any measurements of the plasma parameters, their results are not tabulated.

For multiplets Nos. 57 and 82 in the table below, we have grouped spectral lines together that appear to belong to the same multiplet. However, two different parent terms are involved. In each case, we have separated by a space these two groups of lines that are located at very different wavelengths.

References

[1] D. Iriarte, M. Romeo y Bidegain, G. Bertuccelli, and H. O. Di Rocco, Phys. Scr. **55**, 181 (1997).
[2] M. Romeo y Bidegain, D. Iriarte, G. Bertuccelli, and H. O. Di Rocco, Phys. Scr. **57**, 495 (1998).
[3] H. O. Di Rocco, G. Bertuccelli, J. Reynas Almandos, F. Bredice, and M. Gallardo, J. Quant. Spectrosc. Radiat. Transf. **41**, 161 (1989).

Key data on experiments

Reference	Plasma source	Method of measurement: Electron density	Method of measurement: Temperature	Remarks
1, 2	Pulsed capillary discharge	Stark widths of five Xe II lines	Boltzmann plot of five Xe II lines	

Numerical results for Xe III

No.	Transition array	Multiplet	Wavelength (Å)	Temperature (K)	Electron density (10^{17} cm^{-3})	w_m (Å)	w_m/w_{th}	d_m (Å)	d_m/d_{th}	Acc.	Reference
1	$5d-6p$	^{3}D°–^{5}P	3384.10	29 000	0.24	0.80				B	2
2		^{3}D°–^{3}P	3023.83	29 000	0.24	0.84				B	2
3		^{1}D°–^{5}P	3601.87	29 000	0.24	0.50				B	2
4		^{1}P°–^{3}P	3026.52	29 000	0.24	0.78				B	2
			3196.51	29 000	0.24	0.70				B	2
5		^{3}D°–^{3}P	3522.80	29 000	0.24	0.65				B	2
			3236.84	29 000	0.24	0.51				B	2
			3242.86	29 000	0.24	0.73				B	2
6		^{3}D°–^{5}P	3591.98	29 000	0.24	0.51				B	2
			3884.99	29 000	0.24	0.47				B	2
7	$6s-6p$	^{5}S°–^{3}P	3468.22	29 000	0.236	0.62				B	1
			3268.98	29 000	0.236	0.63				B	1
8		^{5}S°–^{5}P	3624.06	29 000	0.236	0.77				B	1
			3950.59	29 000	0.236	0.67				B	1
			3922.55	29 000	0.236	0.66				B	1
9	$5d-6p$	^{3}F°–^{3}P	3903.67	29 000	0.24	0.47				B	2
			3653.09	29 000	0.24	0.49				B	2
10		^{3}F°–^{3}F	3083.53	29 000	0.24	0.81				B	2
11	$6s-6p$	^{3}S°–^{3}P	3781.00	29 000	0.236	0.61				B	1
			4050.07	29 000	0.236	0.53				B	1
			3676.63	29 000	0.236	0.54				B	1
12		^{3}S°–^{5}P	4683.55	29 000	0.236	0.45				B	1
13	$5d-6p$	^{3}G°–^{3}F	3091.05	29 000	0.24	0.93				B	2
14		^{3}G°–^{3}P	4216.71	29 000	0.24	0.37				B	2
15		^{1}G°–^{1}F	3150.97	29 000	0.24	0.90				B	2
16		^{3}D°–^{3}D	3444.24	29 000	0.24	0.53				B	2
			3880.46	29 000	0.24	0.50				B	2
17	$6s-6p$	^{3}D°–^{3}D	4109.08	29 000	0.236	0.51				B	1
			3623.13	29 000	0.236	0.56				B	1
18	$5d-6p$	^{3}D°–^{1}P	3196.25	29 000	0.24	0.61				B	2
19		^{3}D°–^{3}F	3640.99	29 000	0.24	0.54				B	2
20	$6s-6p$	^{3}D°–^{3}F	3841.53	29 000	0.236	0.54				B	1
			3579.70	29 000	0.236	0.69				B	1
21	$6s-4f$	^{3}D°–^{5}F	3153.00	29 000	0.24	0.72				B	2
			3103.47	29 000	0.24	0.86				B	2
22	$6s-6p$	^{3}D°–^{5}F	3357.99	29 000	0.236	0.63				B	1

Numerical results for Xe III—Continued

No.	Transition array	Multiplet	Wavelength (Å)	Temperature (K)	Electron density (10^{17} cm^{-3})	w_m (Å)	w_m/w_{th}	d_m (Å)	d_m/d_{th}	Acc.	Reference
23	$5d-4f$	^{1}D°–^{5}F	3331.65	29 000	0.24	0.56				B	2
			3276.39	29 000	0.24	0.61				B	2
24	$5d-6p$	^{1}D°–^{3}D	3295.94	29 000	0.24	0.66				B	2
			3861.04	29 000	0.24	0.48				B	2
25		^{1}D°–^{3}P	3151.83	29 000	0.24	0.78				B	2
26		^{1}D°–^{1}P	3552.12	29 000	0.24	0.49				B	2
27	$6s-6p$	^{3}D°–^{3}D	4145.74	29 000	0.236	0.58				B	1
			4794.49	29 000	0.236	0.34				B	1
28		^{3}D°–^{3}F	4434.17	29 000	0.236	0.47				B	1
			4537.38	29 000	0.236	0.41				B	1
29	$6s-4f$	^{3}D°–^{3}F	3164.47	29 000	0.24	1.01				B	2
30	$6s-6p$	^{3}D°–^{3}F	4176.53	29 000	0.236	0.59				B	1
			3583.65	29 000	0.236	0.68				B	1
31		^{3}D°–^{1}P	3791.67	29 000	0.236	0.56				B	1
32	$6s-4f$	^{3}D°–^{5}F	3607.02	29 000	0.24	0.59				B	2
			3542.35	29 000	0.24	0.66				B	2
33	$6s-6p$	^{3}D°–^{1}F	3877.82	29 000	0.236	0.58				B	1
34	$5d-6p$	^{3}P°–^{3}P	3615.86	29 000	0.24	0.55				B	2
			3654.61	29 000	0.24	0.44				B	2
			3965.45	29 000	0.24	0.42				B	2
35		^{3}D°–^{1}D	3340.67	29 000	0.24	0.64				B	2
36		^{3}D°–^{3}F	4869.40	29 000	0.24	0.34				B	2
37	$5d-4f$	^{3}D°–^{5}F	4028.56	29 000	0.24	0.44				B	2
38	$5d-6p$	^{3}D°–^{3}P	3841.87	29 000	0.24	0.56				B	2
39	$6s-6p$	^{1}D°–^{3}P	3992.85	29 000	0.236	0.59				B	1
40		^{1}D°–^{1}P	4657.78	29 000	0.236	0.36				B	1
41	$6s-4f$	^{1}D°–^{5}F	4285.89	29 000	0.24	0.42				B	2
			4194.87	29 000	0.24	0.30				B	2
42	$6s-6p$	^{1}D°–^{1}F	4673.67	29 000	0.236	0.39				B	1
43		^{1}D°–^{1}D	3454.27	29 000	0.236	0.62				B	1
44	$5d-4f$	^{3}D°–^{5}F	4213.99	29 000	0.24	0.62				B	2
			4309.32	29 000	0.24	0.40				B	2
45		^{3}D°–^{3}F	3246.85	29 000	0.24	0.65				B	2
46	$5d-6p$	^{3}D°–^{3}F	4272.58	29 000	0.24	0.49				B	2
47	$5d-4f$	^{3}D°–^{3}F	3689.83	29 000	0.24	0.44				B	2
48	$5d-6p$	^{3}D°–^{1}D	3467.22	29 000	0.24	0.62				B	2
49		^{3}F°–^{3}P	3054.48	29 000	0.24	0.83				B	2
50		^{3}F°–^{3}D	3340.06	29 000	0.24	0.59				B	2
			3065.19	29 000	0.24	0.95				B	2
51		^{3}F°–^{3}P	4387.47	29 000	0.24	0.37				B	2
52	$5d-4f$	^{3}F°–^{5}F	4743.87	29 000	0.24	0.34				B	2
53	$5d-6p$	^{3}F°–^{1}D	3745.71	29 000	0.24	0.53				B	2
54	$5d-4f$	^{3}F°–^{3}F	3494.82	29 000	0.24	0.58				B	2
55	$5d-6p$	^{3}F°–^{3}F	4712.58	29 000	0.24	0.37				B	2
56		^{3}S°–^{3}D	3314.87	29 000	0.24	0.62				B	2
			3644.14	29 000	0.24	0.54				B	2
57		^{3}S°–^{3}P	3304.05	29 000	0.24	0.93				B	2
			3306.80	29 000	0.24	0.68				B	2
			4927.51	29 000	0.24	0.37				B	2
58		^{3}S°–^{1}D	4132.40	29 000	0.24	0.45				B	2
59		^{3}P°–^{3}P	3370.65	29 000	0.24	0.68				B	2
60	$5d-4f$	^{3}P°–^{3}F	3009.03	29 000	0.24	1.18				B	2
61		^{3}P°–^{3}G	3339.50	29 000	0.24	0.43				B	2
62	$5d-6p$	^{3}P°–^{3}D	3379.03	29 000	0.24	0.52				B	2
63	$5d-4f$	^{1}F°–^{3}G	3280.50	29 000	0.24	0.61				B	2
64	$5d-6p$	^{1}F°–^{1}D	4240.24	29 000	0.24	0.50				B	2
65	$5d-4f$	^{1}F°–^{3}F	3915.31	29 000	0.24	0.50				B	2
66	$6p-6d$	^{5}P–^{5}D°	3004.26	29 000	0.24	1.25				B	2
			2992.89	29 000	0.24	0.99				B	2
67		^{3}P–^{5}D°	3099.87	29 000	0.24	0.93				B	2
			3102.69	29 000	0.24	0.96				B	2
68	$6p-7s$	^{3}P–^{3}S°	2985.53	29 000	0.24	1.07				B	2
69	$5d-6p$	^{3}P°–^{3}P	3618.86	29 000	0.24	0.52				B	2

Numerical results for Xe III—Continued

No.	Transition array	Multiplet	Wavelength (Å)	Temperature (K)	Electron density (10^{17} cm^{-3})	w_m (Å)	w_m/w_{th}	d_m (Å)	d_m/d_{th}	Acc.	Reference
70	$6s-6p$	^{3}P°–^{3}P	3632.14	29 000	0.236	0.59				B	1
			3765.85	29 000	0.236	0.62				B	1
71		^{3}P°–^{3}D	3776.32	29 000	0.236	0.56				B	1
			4043.23	29 000	0.236	0.57				B	1
			4209.58	29 000	0.236	0.60				B	1
72	$6s-4f$	^{3}P°–^{1}P	3124.95	29 000	0.24	1.03				B	2
73	$6p-6d$	^{3}P–^{5}D°	3278.44	29 000	0.24	0.77				B	2
74	$6p-7s$	^{3}P–^{3}S°	3227.16	29 000	0.24	0.68				B	2
75	$5d-6p$	^{3}D°–^{3}D	3256.25	29 000	0.24	0.62				B	2
76	$5d-4f$	^{3}D°–^{3}D	3509.77	29 000	0.24	0.63				B	2
			3020.33	29 000	0.24	0.88				B	2
77	$5d-6p$	^{3}D°–^{3}S	3539.94	29 000	0.24	0.62				B	2
78		^{3}D°–^{1}D	5524.33	29 000	0.24	0.41				B	2
79		^{3}P°–^{1}D	3403.91	29 000	0.24	0.56				B	2
80	$5d-4f$	^{3}P°–^{3}D	3090.00	29 000	0.24	1.09				B	2
81	$5d-6p$	^{3}P°–^{3}S	3636.02	29 000	0.24	0.54				B	2
82		^{3}D°–^{3}P	3340.37	29 000	0.24	0.64				B	2
			4413.06	29 000	0.24	0.44				B	2
			4417.97	29 000	0.24	0.40				B	2
83		^{3}D°–^{1}D	3494.51	29 000	0.24	0.54				B	2
			3620.00	29 000	0.24	0.63				B	2
84		^{3}D°–^{3}D	3544.86	29 000	0.24	0.47				B	2
85	$5d-4f$	^{3}D°–^{3}D	3267.05	29 000	0.24	0.50				B	2
86	$6s-6p$	^{3}P°–^{1}P	3708.15	29 000	0.236	0.53				B	1
87	$6s-4f$	^{3}P°–^{1}D	3235.73	29 000	0.24	0.51				B	2
88	$6s-6p$	^{3}P°–^{1}D	3985.96	29 000	0.236	0.50				B	1
89	$6s-4f$	^{3}P°–^{3}D	3562.22	29 000	0.24	0.56				B	2
90		^{3}P°–^{3}P	3390.64	29 000	0.24	0.57				B	2
91		^{3}P°–^{1}F	3240.47	29 000	0.24	0.45				B	2
92	$6s-6p$	^{1}P°–^{1}D	4060.45	29 000	0.236	0.46				B	1
93	$6s-4f$	^{1}P°–^{1}D	3284.64	29 000	0.24	0.72				B	2
94	$6s-6p$	^{1}P°–^{1}P	3772.53	29 000	0.236	0.66				B	1
95	$5d-4f$	^{3}P°–^{3}D	3562.99	29 000	0.24	0.66				B	2
96	$5d-6p$	^{1}D°–^{3}P	4078.70	29 000	0.24	0.43				B	2
97	$5d-4f$	^{1}D°–^{3}P	3757.98	29 000	0.24	0.42				B	2
98	$5d-6p$	^{1}D°–^{1}P	4152.04	29 000	0.24	0.48				B	2
99	$5d-4f$	^{1}D°–^{3}D	3969.91	29 000	0.24	0.49				B	2
100	$5d-6p$	^{1}D°–^{1}D	4503.41	29 000	0.24	0.44				B	2
101	$6p-6d$	^{3}F–^{3}F°	2994.67	29 000	0.24	0.96				B	2
102	$5d-6p$	^{1}F°–^{1}D	4748.94	29 000	0.24	0.45				B	2
103	$5d-4f$	^{1}F°–^{1}D	3721.03	29 000	0.24	0.43				B	2
104	$6p-6d$	^{1}F–^{3}G°	3141.63	29 000	0.24	0.81				B	2
105		^{1}F–^{1}G°	3114.41	29 000	0.24	0.89				B	2
106	$6p-7s$	^{1}F–^{3}D°	3153.44	29 000	0.24	0.75				B	2
107		^{1}P–^{3}D°	3184.27	29 000	0.24	0.70				B	2
108	$6p-6d$	^{1}P–^{3}F°	3177.11	29 000	0.24	0.65				B	2
109		^{3}P–^{3}S°	3014.59	29 000	0.24	0.85				B	2
110	$4f-6d$	^{5}F–^{3}G°	3344.93	29 000	0.24	0.53				B	2
111		^{5}F–^{1}G°	3314.26	29 000	0.24	0.70				B	2
112	$6p-7s$	^{3}F–^{3}D°	2986.11	29 000	0.24	1.10				B	2
113	$6p-6d$	^{3}F–^{3}G°	2984.58	29 000	0.24	0.87				B	2
114		^{3}D–^{3}G°	2997.50	29 000	0.24	0.93				B	2
115	$4f-6d$	^{5}F–^{3}G°	3001.52	29 000	0.24	0.99				B	2
116		^{5}F–^{3}F°	3435.74	29 000	0.24	0.60				B	2
			3362.77	29 000	0.24	0.58				B	2
117		^{5}F–^{3}S°	3102.36	29 000	0.24	0.96				B	2
118	$6p-6d$	^{3}P–^{3}S°	3222.99	29 000	0.24	0.63				B	2
			3120.52	29 000	0.24	0.88				B	2
119	$6p-7s$	^{3}P–^{1}D°	3080.42	29 000	0.24	0.97				B	2
120	$4f-6d$	^{3}F–^{1}G°	3802.98	29 000	0.24	0.51				B	2
121	$6p-7s$	^{1}D–^{1}D°	3501.65	29 000	0.24	0.63				B	2
122	$6p-6d$	^{1}D–^{1}F°	3138.28	29 000	0.24	1.12				B	2
123		^{1}D–^{1}P°	3244.13	29 000	0.24	0.56				B	2

Numerical results for Xe III—Continued

No.	Transition array	Multiplet	Wavelength (Å)	Temperature (K)	Electron density (10^{17} cm^{-3})	w_m (Å)	w_m/w_{th}	d_m (Å)	d_m/d_{th}	Acc.	Reference
124		^{1}D–^{1}D°	3185.21	29 000	0.24	0.82				B	2
125	$4f-6d$	^{3}F–^{3}G°	3768.93	29 000	0.24	0.84				B	2
126	$6p-6d$	^{3}D–^{3}D°	3042.04	29 000	0.24	0.83				B	2
127	$4f-6d$	^{3}G–^{3}F°	4641.40	29 000	0.24	0.40				B	2

Zinc

Zn II

Ground state: $1s^2 2s^2 2p^6 3s^2 3p^6 3d^{10} 4s\ ^2S_{1/2}$
Ionization energy: 17.964 eV = 144 892.6 cm^{-1}

Djenize *et al.*[1] have observed Zn II lines with a pulsed arc end-on, on a shot-to-shot basis. Zinc was deposited on the electrode surface and sputtered into the SF_6 carrier gas. The line intensities were reproducible within 18%. Effects of the inhomogeneous plasma end layers were not discussed. Self-absorption was assumed to be negligible due to the manner in which the element was introduced into the plasma.

The authors estimate that due to the large mass and small concentration of emitters, the Doppler, van der Waals and resonance broadening are negligible. But the line profiles are corrected for instrumental broadening.

The results for the Stark widths of the $4p-5s$ and $5s-5p$ transitions are puzzling. Converted to the frequency scale, the $4p-5s$ width is twice as large as the $5s-5p$ width. But the latter is expected to be the larger because the upper quantum state has the higher angular momentum. Indeed, calculation with the modified semiempirical approach[4] yields a ratio of 12:1 for the Stark widths in the reversed sense from the experiment.

The Stark width measured for the 2062 Å line was compared with different versions of the semiempirical formula,[2,3] and the experimental value is about a factor of 3 larger. No Stark shifts were detected for the lines at 2062 and 2558 Å.

References

[1] S. Djenize, A. Srećković, J. Labat, R. Konjević, and L. Popović, Phys. Rev. A **44**, 410 (1991).
[2] H. R. Griem, Phys. Rev. **165**, 258 (1968).
[3] M. S. Dimitrijević and N. Konjević, Astron. Astrophys. **172**, 345 (1987).
[4] L. C. Popović, I. Vince, and M. S. Dimitrijević, Astron. Astrophys., Suppl. Ser. **102**, 17 (1993).

Key data on experiments

Reference	Plasma source	Method of measurement: Electron density	Method of measurement: Temperature	Remarks
1	Low-pressure pulsed arc	Laser interferometer at 6328 Å	Boltzmann plot of eight F II spectral lines	

Numerical results for Zn II

No.	Transition array	Multiplet	Wavelength (Å)	Temperature (K)	Electron density (10^{17} cm^{-3})	w_m (Å)	w_m/w_{th}	d_m (Å)	d_m/d_{th}	Acc.	Reference
1	$4s-4p$	^{2}S–^{2}P°	2061.91	33 000	1.15	0.054				D	1
2	$4p-3d^9 4s^2$	^{2}P°–^{2}D	5894.35	33 000	1.15	0.528		0.054		B,C	1
			7478.79	33 000	1.15	0.516				B	1
3	$4p-5s$	^{2}P°–^{2}S	2557.96	33 000	1.15	0.118				C	1
4	$4d-4f$	^{2}D–^{2}F°	4911.66	33 000	1.15	0.420		0.048		B,C	1
5	$5s-5p$	^{2}S–^{2}P°	7588.48	33 000	1.15	0.512		0.066		B,C	1